

NASA

AD-A278 849

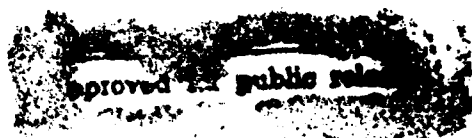


Earth Resources
A Continuing
Bibliography
with Indexes

NASA SP-7041(55)
November 1987



National Aeronautics and
Space Administration



DTIC
ELECTE
MAY 04 1994
S G D

es Earth Resource
s Earth Resources
Earth Resources E
th Resources Ear
Resources Earth
Resources Earth R
resources Earth Re

ED 3

ACCESSION NUMBER RANGES

Accession numbers cited in this Supplement fall within the following ranges.

STAR (N-10000 Series) N87-20171 — N87-25266

IAA (A-10000 Series) A87-31363 — A87-42684

EARTH RESOURCES

A CONTINUING BIBLIOGRAPHY WITH INDEXES

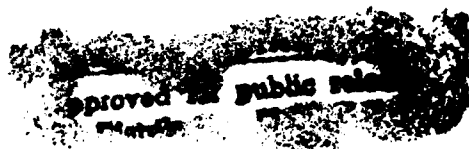
Issue 55

A selection of annotated references to unclassified reports and journal articles that were introduced into the NASA scientific and technical information system and announced between July 1 and September 30, 1987 in

- *Scientific and Technical Aerospace Reports (STAR)*
- *International Aerospace Abstracts (IAA).*

Accession For	
NTIS CRA&I	<input checked="" type="checkbox"/>
DTIC TAB	<input type="checkbox"/>
Unannounced	<input type="checkbox"/>
Justification	
By	
Distribution /	
Availability Codes	
Dist	Avail and/or Special
A-1	

94-13358



DTIC QUALITY INFORMATION



Scientific and Technical Information Division 1987
National Aeronautics and Space Administration
Washington, DC

94 5 03 09 7

This bibliography was prepared by the NASA Scientific and Technical Information Facility operated for the National Aeronautics and Space Administration by RMS Associates.

INTRODUCTION

The technical literature described in this continuing bibliography may be helpful to researchers in numerous disciplines such as agriculture and forestry, geography and cartography, geology and mining, oceanography and fishing, environmental control, and many others. Until recently it was impossible for anyone to examine more than a minute fraction of the Earth's surface continuously. Now vast areas can be observed synoptically, and changes noted in both the Earth's lands and waters, by sensing instrumentation on orbiting spacecraft or on aircraft.

This literature survey lists 368 reports, articles, and other documents announced between July 1 and September 30, 1987 in *Scientific and Technical Aerospace Reports (STAR)*, and *International Aerospace Abstracts (IAA)*.

The coverage includes documents related to the identification and evaluation by means of sensors in spacecraft and aircraft of vegetation, minerals, and other natural resources, and the techniques and potentialities of surveying and keeping up-to-date inventories of such riches. It encompasses studies of such natural phenomena as earthquakes, volcanoes, ocean currents, and magnetic fields; and such cultural phenomena as cities, transportation networks, and irrigation systems. Descriptions of the components and use of remote sensing and geophysical instrumentation, their subsystems, observational procedures, signature and analyses and interpretive techniques for gathering data are also included. All reports generated under NASA's Earth Resources Survey Program for the time period covered in this bibliography are also included. The bibliography does not contain citations to documents dealing mainly with satellites or satellite equipment used in navigation or communication systems, nor with instrumentation not used aboard aerospace vehicles.

The selected items are grouped in nine categories. These are listed in the Table of Contents with notes regarding the scope of each category. These categories were especially chosen for this publication, and differ from those found in *STAR* and *IAA*.

Each entry consists of a standard bibliographic citation accompanied by an abstract. The citations include the original accession numbers from the respective announcement journals.

Under each of the nine categories, the entries are presented in one of two groups that appear in the following order:

- IAA* entries identified by accession number series A87-10,000 in ascending accession number order;

- STAR* entries identified by accession number series N87-10,000 in ascending accession number order.

After the abstract section, there are seven indexes:

- subject, personal author, corporate source, foreign technology, contract number, report/ accession number, and accession number.

TABLE OF CONTENTS

	Page
Category 01 Agriculture and Forestry	1
Includes crop forecasts, crop signature analysis, soil identification, disease detection, harvest estimates, range resources, timber inventory, forest fire detection, and wildlife migration patterns.	
Category 02 Environmental Changes and Cultural Resources	12
Includes land use analysis, urban and metropolitan studies, environmental impact, air and water pollution, geographic information systems, and geographic analysis.	
Category 03 Geodesy and Cartography	14
Includes mapping and topography.	
Category 04 Geology and Mineral Resources	17
Includes mineral deposits, petroleum deposits, spectral properties of rocks, geological exploration, and lithology.	
Category 05 Oceanography and Marine Resources	19
Includes sea-surface temperature, ocean bottom surveying imagery, drift rates, sea ice and icebergs, sea state, fish location.	
Category 06 Hydrology and Water Management	34
Includes snow cover and water runoff in rivers and glaciers, saline intrusion, drainage analysis, geomorphology of river basins, land uses, and estuarine studies.	
Category 07 Data Processing and Distribution Systems	36
Includes film processing, computer technology, satellite and aircraft hardware, and imagery.	
Category 08 Instrumentation and Sensors	43
Includes data acquisition and camera systems and remote sensors.	
Category 09 General	56
Includes economic analysis.	
Subject Index	A-1
Personal Author Index	B-1
Corporate Source Index	C-1
Foreign Technology Index	D-1
Contract Number Index	E-1
Report Number Index	F-1
Accession Number Index	G-1

TYPICAL REPORT CITATION AND ABSTRACT

NASA SPONSORED
 ↓
ON MICROFICHE

ACCESSION NUMBER → **N87-13900*** # Pennsylvania State Univ., University Park. Dept. of Meteorology. ← **CORPORATE SOURCE**

TITLE → **ANALYSIS OF THE INFLOW AND AIR-SEA INTERACTIONS IN HURRICANE FREDERIC (1979) Final Report**

AUTHORS → J. KAPLAN and W. M. FRANK Dec. 1986 119 p

CONTRACT NUMBER → (Contract NAG5-398) ← **PUBLICATION DATE**

REPORT NUMBERS → (NASA-CR-180014; NAS 1.26:180014) Avail: NTIS HC A06/MF A01 CSCL 55C ← **AVAILABILITY SOURCE**

COSATI CODE →

An unusually large amount of aircraft, rawinsonde, satellite, ship and buoy data from hurricane Frederic (1979) are composited over a 40 hr period. These are combined with Frank's (1984) analysis of Frederic's core and Powell's (1982) surface wind analysis to analyze Frederic's three dimensional low level structure between the storm center and a radius of 10 deg. latitude. The analysis is improved significantly by determining the levels at which low level cloud motion winds (CMW's) are in the best agreement with verification wind data and then adjusting the winds to uniform analysis levels. Due to the unusually good low level wind resolution afforded by this data set, it is possible to obtain kinematically derived fields of vorticity, divergence and vertical velocity. These analyses are observed to be internally consistent and should prove useful for future analysis. Analysis of Frederic's surface to 560 m angular momentum budget beyond 2 deg. radius indicates that surface drag coefficients increase slightly with increasing radius and decreasing wind speed. Estimates of storm rainfall obtained by performing a moisture budget between the surface and the top of the inflow layer show that most storm rainfall falls inside about 4 deg. radius and that substantial underestimation of storm rainfall occurs when all low level CMW's are assigned to 560 m. Author

TYPICAL JOURNAL ARTICLE CITATION AND ABSTRACT

NASA SPONSORED
 ↓
ON MICROFICHE

ACCESSION NUMBER → **A87-14176*** # National Aeronautics and Space Administration. Langley Research Center, Hampton, Va.

TITLE → **VARIABILITY OF EARTH-EMITTED RADIATION FROM ONE YEAR OF NIMBUS-6 ERB DATA**

AUTHOR → T. D. BESS (NASA, Langley Research Center, Hampton, VA) ← **AUTHOR'S AFFILIATION**

JOURNAL TITLE → Journal of the Atmospheric Sciences (ISSN 0022-4928), vol. 43, July 15, 1986, p. 1445-1453. refs

Outgoing longwave radiation (OLR) measurements from the Nimbus-6 ERB wide field-of-view instrument are used to study daytime and nighttime radiation variability on a 15 deg regional, zonal, and global scale. An analysis of components of variance is used to determine how much of the total variability is due to between-region and within-region variance. Most of the analysis is on July and January data from one year of Nimbus-6 ERB. Different geographical scales are considered: regions within latitude zones and latitude zones within hemispheres. Results show that much of the variability is spatial, peaks in the tropics and subtropics, and is concentrated in the Northern Hemisphere. Daytime variability is generally larger than nighttime variability for July but not for January. Variance in OLR in the tropics and subtropics is largely a function of cloud variability. Author

EARTH RESOURCES

A Continuing Bibliography (Issue 55)

NOVEMBER 1987

01

AGRICULTURE AND FORESTRY

Includes crop forecasts, crop signature analysis, soil identification, disease detection, harvest estimates, range resources, timber inventory, forest fire detection, and wildlife migration patterns.

A87-31411*# National Aeronautics and Space Administration. National Space Technology Labs., Bay Saint Louis, Miss.

MULTIPOLARIZATION SAR DATA FOR SURFACE FEATURE DELINEATION AND FOREST VEGETATION CHARACTERIZATION

SHIH-TSENG WU and STEVEN A. SADER (NASA, National Space Technology Laboratories, Bay Saint Louis, MS) *IEEE Transactions on Geoscience and Remote Sensing* (ISSN 0196-2892), vol. GE-25, Jan. 1987, p. 67-76. refs

This paper presents the utility of multipolarization Synthetic Aperture Radar (SAR) data for surface feature delineation and forest vegetation characterization. Three channels of radioed data (VV/HH, VH/HH, and VH/VV) are generated from the HH, VV, and VH polarization data (V = vertical, H = horizontal). The radioed data are linearly stretched to yield a digital number within a range of 0 to 255. The techniques for reducing SAR speckle noise and for measuring the degree of separation are discussed. For surface feature delineation, the results indicate that cross polarization as well as cross polarization radioed data better delineate those surface features that are difficult to separate by like polarization data. The results suggest using a median value filtering technique to reduce within-plot data fluctuation to increase the separability measure. For forest vegetation characterization, the results indicate that multipolarization SAR data may be used to estimate forest properties such as total-tree biomass, basal area, and tree height.

Author

A87-31413* Michigan Univ., Ann Arbor.

RELATING POLARIZATION PHASE DIFFERENCE OF SAR SIGNALS TO SCENE PROPERTIES

FAWWAZ T. ULABY, MYRON C. DOBSON, KYLE C. MCDONALD, THOMAS B. A. SENIOR (Michigan, University, Ann Arbor), and DANIEL HELD (California Institute of Technology, Jet Propulsion Laboratory, Pasadena) *IEEE Transactions on Geoscience and Remote Sensing* (ISSN 0196-2892), vol. GE-25, Jan. 1987, p. 83-92.

This paper examines the statistical behavior of the phase difference Delta-phi between the HH-polarized and VV-polarized backscattered signals recorded by an L-band SAR over an agricultural test site in Illinois. Polarization-phase difference distributions were generated for about 200 agricultural fields for which ground information had been acquired in conjunction with the SAR mission. For the overwhelming majority of cases, the Delta-phi distribution is symmetric and has a single major lobe centered at the mean value of the distribution Delta-phi. Whereas the mean Delta-phi was found to be close to zero degrees for bare soil, cut vegetation, alfalfa, soybeans, and clover, a different pattern was observed for the corn fields; the mean Delta-phi increased with increasing incidence angle Theta = 35 deg. The explanation proposed for this variation is that the corn canopy,

most of whose mass is contained in its vertical stalks, acts like a uniaxial crystal characterized by different velocities of propagation for waves with horizontal and vertical polarization. Thus, it is hypothesized that the observed backscatter is contributed by a combination of propagation delay, forward scatter by the soil surface, and specular bistatic reflection by the stalks. Model calculations based on this assumption were found to be in general agreement with the phase observations.

Author

A87-31414*# National Aeronautics and Space Administration. Goddard Space Flight Center, Greenbelt, Md.

SIGNATURE-EXTENDABLE TECHNOLOGY - GLOBAL SPACE-BASED CROP RECOGNITION

FORREST G. HALL (NASA, Goddard Space Flight Center, Greenbelt, MD) and GAUTAM D. BADHWAR (NASA, Johnson Space Center, Houston, TX) *IEEE Transactions on Geoscience and Remote Sensing* (ISSN 0196-2892), vol. GE-25, Jan. 1987, p. 93-103. refs

The use of signature-extendable technology to improve the efficiency of machine processing of remotely sensed data is examined. Temporal profile technology is employed to automatically recognize crops; the technique uses the Kauth and Thomas (1976) transform of Landsat, multidata, and parameters derived from a model of each crop's greenness-time trajectory. The basic characteristics of temporal profile technology and the U.S. based labeling algorithm are described. Consideration is given to signature extension, signature-extendable spaces, and signature-extendable features. The greenness and brightness parameters used in temporal profile technology are derived. The signature extendability of the parameters is evaluated by applying them to the analysis of corn and soybean crops in the U.S. and Argentina. It is noted that the technique is an affordable and efficient method for deriving data on crops on a global basis.

I.F.

A87-32007

WORKSHOP ON SPACE REMOTE SENSING FOR AGRICULTURAL AND THEMATIC MAPPING, BUDAPEST, HUNGARY, APR. 18, 1986, PROCEEDINGS

Workshop sponsored by ESA. Frascati, Italy, Earthnet Programme Office, 1986. 122 p. For individual items see A87-32008 to A87-32010.

Papers are presented on the Earthnet program; remote sensing research in global agricultural productivity; and remote sensing application projects in the United Kingdom. Topics discussed include research activities in agriculture at the Joint Research Centre; remote sensing research and development results from agricultural applications in Hungary; remote sensing and crop production forecasting in Italy; and the use of remote sensing methods for yield forecasting. Consideration is given to remote sensing applications in Poland; the application of remote sensing to agricultural meteorology at the Meteorological Service in Hungary; and mapping crops and their probable water stress using satellite images for better irrigation management.

I.F.

01 AGRICULTURE AND FORESTRY

A87-32008#

REMOTE SENSING RESEARCH IN GLOBAL AGRICULTURAL PRODUCTIVITY

M. F. BAUMGARDNER and C. S. T. DAUGHTRY (Purdue University, West Lafayette, IN) IN: Workshop on Space Remote Sensing for Agricultural and Thematic Mapping, Budapest, Hungary, Apr. 18, 1986, Proceedings . Frascati, Italy, Earthnet Programme Office, 1986, p. 21-31. refs

Problems related to global agricultural productivity are discussed. The uses of remote sensing technology for resource management, in particular for assessing agricultural productivity and land resources, soil classification and mapping, and crop production estimation, are described. Consideration is given to population dynamics and the changing quantity and quality of land resources available for agricultural production. I.F.

A87-32009#

REMOTE SENSING METHODS OF YIELD FORECASTING

D. HAMAR, CS. FERENCZ, J. LICHTENBERGER, GY. TARCSAI (Eotvos Lorand Tudomanyegyetem, Budapest, Hungary), and FERENCZ ARKOS (Budapesti Muszaki Egyetem, Budapest, Hungary) IN: Workshop on Space Remote Sensing for Agricultural and Thematic Mapping, Budapest, Hungary, Apr. 18, 1986, Proceedings . Frascati, Italy, Earthnet Programme Office, 1986, p. 62-78. refs

A brief summary of yield forecasting methods, which are based on remotely sensed (spectral) data, is given. Emphasis is placed on the functional relationship between the different spectral data (or the agronomical variables derived from them) and the estimated yield. Author

A87-32010#

THE APPLICATION OF REMOTE SENSING IN AGRICULTURAL METEOROLOGY AT THE METEOROLOGICAL SERVICE OF THE HPR

P. BOZO, V. VADASZ, L. KETSKEMETI, M. PUTSAY, S. LESZTAK (Országos Meteorológiai Szolgálat, Budapest, Hungary) et al. IN: Workshop on Space Remote Sensing for Agricultural and Thematic Mapping, Budapest, Hungary, Apr. 18, 1986, Proceedings . Frascati, Italy, Earthnet Programme Office, 1986, p. 87-103. Research supported by the Committee for Technological Development, Hungarian Water Management Authority, Magyar Tudományos Akadémia, and Meteorological Service. refs

The use of remote sensing for agricultural meteorology in Hungary is discussed. The interpretation of thermal digital satellite images is examined; methods for geographical rectification and the elimination of atmospheric distortion are proposed. The application of remote sensing to agrometeorological yield estimation is considered. The relationship between plant parameters and remotely sensed data is investigated. Satellite image correction procedures, and the clustering and classification of images are described. I.F.

A87-32090

INFLUENCE OF DIFFERENT NITROGEN AND IRRIGATION TREATMENTS ON THE SPECTRAL REFLECTANCE OF BARLEY

JOHAN KLEMAN and ERIK FAGERLUND (Stockholm, Universitet, Sweden) Remote Sensing of Environment (ISSN 0034-4257), vol. 21, Feb. 1987, p. 1-14. Research supported by the Swedish Board for Space Activities and Naturvetenskapliga Forskningsradet. refs

The information contained in the 0.4-2.4 micron range of a spectroradiometer was evaluated with the aim of finding information parameters different from the IR/red ratio and the related parameters. Reflectance measurements, performed in a nadir looking direction from a mobile platform 15 m above ground, were carried out for twelve plots of barley treated at two irrigation and three fertilization levels; and the reflectance factors of single spectral bands, reflectance factor ratios, and color coordinates were analyzed in relation to the grain yield and the biomass and water content of the crop. The blue color coordinate Z was the only spectral parameter with potential for discriminating between

the irrigation treatments. The average IR/red ratio during the middle of the season was strongly coupled to the grain yield two months later, but when senescence had started, the $R(0.80)/R(1.65)$ ratio offered a greater potential for grain yield prediction. The reflectance factor $R(2.19)$ decreased with increasing canopy water content up to 800-100 g/sq m, after which an asymptotic reflectance was reached. I.S.

A87-32091

CALIBRATION OF SATELLITE RADIOMETERS AND THE COMPARISON OF VEGETATION INDICES

JOHN C. PRICE (USDA, Remote Sensing Research Laboratory, Beltsville, MD) Remote Sensing of Environment (ISSN 0034-4257), vol. 21, Feb. 1987, p. 15-27. refs

Satellite technology provides a steadily improving capability to monitor surface land use and vegetation. However, the increasing number of satellite sensors has led to a variety of spectral indices which may be used to characterize vegetation. A basis is developed for comparing results from different sensors using instrument calibration coefficients, and the derived radiances are related to reflectances, principal component variables such as greenness, and spectral vegetation indices. Author

A87-32093* New York State Univ., Binghamton.

ESTIMATION OF CANOPY PARAMETERS OF ROW PLANTED VEGETATION CANOPIES USING REFLECTANCE DATA FOR ONLY FOUR VIEW DIRECTIONS

NARENDRA S. GOEL and TOBY GRIER (New York, State University, Binghamton) Remote Sensing of Environment (ISSN 0034-4257), vol. 21, Feb. 1987, p. 37-51. NASA-supported research. refs

A procedure for estimating leaf area index (LAI) and percentage of ground cover (GC) for inhomogeneous row planted vegetation canopies using measurement of canopy reflectance (CR) data for only four directions is presented. This procedure, referred to as 'reconstructive inversion', uses the CR data for these directions to first 'reconstruct' the complete bidirectional surface, which is then used to estimate the canopy parameters using the standard inversion of a CR model technique. The technique has been successfully applied to soybean and corn canopies in various stages of growth. Author

A87-32094

HABITAT MAPPING BY LANDSAT FOR AERIAL CENSUS OF KANGAROOS

GREG J. E. HILL (Queensland, University, Brisbane, Australia) and GAIL D. KELLY (Department of Mapping and Surveying, Remote Sensing Unit, North Quay, Australia) Remote Sensing of Environment (ISSN 0034-4257), vol. 21, Feb. 1987, p. 53-60. Research supported by the University of Queensland and Department of Mapping and Surveying. refs

Landsat MSS imagery was used to map habitat categories used in connection with aerial census work that estimates population levels of kangaroos. A study area featuring typical habitat patterns was selected in the marginal wheat lands of southern, inland Queensland. A series of unsupervised classifications of the imagery provided accurate estimation of the relative proportions and distribution of these habitats. The data form a useful base for programmes that: monitor the numbers and distribution of kangaroos; and attempt to refine aerial census methodology. Author

A87-32095* National Aeronautics and Space Administration. Goddard Space Flight Center, Greenbelt, Md.

CONTINENTAL LAND COVER ASSESSMENT USING LANDSAT MSS DATA

ROSS NELSON (NASA, Goddard Space Flight Center, Greenbelt, MD), DAVID CASE, NED HORNING (Science and Applications Research, Inc., Riverdale, MD), VIRGIL ANDERSON, and SREE PILLAI (Purdue University, West Lafayette, IN) Remote Sensing of Environment (ISSN 0034-4257), vol. 21, Feb. 1987, p. 61-81. refs

A statistical procedure to assess level-II continental resources using Landsat MSS digital data is presented. The statistical procedure involves a two-stage cluster sample within a stratified random sample. The utility of this procedure is assessed by using it to estimate the areal extent of the conifer and hardwood resources of the continental U.S. National estimates of conifer and hardwood derived using this sampling procedure were within 3 percent of U.S. Forest Service (USFS) figures. According to the Landsat-based study, 11 percent of the country is conifer forest and 12 percent is hardwood. The corresponding USFS figures are 13 and 15 percent, respectively. Comparison of the MSS classification products and airphotos showed that the conifer cover class was correctly identified 74 percent of the time and hardwood 30 percent of the time. The average classification accuracy countrywide for the four cover types considered (conifer, hardwood, water, and 'other') is 74 percent, and the overall accuracy is 85 percent. The statistical procedure provides a method of incorporating Landsat MSS digital data as a second state for level-II continental resource assessment. Alternate data sources, e.g., satellite and aircraft photographic imagery, may also be used in conjunction with this statistical model. Author

A87-32098* National Aeronautics and Space Administration. Lyndon B. Johnson Space Center, Houston, Tex.

LANDSAT CLASSIFICATION OF ARGENTINA SUMMER CROPS

D. D. BADHWAR (NASA, Johnson Space Center, Houston, TX), C. E. GARGANTINI, and F. V. REDONDO (Comision Nacional de Investigaciones Espaciales, Centro de Sensores Remotes, Buenos Aires, Argentina) Remote Sensing of Environment (ISSN 0034-4257), vol. 21, Feb. 1987, p. 111-117. refs

A Landsat MSS and TM classification approach based on three features derived from the greenness profile has proved very effective in separating and identifying corn, soybeans, and other ground cover classes in the U.S. The objective of this study is to investigate the separation of summer crops in Argentina, one of the most important commodity exporters, using the same greenness profile features that have proved effective in the U.S. Corn Belt. The area chosen for study is a more complex cropping practice area located in the north-west corner of Buenos Aires province in Pampa Humeda, where corn, soybean, sorghum, sunflower, and pastures are cultivated. It is shown that the profile features can provide very effective separation, except in the case of corn from sorghum. Separation between corn and soybeans was found to be greater than in the U.S. This study suggests that the automatic, unsupervised classification approach developed in the U.S., with relatively minor modification, can be used for summer crop area estimation in Argentina. Author

A87-32495

GLOBAL VEGETATION MONITORING USING NOAA VEGETATION INDEX DATA

HARUHIISA SHIMODA, KIYONARI FUKUE, TSUKASA HOSOMURA, and TOSHIBUMI SAKATA (Tokai University, Tokyo, Japan) IN: International Symposium on Space Technology and Science, 15th, Tokyo, Japan, May 19-23, 1986, Proceedings. Volume 2. Tokyo, AGNE Publishing, Inc., 1986, p. 1625-1630.

The method for deriving a global vegetation map from the NOAA-AVHRR vegetation index data (VID) is presented, using a one-week data set of AVHRR measurements. Daytime data were sampled and mosaicked by the lowest radiance principle, thus eliminating most cloud cover from the results. Large shading effects caused by the sun-angle deviations were eliminated using a

luminance-of-the-earth-surface equation. The classification was executed using a maximum likelihood method with four channels of VID. Training areas, composed of 67 categories, were selected from the World Vegetation Map of James et al. (1981); after the classification, these 67 categories were unified to 17 general categories, and the classified image was transformed to longitude and latitude coordinates. The results have demonstrated the suitability of the NOAA VID for worldwide vegetation monitoring, although the remaining clouds are still a problem. I.S.

A87-32498

RELATION BETWEEN PRECIPITATION AND BRIGHTNESS OF EARTH SURFACE IN THE NOAA/GVIP DATA

YASUNORI NAKAYAMA and SOTARO TANAKA (Remote Sensing Technology Center of Japan, Tokyo) IN: International Symposium on Space Technology and Science, 15th, Tokyo, Japan, May 19-23, 1986, Proceedings. Volume 2. Tokyo, AGNE Publishing, Inc., 1986, p. 1643-1650.

Brightness of the earth surface seen in the data of NOAA/GVIP is related to the precipitation at the land. This statistical law was found by comparing the GVIP data with the corresponding precipitation data. The correlation coefficients were 0.85 and 0.84 in the case of global data in 1983 and 1984. Also correlation coefficient of 0.89 was obtained in the case of Lake Chad area. Author

A87-32954

REFLECTANCE CHARACTERISTICS AND ITS APPLICATION IN THE CLASSIFICATION OF NIGERIAN SAVANNA SOILS

AYODELE FAGBAMI (Ibadan, University, Nigeria) Geocarto International, no. 4, 1986, p. 39-47. refs

A87-33298* Centre de Recherches en Physique de l'Environnement, Issy-les-Moulineaux (France).

EVALUATION OF A SURFACE/VEGETATION PARAMETERIZATION USING SATELLITE MEASUREMENTS OF SURFACE TEMPERATURE

O. TACONET, T. CARLSON, R. BERNARD, and D. VIDAL-MADJAR (Centre de Recherches en Physique de l'Environnement Terrestre et Planetaire, Issy-les-Moulineaux, France) Journal of Climate and Applied Meteorology (ISSN 0733-3021), vol. 25, Nov. 1986, p. 1752-1767. CNES-CNRS-supported research. refs (Contract NAG5-114)

Ground measurements of surface-sensible heat flux and soil moisture for a wheat-growing area of Beauce in France were compared with the values derived by inverting two boundary layer models with a surface/vegetation formulation using surface temperature measurements made from NOAA-AVHRR. The results indicated that the trends in the surface heat fluxes and soil moisture observed during the 5 days of the field experiment were effectively captured by the inversion method using the remotely measured radiative temperatures and either of the two boundary layer methods, both of which contain nearly identical vegetation parameterizations described by Taconet et al. (1986). The sensitivity of the results to errors in the initial sounding values or measured surface temperature was tested by varying the initial sounding temperature, dewpoint, and wind speed and the measured surface temperature by amounts corresponding to typical measurement error. In general, the vegetation component was more sensitive to error than the bare soil model. I.S.

01 AGRICULTURE AND FORESTRY

A87-33441* Woods Hole Oceanographic Institution, Mass.
DEFORESTATION IN THE TROPICS - NEW MEASUREMENTS IN THE AMAZON BASIN USING LANDSAT AND NOAA ADVANCED VERY HIGH RESOLUTION RADIOMETER IMAGERY

G. M. WOODWELL (Woods Hole Research Center, MA), R. A. HOUGHTON, T. A. STONE (Marine Biological Laboratory, Woods Hole, MA), R. F. NELSON (NASA, Goddard Space Flight Center, Greenbelt, MD), and W. KOVALICK (Science Applications Research, Lanham, MD). *Journal of Geophysical Research* (ISSN 0148-0227), vol. 92, Feb. 20, 1987, p. 2157-2163. Research supported by the Woods Hole Research Center. refs (Contract DE-AC05-84OR-21400)

A87-35119
GLAI ESTIMATION USING MEASUREMENTS OF RED, NEAR INFRARED, AND MIDDLE INFRARED RADIANCE

P. J. CURRAN and H. D. WILLIAMSON (Sheffield, University, England). *Photogrammetric Engineering and Remote Sensing* (ISSN 0099-1112), vol. 53, Feb. 1987, p. 181-186. refs (Contract NERC-GR/3/5096)

The passive remote sensing of green leaf area index (GLAI) has utilized measurements of red (R) and near-infrared (NIR) radiance. Increased availability of mid-infrared (MIR) radiance data (e.g., 1.55 to 1.75 microns, from Landsat TM band 5) and the correlation between MIR radiance and GLAI has encouraged the use of these wavelengths for GLAI estimation. The aim of this paper is twofold: first, to refine the methodology used for such GLAI estimation, and second, to assess the effect of incorporating MIR radiance data into this methodology. Empirical models based upon airborne multispectral scanner measurements of R, NIR, and MIR radiance were inverted, and the GLAI of grassland was estimated to an accuracy of 18 to 58 percent (95 percent confidence level) for five levels of GLAI and \pm or \pm 0.48 to 0.75 GLAI for a point. Refinement of the methodology increased the accuracy to 60 to 85 percent (95 percent confidence level) for five levels of GLAI and \pm or \pm 0.09 to \pm or \pm 0.12 GLAI for a point. The empirical models provided significantly similar estimates of GLAI regardless of the contribution of MIR radiance. It was concluded that measurements of MIR radiance added little extra information to measurements of R and NIR for the purposes of GLAI estimation. Author

A87-35120
IDENTIFYING VEGETABLE CROPS WITH LANDSAT THEMATIC MAPPER DATA

VICKI L. WILLIAMS, WARREN R. PHILIPSON, and WILLIAM D. PHILPOT (Cornell University, Ithaca, NY). *Photogrammetric Engineering and Remote Sensing* (ISSN 0099-1112), vol. 53, Feb. 1987, p. 187-191. refs (Contract USDA-58-319T-3-0Z08X)

Landsat thematic mapper (TM) data were evaluated for inventorying or monitoring New York State vegetables, which are grown commercially in organic (muckland) or mineral (upland) soils, in fields as small as 2 hectares. Two TM scenes of west-central New York, acquired in July and August 1984, were analyzed digitally with spectral characterizations, enhancements, and supervised classifications being referenced to field-measured reflectances and cropping records. Testing showed single-date classification accuracies of at least 90 percent for three muckland vegetables (onions, lettuce, potatoes), and over 75 percent for three of four upland vegetables (cabbage, sweet corn, potatoes, and mature, but not young, snap beans) for TM data acquired late in the growing season. In addition, visual image analysis of the digitally displayed TM data was capable of easily identifying most of the mature crops studied. Overall, either digital or visual image analysis seems capable of producing reliable classifications of vegetable crops. Author

A87-35121* National Aeronautics and Space Administration
National Space Technology Labs., Bay Saint Louis, Miss
FOREST BIOMASS, CANOPY STRUCTURE, AND SPECIES COMPOSITION RELATIONSHIPS WITH MULTIPOLARIZATION L-BAND SYNTHETIC APERTURE RADAR DATA

STEVEN A. SADER (NASA, National Space Technology Laboratories, Bay Saint Louis, MS). *Photogrammetric Engineering and Remote Sensing* (ISSN 0099-1112), vol. 53, Feb. 1987, p. 193-202. NASA-supported research. refs

The effect of forest biomass, canopy structure, and species composition on L-band synthetic aperture radar data at 44 southern Mississippi bottomland hardwood and pine-hardwood forest sites was investigated. Cross-polarization mean digital values for pine forests were significantly correlated with green weight biomass and stand structure. Multiple linear regression with five forest structure variables provided a better integrated measure of canopy roughness and produced highly significant correlation coefficients for hardwood forests using HV/VV ratio only. Differences in biomass levels and canopy structure, including branching patterns and vertical canopy stratification, were important sources of volume scatter affecting multipolarization radar data. Standardized correction techniques and calibration of aircraft data, in addition to development of canopy models, are recommended for future investigations of forest biomass and structure using synthetic aperture radar. Author

A87-35122
A COMPARISON OF OPTICAL BAR, HIGH-ALTITUDE, AND BLACK-AND-WHITE PHOTOGRAPHY IN LAND CLASSIFICATION

CHARLES T. SCOTT, HANS T. SCHREUDER (USDA, Northeastern Forest Experiment Station, Broomall, PA), and DOUGLAS M. GRIFFITH (USDA, Rocky Mountain Forest and Range Experiment Station, Ft. Collins, CO). *Photogrammetric Engineering and Remote Sensing* (ISSN 0099-1112), vol. 53, Feb. 1987, p. 203-206. refs

For large-area forest surveys, 1981-84 color infrared national high-altitude program (NHAP) and 1983 optical bar color (OBC) infrared photography resulted in equally precise estimates of land-use/land-cover area. Both were only slightly more precise than 1970 black-and-white photography. OBC was the least cost effective because optical bar imagery is usually flown specifically for a survey, whereas NHAP and older black-and-white photography are readily available. Optical bar photography can be used effectively up to 35 degrees from nadir. Author

A87-35307
THE TOPOGRAPHIC EFFECT ON LANDSAT DATA IN GENTLY UNDULATING TERRAIN IN SOUTHERN SWEDEN

KARIN HALL-KONYVES (Lund, Universitet, Sweden). *International Journal of Remote Sensing* (ISSN 0143-1161), vol. 8, Feb. 1987, p. 157-168. Research sponsored by the Swedish Board for Space Activities. refs

The purpose of this study was to investigate the effect of topography on Landsat satellite data in gently undulating terrain. Gently undulating terrain is in this work defined as terrain dominated by slopes of between 1 and 15 deg. For three various solar elevations (38, 44 and 52 deg) digital Landsat MSS and TM data were merged with digital elevation data. In an agricultural region in southern Sweden 135 cultivated fields, 50 pasture sites and 117 forest sites with a total number of 88,800 pixels were studied. The relationship between Landsat response variation and topographic parameters within cultivated fields and forest areas was weak. For some pasture covers a topographic effect was identified. Author

A87-35309* National Aeronautics and Space Administration. Goddard Space Flight Center, Greenbelt, Md.

QUANTIFYING SPATIAL AND TEMPORAL VARIABILITIES OF MICROWAVE BRIGHTNESS TEMPERATURE OVER THE U.S. SOUTHERN GREAT PLAINS

J. CHOUDHURY, M. OWE, J. P. ORMSBY, A. T. C. CHANG, R. WANG (NASA, Goddard Space Flight Center, Greenbelt, MD), S. N. GOWARD (Maryland, University, College Park), and R. GOLUS (Science Applications Research, Lanham, MD). *International Journal of Remote Sensing* (ISSN 0143-1161), vol. 8, Feb. 1987, p. 177-191. refs

Spatial and temporal variabilities of microwave brightness temperature over the U.S. Southern Great Plains are quantified in terms of vegetation and soil wetness. The brightness temperatures (TB) are the daytime observations from April to October for five years (1979 to 1983) obtained by the Nimbus-7 Scanning Multichannel Microwave Radiometer at 6.6 GHz frequency, horizontal polarization. The spatial and temporal variabilities of vegetation are assessed using visible and near-infrared observations by the NOAA-7 Advanced Very High Resolution Radiometer (AVHRR), while an Antecedent Precipitation Index (API) model is used for soil wetness. The API model was able to account for more than 50 percent of the observed variability in TB, although near correlations between TB and API were generally significant at the 1 percent level. The slope of the linear regression between TB and API is found to correlate linearly with an index for vegetation density derived from AVHRR data. Author

A87-35520* Department of Agriculture, Beltsville, Md.

SALINITY EFFECTS ON THE MICROWAVE EMISSION OF SOILS

THOMAS J. JACKSON (USDA, Hydrology Laboratory, Beltsville, MD) and PEGGY E. ONEILL (NASA, Goddard Space Flight Center, Greenbelt, MD). *IEEE Transactions on Geoscience and Remote Sensing* (ISSN 0196-2892), vol. GE-25, March 1987, p. 214-220. Previously announced in STAR as N87-17302. refs

Controlled plot experiments were conducted to collect L and C band passive microwave data concurrent with ground observations of salinity and soil moisture. Two dielectric mixing models were used with an emission model to predict the emissivity from a bare smooth uniform profile. The models produce nearly identical results when near zero salinity is involved and reproduce the observed data at L band extremely well. Discrepancies at C band are attributed to sampling depth problems. Comparisons of predicted emissivities at various salinities with observed values indicate that the dynamic range of the emissivities can be explained using either of the dielectric mixing models. Evaluation of the entire data set, which included four salinity levels, indicates that for general application the effects of soil salinity can be ignored in interpreting microwave data for estimating soil moisture under most agricultural conditions. ESA

A87-35521

A SOIL THERMAL MODEL FOR REMOTE SENSING

DIEM HO (IBM France, S.A., Paris). *IEEE Transactions on Geoscience and Remote Sensing* (ISSN 0196-2892), vol. GE-25, March 1987, p. 221-229. Research supported by IBM France, S.A., CNES, and CNRS. refs

A simulation model of heat exchange at the soil surface is used to study the effects of the soil characteristics, the initial temperature profile, and the boundary conditions on the surface temperatures. The surface temperature cycle is found to be insensitive to both the initial temperature profile and the lower boundary conditions. The result makes it possible to treat the soil with an analytic steady-state model as a transmission line problem. Its formulation allows the calculation of the soil conducting flux directly from satellite temperature data, without the knowledge of the energy exchange process at the ground surface, provided that the soil thermal inertia is known. A simple inverse model can then be formulated to calculate accurately the soil thermal inertia and soil fluxes using visible and infrared satellite data. The model requires neither the linearization of the flux terms at the ground surface nor the knowledge of the lower boundary condition and the soil initial temperature profile. Author

A87-36109

STATISTICAL EVALUATION OF FOREST CHARACTERISTICS FROM AERIAL AND SPACE PHOTOGRAPHS [STATISTICHESKOE OTSENVANIE KHA RAKTERISTIK LESNYKH OB'EKTOV PO AERO- I KOSMICHESKIM SNIMKAM]

R. I. ELMAN, L. A. KUZENKOV, and N. A. APARINOVA (Vsesoiuznoe Aerofototesoustroitel'noe Ob'edinenie Lesproekt, Moscow, USSR). *Issledovanie Zemli iz Kosmosa* (ISSN 0205-9614), Nov.-Dec. 1986, p. 105-112. In Russian. refs

A method of computer-aided statistical evaluation of forest taxation indices (the forest age, height, diameter, density, and growing stock) from aerial and space photographs is discussed. Procedures for estimating the statistical significance and the efficiency of the results obtained are described along with the verification methods. Using this methodology, estimates of the information content of landscape signatures are obtained from aerial and space photographs, together with the principal taxation indices of the forests in these photographs. I.S.

A87-35310

REMOTE OBSERVATIONS ON CROP PROFILE MODELLING

A. CAMPBELL, E. S. DE BOER (CSIRO, Div. of Mathematics and Statistics, Wembley, Australia), and P. T. HICK (CSIRO, Div. of Groundwater Research, Wembley, Australia). *International Journal of Remote Sensing* (ISSN 0143-1161), vol. 8, Feb. 1987, p. 193-201. Research supported by the Cooperative Bulk Handling. refs

Landsat data are typically available for a number of overpasses during a growing season. There is currently considerable interest in modeling the so-called crop profile for such multitemporal data by a nonlinear profile function of some (spectral) index for the spectral bands. The derived coefficients are used in a subsequent location procedure. This paper outlines some results obtained from an evaluation of the approach for crop data from the wheatbelt of Western Australia. Specifically, the degree of separation of crop classes from pasture classes, as measured by the discriminant index, is compared for analyses based on the original bands, on various spectral indices and on fitted coefficients from a crop profile function describing the temporal change in these indices. For the data considered, a marked loss of discrimination is found in analyses based on various spectral indices, when compared with those based directly on the corresponding discriminant functions (where the linear combination is not constrained to be the same for each time). Analysis of the coefficients for the nonlinear profile functions fitted to the indices results in further loss of separation. Author

A87-35312

COMPARISON OF SUPERVISED MAXIMUM LIKELIHOOD AND DECISION TREE CLASSIFICATION FOR CROP COVER ESTIMATION FROM MULTITEMPORAL LANDSAT MSS DATA

S. BELWARD (Cranfield Institute of Technology, Silsoe, England) and A. DE HOYOS (Oxford University, England). *International Journal of Remote Sensing* (ISSN 0143-1161), vol. 8, Feb. 1987, p. 229-235. Research supported by the Fundacao de Amparo a Pesquisa do Estado de Sao Paulo and British Council. refs

A87-36579

AERIAL AND SPACE INVESTIGATIONS OF SOILS AND VEGETATION (AEROKOSMICHESKIE ISSLEDOVANIYA POCHV I RASTITEL'NOSTI)

KIRILL IAKOVLEVICH KONDRATEV, VLADIMIR VASILEVICH KOZODEROV, and PETR PETROVICH FEDCHENKO Leningrad, Gidrometeoizdat, 1986, 232 p. In Russian. refs

Results of theoretical and experimental studies on the identification and evaluation of soils and vegetation covers using ground, airborne, and spaceborne measurements are presented. The principles underlying the evaluation studies of ground cover from the spectral reflectances are discussed, and several empirical methods of soil and plant identification and classification are examined. Equations relating the remote sensing data with the humus content of the soil, the chlorophyll content of plant leaves, weed populations, and the percentage of ruined plants in a winter crop field are presented. I.S.

A87-36946

RECONNAISSANCE OF VEGETAL FORMATIONS IN A GUINEAN FOREST SECTOR BY MEANS OF LANDSAT IMAGES [RECONNAISSANCE DES FORMATIONS VEGETALES DU SECTEUR FORESTIER GUINEEN A PARTIR DES IMAGES LANDSAT]

MYRIAM ARMAND (Ministere de l'Education Nationale, Bureau des Innovations Pedagogiques et des Technologies Nouvelles, Paris, France) Societe Francaise de Photogrammetrie et de Teledetection, Bulletin (ISSN 0244-6014), no. 103, 1986, p. 33-49. In French. refs

A 1974 Landsat image of a region of the Ivory Coast was digitally processed and the results were compared with available ground truth and airborne photography data. The area is of particular interest because of the drought conditions which have been prevalent in that region of Africa for more than a year, and the concomitant need to monitor the encroachment of desert and human population on arable and forested lands. The 1:200,000 scale Landsat image was used to establish 10 different classes of vegetation in an area which included the interface between a savannah and a forest. Sample tricolor images are provided, along with radiometric histograms from the Landsat channels that were used to develop the different classification indices. M.S.K.

A87-37054

AN APPLICATION OF LOW ALTITUDE MULTISPECTRAL PHOTOGRAPHY TO AGRICULTURAL FIELD TRIALS

JAN G. P.W. CLEVERS (Landbouwhogeschool, Wageningen, Netherlands) and CHARLES HORTON (Polytechnic of Central London, London, England) ITC Journal (ISSN 0303-2434), no. 2, 1986, p. 131-139. refs

In agronomy, field trials are conducted to evaluate the influence of different crop treatments on, for example, leaf area index (LAI) and biomass. In the quantitative analysis, inaccuracies can be large because of small sample sizes; these are inevitable when frequent and destructive sampling must be used. In support of such field trials, an airborne multispectral photographic (MSP) system was designed and used as a low altitude data recording system. The results show the relative dispersion of data acquired by this method to be much smaller compared with agronomic data (e.g., LAI). Treatment effects are therefore more readily detected by MSP than by conventional field sampling methods. Infrared reflectance factors have potential use as an estimator of LAI. Consistency is demonstrated by using a method of calibration and data correction to derive canopy spectral reflectance factors. Low altitude multispectral photography can be used as an inexpensive nondestructive tool for routine spectral measurements in field trials, yielding more precise information about vegetation characteristics than conventional field sampling methods. Author

A87-37278* Maryland Univ., College Park.

CANOPY REFLECTANCE, PHOTOSYNTHESIS, AND TRANSPIRATION. II - THE ROLE OF BIOPHYSICS IN THE LINEARITY OF THEIR INTERDEPENDENCE

P. J. SELLERS (Maryland, University, College Park) Remote Sensing of Environment (ISSN 0034-4257), vol. 21, March 1987, p. 143-183. refs
(Contract NAG5-492)

The ability of satellite sensor systems to estimate area-averaged canopy photosynthetic and transpirative properties is evaluated. The near linear relationship between the simple ratio (SR) and normalized difference (ND) and the surface biophysical properties of canopy photosynthetically active radiation (PAR) absorption, photosynthesis, and bulk stomatal resistance is studied. The models utilized to illustrate the processes of canopy reflectance, photosynthesis, and resistance are described. The dependence of SR, the absorbed fraction of PAR, and canopy photosynthesis and resistance on total leaf area index is analyzed. It is noted that the SR and ND vegetation indices and vegetation-dependent qualities are near-linearly related due to the proportion of leaf scattering coefficient in visible and near IR wavelength regions. The data reveal that satellite sensor systems are useful for the estimation of photosynthesis and transpirative properties. I.F.

A87-37279* Science Applications Research, Lanham, Md.

COMPUTATION OF DIFFUSE SKY IRRADIANCE FROM MULTIDIRECTIONAL RADIANCE MEASUREMENTS

SURAIYA P. AHMAD (Science Applications Research, Lanham, MD), ELIZABETH M. MIDDLETON, and DONALD W. DEERING (NASA, Goddard Space Flight Center, Greenbelt, MD) Remote Sensing of Environment (ISSN 0034-4257), vol. 21, March 1987, p. 185-200. refs
(Contract NAS5-28200)

Accurate determination of the diffuse solar spectral irradiance directly above the land surface is important in characterizing the reflectance properties of these surfaces, especially vegetation canopies. This determination is also needed to infer the net radiation budget of the earth-atmosphere system above these surfaces. An algorithm is developed here for the computation of hemispheric diffuse irradiance using the measurements from an instrument called PARABOLA, which rapidly measures upwelling and downwelling radiances in three selected wavelength bands. The validity of the algorithm is established from simulations. The standard reference data set of diffuse radiances of Dave (1978), obtained by solving the radiative transfer equation numerically for realistic atmospheric models, is used to simulate PARABOLA radiances. Hemispheric diffuse irradiance is estimated from a subset of simulated radiances by using the algorithm described. The algorithm is validated by comparing the estimated diffuse irradiance with the true diffuse irradiance of the standard data set. The validations include sensitivity studies for two wavelength bands (visible, 0.65-0.67 micron; near infrared, 0.81-0.84 micron), different atmospheric conditions, solar elevations, and surface reflectances. In most cases the hemispheric diffuse irradiance computed from simulated PARABOLA radiances and the true irradiance obtained from radiative transfer calculations agree within 1-2 percent. This technique can be applied to other sampling instruments designed to estimate hemispheric diffuse sky irradiance. Author

A87-37281* National Aeronautics and Space Administration. Goddard Space Flight Center, Greenbelt, Md.

INFERRING SPECTRAL REFLECTANCES OF PLANT ELEMENTS BY SIMPLE INVERSION OF BIDIRECTIONAL REFLECTANCE MEASUREMENTS

J. OTTERMAN (NASA, Goddard Space Flight Center, Greenbelt, MD; Tel Aviv University, Israel), D. E. STREBEL (Science Applications Research, Lanham, MD), and K. J. RANSON (NASA, Goddard Space Flight Center, Greenbelt, MD) Remote Sensing of Environment (ISSN 0034-4257), vol. 21, March 1987, p. 215-228. refs

(Contract NAS5-28200; NAS9-16528)

Inverting previously developed explicit expressions for a vertical architecture, bidirectional reflectances measured over corn viewing from the solar quadrant at azimuths near the principal plane are used to determine the spectral reflectances of plant elements. The leaf reflectance values extracted in three visible bands at viewing zenith angles of 70 deg, 60 deg, and 45 deg agree closely with laboratory-measured reflectances of corn leaves. At viewing zenith angle of 30 deg, the inversion breaks down, inasmuch as the inferred plant element reflectances are too high. Satisfactory results are also achieved when the same approach is applied to bidirectional reflectances measured over potted balsam firs, but when applied to soybeans reflectances, the procedure yields unreasonably high leaf reflectances. The failure in this case is attributed to the nonvertical architecture of the soybean canopy; however, for this canopy, inversion based on horizontal architecture is possible. The bidirectional reflectances measured from the solar quadrant, at viewing angles appreciably far from 'hot spot' viewing, approximately equal in magnitude half of the leaf reflectance. The 0.5 ratio is predicted by a previous analysis of opaque horizontal Lambertian facets, as the asymptotic value for a dense canopy at any viewing angle. For soybeans, this ratio applies very closely at 15 deg viewing zenith angle. The results suggest that inversion based on simple architecture, applying explicit expressions, might be of value, either in itself or as a preliminary step before inversion applying complex models. Author

A87-37282

LANDSAT AS AN AID IN EVALUATING THE ADEQUACY OF A GRAIN SILO NETWORK

L. A. SANDHAM (University of the North, Sovenga, Republic of South Africa) and P. A. J. VAN RENSBURG (Rand Afrikaans University, Johannesburg, Republic of South Africa) Remote Sensing of Environment (ISSN 0034-4257), vol. 21, March 1987, p. 229-241. Research supported by the Council for Scientific and Industrial Research, and Oostelike Transvaalse Koöperatie. refs

First, Landsat MSS data were used to determine the area of cultivated cropland in a portion of the Eastern Highveld of the Transvaal, South Africa. A supervised Bayes maximum likelihood classification algorithm was applied resulting in classification accuracy above 75 percent for the study area. Second, the area of cropland thus obtained was combined with a spatially contoured surface of potential yield (per hectare) to determine the size of the potential crop of each silo service area. Third, the potential crop size was used to evaluate the adequacy of the existing silo capacity, thus serving as a possible input for planning extensions to the silo network. Author

A87-37827* Army Medical Research Inst. of Infectious Diseases, Fort Detrick, Md.

DETECTION OF RIFT VALLEY FEVER VIRAL ACTIVITY IN KENYA BY SATELLITE REMOTE SENSING IMAGERY

KENNETH J. LINTHICUM, CHARLES L. BAILEY (U.S. Army, Medical Research Institute of Infectious Diseases, Frederick, MD), F. GLYN DAVIES (Veterinary Research Laboratory, Kabete, Kenya), and COMPTON J. TUCKER (NASA, Goddard Space Flight Center, Greenbelt, MD) Science (ISSN 0036-8075), vol. 235, March 27, 1987, p. 1656-1659. NASA-supported research. refs

Data from the advanced very high resolution radiometer on board the National Oceanic and Atmospheric Administration's polar-orbiting meteorological satellites have been used to infer ecological parameters associated with Rift Valley fever (RVF) viral

activity in Kenya. An indicator of potential viral activity was produced from satellite data for two different ecological regions in Kenya, where RVF is enzootic. The correlation between the satellite-derived green vegetation index and the ecological parameters associated with RVF virus suggested that satellite data may become a forecasting tool for RVF in Kenya and, perhaps, in other areas of sub-Saharan Africa. Author

A87-38094* Department of Agriculture, Beltsville, Md.

TEMPORAL OBSERVATIONS OF SURFACE SOIL MOISTURE USING A PASSIVE MICROWAVE SENSOR

T. J. JACKSON (USDA, Agricultural Systems Research Institute, Beltsville, MD) and P. O'NEILL (NASA, Goddard Space Flight Center, Greenbelt, MD) Remote Sensing of Environment (ISSN 0034-4257), vol. 21, April 1987, p. 281-296. refs

A series of 10 aircraft flights was conducted over agricultural fields to evaluate relationships between observed surface soil moisture and soil moisture predicted using passive microwave sensor observations. An a priori approach was used to predict values of surface soil moisture for three types of fields: tilled corn, no-till corn with soybean stubble, and idle fields with corn stubble. Acceptable predictions were obtained for the tilled corn fields, while poor results were obtained for the others. The source of error is suspected to be the density and orientation of the surface stubble layer; however, further research is needed to verify this explanation. Temporal comparisons between observed, microwave predicted, and soil water-simulated moisture values showed similar patterns for tilled well-drained fields. Divergences between the observed and simulated measurements were apparent on poorly drained fields. This result may be of value in locating and mapping hydrologic contributing areas. Author

A87-38095

NADIR LOOKING AIRBORNE RADAR AND POSSIBLE APPLICATIONS TO FORESTRY

R. BERNARD, M. E. FREZAL, D. VIDAL-MADJAR (Centre de Recherches en Physique de l'Environnement Terrestre et Planetaire, Issy-les-Moulineaux, F), D. GUYON, and J. RIOM (Institut National de la Recherche Agronomique, Cestas, France) Remote Sensing of Environment (ISSN 0034-4257), vol. 21, April 1987, p. 297-309. refs

It is shown that investigators can use an airborne radar with high range resolution to measure the height and planting density of trees in forests. Based on C-band, nadir looking airborne radar data from a site in Southwest France, a single-scattering model is developed and verified to aid in the interpretation of such data. Author

A87-38097* Purdue Univ., West Lafayette, Ind.

VARIATIONS IN THE POLARIZED LEAF REFLECTANCE OF SORGHUM BICOLOR

LOIS GRANT, C. S. T. DAUGHTRY (Purdue University, West Lafayette, IN), and V. C. VANDERBILT (NASA, Ames Research Center, Moffett Field, CA; Purdue University, West Lafayette, IN) Remote Sensing of Environment (ISSN 0034-4257), vol. 21, April 1987, p. 333-339. refs

(Contract NAG5-269)

The polarized reflectance factor, R_q , of sorghum (*Sorghum bicolor*, L.) leaves from field-grown plants was measured in situ in the summers of 1983 and 1984. In 1983, three leaves of two randomly selected plants were measured at 2-week intervals. The value of R_q varied, depending on leaf and day of measurement. Measured values of R_q for the adaxial leaf surface ranged from 16 to 53; for the abaxial leaf surface the values ranged from 28 to 69. In 1984, measurements consisted of repeated observations made on the same leaf at biweekly intervals. The values of R_q from the adaxial leaf surface ranged from 26 to 38. Values of R_q from the abaxial leaf surface increased throughout the season, from 16 to 45. Differences in R_q were attributed to changes in surface details of the leaf. Author

A87-39185

REMOTE SENSING OF VEGETATION CHANGE NEAR INCO'S SUDBURY MINING COMPLEXES

J. A. E. ALLUM (Inco, Ltd., Exploration Dept., Mississauga, Canada) and B. R. DREISINGER (Inco, Ltd., Safety and Environmental Control, Copper Cliff, Canada) *International Journal of Remote Sensing* (ISSN 0143-1161), vol. 8, March 1987, p. 399-416.

Using Landsat data for different years between 1973 and 1983, vegetation change maps were produced for two areas in the vicinity of Inco's mining complexes. Field checking showed that for more than 80 percent of the sites inspected, causes for the vegetation changes recorded on the maps could be determined. The system used provides a cost-effective method of monitoring major vegetation changes over a number of years, but it is not suitable for monitoring slow, progressive, vegetation changes over short periods. Author

A87-39187* Canada Centre for Remote Sensing, Ottawa (Ontario).

PROCEDURES FOR THE DESCRIPTION OF AGRICULTURAL CROPS AND SOILS IN OPTICAL AND MICROWAVE REMOTE SENSING STUDIES

J. CIHLAR (Canada Centre for Remote Sensing, Ottawa, Canada), M. C. DOBSON (Michigan, University, Ann Arbor), T. SCHMUGGE (NASA, Goddard Space Flight Center, Greenbelt, MD), P. HOOGEBOOM (Nederlandsche Centrale Organisatie voor Toegepast Natuurwetenschappelijk Onderzoek, The Hague, Nethe, A. R. P. JANSE (Landbouwhogeschool, Wageningen, Netherlands) et al. *International Journal of Remote Sensing* (ISSN 0143-1161), vol. 8, March 1987, p. 427-439. refs

This paper describes procedures for characterizing agricultural crops and soils in remote sensing studies. The procedures are based on the accumulated experience of a number of researchers active in this field. Therefore, they represent a compromise between the theoretically desirable and the practically feasible, and should thus be an effective aid in further studies of this type. Although the guidelines were prepared specifically for microwave studies, adjustments were made to render the procedures applicable to optical studies as well. Given the increasing number of research teams involved in remote sensing applied to agriculture, there is an opportunity to acquire a broad data base on soils and crops in various geographic regions. To allow intercomparisons of such data, they must be obtained in a consistent manner. By following the proposed procedures and reporting results using the parameters described here, such intercomparisons should be possible on a continental or a global scale. Author

A87-39191* National Oceanic and Atmospheric Administration, Washington, D. C.

SATELLITE DETECTION OF TROPICAL BURNING IN BRAZIL

MICHAEL MATSON (NOAA, National Environmental Satellite, Data, and Information Service, Washington, DC) and BRENT HOLBEN (NASA, Goddard Space Flight Center, MD) *International Journal of Remote Sensing* (ISSN 0143-1161), vol. 8, March 1987, p. 509-516. refs

Tropical burning often occurs in remote areas of the world. Satellite remote sensing is the only practical solution for detecting and monitoring this burning. The capability of the Advanced Very High Resolution Radiometer on board the National Oceanic and Atmospheric Administration polar orbiting satellites to detect tropical fire activity in the Manaus, Brazil area is demonstrated. Author

A87-39194* National Aeronautics and Space Administration, Goddard Space Flight Center, Greenbelt, Md.

MONITORING VEGETATION USING NIMBUS-7 SCANNING MULTICHANNEL MICROWAVE RADIOMETER'S DATA

B. J. CHOUDHURY, C. J. TUCKER (NASA, Goddard Space Flight Center, Greenbelt, MD), R. E. GOLUS (Science Applications Research, Lanham, MD), and W. W. NEWCOMB (RMS Technologies, Inc., Landover, MD) *International Journal of Remote Sensing* (ISSN 0143-1161), vol. 8, March 1987, p. 533-538. refs

Field studies and radiative transfer model calculations have shown that brightness temperature at high microwave frequencies is strongly affected by vegetation. The daytime observations for six consecutive years (1979 to 1984) over the Sahara, Senegalese Sahel, Burkina Fasso (Upper Volta), and U.S. Southern Great Plains at 37 GHz frequency of the Scanning Multichannel Microwave Radiometer (SMMR) on board the Nimbus-7 satellite are analyzed, and a high correlation with the normalized difference vegetation index derived from the Advanced Very High Resolution Radiometer on board the NOAA-7 satellite is found. The SMMR data appear to provide a valuable new long-term global data set for monitoring vegetation. In particular, the differing responses of vegetation (for example, annual grasses versus woody plants) to drought and the stability of the desert/steppe boundary of northern Africa might be studied using the time series data. Author

A87-40244* National Aeronautics and Space Administration, Goddard Space Flight Center, Greenbelt, Md.

CONCERNING THE RELATIONSHIP BETWEEN EVAPOTRANSPIRATION AND SOIL MOISTURE

PETER J. WETZEL (NASA, Goddard Space Flight Center, Greenbelt, MD) and JY-TAI CHANG (SASC Technologies, Inc., Hyattsville, MD) *Journal of Climate and Applied Meteorology* (ISSN 0733-3021), vol. 26, Jan. 1987, p. 18-27. NASA-sponsored research. refs

The relationship between the evapotranspiration and soil moisture during the drying, supply-limited phase is studied. A second scaling parameter, based on the evapotranspirational supply and demand concept of Federer (1982), is defined; the parameter, referred to as the threshold evapotranspiration, occurs in vegetation-covered surfaces just before leaf stomata close and when surface tension restricts moisture release from bare soil pores. A simple model for evapotranspiration is proposed. The effects of natural soil heterogeneities on evapotranspiration computed from the model are investigated. It is observed that the natural variability in soil moisture, caused by the heterogeneities, alters the relationship between regional evapotranspiration and the area average soil moisture. I.F.

A87-40248* National Aeronautics and Space Administration, Goddard Space Flight Center, Greenbelt, Md.

SOIL MOISTURE ESTIMATION USING GOES-VISSR INFRARED DATA - A CASE STUDY WITH A SIMPLE STATISTICAL METHOD

PETER J. WETZEL (NASA, Goddard Space Flight Center, Greenbelt, MD) and ROBERT H. WOODWARD (General Software Corp., Landover, MD) *Journal of Climate and Applied Meteorology* (ISSN 0733-3021), vol. 26, Jan. 1987, p. 107-117. refs

Five days of clear sky observations of Kansas and Nebraska are used to examine the statistical relationship between soil moisture and infrared surface temperature observations taken from a geosynchronous satellite. Linear regression is used to relate soil moisture to surface temperature and other variables that represent wind speed, vegetation cover, and low-level temperature advection. Results show good agreement between estimated and observed soil moisture features on each of the 5 days. The average coefficient of determination for five pseudoindependent tests in which the test day is held out of the regression is 0.71. It is shown that a depletion coefficient of 0.92, when used to compute antecedent precipitation index (API), produces the best correlation between API and soil moisture as inferred from GOES thermal infrared data. By averaging daily predicted values over the 5-day rain-free case study period, 92 percent of the variance of the morning surface temperature change is explained by a simple

multiple linear regression with all independent variables, or, alternatively, 85 percent of the observed variance in API is explained. It is concluded that this approach can distinguish at least four classes of soil wetness, but the necessity for measurement of surface advection may limit its usefulness in remote areas. Author

A87-40301* National Aeronautics and Space Administration. National Space Technology Labs., Bay Saint Louis, Miss.

AIRBORNE REMOTE SENSING OF FOREST BIOMES

STEVEN A. SADER (NASA, National Space Technology Laboratories, Bay Saint Louis, MS) Geocarto International, vol. 2, March 1987, p. 9-17. refs

Airborne sensor data of forest biomes obtained using an SAR, a laser profiler, an IR MSS, and a TM simulator are presented and examined. The SAR was utilized to investigate forest canopy structures in Mississippi and Costa Rica; the IR MSS measured forest canopy temperatures in Oregon and Puerto Rico; the TM simulator was employed in a tropical forest in Puerto Rico; and the laser profiler studied forest canopy characteristics in Costa Rica. The advantages and disadvantages of airborne systems are discussed. It is noted that the airborne sensors provide measurements applicable to forest monitoring programs. I.F.

A87-40302

MONTANE VEGETATION STRATIFICATION THROUGH DIGITAL PROCESSING OF LANDSAT MSS DATA

PARTH SARATHI ROY (Indian Institute of Remote Sensing, Dehra Dun, India) Geocarto International, vol. 2, March 1987, p. 19-26. refs

Vegetation stratification in mountainous terrain using space remote sensing techniques is complicated due to varying illumination condition and altitudinal control of vegetation. The present study deals with digital techniques to stratify vegetation in a test area of Arunachal Pradesh (India) using Landsat multispectral data. Various band ratio combinations have been tried to reduce effect of varying illumination and to enhance subtle variation in broad vegetation types. Normalized vegetation index has been found to enhance maximum features. Hence, an attempt was made to improve classification accuracy and identify certain vegetation classes using supervised classification of transformed Landsat multispectral data with normalized difference index, otherwise not possible using normal Landsat MSS data. Author

A87-40303* Maryland Univ., College Park.

COMPARISON OF NORTH AND SOUTH AMERICAN BIOMES FROM AVHRR OBSERVATIONS

SAMUEL N. GOWARD, DENNIS DYE (Maryland, University, College Park), ARLENE KERBER, and VIRGINIA KALB (NASA, Goddard Space Flight Center, Greenbelt, MD) Geocarto International, vol. 2, March 1987, p. 27-39. NASA-supported research. refs (Contract NCC5-26)

Previous analysis of the North American continent with AVHRR-derived vegetation index measurements showed a strong relation between known patterns of vegetation seasonality, productivity and the spectral vegetation index measurements. This study extends that analysis to South America to evaluate the degree to which these findings extend to tropical regions. The results show that the spectral vegetation index measurements provide a general indicator of vegetation activity across the major biomes of the Western Hemisphere of the earth, including tropical regions. The satellite-observed patterns are strongly related to the known climatology of the continents and may offer a means to improve understanding of global bioclimatology. For example, South America is shown to have a longer growing season with much earlier spring green-up than North America. The time integral of the measurements, computed from 12 composited monthly values, produces a value that is related to published net primary productivity data. However, limited net primary production data does not allow complete evaluation of satellite-observed contrasts between North and South American biomes. These results suggest that satellite-derived spectral vegetation index measurements are of

great potential value in improving knowledge of the earth's biosphere. Author

A87-40304

THE USE OF AVHRR DATA IN OPERATIONAL AGRICULTURAL ASSESSMENT IN AFRICA

GARY E. JOHNSON, CLARENCE M. SAKAMOTO (NOAA, Climatic Impact Assessment Div., Columbia, MO), and ALBERT VAN DIJK (Cooperative Institute for Applied Meteorology, Columbia, MO) Geocarto International, vol. 2, March 1987, p. 41-60. Research supported by the Agency for International Development and NOAA. refs

A87-40944* Scranton Univ., Pa.

REMOTE SENSING OF COASTAL WETLANDS

M. A. HARDISKY (Scranton, University, PA), V. KLEMAS (Delaware, University, Newark), and M. F. GROSS BioScience (ISSN 0006-3568), vol. 36, July-Aug. 1986, p. 453-460. Research supported by the Tinker Foundation and University of Delaware. refs

(Contract NOAA-NA-85AADSG033; NAGW-374; NSF DAR-80-17836)

Various aircraft and satellite sensors for detecting and mapping wetlands properties are examined. The uses of color IR photography to map coastal vegetation, and of Landsat MSS and TM and SPOT data to quantify biomass and productivity for large wetland areas are discussed. For spectral estimation of biomass and productivity, the relation between radiance and biomass needs to be studied; the quantity and orientation of dead biomass and the amount of soil reflectance in comparison with vegetation reflectance in a given target area affect the spectral estimation of biomass. The radiometric evaluation of brackish wetland, and remote sensing in mangroves are described. The collection of images in narrow, contiguous spectral band using imaging spectrometry is considered. I.F.

A87-41428

A SOIL MAP THROUGH LANDSAT SATELLITE IMAGERY IN A PART OF THE AURANGA CATCHMENT IN THE RANCHI AND PALAMOU DISTRICTS OF BIHAR, INDIA

R. R. BISWAS (All India Soil and Land Use Survey Organization, Dept. of Agriculture and Cooperation, Calcutta, In International Journal of Remote Sensing (ISSN 0143-1161), vol. 8, April 1987, p. 541-543. refs

A87-41430

A POLAR PLATFORM FOR THE REMOTE SENSING NEEDS OF ECOLOGY AND AGRICULTURE - A VIEW FROM THE U.K.

P. J. CURRAN and S. E. PLUMMER (Sheffield, University, England) International Journal of Remote Sensing (ISSN 0143-1161), vol. 8, April 1987, p. 555-567. refs (Contract NERC-P60/G6/16)

The main characteristics of the proposed polar-orbiting remote sensing satellites to be implemented in the Space Station program are described. The potential benefits of the polar platforms to remote sensing are discussed. The remote sensing needs of UK scientists in the areas of ecology and agriculture are examined. I.F.

A87-41434

RICE CROP IDENTIFICATION AND AREA ESTIMATION USING REMOTELY-SENSED DATA FROM INDIAN CROPPING PATTERNS

P. P. NAGESWARA RAO and V. R. RAO (Indian Space Research Organization, National Natural Resources Management System Office, Bangalore, International Journal of Remote Sensing (ISSN 0143-1161), vol. 8, April 1987, p. 639-650. refs

A87-41771

PHASE PORTRAITS OF VEGETATION DEVELOPMENT TRAJECTORIES IN A MULTIDIMENSIONAL SPECTRAL ATTRIBUTE SPACE [FAZOVYE PORTRETY TRAEKTORII RAZVITIYA RASTITEL'NOSTI V MNOGOMERNOM SPEKTRAL'NOM PRIZNAKOVOM PROSTRANSTVE]

L. N. VASIL'EV (AN SSSR, Institut Geografii, Moscow, USSR) Akademiia Nauk SSSR, Doklady (ISSN 0002-3264), vol. 293, no. 3, 1987, p. 705, 706. In Russian.

In view of the sensitivity of the spectral brightness characteristics of vegetation and soil to meteorological conditions and changes in the terrain components, the objective of the experiment reported here was to evaluate changes in these characteristics for the totality of agricultural crops rather than for each crop individually. The experiment was carried out in 1979-1983 using space imagery obtained by the Salyut station and aerial photography. The phase trajectories obtained in a multidimensional spectral attribute space have yielded a characteristic of the seasonal crop development within a homogeneous agricultural area which can be used to monitor the state of crops in such an area on the basis of satellite and aerial data. T.K.

N87-20619 Delaware Univ., Newark.

REAL-TIME CROP ASSESSMENT USING COLOR THEORY AND SATELLITE DATA Ph.D. Thesis

RUSSELL ANDREW AMBROZIAK 1986 219 p
Avail: Univ. Microfilms Order No. DA8629273

A new color coordinate system for satellite image display is developed and applied to crop monitoring using AVHRR data over the African Sahel. The system, called the Ambroziak Color Coordinate System (ACCS), is the result of applying color theory, models of human vision, and analyses of the unique constraints put on remote sensing for agriculture by the interaction of the vegetation's and atmosphere's time scales of change. The new color system allows real-time quantitative analysis of crops to be done in support of regional and national food security programs. The need for such a system is demonstrated by the severe food shortages in parts of Africa over the past several years and the delayed reports of existing problems. Based on the analysis of the strengths and weaknesses of false color IR images in existing crop monitoring systems which use remotely sensed data, the steps necessary to improve the usefulness of the image without sacrificing its strengths are outlined. The result is the development of the ACCS. The ACCS is then used to produce high resolution, effective cumulative rainfall analyses of the African Sahel and Horn regions. Dissert. Abstr.

N87-21408# National Aerospace Lab., Amsterdam (Netherlands). Space Div.

FOUNDATIONS AND APPLICATIONS OF MULTISPECTRAL SCANNING IN AGRICULTURE

N. J. J. BUNNIK 5 Feb. 1985 46 p In DUTCH; ENGLISH summary Presented at the Royal Society for Physics Dilgentia, The Netherlands, 5 Nov. 1985
(NLR-MP-85015-U; ETN-87-99283) Avail: NTIS HC A03/MF A01

Remote sensing techniques in the visible and near IR ranges for crop yield forecasting and crop disease identification are treated. The interaction of crops and soils with short wave radiation in the optical spectrum is discussed in order to derive the necessary information regarding the spectral distribution of reflected sunlight. The modeling of vegetation canopies is described in relation to yield measurement techniques. The operating principles of multispectral scanning are given, together with examples. ESA

N87-22280 Missouri Univ., Columbia.

A CROP CONDITION AND CROP YIELD ESTIMATION METHOD BASED ON NOAA/AVHRR SATELLITE DATA Ph.D. Thesis

ALBERT VANDIJK 1986 215 p
Avail: Univ. Microfilms Order No. DA8701412

The objective was to develop a crop condition and yield assessment method based on NOAA/Advanced Very High Resolution Radiometer (AVHRR) satellite data for the Sahel and Horn countries of Africa. The method consists of the following

steps. (1) Noise in the NOAA/AVHRR satellite data can cause misinterpretation. A proposed procedure reduces the noise by calculating a vegetation index from satellite data that is a measure of the green biomass. The index is then sampled and averaged in time and space and smoothed by applying an algorithm. (2) NOAA satellite data covering large areas are available every week. A system has been developed to pinpoint areas with abnormal vegetation conditions. (3) The yield estimation method is based on the following idea. In Africa a low percentage of the potential agricultural land is used. During grain-filling of a crop, when the green biomass decreases, the vegetation index of the crop decreases. However, the crop's contribution to the vegetation index of the entire area will be small. As a result, the following rule applies: a high vegetation index during the grain filling stage of a crop indicates a large amount of biomass, favorable growing conditions during that critical period, and a large yield. Regression analysis was performed to establish relationships between yields of millet, sorghum, and groundnuts and the vegetation values during the reproductive phase of these crops.

Dissert. Abstr.

N87-22296# Michigan Univ., Ann Arbor. School of Natural Resources.

EVALUATION OF THE AIRBORNE IMAGING SPECTROMETER FOR REMOTE SENSING OF FOREST STAND CONDITIONS Final Technical Report

CHARLES E. OLSON, JR. May 1986 86 p

(Contract JPL-956578)

(NASA-CR-180918; JPL-9950-1281; NAS 1.26:180918) Avail: NTIS HC A05/MF A01 CSCL 14B

Five pairs of plots were established in forest stands with one of each pair trenched and covered to prevent precipitation from reaching the tree roots. High winds and falling limbs destroyed the covers on three of the plots. The two remaining plots were in a red pine plantation and in a natural stand of sugar maple. Trees in both plots developed levels of moisture stress more than nine bars higher than control trees on the dates of overflights with the Airborne Imaging Spectrometer (AIS) and the Collins' Airborne Spectroradiometer (CAS). Hemispherical reflectance from stressed and control trees was measured with a Beckman DK2A spectrophotometer. On the day of the AIS overflight, stressed maple foliage was less reflective than the control from 1000 to 1300 nm, but more reflective at wavelengths longer than 1300 nm. Pine foliage was less reflective than the control from 1000 to 1600 nm, but the difference was small at wavelengths longer than 1350 nm. AIS data collected showed brightness values for both maple and pine to be lower than for the controls from 1000 to 1300 nm. CAS data were used to determine the gain in species identification accuracy obtainable with high spectral resolution data. Author

N87-22336# Missouri Univ., Columbia. Cooperative Inst. for Applied Meteorology.

A REVIEW OF NATIONAL AND INTERNATIONAL ACTIVITIES ON MODELING THE EFFECTS OF INCREASED CO2 CONCENTRATIONS ON THE SIMULATION OF REGIONAL CROP PRODUCTION: A REPORT ON LINKAGE BETWEEN CLIMATE AND CROP MODELS Progress Report

W. L. DECKER and R. ACHUTUNI 1 Jan. 1987 47 p

(Contract DE-FG02-86ER-60444)

(DE87-005994; DOE/ER-60444/T1) Avail: NTIS HC A03/MF A01

General circulation models have been used to estimate the probable changes in climate due to increased levels of carbon dioxide. These models, generally, project increases in the mean surface temperatures; but changes in precipitation due to CO2 enrichment are not as clear. Some process models, which utilize a minimum amount of empiricism, can be adopted for use in studying the impacts of both climate change scenarios and the direct effects of CO2 fertilization. The CERES-Maize, CERES-Wheat, SORGF, GLYCIM, and SOYGRO are among those classified for this use. A great deal of effort is directed toward these developments. WMO/UNEP/ICSU has sponsored at least

two European meetings but with only limited success for testing production models. A similar effort has been conducted by the Commission of European Communities. An attempt has been made to modify the CERES models, which have been used in climate studies, for use in simulation of the direct effects. Initial simulations involving this modification, show that doubling CO₂ will increase corn production 12 to 30% at locations in northern Illinois for the four-year period 1982 to 1985. Photosynthesis influenced yields more than decreased transpiration. DOE

N87-23032# Missouri Univ., Columbia. Dept. of Atmospheric Sciences.

THE IMPACT OF CLIMATE CHANGE FROM INCREASED ATMOSPHERIC CARBON DIOXIDE ON AMERICAN AGRICULTURE

WAYNE L. DECKER, VERNON K. JONES, and RAO ACHUTUNI
May 1986 108 p

(Contract W-7405-ENG-48)

(DOE/NBB-0077) Avail: NTIS HC A06/MF A01

The impact of climate change on crop production and animal production are discussed. Genetic selection, cropping patterns, farm management techniques, pest management, forage production and water availability are among the topics considered. R.J.F.

N87-24010*# National Aeronautics and Space Administration. Lyndon B. Johnson Space Center, Houston, Tex.

ERROR ANALYSIS OF LEAF AREA ESTIMATES MADE FROM ALLOMETRIC REGRESSION MODELS

A. H. FEIVESON and R. S. CHHIKARA 14 Jul. 1986 44 p

(Contract NAG5-548)

(NASA-TM-89220; NAS 1.15:89220) Avail: NTIS HC A03/MF A01 CSCL 02F

Biological net productivity, measured in terms of the change in biomass with time, affects global productivity and the quality of life through biochemical and hydrological cycles and by its effect on the overall energy balance. Estimating leaf area for large ecosystems is one of the more important means of monitoring this productivity. For a particular forest plot, the leaf area is often estimated by a two-stage process. In the first stage, known as dimension analysis, a small number of trees are felled so that their areas can be measured as accurately as possible. These leaf areas are then related to non-destructive, easily-measured features such as bole diameter and tree height, by using a regression model. In the second stage, the non-destructive features are measured for all or for a sample of trees in the plots and then used as input into the regression model to estimate the total leaf area. Because both stages of the estimation process are subject to error, it is difficult to evaluate the accuracy of the final plot leaf area estimates. This paper illustrates how a complete error analysis can be made, using an example from a study made on aspen trees in northern Minnesota. The study was a joint effort by NASA and the University of California at Santa Barbara known as COVER (Characterization of Vegetation with Remote Sensing).

Author

N87-24593# Sandia National Labs., Albuquerque, N. Mex.
MEASURED RADAR RETURN AT THE NEAR VERTICAL FROM FORESTED TERRAINS

D. A. JELINEK May 1987 57 p

(Contract DE-AC04-76DP-00789)

(DE87-009384; SAND-86-2618) Avail: NTIS HC A04/MF A01

This report presents the results of measurements that were made of the radar return from forested terrains. Measurements were taken while making straight and level passes with a helicopter over nearly pure stands of dense conifer and deciduous forests which were located on very flat terrain. The measurements were made using a 20-nanosecond pulse width, x-band radar and 16-degree-beamwidth antennas pointed straight down. Results are presented in terms of the average return power density at the receiving antenna as a function of round-trip delay for each forest for altitudes above the forest floor ranging from 100 to 1000 feet.

DOE

N87-24733*# California Univ., Santa Barbara. Dept. of Environmental Studies.

EARTH SCIENCE RESEARCH Final Report

DANIEL B. BOTKIN 4 May 1987 9 p

(Contract NAG5-548)

(NASA-CR-180512; NAS 1.26:180512) Avail: NTIS HC A02/MF A01 CSCL 05B

The analysis of ground-truth data from the boreal forest plots in the Superior National Forest, Minnesota, was completed. Development of statistical methods was completed for dimension analysis (equations to estimate the biomass of trees from measurements of diameter and height). The dimension-analysis equations were applied to the data obtained from ground-truth plots, to estimate the biomass. Classification and analyses of remote sensing images of the Superior National Forest were done as a test of the technique to determine forest biomass and ecological state by remote sensing. Data was archived on diskette and tape and transferred to UCSB to be used in subsequent research. B.G.

N87-24735*# National Aeronautics and Space Administration. Lyndon B. Johnson Space Center, Houston, Tex.

NEW DIMENSION ANALYSES WITH ERROR ANALYSIS FOR QUAKING ASPEN AND BLACK SPRUCE

K. D. WOODS, D. B. BOTKIN, and A. H. FEIVESON 1987 66 p

(NASA-TM-89219; NAS 1.15:89219) Avail: NTIS HC A01/MF A01 CSCL 02F

Dimension analysis for black spruce in wetland stands and trembling aspen are reported, including new approaches in error analysis. Biomass estimates for sacrificed trees have standard errors of 1 to 3%; standard errors for leaf areas are 10 to 20%. Bole biomass estimation accounts for most of the error for biomass, while estimation of branch characteristics and area/weight ratios accounts for the leaf area error. Error analysis provides insight for cost effective design of future analyses. Predictive equations for biomass and leaf area, with empirically derived estimators of prediction error, are given. Systematic prediction errors for small aspen trees and for leaf area of spruce from different site-types suggest a need for different predictive models within species. Predictive equations are compared with published equations; significant differences may be due to species responses to regional or site differences. Proportional contributions of component biomass in aspen change in ways related to tree size and stand development. Spruce maintains comparatively constant proportions with size, but shows changes corresponding to site. This suggests greater morphological plasticity of aspen and significance for spruce of nutrient conditions.

Author

N87-24736*# National Aeronautics and Space Administration. Goddard Space Flight Center, Greenbelt, Md.

TEN YEAR CHANGE IN FOREST SUCCESSION AND COMPOSITION MEASURED BY REMOTE SENSING

FORREST G. HALL, DANIEL B. BOTKIN, DONALD E. STREBEL, KERRY K. WOODS, and SCOTT J. GOETZ (Science Applications, Inc., Greenbelt, Md.) 15 Apr. 1987 22 p

(Contract NAG5-548)

(NASA-CR-180948; NAS 1.26:180948) Avail: NTIS HC A02/MF A01 CSCL 02F

Vegetation dynamics and changes in ecological patterns were measured by remote sensing over a 10 year period (1973 to 1983) for 148,406 landscape elements, covering more than 500 sq km in a protected forested wilderness. Quantitative measurements were made possible by methods to detect ecologically meaningful landscape units; these allowed measurement of ecological transition frequencies and calculation of expected recurrence times. Measured ecological transition frequencies reveal boreal forest wilderness as spatially heterogeneous and highly dynamic, with one-sixth of the area in clearings and early successional stages, consistent with recent postulates about the spatial and temporal patterns of natural ecosystems. Differences between managed forest areas and a protected wilderness allow assessment of different management regimes.

Author

01 AGRICULTURE AND FORESTRY

N87-24737*# Aster Consulting Associates, Inc., La Jolla, Calif.
INVERSION OF CANOPY REFLECTANCE MODELS FOR ESTIMATION OF VEGETATION PARAMETERS Final Report
NARENDRA S. GOEL 15 Jun. 1987 20 p
(Contract NAS5-29472)
(NASA-CR-181059; NAS 1.26:181059) Avail: NTIS HC A02/MF A01 CSCL 02F

One of the keys to successful remote sensing of vegetation is to be able to estimate important agronomic parameters like leaf area index (LAI) and biomass (BM) from the bidirectional canopy reflectance (CR) data obtained by a space-shuttle or satellite borne sensor. One approach for such an estimation is through inversion of CR models which relate these parameters to CR. The feasibility of this approach was shown. The overall objective of the research carried out was to address heretofore uninvestigated but important fundamental issues, develop the inversion technique further, and delineate its strengths and limitations. Author

N87-24801# Wageningen Agricultural Univ. (Netherlands).
DETERMINATION OF SPECTRAL REFLECTANCE OF CROPS DURING GROWTH FROM CALIBRATED MULTISPECTRAL SMALL FORMAT AERIAL PHOTOGRAPHY
J. H. LOEDEMAN, J. G. P. W. CLEVERS, and C. A. HORTON (Polytechnic, London, England) In ESA Proceedings of the International Symposium on Progress in Imaging Sensors p 519-531 Nov. 1986
Avail: NTIS HC A99/MF A01

Spectral reflectance factors of crops in field trials were calculated from radiometrically calibrated multispectral aerial photography. The objectives required matching defined spectral bands; film processing under sensitometric control; radiometric correction for effects due to atmosphere and camera; and synthesis of densitometry and photogrammetry. Under meteorological conditions in the Netherlands nearly instant availability of a recording system is needed. Recordings were executed with standard 70 mm cameras, films, and gelatin filters. Densitometry was done using a Macbeth TD-504 modified to a scanning densitometer, interfaced with an HP-85 computer. Results are comparable with those of ground based radiometry. ESA

02

ENVIRONMENTAL CHANGES AND CULTURAL RESOURCES

Includes land use analysis, urban and metroplitan studies, environmental impact, air and water pollution, geographic information systems, and geographic analysis.

A87-32196*# Virginia Univ., Charlottesville.
TRACE GAS EXCHANGES AND TRANSPORTS OVER THE AMAZONIAN RAIN FOREST
MICHAEL GARSTANG, STEVE GRECO, JOHN SCALA (Virginia, University, Charlottesville), ROBERT HARRISS, EDWARD BROWELL, GLENN SACHSE (NASA, Langley Research Center, Hampton, VA), JOANNE SIMPSON, WEI-KUO TAO (NASA, Goddard Space Flight Center, Greenbelt, MD), and ARNOLD TORRES (NASA, Wallops Flight Center, Wallops Island, VA) AMS, International Conference on Southern Hemisphere Meteorology, Wellington, New Zealand, Dec. 1-5, 1986, Paper. 5 p. refs (Contract NCC1-95)

Early results are presented from a program to model deep convective transport of chemical species by means of in situ data collection and numerical models. Data were acquired during the NASA GTE Amazon Boundary Layer Experiment in July-August 1985. Airborne instrumentation, including a UV-DIAL system, collected data on the O₃, CO, NO, temperature and water vapor profiles from the surface to 400 mb altitude, while GOES imagery tracked convective clouds over the study area. A two-dimensional cloud model with small amplitude random temperature fluctuations

at low levels, which simulated thermals, was used to describe the movements of the chemical species sensed in the convective atmosphere. The data was useful for evaluating the accuracy of the cloud model, which in turn was effective in describing the circulation of the chemical species. M.S.K.

A87-32493
ESTIMATION OF ROUGHNESS OF THE EARTH'S SURFACE USING LANDSAT MSS DATA ON THE ASSUMPTION OF RECIPROCITY ON LIGHT SCATTERING
HIROSHI OKAYAMA (Chiba University, Japan) and IWAO OGURA (Tokyo, University, Japan) IN: International Symposium on Space Technology and Science, 15th, Tokyo, Japan, May 19-23, 1986, Proceedings. Volume 2. Tokyo, AGNE Publishing, Inc., 1986, p. 1607-1611. refs

Using ground-glass samples of various degree of roughness to simulate the roughness of the earth's surface, the indicatrices which represent the angular distribution of the scattered light were obtained, and Minnaert's (1941) constants of the respective samples were determined. After it was verified that the scattered light from a sphere fulfills the reciprocity law, the indicatrices of a coastal area and of several Tokyo districts (representing a residential, a mixed residence and business, and a downtown area) were obtained using Landsat MSS data. It was shown that the Minnaert constant of the downtown area (1.60) is substantially greater than that of the coastal area (0.923), with the value of the mixed residential-business area next highest. The Minnaert constant value for the downtown area was approximately the same as that for the ground glass with a mesh number 3000. I.S.

A87-32494
LANDCOVER CHANGE IN HIROSHIMA DURING 1979/1984 DETECTED BY LANDSAT MSS AND TM DATA
KAZUAKI KAMEDA, SHUUHEI UMEZONO (Nihon University, Tokyo, Japan), YUZO SUGA (Hiroshima Institute of Technology, Japan), SOTARO TANAKA, and TOSHIRO SUGIMURA (Remote Sensing Technology Center of Japan, Tokyo) IN: International Symposium on Space Technology and Science, 15th, Tokyo, Japan, May 19-23, 1986, Proceedings. Volume 2. Tokyo, AGNE Publishing, Inc., 1986, p. 1613-1618.

A87-32496
FUNDAMENTAL STUDY ON SYSTEMATIZATION OF SELECTING NEW DEVELOPMENT AREA WITH LANDSAT DATA AND TOPOGRAPHIC INFORMATIONS
TAICHI OSHIMA and KIYOE MIYASHITA (Hosei University, Koganei, Japan) IN: International Symposium on Space Technology and Science, 15th, Tokyo, Japan, May 19-23, 1986, Proceedings. Volume 2. Tokyo, AGNE Publishing, Inc., 1986, p. 1631-1636.

Criteria of land selection on the basis of remote-sensing data are developed in connection with the concept planning stage of a land utilization program. The overlay processing of multidimensional information is used to select appropriate lands on the basis of a combination of Landsat data and topographical information. Results corresponding to regions near Hachioji and Musashi Fuchu are discussed. K.K.

A87-32953
POLARIZATION, LAND USE TYPE AND INTRAURBAN LOCATION AS VARIABLES IN SAR MAPPING ACCURACY
FLOYD M. HENDERSON (New York, State University, Albany) Geocarto International, no. 4, 1986, p. 27-37. refs (Contract NSF SES-81-12797)

Dual-polarized X-band airborne synthetic aperture radar imagery of Los Angeles, CA is employed to examine the relationship among urban land use category identification, category location within an urban area, and radar polarization. Results indicate that HV polarized imagery may be preferred for urban land use mapping as the signal response is less sensitive to target orientation and surface scatter. That is, there was more category related variation in tone and texture. For both polarizations there were significant differences in identification accuracy among land use classes and

the ability to identify a single land use type varied across the study area, but not equally. A major problem relative to developing applications was the inability to distinguish Commercial-Services and Industrial activity from other categories. Author

A87-33292**LIDAR OBSERVATION OF ELEVATED POLLUTION LAYERS OVER LOS ANGELES**

ROGER M. WAKIMOTO (California, University, Los Angeles) and JAMES L. MCELROY (EPA, Environmental Monitoring Systems Laboratory, Las Vegas, NV) *Journal of Climate and Applied Meteorology* (ISSN 0733-3021), vol. 25, Nov. 1986, p. 1583-1599. Research sponsored by the California Air Resources Board, South Coast Air Quality Management District, and EPA. refs

Elevated pollution layers are observed over Los Angeles with an aircraft equipped with a downward-looking lidar. For the first time, detailed ancillary upper-air kinematic and thermodynamic data were collected simultaneously to aid in the interpretation of these elevated layers. It is concluded that upper-level winds within the inversion, orographic effects, and thermally induced changes in the depth of the mixed layer control the evolution of these layers. Author

A87-35523**COMPARISON OF LANDSAT MSS AND TM DATA FOR URBAN LAND-USE CLASSIFICATION**

SIAMAK KHORRAM, JOHN A. BROCKHAUS, and HEATHER M. CHESHIRE (North Carolina State University, Raleigh) *IEEE Transactions on Geoscience and Remote Sensing* (ISSN 0196-2892), vol. GE-25, March 1987, p. 238-243. Research supported by North Carolina State University. refs

A supervised classification of digital Landsat Multispectral Scanner (MSS) data for the Raleigh, NC, metropolitan area was conducted in 1982. These data were categorized into 10 land-use/land-cover representative of the area. Digital Landsat Thematic Mapper (TM) data, for the Raleigh metropolitan area, were obtained in 1985 and analyzed for comparison to the MSS data. A stratified classification based upon principal components analysis was applied to the TM data, classifying the data into the 10 land-use/land-cover categories used in the analysis of the MSS data. Comparison of photo-interpreted land-use types and Landsat derived land-use types indicates that TM data provides significantly higher classification accuracies than can be obtained from MSS data. However, an increase in confusion between urban cover types was observed for the classified TM data over the MSS data. It is felt that the stratified classification approach was instrumental in reducing classification errors between general land-use/land-cover types such as urban areas, coniferous forests, and deciduous forests. It is not clear that the information extracted from the TM data regarding the urban environment will be of much more use to city planners than that obtained from MSS data. Author

A87-36125**THE POSSIBILITY OF USING SATELLITE MEASUREMENTS OF METHANE IN THE ATMOSPHERE TO STUDY THE GLOBAL-DISTRIBUTION CHARACTERISTICS OF ITS SOURCES [O VOZMOZHNOSTI ISPOL'ZOVANIYA SPUTNIKOVYKH IZMERENII METANA V ATMOSFERE DLIA IZUCHENIYA OSOBNOSTEI GLOBAL'NOGO RASPREDELENIYA EGO ISTOCHNIKOV]**

F. M. GADZHIR-ZADE, I. S. GULIEV, and A. A. FEIZULLAEV (AN ASSR, Nauchno-Proizvodstvennoe Ob'edinenie Kosmicheskikh Issledovaniy, Azerbaidzhan SSR) *Akademiia Nauk Azerbaidzhanskoi SSR, Doklady* (ISSN 0002-3078), vol. 42, no. 6, 1986, p. 47-50. In Russian. refs

A87-36363**ENVIRONMENTAL PROTECTION FROM SPACE**

IULIAN NOVIKOV (AN SSSR, Moscow, USSR) *Space* (ISSN 0267-954X), vol. 3, Mar.-Apr. 1987, p. 36, 37.

The use of remote sensing satellites for monitoring pollution is discussed. The visible, near-IR, and IR regions of the spectrum

are utilized to study pollution and its effect on the environment. The processing of the satellite data by adding false color to zones differing in density and structure is described. The data are applicable for geologists, land surveyors, foresters, oil workers, and environmental protection specialists. I.F.

A87-37277**TESTING THE CONSISTENCY FOR MAPPING URBAN VEGETATION WITH HIGH-ALTITUDE AERIAL PHOTOGRAPHS AND LANDSAT MSS DATA**

FRANK G. SADOWSKI (TGS Technology, EROS Data Center, Sioux Falls, SD), JAMES A. STURDEVANT (USGS, EROS Data Center, Sioux Falls, SD), and ROWAN A. ROWNTREE (USDA, Northeastern Forest Experiment Station, Syracuse, NY) *Remote Sensing of Environment* (ISSN 0034-4257), vol. 21, March 1987, p. 129-141. refs

Two methods of analysis were evaluated for mapping urban vegetation on high-altitude, color-infrared aerial photographs and Landsat MSS data of Syracuse, NY. The first method consisted of defining the spatial patterns (strata) of urban vegetation occurrence. The second method discriminated woody and herbaceous vegetation classes within defined strata. Emphasis was placed on evaluating the consistency of each method. Results indicate that consistent spatial patterns of urban vegetation strata were not achieved on either of the two data types tested due to the spatial complexity of the urban vegetation. However, for discriminating woody and herbaceous vegetation classes within defined strata, good consistency was noted among the interpreters of the high-altitude aerial photographs. The coarse spatial resolution of the Landsat MSS data resulted in low precision for identifying these two vegetation classes in this highly urbanized area. Where photointerpretation efforts are intended for mapping vegetation within numerous urban areas, the estimation of proportions of vegetation classes within defined strata should be a data analysis procedure more objective and consistently repeatable than is the delineation of vegetation patterns. Author

A87-37280* George Mason Univ., Fairfax, Va.**AN ASSESSMENT OF LANDSAT MSS AND TM DATA FOR URBAN AND NEAR-URBAN LAND-COVER DIGITAL CLASSIFICATION**

BARRY HAACK (George Mason University, Fairfax, VA), NEVIN BRYANT, and STEVEN ADAMS (California Institute of Technology, Jet Propulsion Laboratory, Pasadena) *Remote Sensing of Environment* (ISSN 0034-4257), vol. 21, March 1987, p. 201-213. refs

(Contract NAS7-918)

The information content of Landsat TM and MSS data was examined to assess the ability to digitally differentiate urban and near-urban land covers around Miami, FL. This examination included comparisons of unsupervised signature extractions for various cover types, training site statistics for intraclass and interclass separability, and band and band combination selection from an 11-band multisensor data set. The principal analytical tool used in this study was transformed divergence calculations. The TM digital data are typically more useful than the MSS data in the homogeneous near-urban land-covers and less useful in the heterogeneous urban areas. Author

A87-39182* National Aeronautics and Space Administration. Goddard Inst. for Space Studies, New York, N.Y.**DERIVING SURFACE ALBEDO MEASUREMENTS FROM NARROW BAND SATELLITE DATA**

CHRISTOPHER L. BREST (NASA, Goddard Institute for Space Studies, New York) and SAMUEL N. GOWARD (Maryland, University, College Park) *International Journal of Remote Sensing* (ISSN 0143-1161), vol. 8, March 1987, p. 351-367. refs

(Contract NCC5-20)

A target calibration procedure for obtaining surface albedo from satellite data is presented. The methodology addresses two key issues, the calibration of remotely-sensed, discrete wavelength, digital data and the derivation of an albedo measurement (defined over the solar short wave spectrum) from spectrally limited

02 ENVIRONMENTAL CHANGES AND CULTURAL RESOURCES

observations. Twenty-seven Landsat observations, calibrated with urban targets (building roof-tops and parking lots), are used to derive spatial and seasonal patterns of surface reflectance and albedo for four land cover types: city, suburb, farm and forest.

Author

A87-39188

URBAN LAND USE SEPARABILITY AS A FUNCTION OF RADAR POLARIZATION

FLOYD M. HENDERSON and KELLY A. MOGILSKI (New York, State University, Albany) *International Journal of Remote Sensing* (ISSN 0143-1161), vol. 8, March 1987, p. 441-448. refs

In this study the relationship between urban land use features and radar polarization was examined. Statistical tests were applied to density readings of HH- and HV-polarized X-band SAR imagery to determine: (1) differences in signal return among urban land use categories within a single polarization and (2) variations in signal return between polarizations for individual land use categories. Only one category produced a statistical difference between polarizations. Although some categories were separable on both polarizations, others were separable only on a single polarization. Possible reasons are discussed along with an observed clustering of classes by signal response/grey tone.

Author

A87-39593#

STRATEGIES AND TECHNOLOGIES FOR MONITORING THE ENVIRONMENT

DIETER LEICHT *Dornier Post* (English Edition) (ISSN 0012-5563), no. 1, 1987, p. 34-36.

Various methods of environmental monitoring are discussed. Some applications for and the different types of sensors utilized in space and airborne environmental monitoring are described. Satellite-borne remote sensing is useful for detecting pollutants in the atmosphere and on the earth's surface and for monitoring meteorological parameters; the sensors used in satellite remote sensing operate in the visible, IR, and microwave ranges. Aircraft-based monitoring employs various sensor packages, which include SLAR, microwave radiometer, IR/UV scanner, laser fluorosensor, and cameras, to detect ocean pollution. Consideration is given to ground-based equipment used in the monitoring of air and water quality and nuclear power plants. I.F.

A87-42255

USE OF MAPS, AERIAL PHOTOGRAPHS, AND OTHER REMOTE SENSOR DATA FOR PRACTICAL EVALUATIONS OF HAZARDOUS WASTE SITES

JOHN GRIMSON LYON (Ohio State University, Columbus) *Photogrammetric Engineering and Remote Sensing* (ISSN 0099-1112), vol. 53, May 1987, p. 515-519. Research sponsored by the Ohio State University. refs
(Contract NOAA-04/M01-B4; NOAA-NA-81AAD0095)

Aerial photographs and remote sensor data were used to identify and inventory hydrologic, soil, and vegetative conditions indicative of hazardous waste sites. Several papers and their results demonstrate the utility of these data and techniques for engineering applications. A combination of aerial photos, remote sensing, maps, and advanced evaluation techniques provided more information than traditional engineering techniques alone.

Author

N87-23015# Louisiana State Univ., Baton Rouge. Remote Sensing and Image Processing Lab.

THE INTEGRATION OF SPECTRAL AND SPATIAL ANALYSIS FOR LAND USE CLASSIFICATION Final Report, 27 Sep. 1982 - 30 Sep. 1986

CHARLES A. HARLOW Dec. 1986 24 p
(Contract DAAG29-82-K-0189)
(AD-A178703; ARO-19327.9-GS) Avail: NTIS HC A02/MF A01
CSCL 17H

This report describes the research conducted through September 1986 on the investigation of vision systems for aerial scenes. The projects reported on include: (1) Defining Measures Related to Perceptual Properties, (2) Texture Operators and their

Application to Vision Systems, (3) Structure of Vision Systems for Aerial Scenes, and (4) General Purpose Spatial Operators. GRA

N87-24747# IBM France S. A., Paris. Science Center.

TOWARDS AN AUTOMATIC IDENTIFICATION OF URBAN TEXTURES [VERS UNE IDENTIFICATION AUTOMATIQUE DES TISSUS URBAINS]

M. ARMAND and M. HERNANDEZ *In* ESA Proceedings of the International Symposium on Progress in Imaging Sensors p 73-85 Nov. 1986 *In* FRENCH; ENGLISH summary Original document contains color illustrations

Avail: NTIS HC A99/MF A01

Use of LANDSAT-5 Thematic Mapper imagery in urban planning and management was investigated. Urban structures and textures were analyzed, and the methodology of the photointerpreter was simulated. The radiometric properties were used for two types of Bayesian classifications: a general classification to identify the large homogeneous entities of the image, and a classification of primitives (urban, vegetation, streets). A moving window was applied to determine the percentage for each primitive contained in the corresponding homogeneous entity. Results were compared with existing urban cartography. The semiautomatic classification method works well, even if the division into zones is rather rough.

ESA

03

GEODESY AND CARTOGRAPHY

Includes mapping and topography.

A87-31591

A NEW COVARIANCE MODEL FOR INERTIAL GRAVIMETRY AND GRADIOMETRY

RENE FORSBERG (Geodetic Institute, Charlottenlund, Denmark) *Journal of Geophysical Research* (ISSN 0148-0227), vol. 92, Feb. 10, 1987, p. 1305-1310. refs
(Contract NATO-320/82)

A self-consistent covariance model for the earth's anomalous gravity field is presented within the framework of the planar approximation. The model features simple, closed formulas for autocovariances and cross covariances of geoid undulations, gravity anomalies, deflections of the vertical, and second-order gradients, both at the reference plane and aloft. Furthermore the main spectral decay of the model gravity power spectral density corresponds closely to Kaula's (1966) rule, thus yielding good fits to actual gravity field spectral characteristics. The outlined model may be viewed as the planar equivalent to the spherical Tscherning-Rapp (1974) model. The analytical model is characterized by three free parameters: the gravity anomaly variance a 'shallow' depth parameter, and a 'compensating' depth. These parameters act as scale factor, high-frequency attenuation, and low-frequency attenuation, respectively. The shallow depth parameter corresponds to twice the Bjerhammer sphere depth of spherical harmonic analysis, while the compensating depth is introduced as an arbitrary mathematical convenience, necessary to obtain finite values for gravity and geoid variance.

Author

A87-33375

INVESTIGATION OF TECTONIC DEFORMATIONS USING GLOBAL SATELLITE LASER RANGING DATA

R. DIETRICH and G. GENDT (Akademie der Wissenschaften der DDR, Zentralinstitut fuer Physik der Erde, Potsdam, East Germany) *Gerlands Beitrage zur Geophysik* (ISSN 0016-8696), vol. 95, 1986, p. 453-458. refs

Satellite laser ranging and orbital modeling of artificial satellites have both reached the sub-decimeter level of accuracy. The observations of satellite Lageos during the international MERIT-Campaign (September 1983-October 1984; about 30 stations) and the orbital model POTSDAM-5 were used to compute

a global station-coordinate set of high accuracy. Next, different methods for the determination of station motions are investigated. The data are used for an estimation of model accuracy as well as for determination of relative motion in a special case. Author

A87-34186

THE DETERMINATION OF EARTH-ROTATION PARAMETERS FROM SATELLITE LASER RANGING [K VOPROSU OPREDELENIIA PARAMETROV VRASHCHENIIA ZEMLI PO LAZERNYM NABLIUDENIIAM ISZ]

I. M. TSIUPAK (L'vovskii Politekhnikeskii Institut, Lvov, Ukrainian SSR) Kinematika i Fizika Nebesnykh Tel (ISSN 0233-7665), vol. 3, Jan.-Feb. 1987, p. 78-83. In Russian. refs

A technique for determining earth-rotation parameters (ERP) from satellite laser ranging is described. Allowance is made for the influence of ERP on the calculated vector of the satellite's state and on the joint determination of the orbital parameters, pole coordinates, and sidereal time using a priori information. Lageos laser data obtained in the MERIT campaign are treated using the proposed technique. K.K.

A87-35308

GEOCHRONOLOGICAL STUDIES OF STRANGLINES OF SAURASHTRA, INDIA, DETECTED BY REMOTE SENSING TECHNIQUES

M. BASKARAN, B. L. K. SOMAYAJULU (Physical Research Laboratory, Ahmedabad, India), BALDEV SAHAI, and R. K. SOOD (Indian Space Research Organisation, Space Applications Centre, Ahmedabad, India) International Journal of Remote Sensing (ISSN 0143-1161), vol. 8, Feb. 1987, p. 169-176. refs

Using remote sensing techniques, four strandlines parallel to the present coastline were detected in the 16-18 km wide coastal belt of the Saurashtra peninsula in western India. Geochronological studies of the miliolites, the principal deposit of this area, using the Th-230/U-234 method, yielded ages ranging from 52 to 235 thousand years. With strong evidence in favor of tectonic instability in the region, the average uplift rates of the strandlines are calculated to range from 0.12 to 0.58 mm/year. Author

A87-36126

INTERNATIONAL CONFERENCE ON EARTH ROTATION AND THE TERRESTRIAL REFERENCE FRAME, COLUMBUS, OH, JULY 31-AUG. 2, 1985, PROCEEDINGS. VOLUMES 1 & 2

Conference sponsored by IAU, International Association of Geodesy, International Union of Geodesy and Geophysics, and International Council of Scientific Unions. Columbus, OH, Ohio State University (Reports on the MERIT-COTES Campaign on Earth Rotation and Reference Systems, Part II), 1986. Vol. 1, 428 p.; vol. 2, 444 p. For individual items see A87-36127 to A87-36177.

Reports are presented on the MERIT-COTES campaign on techniques in astrometry, satellite laser ranging, lunar laser ranging, very long baseline interferometry, and on combinations of techniques. Consideration is also given to short periodic and irregular variations in earth orientation parameters and atmospheric effects, intercomparisons of reference frames and standards, and future instrumentation and computational techniques for measuring earth rotation parameters. Papers are presented on the precision and accuracy of earth rotation determinations derived from optical astrometry, the performance of NASA laser ranging systems during MERIT, a stable method for estimation of laser ranging, a laser network designed for lunar ranging and earth satellite ranging, and combination of recent polar motion observations. Also included are papers on water storage effects on the earth's rotation, a geodetic intercomparison network for evaluating space techniques, reference frame intercomparisons, and polar motion-induced gravity. I.S.

A87-36164#

GINFEST - GEODETIC INTERCOMPARISON NETWORK FOR EVALUATING SPACE TECHNIQUES

VIDAL ASHKENAZI (Nottingham University, England) IN: International Conference on Earth Rotation and the Terrestrial Reference Frame, Columbus, OH, July 31-Aug. 2, 1985, Proceedings. Volume 2. Columbus, OH, Ohio State University, 1986, p. 584-589.

Details are given of a geodetic network connecting the major radio telescopes and SLR facilities in Western and Central Europe, which is to be used in a co-location exercise involving VLBI, CERI, SLR observations, with the aim of evaluating the relative accuracies and system biases of these geodetic space observation techniques. Author

A87-36166*#

National Aeronautics and Space Administration. Goddard Space Flight Center, Greenbelt, Md.

CREATION OF A GLOBAL GEODETIC NETWORK USING MARK III VLBI

CHOPO MA, THOMAS A. CLARK, and JAMES W. RYAN (NASA, Goddard Space Flight Center, Greenbelt, MD) IN: International Conference on Earth Rotation and the Terrestrial Reference Frame, Columbus, OH, July 31-Aug. 2, 1985, Proceedings. Volume 2. Columbus, OH, Ohio State University, 1986, p. 601-608. refs

The positions of 15 permanent VLBI stations have been determined using Mark III with one-sigma uncertainties of less than 5 cm except for three stations in the Pacific. 46070 delay/delay rate observations acquired by the Crustal Dynamics Project and Polaris/IRIS from 1980-84 were included in a least squares solution to estimate the station positions, 44 radio source positions, and earth orientation parameters. Author

A87-36176*# Colorado Univ., Boulder.

POLAR MOTION-INDUCED GRAVITY

JOHN M. WAHR (Colorado, University, Boulder) IN: International Conference on Earth Rotation and the Terrestrial Reference Frame, Columbus, OH, July 31-Aug. 2, 1985, Proceedings. Volume 2. Columbus, OH, Ohio State University, 1986, p. 736-741. refs (Contract NAS5-27644)

Variations in the geocentric position of the earth's rotation axis (polar motion) cause deformation within the earth. The effects of this deformation on surface gravity and on radial and horizontal positions of points on the earth's surface are estimated. The effects of the oceans and of the earth's anelasticity on this deformation are found to be negligible. Peak-to-peak variations in surface gravity of 10 microgals or more, and in radial motion of 1-2 cm are possible over six months or so. These numbers are small enough that they can probably not be used to learn about the earth; however, they are large enough to noticeably affect present high-quality geodetic observations. Author

A87-37918

GLOBAL IMAGES OF THE EARTH'S INTERIOR

ADAM M. DZIEWONSKI and JOHN H. WOODHOUSE (Harvard University, Cambridge, MA) Science (ISSN 0036-8075), vol. 236, April 3, 1987, p. 37-48. refs (Contract NSF EAR-81-20944; NSF EAR-82-13330; NSF EAR-83-17594; NSF EAR-84-18332; NSF EAR-85-11400)

Global seismic imaging is reviewed. The systematic and rapid progression away from the spherically symmetric earth models developed during the first three quarters of this century is recalled, showing the progression toward three-dimensional maps of the earth's interior which now span regions from the bottom of the crust to the inner core of the earth. The surprising finding is addressed that the inner core appears to be anisotropic with the axis of symmetry aligned with the axis of rotation. C.D.

03 GEODESY AND CARTOGRAPHY

A87-41380* Jet Propulsion Lab., California Inst. of Tech., Pasadena.

GPS-BASED GEODESY IN CALIFORNIA, MEXICO AND THE CARIBBEAN

W. G. MELBOURNE, T. H. DIXON, J. M. DAVIDSON, and C. L. THORNTON (California Institute of Technology, Jet Propulsion Laboratory, Pasadena) IN: PLANS '86 - Position Location and Navigation Symposium, Las Vegas, NV, Nov. 4-7, 1986, Record. New York, Institute of Electrical and Electronics Engineers, 1986, p. 219-229. refs

Thw NASA GPS-based geophysical geodetics system will be capable of 1-3 cm relative position accuracies on regional baselines and GPS ephemerides with submeter accuracies. Simultaneity and mutual visibility allow high differential carrier phase and group delay measurements to be obtained without clock errors. Both mobile GPS terminal sites and fiducial sites whose locations are accurately maintained by independent VLBI and SLR systems are to be used. A system validation and multiyear measurement program is under way. O.C.

A87-41383

USING THE GLOBAL POSITIONING SYSTEM (GPS) FOR HIGH PRECISION GEODETIC SURVEYS - HIGHLIGHTS AND PROBLEM AREAS

G. BEUTLER, W. GURTNER, M. ROTHACHER, T. SCHILDKNECHT, and I. BAUERSIMA (Bern, Universitaet, Switzerland) IN: PLANS '86 - Position Location and Navigation Symposium, Las Vegas, NV, Nov. 4-7, 1986, Record. New York, Institute of Electrical and Electronics Engineers, 1986, p. 243-250. refs

Although only partially deployed the GPS could be applied successfully to a big variety of high precision surveys ranging from the measurement of short ultra-precise terrestrial baselines to the establishment of networks of continental size. This development is illustrated with a typical example for small-scale surveys (CERN-LEP control net) and two for large scale surveys (1984 Alaska GPS experiment and 1985 High precision baseline test /HPBL-test/). Typical problem areas (atmospheric refraction effects, orbit quality) are discussed. The accuracy obtainable with GPS today is demonstrated by comparison with terrestrial surveys for the small networks, with VLBI measurements for large networks. Author

N87-20618 Bayerische Akademie der Wissenschaften, Munich (West Germany). Bayerische Kommission fuer die Internationale Erdmessung.

REPORT ON THE SPECIAL PROGRAM 78 SATELLITE GEODESY OF THE TECHNICAL UNIVERSITY OF MUNICH Progress Report, 1984-1985 [DIE ARBEITEN DES SONDERFORSCHUNGSBEREICHES 78 SATELLITENGEODAESIE DER TECHNISCHEN UNIVERSITAET MUENCHEN 1984 UND 1985]

MANFRED SCHNEIDER 1986 346 p In GERMAN (ASTRON-GEODAET-ARB-48; ISBN-3-7696-9791-X; ISSN-0340-7691; ETN-87-98974) Avail: Issuing Activity

In the project, laser range finding software and sequential storage system development for satellite observation, the thermal behavior and radiation quality of an Nd-glass slab laser, laser and receiver developments, and a concept for a Moon and satellite laser range finder were studied. A mobile laser range finder was examined. The operation and development of a receiver unit for radio interferometry was investigated. Microwave Doppler and global positioning measurements were performed. Universal time, terrestrial, meteorological, and seismological supplemental measurements were conducted. Gradiometer concepts were examined. The influence of lithosphere boundary waves on the geoid was studied. In the field of the Earth-Moon systems dynamics ephemeride calculations, satellite orbits and laser time-of-flight, satellite gradiometry, the Newton-Euler equation of motion, and relativistic effects were investigated. The astrometric and geodetic-geophysical application of interferometric methods was examined. ESA

N87-22282# Institut fuer Angewandte Geodaesie, Frankfurt am Main (West Germany).

REPORTS ON CARTOGRAPHY AND GEODESY, SERIES 1, NUMBER 96 [NACHRICHTEN AUS DEM KARTEN- UND VERMESSUNGSWESEN, REIHE 1, HEFT NR. 96]

1985 40 p In GERMAN, ENGLISH and FRENCH (ISSN-0469-4236; ETN-87-99328) Avail: NTIS HC A03/MF A01

A collocation experiment with laser systems and a time-transfer experiment as well as the timing-system of the ground station are described. A reconstitution of the graphic triangulation procedure of the Dutch cartographer, Jacob van Deventer (1500 to 1575) is given.

ESA

N87-22286# Institut fuer Angewandte Geodaesie, Frankfurt am Main (West Germany).

REPORTS ON CARTOGRAPHY AND GEODESY, SERIES 1, NUMBER 97 [NACHRICHTEN AUS DEM KARTEN- UND VERMESSUNGSWESEN, REIHE 1, HEFT 97]

1986 111 p In GERMAN, ENGLISH and FRENCH (ISSN-0469-4236; ETN-87-99329) Avail: NTIS HC A06/MF A01

Developments of digital and graphic program systems used for cartography and geodesy are presented. Systems of digital image processing, like the Vicom system and their application in navigation, orthophotomapping, and thematic cartography are discussed. Possibilities of map-projection, such as the development from digital to analog maps are shown. Research activities and fields of application, including regional planning engineering-geodesy as well as the establishment of an official computerized topographic cartographic information system (TOPKIS) are outlined.

ESA

N87-22290# Institut fuer Angewandte Geodaesie, Frankfurt am Main (West Germany).

THE VICOM SYSTEM FOR DIGITAL IMAGE PROCESSING AT THE INSTITUTE OF CARTOGRAPHY OF TECHNICAL UNIVERSITY, HANOVER (WEST GERMANY) [DIE VICOM-ANLAGE ZUR DIGITALEN BILDVERARBEITUNG BEIM INSTITUT FUER KARTOGRAPHIE (IFK) DER UNIVERSITAET HANNOVER]

ERNST JAEGER In its Repts. on Cartography and Geodesy, Series 1, No. 97 p 41-49 1986 In GERMAN; ENGLISH and FRENCH summaries Avail: NTIS HC A06/MF A01

The VICOM system is used for automatic digitizing of cadastral and topographic maps as an alternative to manual digitizing. Hardware and software components of an image processing system for application of processes which can increase the system efficiency are described. Research activities in digital image processing, using the VICOM system, are discussed. ESA

N87-23018*# National Aeronautics and Space Administration, Goddard Space Flight Center, Greenbelt, Md.

QUICK-LOOK GUIDE TO THE CRUSTAL DYNAMICS PROJECT'S DATA INFORMATION SYSTEM

CAREY E. NOLL, JEANNE M. BEHNKE, and HENRY G. LINDER Jun. 1987 82 p (NASA-TM-87818; NAS 1.15:87818) Avail: NTIS HC A05/MF A01 CSCL 08G

Described are the contents of the Crustal Dynamics Project Data Information System (DIS) and instructions on the use of this facility. The main purpose of the DIS is to store all geodetic data products acquired by the Project in a central data bank and to maintain information about the archive of all Project-related data. Access and use of the DIS menu-driven system is described as well as procedures for contacting DIS staff and submitting data requests. Author

N87-23033* Texas Univ., Austin. Center for Space Research. **ALTIMETER MEASUREMENTS FOR THE DETERMINATION OF THE EARTH'S GRAVITY FIELD** Annual Research Technical Report, 18 Mar. 1986 - 14 Mar. 1987

B. D. TAPLEY, B. E. SCHUTZ, and C. K. SHUM 29 Apr. 1987 15 p

(Contract NAG5-746)

(NASA-CR-180520; NAS 1 26.180520) Avail: NTIS HC A02/MF A01 CSCI 08G

The ability of satellite-borne radar altimeter data to measure the global ocean surface with high precision and dense spatial coverage provides a unique tool for the mapping of the Earth's gravity field and its geoid. The altimeter crossover measurements, created by differencing direct altimeter measurements at the subsatellite points where the orbit ground tracks intersect, have the distinct advantage of eliminating geoid error and other nontemporal or long period oceanographic features. In the 1990's, the joint U.S./French TOPEX/POSEIDON mission and the European Space Agency's ERS-1 mission will carry radar altimeter instruments capable of global ocean mapping with high precision. This investigation aims at the development and application of dynamically consistent direct altimeter and altimeter crossover measurement models to the simultaneous mapping of the Earth's gravity field and its geoid, the ocean tides and the quasi-stationary component of the dynamic sea surface topography. Altimeter data collected by SEASAT, GEOS-3, and GEOSAT are used for the investigation.

Author

04

GEOLOGY AND MINERAL RESOURCES

Includes mineral deposits, petroleum deposits, spectral properties of rocks, geological exploration, and lithology.

A87-31410* National Aeronautics and Space Administration. Goddard Space Flight Center, Greenbelt, Md.

SHUTTLE IMAGING RADAR (SIR-B) INVESTIGATIONS OF THE CANADIAN SHIELD - INITIAL REPORT

PAUL D. LOWMAN, JR. (NASA, Goddard Space Flight Center, Greenbelt, MD), JEFF HARRIS (F. G. Bercha and Associates, Ltd., Calgary, Canada), PENNY M. MASUOKA (Science Applications Research, Lanham, MD), VERNON H. SINGHROY (Ministry of National Resources, Ontario Centre for Remote Sensing, Toronto, Canada), and VERNON ROY SLANEY (Geological Survey of Canada, Mineral Resource Div., Ottawa) IEEE Transactions on Geoscience and Remote Sensing (ISSN 0196-2892), vol. GE-25, Jan. 1987, p. 55-66. refs

Two of the 43 Shuttle Imaging Radar (SIR-B) experiments carried out from the 41-G shuttle mission in 1984 involved a 2600-km swath across the Canadian Shield, with the objectives of studying the structure of province boundaries and developing techniques for the geologic use of orbital radar. Despite degraded single incidence angle imagery resulting from system problems, valuable experience has been obtained with data over a test site near Bancroft, Ontario. It has been found that even subdued glaciated topography can be effectively imaged, variations in backscatter being caused by variations in local incidence angle rather than shadowing. It has been demonstrated that small incidence angles are more sensitive to topography than large angles. Backscatter is extremely sensitive to look direction, topographic features nearly normal to the illumination being highlighted, and those nearly parallel to it being suppressed. It is concluded that orbital radar can provide a valuable tool for geologic studies of the Canadian Shield and similar areas, if suitable look angles and at least two look directions can be utilized for each area.

Author

A87-32478

EXPLORATION OF GEOMAGNETIC FIELD ANOMALY WITH BALLOON FOR GEOPHYSICAL RESEARCH

WEN-KUI JIA (Chinese Academy of Sciences, Space Science and Technology Center, Beijing, People's Republic of China) IN International Symposium on Space Technology and Science, 15th, Tokyo, Japan, May 19-23, 1986, Proceedings Volume 2 Tokyo, AGNE Publishing, Inc., 1986, p. 1503-1509

The use of a balloon to explore the geomagnetic field anomaly in the area east of Beijing is demonstrated. The present results are compared with those of aerial surveys. Descriptions are given of the fluxgate magnetometer, the sensor's attitude control and measurement, and data transmission and processing. At an altitude of about 30 km, a positive anomaly of the vertical component of about 100 nanoteslas was measured. The results suggest that, for this particular area, the shallow layer of a small-scale geological structure differs from the deep layer of a large-scale geological structure.

T.K.

A87-35522

MID-INFRARED REMOTE SENSING SYSTEMS AND THEIR APPLICATION TO LITHOLOGIC MAPPING

JOHN E. EBERHARDT, JOHN G. HAUB (CSIRO, Lucas Heights Research Laboratories, Australia), ANDREW A. GREEN (CSIRO, Div. of Mineral Physics and Mineralogy, North Ryde, Australia), RONALD J. P. LYON (Stanford University, CA), and ARTHUR W. PRYOR (Macquarie University, North Ryde, Australia) IEEE Transactions on Geoscience and Remote Sensing (ISSN 0196-2892), vol. GE-25, March 1987, p. 230-237. refs

Mid-infrared remote lithologic mapping by emittance and by reflectance are assessed in laboratory experiments. The emittance spectra of various rocks and minerals, measured in the 8-13-micron atmospheric transmission window, are compared with reflectance data measured in the range of 9.2-11.2-micron using a line-tuned CO₂ laser. It is concluded that the reflectance data are more useful for lithologic discrimination than the passive emittance data. An experimental laser suitable for terrain mapping from a low-flying aircraft is described. The low-pressure longitudinal discharge CO₂ laser has a rotating mirror to scan the diffraction grating and generates 90 bursts of pulses per second. Each 1-ms burst contains 92 pulses at 92 CO₂ laser wavelengths. The mean output power is 12 W and the average pulse power is 370 W. With that power, and using incoherent detection, a signal-to-noise ratio of better than 100:1 should be obtained from terrain with an albedo of 0.01 at a height of 500 m.

Author

A87-36104

THE GEOMETRY OF THE INTERSECTIONS OF TECTONIC STRUCTURES DETECTED ON SATELLITE IMAGES [GEOMETRICHESKIE PERESECHENIIA TEKTONICHESKIKH STRUKTUR, VYAVLIAEMYKH NA KOSMICHESKIKH SNIMKAKH]

M. I. BURLESHIN (Proizvodstvennoe Geologicheskoe Ob'edinenie Gidrospeetsgeologiya, Moscow, USSR) Issledovanie Zemli iz Kosmosa (ISSN 0205-9614), Nov.-Dec. 1986, p. 32-37. In Russian. refs

Using a number of interpreted satellite images of the Turan platform, four groups of tectonic structures were identified: structures oriented either longitudinally or transversely with respect to the basic folding pattern of the platform, structures that are intermediate between the longitudinal and transverse structures, and ring structures. These structures were seen to intersect forming two types of intersections. The first type comprises intersections between the longitudinal, transverse, and intermediate structures, forming orthogonal, diagonal, or complex patterns. The second type includes those between the longitudinal and ring structures. These types of intersections can have 'superimposed', 'enclosed', and 'displaced' configurations. The correlations between the intersection patterns observed and the geological features of the area are discussed.

I.S.

A87-36105

THE GEOSTRUCTURAL CHARACTERISTICS OF THE RIFT ZONE ON THE LAMBERT GLACIER (ANTARCTICA) ACCORDING TO SPACE IMAGES [OSOBENNOSTI GEOLOGICHESKOGO STROENIYA RIFTOVOI ZONY LEDNIKA LAMBERTA /ANTARKTIDA/ PO DANNYM DESHIFRIROVANIYA KOSMICHESKIKH SNIMKOV]

V. M. BUDKO and V. S. SHALAEV (Proizvodstvennoe Geologicheskoe Ob'edinenie Aerogeologii, Leningrad, USSR) *Issledovanie Zemli iz Kosmosa* (ISSN 0205-9614), Nov.-Dec. 1986, p. 38-47. In Russian. refs

Cosmos-satellite images of the Lambert glacier rift zone were interpreted to reveal the zone's geological features. A schematic map (on the scale of 1:1,000,000) of faults and tectonic structures compiled on the basis of the interpreted images reveals about 10 ring structures and an ancient tectonic zone. Two types of faults were identified on the map: the first comprising the disjunctions forming the largest grabens, or riftogenic faults; and the second comprising all other dislocations. Statistical analysis of the interpretation results has demonstrated good agreement between predicted and identified faults. The ore-controlling significance of the ancient tectonic zone (dating to the Ross Orogeny) is inferred. I.S.

A87-36525

FAULT PATTERNS BY SPACE REMOTE SENSING AND THE ROTATION OF WESTERN OREGON DURING CENOZOIC TIMES

MICHEL CHAPLET, JEAN CHOROWICZ, and FRANCOIS ROURE (Paris VI, Universite, France) *Earth and Planetary Science Letters* (ISSN 0012-821X), vol. 81, no. 4, Feb. 1987, p. 425-433. refs

MSS-Landsat images (bands 6 and 7) as well as previous studies were used to interpret fault patterns in western Oregon in terms of the rotations detected by paleomagnetism. These fault zones show a great concentration between the Cascade Range and the Idaho Batholite and have several distinct trends. The north-south striking structures are attributed to the Basin and Range province, while the large NW-SE right-lateral fault zones are interpreted as resulting from an extension between the Cascades Arc and the Olympic-Wallowa lineament. The latter was a paleoplate boundary during pre-Eocene times. This extension, beginning during Late Eocene/Oligocene times and continuing through recent times, is accompanied by a migration of the rotation pole from southeast to northwest, and by a clockwise rotation of the Coast Range-Klamath Mountain-Cascade Range block, induced by the subduction of the Farallon plate. Author

A87-36925

FIRST RESULTS OF LATERITIC COVER MAPPING WITH SPOT IMAGES THE KANGABA REGION (SOUTH-MALI) [PREMIERS RESULTATS DE CARTOGRAPHIE DES COUVERTURES LATERITIQUES PAR IMAGES SPOT, REGION DE KANGABA (SUD-MALI)]

CLAUDE ROQUIN, TOUNDE DANDJINO, PHILIPPE FREYSSINET, JEAN-CLAUDE PION, and YVES TARDY (CNRS, Centre de Sedimentologie et de Geochimie de la Surface, Strasbourg, France) *Academie des Sciences (Paris), Comptes Rendus, Serie II Mecanique, Physique, Chimie, Sciences de l'Univers, Sciences de la Terre* (ISSN 0249-6305), vol. 304, no. 8, Feb. 28, 1987, p. 321-326. In French. CNES-supported research. refs

A detailed mapping method is applied to multispectral SPOT images of the Kangaba region of South-Mali obtained on April 5, 1986, and the relationship between lateritic landscapes and the mineral and element contents of the soil is successfully demonstrated. The process distinguishes between the sandy surface deposits in the thalwegs which are rich in quartz and sparse in vegetation, and the ferruginous duricrusts on the plateaus whose vegetation density varies with kaolinite content. The study reveals elements relating the geochemical evolution of duricrusts to the surface drainage conditions and the development of vegetation cover. R.R.

A87-39186

PREDICTING THE LOCATION OF KIMBERLITE FROM A PROBABILITY ANALYSIS OF LINEAR STRUCTURE ON REMOTE SENSING DATA

PIN-QING WANG (Centre for Remote Sensing in Geology, Beijing, People's Republic of China) *International Journal of Remote Sensing* (ISSN 0143-1161), vol. 8, March 1987, p. 417-426. refs

The relation between linear structure and mineral deposits is examined. The use of linear structure on a remote sensing image to predict the location of kimberlite is described. Statistical analysis and probability calculations are applied to remote sensing images of a test site in northeastern China. A probability contour map of kimberlite in the area is derived, and a correlation between the kimberlite locations and the linear structure distributions from the remote sensing images is detected. I.F.

A87-39193

A SOFTWARE DEFOLIANT FOR GEOLOGICAL ANALYSIS OF BAND RATIOS

S. J. FRASER and A. A. GREEN (CSIRO, Div. of Mineral Physics and Mineralogy, North Ryde, Australia) *International Journal of Remote Sensing* (ISSN 0143-1161), vol. 8, March 1987, p. 525-532. Research sponsored by the Australian Mineral Industries Research Association. refs

Vegetation impedes the geological analysis of band ratio images, because it is both widely distributed in the surficial environment and can be spectrally similar to ferric oxides and clays when sampled by broad-band imaging devices. This problem is addressed by a technique called 'directed principal component analysis' (DPCA) that involves calculating principal components on two input band ratio images. One ratio is a geological discriminant, confused by the presence of vegetation; the second ratio is chosen for its suitability as a vegetation index. Once computed, the second DPC has the properties of a geological discriminant, but is less influenced by vegetation. The effects of vegetation, which are strongly correlated between the two input ratios, contribute chiefly to the first DPC. This simple method, applied selectively to airborne thematic mapper data, substantially reduces the effects of vegetation. Author

A87-39468

HIGH RESOLUTION REMOTE SENSING OF SPATIALLY AND SPECTRALLY COMPLEX COAL SURFACE MINES OF CENTRAL PENNSYLVANIA - A COMPARISON BETWEEN SIMULATED SPOT MSS AND LANDSAT-5 THEMATIC MAPPER

NANCY F. PARKS, GARY W. PETERSEN, and GEORGE M. BAUMER (Pennsylvania State University, University Park) *Photogrammetric Engineering and Remote Sensing* (ISSN 0099-1112), vol. 53, April 1987, p. 415-420. refs (Contract DE-AC02-83ER-60182)

A87-39790

SPACELAB DATA - A NEW CONTRIBUTION FOR STRUCTURAL INTERPRETATIONS OF REMOTELY SENSED DATA IN GEOLOGY

ANNICK BLUSSON (Paris XI, Universite, Orsay; IBM France, S.A., Centre Scientifique, Paris) *Earth, Moon, and Planets* (ISSN 0167-9295), vol. 38, May 1987, p. 1-11. CNES-CNRS-supported research. refs

This study deals with the comparison between Landsat MSS usual data, extensively used in the past, and new Spacelab photographs for geological application. Both data have been processed, but the best results were obtained by interpreting original data. Classical image processing techniques were applied but they did not help much apart from geometrical correction which is essential for Landsat MSS images. Geological and structural interpretations were conducted for both types of data and compared. The results show that, even if Landsat MSS images provide a good approach for geological mapping, Spacelab photos allow more accurate and detailed interpretations. This is mostly due to the 20-meters resolution of the photos (80 meters for Landsat), and also to the potentiality of stereoscopic view (not immediate with Landsat). Spacelab data seem to be today the

best document a geologist can use to produce geologic and structural maps. Author

N87-22319* Bechtel National, Inc., San Francisco, Calif.
TECTONIC EVALUATION OF THE NUBIAN SHIELD OF NORTHEASTERN SUDAN USING THEMATIC MAPPER IMAGERY Final Report

CAROL TOSAYA, DAVID HARNISH, and RICHARD DAY Apr. 1987 255 p Original contains color illustrations Document contains maps as supplements
(Contract NAS5-28757)
(NASA-CR-180575; NAS 1.26:180575) Avail: Issuing Activity
CSCS 08B

Owing to the size, inaccessibility, and harsh, arid climate of the Red Sea Hills, remotely sensed satellite imagery is well suited for analysis of the region. An area of approximately 125,000 sq km of the northernmost Red Sea Hills, which contains the greatest amount of published geologic data using LANDSAT Thematic Mapper (TM) imagery was selected. The regional structure and lithotectonic provinces were defined and delineated. The tectonic evolution of the Nubian Shield was evaluated based on the image interpretation and the compiled tectonic maps. B.G.

N87-24043# Texas Univ., Austin. Bureau of Economic Geology.

LANDSAT-BASED LINEAMENT ANALYSIS, EAST TEXAS BASIN, AND STRUCTURAL HISTORY OF THE SABINE UPLIFT AREA, EAST TEXAS AND NORTH LOUISIANA Topical Report, Mar. 1984 - Nov. 1986

R. W. BAUMGARDNER and M. L. W. JACKSON 2 Mar. 1987 128 p
(Contract GRI-5082-211-0708)
(PB87-176327; GRI-87/0077) Avail: NTIS HC A07/MF A01
CSCS 08G

The relationship between subsurface structure and lineaments was examined. More than 2,200 lineaments were mapped from 1:250,000-scale LANDSAT images. Vector sums of greater-than-average values of length-weighted frequency define significant peaks of lineament orientation. For all lineaments, significant peaks occur at 325 degrees and 21 degrees. The northwest peak parallels mean azimuth of borehole elongations in Cotton Valley sandstone wells throughout East Texas. Lineament density delineates major fault zones. These results suggest that lineaments and subsurface structures results from like-oriented stresses. Identification of the timing, extent, and orientation of arching episodes in the Sabine Uplift areas is important in developing a structural history of the area. GRA

05

OCEANOGRAPHY AND MARINE RESOURCES

Includes sea-surface temperature, ocean bottom surveying imagery, drift rates, sea ice and icebergs, sea state, fish location.

A87-31572#

A CURIOUS SEA-SURFACE-TEMPERATURE PHENOMENON OBSERVED BY METEOSAT

D. R. KINDRED (ESA, European Space Organizations Centre, Darmstadt, West Germany) ESA Bulletin (ISSN 0376-4265), no. 48, Nov. 1986, p. 43-49.

Meteosat data processing procedures are described, noting their application to a sea surface-temperature (SST) anomaly observed on Aug. 26, 1985. SSTs are mainly determined from water vapor band data corrected atmospheric absorption. Several SSTs are acquired to form a composite image of the slowly-varying condition, and compared with reference fields developed from previously measured fields and, as an option, in situ ship data. The anomaly consisted of Mediterranean SSTs 5-10 C above those expected. Cool, fresh maritime air had entered the western Mediterranean,

05 OCEANOGRAPHY AND MARINE RESOURCES

accompanied by 15 kt surface winds, while the existing pressure gradient allowed quiet, calm hot weather to remain in the eastern Mediterranean. The passage of the frontal system caused significant mixing of the waters of the western region, thereby invalidating much of the SST data. M.S.K.

A87-31592

WEST ANTARCTIC ICE STREAMS DRAINING INTO THE ROSS ICE SHELF CONFIGURATION AND MASS BALANCE

SION SHABTAIE and CHARLES R. BENTLEY (Wisconsin, University, Madison) Journal of Geophysical Research (ISSN 0148-0227), vol. 92, Feb. 10, 1987, p. 1311-1336. refs
(Contract NSF DPP-81-20332; NSF DPP-84-12404)

Airborne radar sounding data, collected in 1984-1985, for the West Antarctic inland ice sheet, the Ross Ice Shelf, and the Crary Ice Rise are examined, and utilized to map the boundaries of the ice streams and their flow bands on the Ross Ice Shelf. In order to relate surface elevation data from satellite observations to sea level, three geoidal models (GEM 9, 10, and 10C) are evaluated by comparing them with elevations obtained from a hydrostatic model. The best correlation was observed between the GEM 10C model and the hydrostatic model with a difference of only 0.4 + or - 2.7 m. Consideration is given to the mass balance of the inland ice and of the Ross Ice Shelf. The surface elevation map derived with these data reveal that: (1) the three streams are up to 500 km long; (2) the surface of the streams A and B are crevassed and the boundaries are marked by chaotic, incoherent bands of surface crevasses; however, stream C has no crevasses; and (3) streams A and B overlie a deep subglacial channel and stream C is over a smoother and shallower subglacial trough. The overall net balance for this portion of the West Antarctic inland ice is estimated as -23 + or - 15 cu km/yr, and the volume melt rate for the Ross Ice Shelf is calculated as 60 + or - 15 cu km/yr, corresponding to a mean melt rate of 0.12 + or - 0.03 m/yr. I.F.

A87-31631

VHF RADAR FOR OCEAN SURFACE CURRENT AND SEA STATE REMOTE SENSING

P. BROCHE, P. FORGET, J. C. DE MAISTRE, J. L. DEVENON, and M. CROCHET (Toulon et Var, Universite, Toulon, France) Radio Science (ISSN 0048-6604), vol. 22, Jan.-Feb. 1987, p. 69-75. Research supported by the Institut National d'Astronomie et Geophysique, Conseil Regional de Provence-Cote d'Azur, and CNRS. refs

A meteorological ST radar operating at a frequency of 47.8 MHz has been used for remote sensing of sea state. General features of the Doppler spectra of the echoes are found to be the same as those obtained at HF; however, space resolution and intrinsic accuracy of the current velocity measurements can be significantly improved. Arguments are presented to suggest a potential range of a few tens of kilometers on the open sea if the full capabilities of ST radars are used. The experiment also shows that, when it is possible, the range could be extended by increasing the altitude of the radar. Author

A87-32097

MEASUREMENT OF THE SURFACE EMISSIVITY OF TURBID WATERS

WEN-YAO LIU, R. T. FIELD, R. G. GANTT, and V. KLEMAS (Delaware, University, Newark) Remote Sensing of Environment (ISSN 0034-4257), vol. 21, Feb. 1987, p. 97-109. refs
(Contract NSF CEE-82-10857)

Knowledge of sea surface emissivity is an important factor in measuring valid thermal IR radiometric temperatures from viewing positions both near the sea surface and from satellite platforms. In the latter case, it is found that the effect of as little as a 0.01 change in emissivity from a blackbody assumption may create an increase of as much as 1.0 C in recovered temperature in dry atmospheres, where recovered temperatures are radiometric temperatures obtained by applying the Planck function to radiances received at the satellite. As atmospheric moisture increases to around 5 g/sq cm variations in emissivity of the same order have

05 OCEANOGRAPHY AND MARINE RESOURCES

negligible effect on recovered sea surface temperatures. Laboratory measurements of fresh (tap) and sea water samples with a Barnes 8-14 micron PRT-5 radiometer show distinctive differences in the behavior of emissivity with changes in suspended sediment concentrations for both organic and inorganic materials. Tap water emissivity remains essentially invariant at 0.980 over a wide range of concentrations. In contrast, however, sea-water emissivity values show an immediate but steady decrease from 0.975 to a value 0.970, with increasing suspended sediment loading up to around 100 mg/l, where emissivity levels off until it falls again to a value of 0.962 at concentrations of 10,000 mg/l. Consequently, emissivity variations should not be neglected in making thermal measurements of coastal waters. Author

A87-32490

AUSTRALIAN UTILIZATION AND RESEARCH INTO REMOTE SENSING

KENNETH G. MCCracken (CSIRO, Office of Space Science and Applications, Canberra, Australia) IN: International Symposium on Space Technology and Science, 15th, Tokyo, Japan, May 19-23, 1986, Proceedings. Volume 2. Tokyo, AGNE Publishing, Inc., 1986, p. 1587-1592. refs

Uses of remote sensing (by the NOAA, NIMBUS, Landsat, Shuttle, and ARGOS-system instruments) in the mapping and management of the Australian continent are discussed together with recent research results and important research initiatives. Particular attention is given to the results obtained in mapping ocean currents and reefs and in predicting the areas of highest erosion risk. Recent results indicate that large long-lived eddies in the Tasman Sea exhibit angular momenta that vary as the 1.8th power of radius; in addition, a major new current system was discovered that travels along the southern coastline of the Australian continent. Based on Landsat data, a classification procedure was developed that provides bathymetric and geomorphological classifications of coral reefs, and an autocorrelation technique is being developed to quantify erosion in arid range lands. I.S.

A87-32497

MONITORING OF SNOW AND ICE IN HOKKAIDO ISLAND USING MULTITEMPORAL NOAA-AVHRR DATA

SHOJI TAKEUCHI, KANAME TAKEDA (Remote Sensing Technology Center of Japan, Tokyo), and HIROAKI OCHIAI (Toba Merchant Marine College, Japan) IN: International Symposium on Space Technology and Science, 15th, Tokyo, Japan, May 19-23, 1986, Proceedings. Volume 2. Tokyo, AGNE Publishing, Inc., 1986, p. 1637-1642.

A87-32499

MARINE OBSERVATION SATELLITE-1 (MOS-1)

YOSHIHIRO ISHIZAWA, TAKESHI MASUDA, and SUSUMU YOSHITOMI (National Space Development Agency of Japan, Tokyo) IN: International Symposium on Space Technology and Science, 15th, Tokyo, Japan, May 19-23, 1986, Proceedings. Volume 2. Tokyo, AGNE Publishing, Inc., 1986, p. 1651-1657.

The MOS-1 satellite, Japan's first remote sensing satellite, was scheduled for launch in early 1987 on-board the NASDA N-II launch vehicle. MOS-1 is to be used as a testbed for earth observation technologies, perform remote sensing of the sea and atmosphere, and enable basic research on a data acquisition system. Designed for a 2 yr lifetime, the satellite carries a multispectral electronic self-scanning radiometer, a visible and thermal IR radiometer, and a microwave scanning radiometer. The spacecraft is three axis stabilized with a controlled bias momentum apparatus. The instrumental operational components and performance capabilities, telemetry systems and ground segment are summarized. M.S.K.

A87-32503

THE FRENCH SPACE OCEANOGRAPHY PROGRAM

JEAN-LOUIS FELLOUS IN: International Symposium on Space Technology and Science, 15th, Tokyo, Japan, May 19-23, 1986, Proceedings. Volume 2. Tokyo, AGNE Publishing, Inc., 1986, p. 1689-1692.

The French Space Oceanography Program, aimed at improving current knowledge and understanding of the oceans and their role in climate, and at promoting potential applications of ocean observations from space, involves a series of flight instruments and dedicated satellite missions. Projects currently under development such as TOPEX-POSEIDON (a satellite system designed to make accurate, global measurements of the surface topography of the oceans) and ESA's ERS-1 are discussed in detail. Other projects of interest for space oceanography are the ARGOS data collection and platform location satellite system, and the first SPOT high resolution visible imagery satellite. T.K.

A87-32770* Texas Univ., Austin.

BIHARMONIC SPLINE INTERPOLATION OF GEOS-3 AND SEASAT ALTIMETER DATA

DAVID T. SANDWELL (Texas, University, Austin) Geophysical Research Letters (ISSN 0094-8276), vol. 14, Feb. 1987, p. 139-142. refs
(Contract NAG5-787)

An algorithm is presented for determining the minimum curvature surface passing through a set of nonuniformly spaced data points. The curve is generated as a linear combination of Green functions for the biharmonic operator at each data point, with the amplitudes of the functions adjusted so that the interpolating surfaces passes through each point. The function passing through the points can be regarded as a spline to which point forces are applied, defining the minimum curvature between the points. The technique was used to combine the along track slopes of the GEOS-3 and Seasat altimeter data into a consistent geoid height map of the Caribbean area, covering 0.5 million data points in the process. Sample images are provided and new topographic features that are revealed are discussed. M.S.K.

A87-32951

CORAL REEF REMOTE SENSING APPLICATIONS

DEBORAH A. KUCHLER, DAVID L. B. JUPP (CSIRO, Div. of Water and Land Resources, Canberra, Australia), DANIEL B. VAN R. CLAASEN (Great Barrier Reef Marine Park Authority, Townsville, Australia), and WILLIAM BOUR (Office de la Recherche Scientifique et Technique d'Outre-Mer, Noumea, New Caledonia) Geocarto International, no. 4, 1986, p. 3-15. Research supported by the Great Barrier Reef Marine Park Authority. refs

The application of remote sensing technology to coral reef research, management, and development is discussed. Consideration is given to reef geography, reef form, surface cover, vegetation, and oceanography. The remotely sensed data are utilized to provide information for coral reef resource assessment, to plan and map shipping routes, to locate potential fishing grounds, to study water circulation patterns, to analyze reef topography and morphology, and to develop maps of reef covers and reef vegetation. The use of remote sensing data in coral calcification and accretion studies is examined. I.F.

A87-32976#

OBSERVATIONS OF INTERMITTENT CUMULUS CONVECTION IN THE BOUNDARY LAYER

BURGHARD BRUEMMER (Hamburg, Universitaet, West Germany) and MELCHIOR WENDEL (Max-Planck-Institut fuer Meteorologie, Hamburg, West Germany) Royal Meteorological Society, Quarterly Journal (ISSN 0035-9009), vol. 113, Jan. 1987, p. 19-36. refs

During the September 1, 1978 radiosonde and tethered balloon measurements performed for the 1978 Joint Air Sea Interaction in the NE Atlantic, two cloud layers (cumulus below stratocumulus) were observed below an inversion at about 900 m. Cumulus clouds alternately appeared and disappeared; on September 1, a relatively large vertical shear was observed together with an inflection point in the profile of the wind component normal to the mean wind

direction. The small air-sea temperature difference and large dynamical contribution to cloud generation suggest an interaction between large scale processes generating a favorable mean wind shear profile and dynamically forced convection. The relative airflow in and around active cumulus clouds was characterized by updrafts within the clouds and downdrafts at the cloud edges; the thermodynamic properties of these phenomena are discussed.

O.C.

A87-32982*# Purdue Univ., West Lafayette, Ind.
CONVECTIVE HEATING AND PRECIPITATION ESTIMATES FOR THE TROPICAL SOUTH PACIFIC DURING FGGE, 10-18 JANUARY 1979

BERNARD L. MILLER and DAYTON G. VINCENT (Purdue University, West Lafayette, IN) Royal Meteorological Society, Quarterly Journal (ISSN 0035-9009), vol. 113, Jan. 1987, p. 189-212. NOAA-supported research. refs
 (Contract NAS8-35187; NSF ATM-84-05748)

Heat and moisture budgets are computed during part of the FGGE Special Observing Period-1 for an area containing the South Pacific convergence zone, deriving 12-hour precipitation rate estimates as residuals and comparing them with those derived from a GOES IR technique. Heat budget estimates are generally in good agreement with the IR estimates; the axis of maximum precipitation derived from the heat budget is well aligned with the lowest values of outgoing long wave excitation, which represent high, cold cloud tops resulting from deep cumulus convection. The vertical advection term is found to be the dominant term in the heat budget; this, together with radiative cooling, yields the approximate balance between adiabatic cooling and diabatic heating.

O.C.

A87-33430* National Aeronautics and Space Administration, Langley Research Center, Hampton, Va.
OH MEASUREMENT NEAR THE INTERTROPICAL CONVERGENCE ZONE IN THE PACIFIC

L. I. DAVIS, JR., JOHN V. JAMES, CHARLES C. WANG (Ford Motor Co., Dearborn, MI), CHUAN GUO, PETER T. MORRIS (Wayne State University, Detroit, MI), and JACK FISHMAN (NASA, Langley Research Center, Hampton, VA) Journal of Geophysical Research (ISSN 0148-0227), vol. 92, Feb. 20, 1987, p. 2020-2024. NASA-DOE-supported research. refs

Airborne measurements of OH were made near the Intertropical Convergence Zone in the Pacific, and the averaged results for each data run were compared with those calculated from a photochemical model. The measured OH concentrations were found to vary along the flight path. Possible causes for the observed variations are discussed.

Author

A87-33431* National Center for Atmospheric Research, Boulder, Colo.
MEASUREMENTS OF NITRIC OXIDE IN THE BOUNDARY LAYER AND FREE TROPOSPHERE OVER THE PACIFIC OCEAN

B. A. RIDLEY (National Center for Atmospheric Research, Boulder, CO), M. A. CARROLL (Cooperative Institute for Research in Environmental Sciences, Boulder, CO), and G. L. GREGORY (NASA, Langley Research Center, Hampton, VA) Journal of Geophysical Research (ISSN 0148-0227), vol. 92, Feb. 20, 1987, p. 2025-2047. NASA-NSF-supported research. refs

Measurements of NO and O₃ are presented from 13 aircraft flights made over the Pacific Ocean in the autumn of 1983 during one phase of the NASA Global Tropospheric Experiment. All of the flights were made between 15 deg and 42 deg N and from the coast of California to west of the Hawaiian Islands. Within the upper marine boundary layer the median daytime mixing ratio of NO was near 1 part per trillion by volume (pptv). Values of NO less than 10 pptv were often observed up to altitudes near 6 km. Thus for the location and season of the measurements, a net photochemical destruction of O₃ would be anticipated for the boundary layer region and to altitudes of 2-3 km. At higher altitudes of 7-11 km in the free troposphere, larger mixing ratios and greater variability were usually observed for NO. Both features are

consistent with observed examples of injection of NO and O₃ from the lower stratosphere and with the injection of NO from towering, electrically active, cumulonimbus clouds.

Author

A87-33432* Georgia Inst. of Tech., Atlanta
FREE TROPOSPHERIC AND BOUNDARY LAYER MEASUREMENTS OF NO OVER THE CENTRAL AND EASTERN NORTH PACIFIC OCEAN

D. D. DAVIS, J. D. BRADSHAW, M. O. RODGERS, S. T. SANDHOLM, and S. KESHENG (Georgia Institute of Technology, Atlanta) Journal of Geophysical Research (ISSN 0148-0227), vol. 92, Feb. 20, 1987, p. 2049-2070. refs
 (Contract NAG1-50)

Reported in this paper are the Georgia Institute of Technology NO results from the fall 1983 NASA GTE/CITE 1 Airborne Field Sampling Program. These data were predominantly collected over a geographical area defined by the eastern and central North Pacific Ocean, spanning the latitude range of 15-42 deg N. These NO measurements were taken using the two-photon laser-induced fluorescence technique. The data show a general trend of increasing levels of NO from the boundary layer up to altitudes of nearly 10 km. The average midday value of NO at altitudes of less than or equal to 1.8 km was 4 parts per trillion by volume (pptv), and at about 6 km, 20 pptv, whereas that at about 9 km was 25-35 pptv, the higher value reflecting the inclusion of NO data collected from the outflow region of two electrically active cumulonimbus clouds. The high-altitude NO data strongly suggest that at least during the time of the GTE flight operation, the major sources of NO for remote regions of the Pacific Ocean were those resulting from lightning and the downward transport of stratospheric air.

Author

A87-33435*# National Aeronautics and Space Administration, Washington, D.C.
CARBON MONOXIDE MEASUREMENTS OVER THE EASTERN PACIFIC DURING GTE/CITE 1

ESTELLE P. CONDON, EDWIN F. DANIELSEN (NASA, Ames Research Center, Moffett Field, CA), GLEN W. SACHSE, and GERALD F. HILL (NASA, Langley Research Center, Hampton, VA) Journal of Geophysical Research (ISSN 0148-0227), vol. 92, Feb. 20, 1987, p. 2095-2102. NASA-supported research. refs

As part of the Global Tropospheric Experiment's Chemical Instrumentation Test and Evaluation (GTE/CITE 1) intercomparison, carbon monoxide (CO) measurements were made from the NASA CV-990 aircraft during the fall of 1983 and again in the spring of 1984. The experimental measurements for CO obtained during those flight series over the eastern and mid-Pacific are presented here. Data were acquired from 10 to 20 deg N latitude over the mid-Pacific and from 30 to 37 deg N latitude over the eastern Pacific off the coast of California. A seasonal variation of approximately 34 parts per billion by volume was measured over the altitudes and latitudes sampled, and a small latitudinal variation was also noted. The data are discussed in terms of the meteorological context in which they were collected.

Author

A87-34447
REMOTE-SENSING METHOD FOR DETERMINING MONTHLY PRECIPITATION SUMS USING METEOR-SATELLITE DATA ON THE ATLANTIC OCEAN [DISTANTSIONNYI METOD OTSENKI MESIACHNYKH SUMM OSADKOV PO DANNYM ISZ 'METEOR' NA AKVATORII ATLANTICHESKOGO OKEANA]

A. A. ISAEV and O. N. NASONOVA IN: Aviation and satellite climatology. Moscow, Gidrometeoizdat, 1986, p. 50-54. In Russian.

The possibility of determining monthly precipitation sums under open-ocean conditions on the basis of Meteor-satellite cloud-cover data is examined for the example of the North Atlantic. Detailed multiyear maps of cloud cover, precipitation indices, and precipitation were compiled along with precipitation maps for individual years during 1975-1978 and 1980-1981 for October for the North Atlantic. The results obtained indicate that reliable

estimates of precipitation can be obtained from satellite data for regions where an observation network is absent. B.J.

A87-35148#

SEA SURFACE TEMPERATURE MEASUREMENT FROM SPACE ALLOWING FOR THE EFFECT OF THE STRATOSPHERIC AEROSOLS

T. TAKASHIMA and Y. TAKAYAMA (Meteorological Research Institute, Tsukuba, Japan) *Papers in Meteorology and Geophysics* (ISSN 0031-126X), vol. 37, Sept. 1986, p. 193-204. refs

A method of deriving the sea surface temperature (SST) from space is described by using the infrared channels of NOAA-AVHRR radiometer with reference to a model atmosphere-ocean system. It was found that, when free of stratospheric aerosols, the combined use of channels 3 (3.7 microns), 4 (11 microns) and 5 (12 microns) is effective for the SST derivation for a moderate amount of precipitable water. However, in the case of a large amount of water vapor, its vertical profile has to be simultaneously determined to correct for the water vapor effect. Furthermore, to evaluate the effect of the stratospheric aerosols on SST, the visible channels are also utilized for the atmospheric correction where the radiation from the atmosphere is affected more by the presence of stratospheric aerosols. Author

A87-35314

DETERMINATION OF THE VELOCITY OF OCEAN GYRES THROUGH SYNTHETIC APERTURE RADAR

N. K. VYAS and H. I. ANDHARIA (Indian Space Research Organisation, Space Applications Centre, Ahmedabad, India) *International Journal of Remote Sensing* (ISSN 0143-1161), vol. 8, Feb. 1987, p. 243-249. refs

The simple optical image undergoes blurring due to target motion, but the more complex aperture synthesis process of the Synthetic Aperture Radar (SAR) results in a shift in the position of the moving target. The different parts of an extended nonlinear target (such as an ocean eddy) are differentially shifted in the image plane and this leads to a geometric distortion of the shape of the target. In this paper, an attempt is made to analyze this distortion factor for the case of an ocean gyre and to express it as a function of the velocity of the gyre. The relationship thus arrived at has been applied to the innermost ring of an Atlantic Ocean gyre image by Shuttle Imaging Radar A. The velocity values (speed and direction) are retrieved under the assumption that the target ocean ring is circular in nature. The method appears promising for deriving the velocity field of the ocean gyres through SAR observations from remote platforms. Simultaneous optical observations, if available, will allow the estimation of velocity for ocean gyres/eddies with arbitrary shapes, without the necessity of assuming circularity. Author

A87-35315

LANDSAT IMAGE ENHANCEMENT STUDY OF POSSIBLE SUBMERGED SAND-DUNES IN THE ARABIAN GULF

KHATTAB G. AL-HINAI, JOHN MCMAHON MOORE, and PETER R. BUSH (Imperial College of Science and Technology, London, England) *International Journal of Remote Sensing* (ISSN 0143-1161), vol. 8, Feb. 1987, p. 251-258. Research sponsored by the University of Petroleum and Minerals (Saudi Arabia). refs

Digital image enhancement of selected Landsat Multispectral Scanner (MSS) image data for the coastal area of eastern Saudi Arabia reveals large sandbanks in relatively clear water, 8-10 m deep. The Landsat MSS imagery of wave length range 0.5-0.6 microns was masked digitally to remove onshore spectral data, and the contrast range of sea areas enhanced to display tonal variations which correspond in form to major barchanoid-shaped shoals on the sea floor. The shape, scale and orientation of the sandbanks suggest that they may be submerged aeolian dunes. If these sandbanks are submerged dunes, they predate the last eustatic sea level rise (8000-10,000 years BP) and must have been stabilized by cementation prior to submergence in order to survive palaeowind and current erosive action. Author

A87-35515

THE DEPENDENCE OF SEA-SURFACE MICROWAVE EMISSION ON WIND SPEED, FREQUENCY, INCIDENCE ANGLE, AND POLARIZATION OVER THE FREQUENCY RANGE FROM 1 TO 40 GHz

YASUNORI SASAKI, ICHIO ASANUMA, KEI MUNEYAMA, GENICHI NAITO, and TSUTOMU SUZUKI (Japan Marine Science and Technology Center, Yokosuka) *IEEE Transactions on Geoscience and Remote Sensing* (ISSN 0196-2892), vol. GE-25, March 1987, p. 138-146. refs

A87-35516

SEASONAL AND REGIONAL VARIATIONS OF ACTIVE/PASSIVE MICROWAVE SIGNATURES OF SEA ICE

CHARLES E. LIVINGSTONE, A. LAURENCE GRAY (Canada Centre for Remote Sensing, Ottawa), and KESHAVA P. SINGH (Banaras Hindu University, Varanasi, India) *IEEE Transactions on Geoscience and Remote Sensing* (ISSN 0196-2892), vol. GE-25, March 1987, p. 159-173. refs

Ku-band (13.3 GHz) scatterometer and K-band (19.4 GHz) radiometer data acquired by the CCRS CV-580 aircraft over the period from 1979 to 1982 in Canadian and Danish (Greenland) coastal waters have been analyzed to determine the seasonal and regional variations of microwave sea-ice signatures. A clustering analysis of the like and cross-polarized scattering cross sections and the H polarized emissivity has been used to identify distinct microwave sea-ice signatures for each ice type and to trace the evolution of these signatures with region and season. Ice-type signatures in the high Arctic under cold conditions are quite stable, and major ice classes are readily identified from microwave measurements. Under warmer conditions the signatures change with the structure, moisture content of the snow pack, and with the free water in the surface layers of the underlying ice. Author

A87-35517

MICROWAVE SEA-ICE SIGNATURES NEAR THE ONSET OF MELT

CHARLES E. LIVINGSTONE, A. LAURENCE GRAY, KESHAVA P. SINGH (Canada Centre for Remote Sensing, Ottawa), R. G. ONSTOTT (Kansas, University, Lawrence), and L. D. ARSENAULT (Cold Regions Remote Sensing, Stittsville, Canada) *IEEE Transactions on Geoscience and Remote Sensing* (ISSN 0196-2892), vol. GE-25, March 1987, p. 174-187. refs

On June 22, 1982, the Canada Centre for Remote Sensing's Convair 580 aircraft (CCRS CV-580) made X-band SAR, Ku-band scatterometer, and K-band radiometer measurements of the sea ice in Crozier Channel. Measurements of the physical properties of the ice and snow cover were in progress at a site in the southern portion of the CV-580 measurement area at the time of overflight. The CV-580 X-band SAR and Ku-band scatterometer were cross calibrated with the University of Kansas Heloscat to examine the frequency dependence of surface signatures. Analysis of the combined airborne and surface characterization data set shows that the microwave signatures of the surface, under the conditions present, were dominated by the snow cover and, in bare ice areas, by surface moisture. At frequencies above 9.35 GHz no scattering cross section/brightness temperature signatures could be uniquely related to ice type over the entire experiment area. Author

A87-35873

RAPID ANALYSIS OF SATELLITE RADAR IMAGES OF SEA ICE [OB EKSPRESS-ANALIZE KOSMICHESKIKH RADIOLOKATSIONNYYKH IZOBRAZHENII MORSKIKH L'DOV]

V. S. KRASIUK, M. NAZIROV, P. A. NIKITIN, and E. V. BUKHMAN (Gosudarstvennyi Nauchno-Issledovatel'skii Tsentr Izucheniia Prirodnykh Resursov, Moscow, USSR) *Meteorologiya i Gidrologiya* (ISSN 0130-2906), Feb. 1987, p. 70-75. In Russian. refs

Cosmos-1500 radar images of drifting Ross Sea ice are used to evaluate procedures and possibilities for the digital processing of incoming satellite information. Consideration is given to contour superposition, masking, tonal segmentation, and spatial

differentiation. It is concluded that the use of interactive processing techniques for the rapid analysis of images leads to greater reliability and clarity of the results. K.K.

A87-36101

USE OF SATELLITE ALTIMETRY FOR OCEAN MONITORING [ISPOL'ZOVANIE SPUTNIKOVOI VYSOTOMETRII V ZADACHAKH KONTROLIA ZA SOSTOIANIEM OKEANA]

V. L. DOROFEEV, I. E. TIMCHENKO, and A. B. FEDOTOV (AN USSR, Morskoi Gidrofizicheskii Institut, Sevastopol, Ukrainian SSR) *Issledovanie Zemli iz Kosmosa* (ISSN 0205-9614), Nov.-Dec. 1986, p. 3-10. In Russian. refs

The use of satellite altimetry data on sea-level variations in numerical dynamic stochastic models of the ocean state is demonstrated. The effect of altimeter measurement errors on the sea-level retrieval accuracy was determined using a quasi-geostrophic model of synoptic variations in world-ocean conditions. The approaches described are applicable for the satellite monitoring of the sea-level conditions and ocean currents. I.S.

A87-36107

MEASUREMENT OF THE SPATIAL SPECTRUM OF OCEAN WAVES USING A TWO-FREQUENCY SCATTEROMETER [K OPREDELENIU PROSTRANSTVENNOGO SPEKTRA VOLN S POMOSHCHIU DVUKHCHASTNOGO SKATTEROMETRA]

M. G. BULATOV, M. D. RAEV, E. I. SKVORTSOV, and V. S. ETKIN (AN SSSR, Institut Kosmicheskikh Issledovanii, Moscow, USSR) *Issledovanie Zemli iz Kosmosa* (ISSN 0205-9614), Nov.-Dec. 1986, p. 72-76. In Russian. refs

A two-frequency scatterometer (TFS) aboard an aircraft was used to determine the spatial spectrum of waves on the surface of the Black Sea. A TFS scheme with temporal separation of sounding and reception signals was tested. The method was found to permit measurements of the spectral characteristics of sea waves several meters long. The assessment of the experimentally derived spectral shapes agreed well with the spectral theory of wind waves. I.S.

A87-36945

AIRCRAFT RADIOPOSITIONING FOR AIRBORNE PHOTOGRAPHY DURING HYDROGRAPHIC COASTAL SURVEYS

J. M. CHIMOT and M. LE GOUIC (Service Hydrographique et Oceanographique de la Marine, Brest, France) *Societe Francaise de Photogrammetrie et de Teledetection, Bulletin* (ISSN 0244-6014), no. 103, 1986, p. 11-23. In French. refs

Results are reported from the development of radiopositioning techniques during two coastal hydrographic surveys of the Bay of Lannion using airborne photography. The overflight times were limited low tide of a calm sea with the sun in a clear sky was at least 30 deg over the horizon to ensure that bottom features were visible. The aircraft was flown at a constant altitude ASL while an on-board interrogator acquired positioning data from two, three or four TRIDENT III beacons in the vicinity of the Bay. Signal acquisition was electronically synchronized with photographic exposures and an on-board timing clock. Distances to the beacons were derived on the basis of the time between broadcast of the interrogation signal and the reception of the reply. Techniques used to reduce biases in the resulting position data are described. M.S.K.

A87-37056

PRELIMINARY REPORT ON THE DEVELOPMENT OF MARINE GEOGRAPHIC INFORMATION SYSTEMS

JOAN C. HOCK (NOAA, National Environmental Satellite, Data and Information Service, Washington, DC) *ITC Journal* (ISSN 0303-2434), no. 2, 1986, p. 156-163.

In combination with conventional in situ data gathering, NOAA scientists are using various satellite data sources in an attempt to create marine geographic information systems which could be of great assistance in - among other things monitoring and controlling coastal pollution and in exploiting fishery resources. Unlike

conventional geo-information systems dealing with relatively permanent topographic features, a marine system must accommodate the dynamic marine environment. The following is a preliminary report on progress to date in three test areas. Author

A87-37563* National Aeronautics and Space Administration. Goddard Space Flight Center, Greenbelt, Md.

RECURRING POLYNAS OVER THE COSMONAUT SEA AND THE MAUD RISE

J. C. COMISO (NASA, Goddard Spaceflight Center, Greenbelt, MD) and A. L. GORDON (Lamont-Doherty Geological Observatory, Palisades, NY) *Journal of Geophysical Research* (ISSN 0148-0227), vol. 92, March 15, 1987, p. 2819-2833. NASA-supported research. refs (Contract NSF DPP-85-02386)

Two remarkable deep ocean polynyas observed in the Antarctic region during the winter of 1980, here referred to as the Cosmonaut polynya and the Maud Rise polynya, are discussed. It is proposed that both polynyas are products of deep-reaching convection which introduces warmer deep water into the surface layer. Hydrographic data at both sites indicate the existence of localized doming of the pycnocline. This brings warmer, saltier deep water close to the sea surface, which has been demonstrated to be an effective preconditioner for deep-reaching convection. A possible relationship between the two polynyas is suggested in that both are in the eastern margins of the Weddell Sea. C.D.

A87-37564

LONG WAVES IN THE EQUATORIAL ATLANTIC OCEAN DURING 1983

RICHARD LEGECKIS (NOAA, National Environmental Satellite, Data, and Information Service, Washington, DC) and GILLES REVERDIN (CNRS, Paris, France) *Journal of Geophysical Research* (ISSN 0148-0227), vol. 92, March 15, 1987, p. 2835-2842. CNRS-supported research. refs

The undulations of the sea surface temperature (SST) front during June and July of 1983 are described, and the wave speed, length, and amplitude are estimated based on these observations. The trajectories of several FOCAL buoys are shown to be influenced by the position of the SST front. An attempt is made to resolve the 0.8 C bias found between the NESDIS operational global 100 km SST maps and the FOCAL drifting buoy measurements at 2 m as described by Reverdin et al. (1984). The SST measured by the buoys is compared to the raw satellite data using two advanced very high resolution radiometer (AVHRR) window channels to correct for atmospheric moisture absorption in cloud-free areas. It is demonstrated that there is a dependence of the satellite SST on the satellite zenith angle, and there is a small day-night bias in the satellite data. C.D.

A87-37565

COMPARISON OF SATELLITE-DERIVED SEA SURFACE TEMPERATURES WITH IN SITU SKIN MEASUREMENTS

P. SCHLUESSEL (Kiel, Universitaet, West Germany), H.-Y. SHIN, W. J. EMERY (British Columbia, University, Vancouver, Canada), and H. GRASSL (Forschungszentrum Geesthacht, West Germany) *Journal of Geophysical Research* (ISSN 0148-0227), vol. 92, March 15, 1987, p. 2859-2874. Research supported by the British Columbia Science Council, DFG, and NSERC. refs

Sea surface temperatures (SST) computed from sensor systems on the NOAA polar-orbiting satellites are compared with surface skin temperatures and subsurface temperature measurements. The importance of scan angle correction to define the correct atmospheric path is discussed, and the improvement of SST retrievals using sensor combination is demonstrated with satellite versus ship skin temperature mean differences ranging from 0.55 to 0.73 C for the advanced very high resolution radiometer (AVHRR) alone, from 0.39 to 0.71 C for AVHRR plus the TIROS operational vertical sounder (TOVS), and from 0.22 to 0.33 C for AVHRR plus high resolution infrared sounder (HIRS). The improved accuracy for AVHRR plus HIRS is due to additional correction for

the atmospheric water vapor and temperature structures made possible with some of the HIRS channels. C.D.

A87-37886

SATELLITE MEASUREMENTS OF SEA SURFACE COOLING DURING HURRICANE GLORIA

PETER CORNILLON (Rhode Island, University, Kingston), LOTHAR STRAMMA (Kiel, Universitaet, West Germany), and JAMES F. PRICE (Woods Hole Oceanographic Institution, MA) *Nature* (ISSN 0028-0836), vol. 326, March 26, 1987, p. 373-375. refs (Contract N00014-81-C-0062; N00014-84-C-0134)

Satellite-derived infrared images of the western North Atlantic are used here to study sea surface cooling (SSC) caused by hurricane Gloria (1985). Significant regional variations in SSC are well correlated with hydrographic conditions. The greatest cooling occurred in slope waters north of the Gulf Stream where the seasonal thermocline is shallowest and most compressed. Moderate cooling occurred in the open Sargasso Sea where the thermocline is deeper and more diffused. Little or no cooling occurred in shallow coastal waters which were isothermal before the passage of the hurricane. There is a pronounced right-side asymmetry of SSC with stronger and more extensive cooling found on the right side of the hurricane track. These qualitative results are consistent with the notion that vertical mixing within the upper ocean is the dominant SSC mechanism of hurricanes. C.D.

A87-38826* Johns Hopkins Univ., Laurel, Md. MEASURING OCEAN WAVES FROM SPACE; PROCEEDINGS OF THE SYMPOSIUM, JOHNS HOPKINS UNIVERSITY, LAUREL, MD, APR. 15-17, 1986

ROBERT C. BEAL, ED. (Johns Hopkins University, Laurel, MD) Symposium sponsored by NASA, U.S. Navy, and Johns Hopkins University. Johns Hopkins APL Technical Digest (ISSN 0270-5214), vol. 8, Jan.-Mar. 1987, 165 p. For individual items see A87-38827 to A87-38848.

Papers are presented on ocean-wave prediction; the quasi-universal form of the spectra of wind-generated gravity waves at different stages of their development; the limitations of the spectral measurements and observations of the group structure of surface waves; the effect of swell on the growth of wind wave; operational wave forecasting; ocean-wave models, and seakeeping using directional wave spectra. Consideration is given to microwave measurements of the ocean-wave directional spectra; SIR research; estimating wave energy spectra from SAR imagery, with the radar ocean-wave spectrometer, and SIR-B; the wave-measurement capabilities of the surface contour radar and the airborne oceanographic lidar; and SIR-B ocean-wave enhancement with fast-Fourier transform techniques. Topics discussed include wave-current interaction; the design and applicability of Spectrasat; the need for a global wave monitoring system; the age and source of ocean swell observed in Hurricane Josephine; and the use of satellite technology for insulin treatment. I.F.

A87-38831

THE PRESENT STATUS OF OPERATIONAL WAVE FORECASTING

VINCENT J. CARDONE (Ocean-Weather, Inc., Cos Cob, CT) (NASA, U.S. Navy, and Johns Hopkins University, Symposium on Measuring Ocean Waves from Space, Laurel, MD, Apr. 15-17, 1986) Johns Hopkins APL Technical Digest (ISSN 0270-5214), vol. 8, Jan.-Mar. 1987, p. 24-32. refs

The basic structure and behavior of first- and second-generation waves models, in particular their propagation schemes and source terms, are examined. The capabilities of operational wave-prediction models for storm hindcasting, wave climate assessment, and real-time applications are evaluated. The development of third-generation models based on improved representations of physical processes of wave growth, wave-wave interactions, and wave dissipation is described, and the benefits to be provided by the third-generation models to wave forecasting are discussed. I.F.

A87-38832

THE OPERATIONAL PERFORMANCE OF THE FLEET NUMERICAL OCEANOGRAPHY CENTER GLOBAL SPECTRAL OCEAN-WAVE MODEL

LIANA F. ZAMBRESKY (European Centre for Medium Range Weather Forecasting, Reading, England) (NASA, U.S. Navy, and Johns Hopkins University, Symposium on Measuring Ocean Waves from Space, Laurel, MD, Apr. 15-17, 1986) Johns Hopkins APL Technical Digest (ISSN 0270-5214), vol. 8, Jan.-Mar. 1987, p. 33-36. refs

An operational 72-hour global wave forecast was made at the Fleet Numerical Oceanography Center, but because of the inaccuracy and scarceness of suitable wave observations, the wave forecast remains uninitialized by any observations. Present model performance is given in order to learn what degree of improvement might be expected should directional wave spectral observations from satellites become available. Author

A87-38833

RECENT RESULTS WITH A THIRD-GENERATION OCEAN-WAVE MODEL

GERBRAND J. KOMEN (Koninklijk Nederland Meteorologisch Instituut, DeBilt, Netherlands) (NASA, U.S. Navy, and Johns Hopkins University, Symposium on Measuring Ocean Waves from Space, Laurel, MD, Apr. 15-17, 1986) Johns Hopkins APL Technical Digest (ISSN 0270-5214), vol. 8, Jan.-Mar. 1987, p. 37-41. refs (Contract NATO-27-0523/85)

The applicability of third-generation ocean-wave models is evaluated using the CRAY computer at the European Centre for Medium Range Weather Forecasting. A prototype model was tested for a global run, a regional hindcast of extratropical storms, and a regional hindcast of hurricanes. The test results are compared with observational data and good correlation is observed. The use of satellite wave observations for model validation and data assimilation is examined. I.F.

A87-38835

SOME APPROACHES FOR COMPARING REMOTE AND IN-SITU ESTIMATES OF DIRECTIONAL WAVE SPECTRA

WILLARD J. PIERSON, JR. (City College, New York) (NASA, U.S. Navy, and Johns Hopkins University, Symposium on Measuring Ocean Waves from Space, Laurel, MD, Apr. 15-17, 1986) Johns Hopkins APL Technical Digest (ISSN 0270-5214), vol. 8, Jan.-Mar. 1987, p. 48-54. Research supported by the National Data Buoy Center. refs

Radar imaging systems inherently measure different properties of the spectrum than do the more traditional directional wave buoys. Analysis of the present methods of measuring heave acceleration, pitch, and roll on buoys under development by the National Data Buoy Center (NDBC) explains some of the inconsistencies that have been found not only for NDBC buoys but also for other directional wave buoys. The methods used for buoys can be extended to airborne and spaceborne systems in order to compare spectra estimated by the different systems. Author

A87-38836

THE MICROWAVE MEASUREMENT OF OCEAN-WAVE DIRECTIONAL SPECTRA

WILLIAM J. PLANT (U.S. Navy, Naval Research Laboratory, Washington, DC) (NASA, U.S. Navy, and Johns Hopkins University, Symposium on Measuring Ocean Waves from Space, Laurel, MD, Apr. 15-17, 1986) Johns Hopkins APL Technical Digest (ISSN 0270-5214), vol. 8, Jan.-Mar. 1987, p. 55-59. refs

Basic principles of six microwave techniques that have been used to measure ocean-wave directional spectra from aircraft are described. Three of these techniques - synthetic aperture radar, the short pulse scanning beam spectrometer, and the two-frequency resonance scanning beam spectrometer - are proposed as possible ways to measure global directional spectra from satellites. Author

A87-38839* National Aeronautics and Space Administration. Goddard Space Flight Center, Greenbelt, Md.

THE PHYSICAL BASIS FOR ESTIMATING WAVE-ENERGY SPECTRA WITH THE RADAR OCEAN-WAVE SPECTROMETER
FREDERICK C. JACKSON (NASA, Goddard Space Flight Center, Greenbelt, MD) (NASA, U.S. Navy, and Johns Hopkins University, Symposium on Measuring Ocean Waves from Space, Laurel, MD, Apr. 15-17, 1986) Johns Hopkins APL Technical Digest (ISSN 0270-5214), vol. 8, Jan.-Mar. 1987, p. 70-73. refs

The derivation of the reflectivity modulation spectrum of the sea surface for near-nadir-viewing microwave radars using geometrical optics is described. The equations required for the derivation are presented. The derived reflectivity modulation spectrum provides data on the physical basis of the radar ocean-wave spectrometer measurements of ocean-wave directional spectra. I.F.

A87-38840* National Aeronautics and Space Administration. Goddard Space Flight Center, Greenbelt, Md.

WAVE-MEASUREMENT CAPABILITIES OF THE SURFACE CONTOUR RADAR AND THE AIRBORNE OCEANOGRAPHIC LIDAR

EDWARD J. WALSH (NASA, Goddard Space Flight Center, Greenbelt, MD), DAVID W. HANCOCK, III, DONALD E. HINES (NASA, Wallops Flight Center, Wallops Island, VA), ROBERT N. SWIFT, and JOHN F. SCOTT (EG&G Washington Analytical Services Center, Inc., Pocomoke City, MD) (NASA, U.S. Navy, and Johns Hopkins University, Symposium on Measuring Ocean Waves from Space, Laurel, MD, Apr. 15-17, 1986) Johns Hopkins APL Technical Digest (ISSN 0270-5214), vol. 8, Jan.-Mar. 1987, p. 74-81. refs

The 36-gigahertz surface contour radar and the airborne oceanographic lidar were used in the SIR-B underflight mission off the coast of Chile in October 1984. The two systems and some of their wave-measurement capabilities are described. The surface contour radar can determine the directional wave spectrum and eliminate the 180-degree ambiguity in wave propagation direction that is inherent in some other techniques such as stereophotography and the radar ocean wave spectrometer. The Airborne Oceanographic Lidar can acquire profile data on the waves and produce a spectrum that is close to the nondirectional ocean-wave spectrum for ground tracks parallel to the wave propagation direction. Author

A87-38841

A PRACTICAL METHODOLOGY FOR ESTIMATING WAVE SPECTRA FROM THE SIR-B

FRANK M. MONALDO (Johns Hopkins University, Laurel, MD) (NASA, U.S. Navy, and Johns Hopkins University, Symposium on Measuring Ocean Waves from Space, Laurel, MD, Apr. 15-17, 1986) Johns Hopkins APL Technical Digest (ISSN 0270-5214), vol. 8, Jan.-Mar. 1987, p. 82-86. refs

A step-by-step procedure is outlined to convert synthetic aperture radar imagery into estimates of ocean surface-wave spectra. The procedure is based on a linearized version of a model that relates synthetic aperture radar image intensity spectra and wave slope- or height-variance spectra. The outlined procedure is applied to synthetic aperture radar imagery from the Shuttle Imaging Radar mission and is shown to produce spectra that, except in the lowest sea state, are highly correlated with two-dimensional spectra measured independently. Author

A87-38843* National Oceanic and Atmospheric Administration, Seattle, Wash.

THE AGE AND SOURCE OF OCEAN SWELL OBSERVED IN HURRICANE JOSEPHINE

FRANK I. GONZALEZ (NOAA, Pacific Marine Environmental Laboratory, Seattle, WA), BENJAMIN M. HOLT (California Institute of Technology, Jet Propulsion Laboratory, Pasadena), and DAVID G. TILLEY (Johns Hopkins University, Laurel, MD) (NASA, U.S. Navy, and Johns Hopkins University, Symposium on Measuring Ocean Waves from Space, Laurel, MD, Apr. 15-17, 1986) Johns Hopkins APL Technical Digest (ISSN 0270-5214), vol. 8, Jan.-Mar. 1987, p. 94-99. refs

A simple kinematic model is applied to SIR-B observations in the far field of Hurricane Josephine in order to estimate the swell origin in space and time. The SIR data was obtained on October 12, 1984, and the geometry of the hurricane swell kinematic model is described. Estimates of the wavenumber and wave age and generation regions of the system are graphically presented and examined. The data reveal that the waves of Hurricane Josephine were generated 0-9 hours before the SIR-B overpass. I.F.

A87-38845* Johns Hopkins Univ., Laurel, Md.

SPECTRASAT - A HYBRID ROWS/SAR APPROACH TO MONITOR OCEAN WAVES FROM SPACE

ROBERT C. BEAL (Johns Hopkins University, Laurel, MD) (NASA, U.S. Navy, and Johns Hopkins University, Symposium on Measuring Ocean Waves from Space, Laurel, MD, Apr. 15-17, 1986) Johns Hopkins APL Technical Digest (ISSN 0270-5214), vol. 8, Jan.-Mar. 1987, p. 107-115. Research supported by the Johns Hopkins University, NASA, and U.S. Navy. refs

Evidence from both Seasat and the Shuttle Imaging Radar indicates that Doppler contamination in synthetic aperture radar (SAR) at the shorter azimuth (along-track) ocean wavelengths can seriously limit the instrument performance. Although the problem is alleviated at low orbital altitudes, it is never completely eliminated, particularly for higher wave slopes. By combining a SAR with a conically scanning altimeter (a radar ocean-wave spectrometer) on a common low-altitude platform, the disadvantages of each tend to be offset by the advantages of the other. Thus, a hybrid combination of the two may be the most practical approach to monitoring ocean waves from space. Author

A87-38846* National Aeronautics and Space Administration. Goddard Space Flight Center, Greenbelt, Md.

THE RADAR OCEAN-WAVE SPECTROMETER

FREDERICK C. JACKSON (NASA, Goddard Space Flight Center, Greenbelt, MD) (NASA, U.S. Navy, and Johns Hopkins University, Symposium on Measuring Ocean Waves from Space, Laurel, MD, Apr. 15-17, 1986) Johns Hopkins APL Technical Digest (ISSN 0270-5214), vol. 8, Jan.-Mar. 1987, p. 116-127. refs

The scanning-beam Radar Ocean-Wave Spectrometer (ROWS) technique is described. The derivation of a spectrum for the reflectivity modulation as a function of range is examined. The usefulness of the ROWS technique was initially validated using aircraft data obtained in 1978 with the GSFC Ku-band pulse-compression radar; additional examples of aircraft data which verify the effectiveness of the ROWS technique are presented. The development of a ROWS mode for Spectrasat is discussed. Consideration is given to the incidence angle, twin beam option for cross-section roll-off and wind vector determination, rotation rate, antenna and footprint dimensions, integration time, sphericity effects, and a processor configuration. A design for the ROWS-mode time-domain processor on Spectrasat is proposed. The performance of the system is evaluated, and it is determined that the system performs well. I.F.

05 OCEANOGRAPHY AND MARINE RESOURCES

A87-38847

SPECTRASAT INSTRUMENT DESIGN USING MAXIMUM HERITAGE

JOHN L. MACARTHUR (Johns Hopkins University, Laurel, MD) (NASA, U.S. Navy, and Johns Hopkins University, Symposium on Measuring Ocean Waves from Space, Laurel, MD, Apr. 15-17, 1986) Johns Hopkins APL Technical Digest (ISSN 0270-5214), vol. 8, Jan.-Mar. 1987, p. 128-132. Research supported by the Johns Hopkins University.

The design and components of the Spectrasat RA/ROWS/SAR (radar altimeter/radar ocean wave spectrometer/synthetic aperture radar) are described. The C-band power amplifier uses a waveform with a high pulse-repetition-frequency burst in which 102.4 microsec pulses are transmitted at a rate of about 5 kHz; the transmission and reception schemes for the amplifier are illustrated. The basic features of the instrument are discussed. The receiver design is examined; in the altimeter mode, the local oscillator is a chirped pulse that matches the transmitted chirp to implement full-deramp processing and to transform range offset to frequency offset and at the other times, the Ku-band local oscillator is a continuous wave signal to process the off-nadir ROWS returns. The design and functions of the ROWS and SAR processors are considered.

I.F.

A87-38848

A SPECTRASAT SYSTEM DESIGN BASED ON THE GEOSAT EXPERIMENT

CHARLES C. KILGUS and WILLIAM E. FRAIN (Johns Hopkins University, Laurel, MD) (NASA, U.S. Navy, and Johns Hopkins University, Symposium on Measuring Ocean Waves from Space, Laurel, MD, Apr. 15-17, 1986) Johns Hopkins APL Technical Digest (ISSN 0270-5214), vol. 8, Jan.-Mar. 1987, p. 133-137. Research supported by the Johns Hopkins University.

The design and components of the Spectrasat system which operates in a 275-km altitude, sun-synchronous orbit and simultaneously measures wave spectra at C- and Ku-bands are described. The Spectrasat spacecraft, with a configuration based on Geosat, provides the systems needed to support the radar instrument. The components and functions of the command, telemetry, Doppler, power, attitude control, and velocity control systems are examined. The ground support for Spectrasat is discussed. Spectrasat stores data for about 9 hrs and then transmits it to the Johns Hopkins University Applied Physics Laboratory for archiving, processing, and distributing. Consideration is given to the RF, digital, and computer elements of the ground station, and the command, control, and monitor; sensor data record; and real-time data record software packages.

I.F.

A87-39176 San Diego State Univ., Calif.

REMOTELY-SENSED TRACERS FOR HYDRODYNAMIC SURFACE FLOW ESTIMATION

D. A. STOW (San Diego State University, CA) International Journal of Remote Sensing (ISSN 0143-1161), vol. 8, March 1987, p. 261-278. Research supported by the University of California and NASA. refs

Research results concerning tracers useful for estimating hydrodynamic surface flow are reported. Tracer characteristics analyzed include spectral signatures, mapping transformations, sensor penetration depths, conservativeness and horizontal variability. Fluorescent dye is limited in usefulness to small area Lagrangean drift estimates. Suspended sediments and salinity are limited to single-date descriptive and Lagrangean drift estimates for estuarine and adjacent coastal waters. Chlorophyll pigments and surface temperature are the most ubiquitous properties and hold the most potential to be useful tracers. This is particularly the case for coarse- to meso-scale circulation of coastal ocean waters. Potential drawbacks of chlorophyll and surface temperatures as tracers must be overcome prior to their successful application for flow estimations by: (1) compensating for nonconservative sources/sinks; (2) achieving imaging precision sufficient to resolve tracer levels at smaller space scale; and (3) acquiring the ability to remove spatially inhomogeneous atmospheric effects.

Author

A87-39178

A TWO-LOOK TECHNIQUE FOR STUDYING ATMOSPHERIC EFFECTS IN OPTICAL SCANNER DATA FOR THE OCEAN

G. KHOSRAVIANI and A. P. CRACKNELL (Dundee, University, Scotland) International Journal of Remote Sensing (ISSN 0143-1161), vol. 8, March 1987, p. 291-308. refs

The traditional method for validating calculated values of chlorophyll concentration in the sea is based on comparisons with in situ point measurements made from ships. An alternative approach based on a two-look method involving data from successive orbits of the Nimbus-7 satellite is presented. The results of some calculations, based on the use of Coastal Zone Color Scanner data, for the Irish Sea viewed from two successive orbits of the Nimbus-7 satellite are presented. The method used involves a first attempt at a self-consistent approach to calculating the aerosol path radiance. Results are presented for two pairs of scenes from Apr. 6, 1980 and May 4, 1980.

Author

A87-39179

THE EFFECT OF A NON-GAUSSIAN POINT TARGET RESPONSE FUNCTION ON RADAR ALTIMETER RETURNS FROM THE SEA SURFACE

P. G. CHALLENGER, M. A. SROKOSZ (Institute of Oceanographic Sciences, Wormley, England), and B. GRECO (European Space Research Institute, Frascati, Italy) International Journal of Remote Sensing (ISSN 0143-1161), vol. 8, March 1987, p. 309-313. refs

In order to derive nonlinear wave parameters from radar altimeter data it is necessary to model the return from the sea surface. Most models assume a Gaussian point target response for the radar, whereas in practice it was found for the Seasat altimeter that the response was non-Gaussian. The effect of a non-Gaussian point target response on the retrieval of nonlinear wave parameters is examined here, using a model based on a Gram-Charlier series. It is found that if the transmitted pulse width is sufficiently small then a non-Gaussian point target response has little effect on the retrieval of nonlinear wave parameters.

Author

A87-39180* Naval Research Lab., Washington, D.C.

AIRBORNE MICROWAVE DOPPLER MEASUREMENTS OF OCEAN WAVE DIRECTIONAL SPECTRA

W. J. PLANT, W. C. KELLER, A. B. REEVES, E. A. ULIANA (U.S. Navy, Naval Research Laboratory, Washington, DC), and J. W. JOHNSON (NASA, Langley Research Center, Hampton, VA) International Journal of Remote Sensing (ISSN 0143-1161), vol. 8, March 1987, p. 315-330. refs

A technique is presented for measuring ocean wave directional spectra from aircraft using microwave Doppler radar. The technique involves backscattering coherent microwave radiation from a patch of sea surface which is small compared to dominant ocean wavelengths in the antenna look direction, and large compared to these lengths in the perpendicular (azimuthal) direction. The mean Doppler shift of the return signal measured over short time intervals is proportional to the mean sea surface velocity of the illuminated patch. Variable sea surface velocities induced by wave motion therefore produce time-varying Doppler shifts in the received signal. The large azimuthal dimension of the patch implies that these variations must be produced by surface waves traveling near the horizontal antenna look direction thus allowing determination of the direction of wave travel. Linear wave theory is used to convert the measured velocities into ocean wave spectral densities. Spectra measured simultaneously with this technique and two laser profilometers, and nearly simultaneous with this technique and two laser profilometers, and nearly simultaneous with a surface buoy, are presented. Applications and limitations of this airborne Doppler technique are discussed.

Author

A87-39462* National Aeronautics and Space Administration. Goddard Space Flight Center, Greenbelt, Md.

TWO-COLOR SHORT-PULSE LASER ALTIMETER MEASUREMENTS OF OCEAN SURFACE BACKSCATTER

JAMES B. ABSHIRE and JAN F. MCGARRY (NASA, Goddard Space Flight Center, Greenbelt, MD) Applied Optics (ISSN 0003-6935), vol. 26, April 1, 1987, p. 1304-1311. refs

The timing and correlation properties of pulsed laser backscatter from the ocean surface have been measured with a two-color short-pulse laser altimeter. The Nd:YAG laser transmitted 70- and 35-ps wide pulses simultaneously at 532 and 355 nm at nadir, and the time-resolved returns were recorded by a receiver with 800-ps response time. The time-resolved backscatter measured at both 330-m and 1291-m altitudes showed little pulse broadening due to the submeter laser spot size. The differential delay of the 355-nm and 532-nm backscattered waveforms were measured with a rms error of about 75 ps. The change in aircraft altitudes also permitted the change in atmospheric pressure to be estimated by using the two-color technique. Author

A87-40250* National Aeronautics and Space Administration. Goddard Inst. for Space Studies, New York, N.Y.

REGIONAL AND SEASONAL VARIATIONS OF SURFACE REFLECTANCE FROM SATELLITE OBSERVATIONS AT 0.6 MICRON

ELAINE MATTHEWS and WILLIAM B. ROSSOW (NASA, Goddard Institute for Space Studies, New York) Journal of Climate and Applied Meteorology (ISSN 0733-3021), vol. 26, Jan. 1987, p. 170-202. refs

A global series of seasonal visible surface reflectance maps derived from NOAA-5 Scanning Radiometer observations is presented. Methods for isolating clear-sky observations from satellite data are evaluated and the magnitude of atmospheric effects (Rayleigh scattering and ozone absorption) are presented. A preliminary analysis of digital vegetation and soils data bases, which were analyzed in conjunction with the satellite observations, is discussed. Regional and global reflectance homogeneity of land-cover types, and snow brightening for types, are presented. Results demonstrate that the statistical approach for isolating clear-sky radiances used in this study obtains accurate enough values for each location to allow meaningful measurements of seasonal, spatial and ecosystem variations in surface reflectance. Author

A87-40281

THE GEOSAT ALTIMETER MISSION - A MILESTONE IN SATELLITE OCEANOGRAPHY

ROBERT CHENEY, BRUCE DOUGLAS, RUSSELL AGREEN, LAURY MILLER, DENNIS MILBERT (NOAA, National Ocean Service, Rockville, MD) et al. EOS (ISSN 0096-3941), vol. 67, Dec. 2, 1986, p. 1354, 1355. refs

The operation of the U.S. Navy Geosat oceanographic altimeter is described, and some principal results are summarized. During the first 18 months of operation after its launch to a 108-deg-inclination orbit in April 1985, Geosat collected 270 million 2-cm-accuracy sea-level observations (including about 35 million crossovers) along 200 million km of ocean. A primary aim is the construction of long time series of sea-level observations over the tropical Pacific. Sample data are presented in graphs and briefly characterized. T.K.

A87-40289* National Aeronautics and Space Administration. Goddard Space Flight Center, Greenbelt, Md.

FEEDBACK BETWEEN ICE FLOW, BAROTROPIC FLOW, AND BAROCLINIC FLOW IN THE PRESENCE OF BOTTOM TOPOGRAPHY

SIRPA HAKKINEN (NASA, Goddard Space Flight Center, Greenbelt, MD) Journal of Geophysical Research (ISSN 0148-0227), vol. 92, April 15, 1987, p. 3807-3820. refs

Coupling between externally driven barotropic flow and locally driven baroclinic flow in the presence of an ice cover and topography is studied. The topography is a necessary ingredient in this coupling. This study shows that the observed mesoscale

activity of the ice edge seen in satellite imagery does not necessarily reflect the mesoscale baroclinic activity in the ocean. Besides oceanic eddies, the ice cover can trace the topographic changes via the coupling to the barotropic flow. A two-layer ocean model coupled to an ice model is constructed to simulate an ice-ocean system with a varying bottom topography. In the absence of wind, forcing the ice cover reflects the externally driven barotropic ocean response, especially topographically forced Taylor columns by forming ice streamers or meanders. Some of these features propagate (advected with the ocean currents) as a whole downstream, creating an image of eddy propagation even though there is no baroclinic structure underneath. When downwelling favorable winds (ice on the left from the wind direction) are turned on, in addition to this background barotropic flow, the Ekman flow in the ocean (toward the open ocean) will enhance the meandering of the ice edge due to the barotropic flow. During upwelling favorable winds, the ice edge stays rather compact, including the case when a strong baroclinic, cyclonic vortex is developing beneath an ice meander supported by the Taylor column in the ocean. Author

A87-40432

ICE-EDGE EDDIES IN THE FRAM STRAIT MARGINAL ICE ZONE

O. M. JOHANNESSEN, J. A. JOHANNESSEN, E. SVENDSEN (Bergen, Universitetet, Norway), R. A. SHUCHMAN (Michigan, Environmental Research Institute, Ann Arbor), W. J. CAMPBELL (USGS, Tacoma, WA) et al. Science (ISSN 0036-8075), vol. 236, April 24, 1987, p. 427-429. Research supported by the Bergen Universitetet, Norges Teknisk-Naturvitens-Rapelige Forskningsrad, Norges Almenvitenskapelige Forskningsrad, Navy, and USGS. refs

Five prominent ice-edge eddies in Fram Strait on the scale of 30 to 40 kilometers were observed over deep water within 77 deg N to 79 deg N and 5 deg W to 3 deg E. The use of remote sensing, a satellite-tracked buoy, and in situ oceanographic measurements showed the presence of eddies with orbital speeds of 30 to 40 cm per second and lifetimes of at least 20 days. Ice ablation measurements made within one of these ice-ocean eddies indicated that melting, which proceeded at rates of 20 to 40 cm per day, is an important process in determining the ice-edge position. These studies give new insight on the formation, propagation, and dissipation of ice-edge eddies. Author

A87-40433

REMOTE SENSING OF THE FRAM STRAIT MARGINAL ICE ZONE

R. A. SHUCHMAN, B. A. BURNS (Michigan, Environmental Research Institute, Ann Arbor), O. M. JOHANNESSEN (Bergen, Universitetet, Norway), E. G. JOSBERGER, W. J. CAMPBELL (USGS, Tacoma, WA) et al. Science (ISSN 0036-8075), vol. 236, April 24, 1987, p. 429-431. refs

(Contract N00014-81-C-0295; N00014-83-C-0404)

Sequential remote sensing images of the Fram Strait marginal ice zone played a key role in elucidating the complex interactions of the atmosphere, ocean, and sea ice. Analysis of a subset of these images covering a 1-week period provided quantitative data on the mesoscale ice morphology, including ice edge positions, ice concentrations, flow size distribution, and ice kinematics. The analysis showed that, under light to moderate wind conditions, the morphology of the marginal ice zone reflects the underlying ocean circulation. High-resolution radar observations showed the location and size of ocean eddies near the ice edge. Ice kinematics from sequential radar images revealed an ocean eddy beneath the interior pack ice that was verified by in situ oceanographic measurements. Author

05 OCEANOGRAPHY AND MARINE RESOURCES

A87-40434

MESOSCALE OCEANOGRAPHIC PROCESSES BENEATH THE ICE OF FRAM STRAIT

T. O. MANLEY, K. L. HUNKINS (Lamont-Doherty Geological Observatory, Palisades, NY), J. Z. VILLANUEVA (Miami, University, FL), J. C. GASCARD, P. F. JEANNIN (Paris VI, Université, France) et al. Science (ISSN 0036-8075), vol. 236, April 24, 1987, p. 432-434. Sponsorship: Centre National pour l'Exploitation des Océans. refs

(Contract CNEXO-84/3147; N00014-76-C-0004; N00014-84-C-0132; N00014-83-K-0020; CEC-CLI-083-F; CNRS-981-022)

A major component of the Fram Strait Marginal Ice Zone Experiment was the investigation of air-sea-ice interactions, processes, and circulation patterns found behind the local ice edge and on scales greater than 10 kilometers (mesoscale and large scale). Neutrally buoyant floats, ice-tethered cyclesondes, and helicopter-based measurements were used to obtain uniquely integrated and consistent views of the mesoscale ocean features beneath the ice cover of Fram Strait. Within the vicinity of the Yermak Plateau, three distinct regions of mesoscale motion were observed that coincided with the shallow topography of the plateau, the northward flowing Atlantic water over the western flank of the plateau, and the strong current-shear zone of the East Greenland Polar Front. A subice meander of the front was also observed, which was probably occluded subsequently. Author

A87-40648* Jet Propulsion Lab., California Inst. of Tech., Pasadena.

REMOTE SENSING AS A RESEARCH TOOL

F. D. CARSEY (California Institute of Technology, Jet Propulsion Laboratory, Pasadena) and H. J. ZWALLY (NASA, Goddard Space Flight Center, Greenbelt, MD) IN: The geophysics of sea ice. New York, Plenum Publishing Corp., 1986, p. 1021-1098. refs

The application of aircraft and spacecraft remote sensing techniques to sea ice surveillance is evaluated. The effects of ice in the air-sea-ice system are examined. The measurement principles and characteristics of remote sensing methods for aircraft and spacecraft surveillance of sea ice are described. Consideration is given to ambient visible light, IR, passive microwave, active microwave, and laser altimeter and sonar systems. The applications of these systems to sea ice surveillance are discussed and examples are provided. Particular attention is placed on the use of microwave data and the relation between ice thickness and sea ice interactions. It is noted that spacecraft and aircraft sensing techniques can successfully measure snow cover; ice thickness; ice type; ice concentration; ice velocity field; ocean temperature; surface wind vector field; and air, snow, and ice surface temperatures. I.F.

A87-40835

THE PROPAGATION OF SHORT SURFACE WAVES ON LONGER GRAVITY WAVES

M. S. LONGUET-HIGGINS (Cambridge University; Institute of Oceanographic Sciences, Wormley, England) Journal of Fluid Mechanics (ISSN 0022-1120), vol. 177, April 1987, p. 293-306. refs

The theoretical variations in the wavelength and steepness of short gravity waves propagated over the surface of a train of longer gravity waves of finite amplitude may be calculated once the orbital accelerations and surface velocities in the longer waves have been accurately determined. Use is presently made of a fully nonlinear theory indicating that for longer waves, the short wave steepness can be increased at the crests of the longer waves by a factor of order 8, compared with its value at the mean level; by contrast, linear theory gives a factor of less than 2. O.C.

A87-41068

MULTILOOK IMAGES OF OCEAN WAVES BY SYNTHETIC APERTURE RADARS

KAZUO OUCHI (King's College, London, England) IEEE Transactions on Antennas and Propagation (ISSN 0018-926X), vol. AP-35, March 1987, p. 313-318. SERC-supported research. refs

A property of multilook processing of synthetic aperture radar (SAR) data is that a time lapse exists between subapertures, so that they contain information about a scattering surface at different times. Reported here is a theoretical study on the images of dynamic ocean waves processed by this technique. It is shown that due to the time lapse the subimages of a moving ocean wave differ in position depending on the look number and the wave phase velocity. Such images cannot be enhanced by the incoherent addition so much as those of stationary surfaces. The difference in image position can be corrected by defocusing the azimuth reference signal by the same amount as for the correction of defocusing induced by the wave motion. Discussions are presented on the correction of image positions and on the effect of defocusing. The property of the time lapse could be applied to estimating not only the phase velocity of ocean waves but also temporal changes in general scattering surfaces. Author

A87-42637

OCEAN OPTICS VIII; PROCEEDINGS OF THE MEETING, ORLANDO, FL, MAR. 31-APR. 2, 1986

MARVIN A. BLIZARD, ED. (U.S. Navy, Office of Naval Research, Arlington, VA) Meeting sponsored by SPIE, Bellingham, WA, Society of Photo-Optical Instrumentation Engineers (SPIE Proceedings. Volume 637), 1986, 379 p. For individual items see A87-42638 to A87-42647. (SPIE-637)

Papers are presented on ocean optics, a polarized view of the earth from orbital altitude, albedos and glitter patterns of a wind-roughened sea surface, a fractal geometric model of light pulse propagation in a multilayer ocean, and a multiple-wavelength method for filtering cloud shadows from oceanic spectral-irradiance profiles. Topics discussed include the use of the specific beam attenuation coefficient for identification of suspended particulate material; polarization modulation scattering measurements of well-characterized marine plankton; optical particle sizing for hydrodynamics; ocean-optical measurements using acoustooptic filtering; a simple, logarithmic light sensor; and a refractometer for use in oceanography. Consideration is given the optical properties of ice and snow in polar oceans; wind and nadir-angle effects on airborne-lidar water-surface returns; and the use of satellite remote sensing for the measurement of primary production in the ocean. I.F.

A87-42638

OPTICAL PROPERTIES OF THE MARINE ATMOSPHERIC BOUNDARY LAYER - AEROSOL PROFILES

K. L. DAVIDSON (U.S. Navy, Naval Postgraduate School, Monterey, CA) and C. W. FAIRALL (Pennsylvania State University, University Park) IN: Ocean optics VIII; Proceedings of the Meeting, Orlando, FL, Mar. 31-Apr. 2, 1986. Bellingham, WA, Society of Photo-Optical Instrumentation Engineers, 1986, p. 18-24. Navy-supported research. refs

The distribution of aerosols in the marine boundary layer can be viewed as a dynamic balance of production, transport and removal processes. The balance of these processes can be represented by a simple mixed-layer model. The vertical distribution of aerosols is dominated by turbulent transport. When mixing is dominated by surface shear or cloudtop cooling (as is typical in mid-latitudes), a single 'well-mixed' layer is sufficient to describe the aerosol profile. When scattered cumulus clouds are present (called the 'trade wind' or 'weak cumulus convection' regime), the well-mixed layer is confined to the region below cloud base. In the region above cloudbase and below cloudtops, strong vertical gradients of aerosol concentration may be observed. A simple parameterization of this gradient is presented. Author

A87-42640* University of South Florida, St. Petersburg.
THE INTERACTION OF LIGHT WITH PHYTOPLANKTON IN THE MARINE ENVIRONMENT

KENDALL L. CARDER (South Florida, University, St. Petersburg, FL), DONALD J. COLLINS (California Institute of Technology, Jet Propulsion Laboratory, Pasadena), MARY JANE PERRY (Washington, University, Seattle), H. LAWRENCE CLARK (NSF, Washington, DC), JORGE M. MESIAS (Pontificia Universidad Catolica de Chile, Talcahuano) et al. IN: Ocean optics VIII; Proceedings of the Meeting, Orlando, FL, Mar. 31-Apr. 2, 1986. Bellingham, WA, Society of Photo-Optical Instrumentation Engineers, 1986, p. 42-55. refs
 (Contract NAGW-465; N00014-84-C-0111)

In many regions of the ocean, the phytoplankton population dominates both the attenuation and scattering of light. In other regions, non-phytoplankton contributions to the absorption and scattering may change the remote sensing reflectance and thus affect the ability to interpret remotely sensed ocean color. Hence, variations in the composition of both the phytoplankton population and of the non-phytoplankton material in the water can affect the optical properties of the sea. The effects of these contributions to the remote sensing reflectance and the submarine light field are modeled using scattering and absorption measurements of phytoplankton cultures obtained at the Friday Harbor Laboratory of the University of Washington. These measurements are used to develop regional chlorophyll algorithms specific to the summer waters of Puget Sound for the Coastal Zone Color Scanner, Thematic Mapper and future Ocean Color Imager, and their accuracies are compared for high chlorophyll waters with little or no Gelbstoff, but with variable detrital and suspended material.

Author

A87-42641
WIND AND NADIR ANGLE EFFECTS ON AIRBORNE LIDAR WATER 'SURFACE' RETURNS

GARY C. GUENTHER (NOAA, National Ocean Service, Rockville, MD) IN: Ocean optics VIII; Proceedings of the Meeting, Orlando, FL, Mar. 31-Apr. 2, 1986. Bellingham, WA, Society of Photo-Optical Instrumentation Engineers, 1986, p. 277-286. refs

The effects of the wind and nadir angle on airborne lidar water surface returns are investigated. The character of the surface return depends on the ratio of the peak volume backscatter power and the peak interface reflection power; analytic expressions are derived for mean values of these quantities. The functionalities of the volume-to-interface peak power ratio on wind speed and direction, off-nadir beam incidence angle, and water clarity parameters are studied. Depth measurement error magnitudes are calculated for a volume return. It is observed, for off-nadir angles and low wind conditions, that the detection of the volume backscatter as the surface return will cause consistent shoal biases whose magnitudes are significant and depend on the pulse location algorithm. Potential methods for reducing the shoal bias are discussed. An expression for the temporal profile of a volume backscatter return is presented, and a method for estimating the scattering coefficient of water from the airborne data is described. I.F.

A87-42642* Bigelow Lab. for Ocean Sciences, West Boothbay Harbor, Maine.

THE RELATIONSHIP BETWEEN PHYTOPLANKTON CONCENTRATION AND LIGHT ATTENUATION IN OCEAN WATERS

DAVID A. PHINNEY and CHARLES S. YENTSCH (Bigelow Laboratory for Ocean Sciences, West Boothbay Harbor, ME) IN: Ocean optics VIII; Proceedings of the Meeting, Orlando, FL, Mar. 31-Apr. 2, 1986. Bellingham, WA, Society of Photo-Optical Instrumentation Engineers, 1986, p. 321-327. refs
 (Contract NAG6-17; N00014-81-C-0043)

The accuracy of chlorophyll estimates by ocean color algorithms is affected by the variability of particulate attenuation; the presence of dissolved organic matter; and the nonlinear inverse relationship between the attenuation coefficient, K, and chlorophyll. Data collected during the Warm Core Rings Program were used to model the downwelling light field and determine the impact of

these errors. A possible mechanism for the nonlinearity of K and chlorophyll is suggested; namely, that changing substrate from nitrate-nitrogen to ammonium causes enhanced blue absorption by photosynthetic phytoplankton in oligotrophic surface waters.

Author

A87-42643* California Univ., La Jolla.
REMOTE SENSING OF CHLOROPHYLL CONCENTRATIONS IN THE NORTHERN GULF OF MEXICO

CHARLES C. TREES (California, University, La Jolla) and SAYED Z. EL-SAYED (Texas A & M University, College Station) IN: Ocean optics VIII; Proceedings of the Meeting, Orlando, FL, Mar. 31-Apr. 2, 1986. Bellingham, WA, Society of Photo-Optical Instrumentation Engineers, 1986, p. 328-334. refs
 (Contract NAS5-22966)

During a 17 month period (November 1978 - March 1980), phytoplankton pigment concentrations were remotely sensed in the northern Gulf of Mexico using the Coastal Zone Color Scanner (CZCS). A total of 29 CZCS orbits were processed into pigment (chlorophyll a + phaeopigments) images and then geometrically warped to a Mercator projection. A correction factor of 1.67 was applied to the pigment concentrations to correct for the tendency of the standard fluorometric method to underestimate chlorophyll a concentrations. The spatial and temporal distributions of pigment fronts were quite variable during this time series. Constant features observed throughout the pigment imagery were the entrainment of coastal waters offshore. The most extensive entrainments occurred during intrusions of the Loop Current. For the 17 month survey, the mean HPLC-corrected pigment concentration was 3.30 + or - 1.45 mg/cu m.

Author

A87-42644* Jet Propulsion Lab., California Inst. of Tech., Pasadena.

A MODEL FOR THE USE OF SATELLITE REMOTE SENSING FOR THE MEASUREMENT OF PRIMARY PRODUCTION IN THE OCEAN

DONALD J. COLLINS, WEI-LIANG YANG (California Institute of Technology, Jet Propulsion Laboratory, Pasadena), DALE A. KIEFER, JANICE BEELER SOOHOO, and CASSON STALLINGS (Southern California, University, Los Angeles) IN: Ocean optics VIII; Proceedings of the Meeting, Orlando, FL, Mar. 31-Apr. 2, 1986. Bellingham, WA, Society of Photo-Optical Instrumentation Engineers, 1986, p. 335-348. refs

A model of primary production based upon the responses of phytoplankton to differing light and nutrient fields is described. This model includes the effects on production of variations in surface pigment concentration, the mixed layer depth, and the dependence on the incident solar irradiance. The model has been tested using in situ data provided by the Southern California Bight Studies of Eppley, et al. (1979), the California Cooperative Fisheries Investigations, the Organization of Persistent Upwelling Structures, and other data sets. A synoptic measure of the distribution of surface pigments is derived from the West Coast Chlorophyll and Temperature Time Series. The features and behavior of the model are presented together with the results of the model verification.

Author

A87-42645* National Oceanic and Atmospheric Administration, Washington, D. C.
COASTAL ZONE COLOR SCANNER IMAGERY OF PHYTOPLANKTON PIGMENT DISTRIBUTION IN ICELANDIC WATERS

DENNIS K. CLARK (NOAA, National Environmental Satellite, Data, and Information Service, Washington, DC) and NANCY G. MAYNARD (California Institute of Technology, Jet Propulsion Laboratory, Pasadena; California, University, La Jolla) IN: Ocean optics VIII; Proceedings of the Meeting, Orlando, FL, Mar. 31-Apr. 2, 1986. Bellingham, WA, Society of Photo-Optical Instrumentation Engineers, 1986, p. 350-357. Navy-supported research. refs

05 OCEANOGRAPHY AND MARINE RESOURCES

A87-42646* National Aeronautics and Space Administration. Goddard Space Flight Center, Greenbelt, Md.

SUNLIGHT INDUCED 685 NM FLUORESCENCE IMAGERY

HONGSUK H. KIM (NASA, Goddard Space Flight Center, Greenbelt, MD) and HEINZ VAN DER PIEPEN (DFVLR, Wessling, West Germany) IN: Ocean optics VIII; Proceedings of the Meeting, Orlando, FL, Mar. 31-Apr. 2, 1986. Bellingham, WA, Society of Photo-Optical Instrumentation Engineers, 1986, p. 358-363. refs

The capability of a new fluorescence method is evaluated using data from an aircraft fluorescence experiment conducted on the Elbe River on August 10-14, 1981. The technique measures chlorophyll concentrations by monitoring sunlight-induced fluorescence at 685 nm. Upwelling radiance spectra and vertical profiles of upwelling radiances are presented and analyzed. The image-processing algorithm used to retrieve fluorescence signals from raw data is described. I.F.

N87-20635# Meteorological Office, Bracknell (England).

OCEAN-ICE PANEL REPORT

T. D. ALLAN and A. MOREL IN ESA Proceedings of the European Symposium on Polar platform Opportunities and Instrumentation for Remote-sensing (ESPOIR) p 85-88 Nov. 1986

Avail: NTIS HC A07/MF A01

Ocean/ice objectives, payload, observation strategy, and data management of Columbus are outlined. Ocean/ice objectives for Columbus should provide continuity to routine remote sensing of the global oceans and ice caps, and over European coastal zones; prepare for an operational system following the experimental and/or pre-operational satellite systems planned to be launched over the next 5yr; develop and test techniques and concepts; provide improved scientific, social and economic benefits; and foster international, interagency cooperative programs aimed at the routine monitoring of the environment. ESA

N87-20659# Research Inst. of National Defence, Linköping (Sweden). Dept. 3.

POTENTIAL OF LASER REMOTE SENSING OF OIL BELOW WATER SURFACE

OVE STEINVALL Nov. 1986 19 p

(FOA-C-30435-3.1; ISSN-0347-3708; ETN-87-99441) Avail: NTIS HC A02/MF A01

An airborne pollution-monitoring system with a laser bathymeter to detect the oil and a laser fluoescensor for verification is proposed. It is estimated that such a system can have a depth range of 10 m in coastal waters. ESA

N87-20710 Wisconsin Univ., Madison.

A TECHNIQUE TO ESTIMATE THE OCEAN SURFACE ENERGY FLUX USING VAS MULTISPECTRAL DATA Ph.D. Thesis

JOHN JOSEPH BATES 1986 164 p

Avail: Univ. Microfilms Order No. DA8605676

A technique is developed to estimate the ocean surface energy flux from multispectral (visible and infrared) data obtained from the visible and infrared spin scan radiometer atmospheric sounder (VAS) on the geostationary GOES satellite. The technique is designed for application in the tropics. The shortwave flux is estimated by application of a simple physical model to visible data. The longwave flux is calculated using a statistical regression algorithm specifically tailored to model tropical cumulus clouds. In order to estimate the latent heat flux, the bulk parameterization is used with the sea surface temperature (SST), low-level moisture, and low-level wind speed, as inputs. Simulation and in-situ matches are used to estimate the expected errors of the method. The model was tested through its application to a case study using several days of data from November of 1982 and 1983 in the eastern tropical Pacific, in order to examine a large SST signal (the El Nino Southern Oscillation, ENSO). The results showed that almost all features on the individual analyses were significant to the 2 sigma level, but that few significant features remained on the difference fields for latent heat flux and net heat flux.

Dissert. Abstr.

N87-20716# Old Dominion Univ., Norfolk, Va.

CONTINENTAL SHELF PROCESSES AFFECTING THE OCEANOGRAPHY OF THE SOUTH ATLANTIC BIGHT Progress Report, 1 Jun. 1986 - 31 May 1987

L. P. ATKINSON Jan. 1987 52 p

(Contract DE-FG05-85ER-60348)

(DE87-005303; DOE/ER-60348/5) Avail: NTIS HC A04/MF A01

As part of a study of continental shelf processes affecting the oceanography of the South Atlantic Bight, data collected during the Spring 1985 SPREX field experiment was processed and analyzed. The goals of the analyses were to: (1) determine the distribution of temperature, salinity, nutrients, and humid fluorescence such that flow fields and distributions of variables could be related to wind forcing events; (2) determine the time change in nutrient concentration and salinity at selected current meter locations; and (3) evaluate the usefulness of tritium as a fresh water tracer in the nearshore region of the South Atlantic Bight. DOE

N87-21497# Istituto di Fisica dell Atmosfera, Rome (Italy).

REMOTELY SENSED SEA SURFACE TEMPERATURE FOR THE ALPINE EXPERIMENT (ALPEX)

G. DALU, A. VIOLA, and S. MARULLO IN WMO Proceedings of the Conference on the Scientific Results of the Alpine Experiment (ALPEX), Volume 1 p 131-138 Jul. 1986 Sponsored by CNR Avail: NTIS MF A01; print copy available from WMO, Geneva, Switzerland

The methodology behind the algorithms used to retrieve the sea surface temperature from infrared radiometric data was examined with a radiative transfer model that simulates the response of the atmosphere for different temperature and water vapor profiles. Linear algorithms are used to evaluate the sea surface temperature from AVHRR data. Although the results obtained show that a nonlinear algorithm is more accurate, a linear algorithm can give better results if it is optimized for a particular region and season. An improved calibration procedure was used to process the data of the AVHRR-2 radiometer. ESA

N87-21533*# Wisconsin Univ., Madison. Space Science and Engineering Center.

QUICK LOOK ATLANTIC OCEAN RAIN MAPS FOR GALE Interim Report

DAVID W. MARTIN and BRIAN AUVINE Mar. 1987 32 p

(Contract NAG5-742)

(NASA-CR-180511; NAS 1.26:180511) Avail: NTIS HC A03/MF A01 CSCL 08C

A set of quick look maps of Atlantic Ocean rainfall were made. The maps are based entirely on information extracted from geostationary satellite images. The maps and the process by which they were made are briefly described. The major shortcomings of such a project are pointed out. For convenience the maps are presented in rectangular format. Each map covers one day. Rainfall is contoured in units of millimeters. Rainfall was estimated by the Arkin technique. B.G.

N87-21534*# National Aeronautics and Space Administration. Goddard Space Flight Center, Greenbelt, Md.

TIDAL ESTIMATION IN THE ATLANTIC AND INDIAN OCEANS, 3 DEG X 3 DEG SOLUTION

BRAULIO V. SANCHEZ, DESIRAJU B. RAO (National Oceanic and Atmospheric Administration, Rockville, Md.), and STEPHEN D. STEENROD (Applied Research Corp., Landover, Md.) Apr. 1987 21 p

(NASA-TM-87812; REPT-87B0163; NAS 1.15:87812) Avail: NTIS HC A02/MF A01 CSCL 08C

An estimation technique was developed to extrapolate tidal amplitudes and phases over entire ocean basins using existing gauge data and the altimetric measurements provided by satellite oceanography. The technique was previously tested. Some results obtained by using a 3 deg by 3 deg grid are presented. The functions used in the interpolation are the eigenfunctions of the velocity (Proudman functions) which are computed numerically from a knowledge of the basin's bottom topography, the horizontal plan

form and the necessary boundary conditions. These functions are characteristic of the particular basin. The gravitational normal modes of the basin are computed as part of the investigation; they are used to obtain the theoretical forced solutions for the tidal constituents. The latter can provide the simulated data for the testing of the method and serve as a guide in choosing the most energetic functions for the interpolation. Author

N87-21980# Joint Publications Research Service, Arlington, Va.
POSSIBILITIES OF USING ARTIFICIAL EARTH SATELLITE DATA FOR COMPUTING HEAT EXCHANGE BETWEEN THE OCEAN AND ATMOSPHERE IN NEWFOUNDLAND ENERGY-ACTIVE ZONE DURING WINTER

D. G. RZHEPLINSKIY and N. N. SHVYRKOV *In its USSR Report: Space (JPRS-USP-87-001) p 180-181 19 Feb. 1987 Transl. into ENGLISH from Issledovaniye Zemli iz Kosmosa (Moscow, USSR), no. 4, Jul. - Aug. 1986 p 32-41*
 Avail: NTIS HC A11/MF A01

Maps of the dynamic topography of the ocean surface in the Newfoundland Energy-Active Zone (NEAZ) were plotted on the basis of three oceanographic surveys made during the winter of 1983 to 1984. During the first survey the main flow of the Gulf Stream at 50 degrees longitude was traced in the latitude zone from 38 to 43 deg N. The second survey revealed no significant changes in circulation and temperature distribution in the test range. Observations made during the third survey confirmed the presence of the main forms of circulation in the region. The test range was regionalized on the basis of types of vertical distribution of temperature and salinity for determining the limits of propagation of different water structures. Three types of vertical structures were defined: structure of slope waters, structure of transformation zone, and vertical North Atlantic structure. It was found that the intensity of the heat flows between the ocean and atmosphere in the NEAZ in winter is dependent largely on the position of the hydrological front separating the North Atlantic central water mass from the remaining water structures and on the specific meteorological synoptic situation. Author

N87-22297# Woods Hole Oceanographic Institution, Mass.
CHART: A COMPUTER PLOTTING PACKAGE FOR THE DISPLAY OF POSITION-DEPENDENT MARINE DATA

A. MARTIN Dec. 1986 57 p Sponsored by Sandia National Labs.
 (PB87-148607; WHOI-86-43) Avail: NTIS HC A04/MF A01
 CSCL 08B

The computer program CHART produces plots of navigation tracks and data points in a choice of 14 projections where navigation coordinates are defined. It was written specifically for the plotting and annotation of geological and geophysical data; however, any data which includes geographical coordinates can be plotted. The package was designed for broad flexibility of application and for ease of use. Chart can be used on any Digital Equipment Corporation VAX machine running VMS. Some additional features of CHART: coastlines, multiple data sets on one grid; empty grid without data points are given. GRA

N87-22382# Coastal Engineering Research Center, Vicksburg, Miss.

DUCK '85 NEARSHORE WAVES AND CURRENTS EXPERIMENT DATA SUMMARY REPORT Final Report

JON M. HUBERTZ, CHARLES E. LONG, PANOLA RIVERS, and WILLIE A. BROWN Feb. 1987 210 p
 (AD-A177419; CERC-MP-87-3) Avail: NTIS HC A10/MF A01
 CSCL 08C

This report provides a summary of mean values of data collected during the nearshore waves and currents experiment which was part of the DUCK '85 field program. The objective of the experiment was to collect data which could be used to study coastal processes and verify numerical models. Data sets such as this provide valuable prototype measurements for validation of theories and techniques which can be used to predict nearshore waves and currents for various climatic conditions. GRA

N87-22386# Jet Propulsion Lab., California Inst. of Tech., Pasadena

THE 1982-1983 EL NINO ATLAS: NIMBUS-7 MICROWAVE RADIOMETER DATA

W. TIMOTHY LIU 15 Feb. 1987 77 p Sponsored by NASA
 (NASA-CR-180914; JPL-PUB-87-5; NAS 1.26.180914) Avail:
 NTIS HC A05/MF A01 CSCL 08C

Monthly maps of sea surface temperature, atmospheric water vapor, and surface level wind speed as measured by the Scanning Multichannel Microwave Radiometer (SMMR) on the Nimbus-7 satellite for the tropical Pacific from June 1982 to October 1983, during one of the most intense El Nino Southern Oscillations (ENSO) episodes, are presented. The non-ENSO annual cycle was compiled by averaging the 1980 and 1981 data for each calendar month and was removed from monthly fields of 1982 and 1983 to reveal the anomalous distributions. The anomaly fields and part of the non-ENSO annual cycle are also presented. This study and earlier evaluations demonstrate that the Nimbus/SMMR can be used to monitor large scale and low frequency variabilities in the tropical ocean. The SMMR data support and extend conventional measurements. The variabilities of the three parameters are found to represent various aspects of ENSO related through ocean atmosphere interaction. Their simultaneous and quantitative descriptions pave the way for the derivation of ocean atmosphere latent heat exchange and further the understanding of the coupled atmospheric and oceanic thermodynamics. Author

N87-22387# Alaska Univ., Fairbanks. Geophysical Inst.
STATISTICAL DESCRIPTION OF THE SUMMERTIME ICE EDGE IN THE CHUKCHI SEA, TASK 2 Final Report

W. J. STRINGER and J. E. GROVES Jan. 1987 217 p
 (Contract DE-AC21-83MC-20037)
 (DE87-001056; DOE/MC-20037/2265) Avail: NTIS HC A10/MF A01

Ice edge data has been analyzed for ice recursion analysis in the Chukchi Sea for a twelve year period. Conclusions drawn include: (1) numerous parameter comparisons describing the great variability of ice extent found in the Chukchi Sea; (2) that for a period of 80 to 100 days beginning with August and continuing through October, ice-free water will exist in the Chukchi Sea south of 70 deg N and 175 deg W. Within these boundaries ice will return (recur) once after it has retreated in the spring, or it will retreat once after it has returned in the fall, less than 50% of the time; (3) ice in the western Chukchi Sea (along the Siberian coast) may provide multi-year ice to the Bering Sea through Bering Strait starting in late fall; (4) melt-back bays (defined by Paquette and Bourke, 1981) created by warm Bering Sea waters channeled by Chukchi Sea bathymetry are persistent and significant features of the Chukchi Sea ice edge. DOE

N87-22388# National Oceanic and Atmospheric Administration, Washington, D. C.

THE AVHRR/HIRS OPERATIONAL METHOD FOR SATELLITE BASED SEA SURFACE TEMPERATURE DETERMINATION

CHARLES WALTON Mar. 1987 65 p
 (NOAA-TR-NESDIS-28) Avail: NTIS HC A04/MF A01

A technique which was used operationally to produce sea surface temperatures from the NOAA polar orbiting satellites between 1976 and 1981 is described. The single window channel technique used before 1976 is described in the NOAA Technical Memorandum NESD 78 while the multiple window channel technique (MCSST) applied since 1981 is well documented. This information bridges the gap between these two periods and provides a continuous record of the evolution of one of NOAA's primary satellite derived meteorological products. Author

05 OCEANOGRAPHY AND MARINE RESOURCES

N87-23016# Naval Postgraduate School, Monterey, Calif.
LASER REFLECTANCE AS A FUNCTION OF ROUGH WATER GLITTER PROFILE M.S. Thesis

CARLTON M. BOURNE Mar. 1987 67 p
(AD-A178774) Avail: NTIS HC A04/MF A01 CSCL 17H

A new remote sensing technique was developed for predicting the expected mean laser radar return from a rough water surface. This technique involved measuring the standard deviations of the upwind and crosswind profiles of the elliptical glitter patterns occurring for illumination of the water surface with a point source near the laser radar system. A pencil beam laser radar from a companion project simultaneously measured the reflected signals from the water surface. The glitter pattern images were recorded with a video camera and recorder. The images for each run were later digitized along their major and minor elliptic axes and averaged over 256 images to produce smooth intensity curves from which the standard deviations were measured. The radar return fluctuated over a large range because of the rapid variation of individual water surface facets, and so was recorded and time averaged for the same interval as the video images. Data sufficient for empirical prediction of expected mean laser return signal were obtained. This is necessary to permit evaluation of the performance of a given laser radar design. The data obtained approximated the predictions of a new model proposed in this work. GRA

N87-23046# European Centre for Medium-Range Weather Forecasts, Reading (England).

THE IMPACT OF INITIAL CONDITIONS AND SST ANOMALIES ON EXTENDED RANGE PREDICTIONS FOR THE EL NINO PERIOD

ULRICH CUBASCH *In* World Climate Program Workshop on Comparison of Simulations by Numerical Models of the Sensitivity of the Atmospheric Circulation to Sea Surface Temperature Anomalies p 110-116 Jul. 1986

Avail: NTIS MF A01; print copy available from WMO, Geneva, Switzerland

The El Nino sea surface temperature (SST) anomaly observed during 1982 to 1983 was used to investigate the impact of anomalous forcing at the lower boundary on the predictability of the atmosphere. In order to test the impact of the SST as a function of the initial conditions, forecasts using the observed or climatological SST adjusted every 5th day, were run starting on December 15, 16, and 17 1982. All experiments were run up to 90 days with the ECMWF spectral model and a resolution of T42L16 (i.e., with a Gaussian grid of 2.8125 deg) from the ECMWF operational 12z analysis. Results show that precipitation can be used as a diagnostic tool for the effect of El Nino on the tropical atmosphere. The difference between the experiments with the observed moving and climatological SST indicates the impact of the El Nino SST anomaly on the atmosphere. ESA

N87-23102# Admiralty Research Establishment, Portland (England).

THE SIR-B MISSION: TOWARDS AN UNDERSTANDING OF INTERNAL WAVES IN THE OCEAN

M. T. BAGG, A. C. EDWARDS, J. R. PERRY, J. C. SCOTT, J. A. STACEY, and J. O. THOMAS Dec. 1986 51 p
(Contract MOD(PE)-NUW-72A/1287)

(ARE-TR-86122; ACCN-74513; BR101469; ETN-87-99809) Avail: NTIS HC A04/MF A01

An internal wave sea truth experiment was conducted in conjunction with SIR-B overflights. Using knowledge obtained from sea truth and radar imagery of internal waves computational and theoretical procedures to model observed surface signatures are presented. The procedures are intended to predict the changing wave action spectral density of the ocean surface short wavelength surface gravity waves as they propagate across the straining region induced at the surface by the underlying internal wave. Variants of the Phillips (1984) formulation of the wave action source and sink terms are used to account for the effects of the wind and wave breaking on the development of the wave action spectral density. Considerable success is achieved in understanding how various signatures arise. ESA

N87-23103# Royal Australian Navy Research Lab., Edgecliff.
STUDIES OF THE EAST AUSTRALIAN CURRENT OFF NORTHERN NEW SOUTH WALES

P. J. MULHERAN Aug. 1986 73 p
(AD-A178461; RANRL-TN-6/86) Avail: NTIS HC A04/MF A01 CSCL 08C

Cruises in November 1982 and May 1983 were conducted to investigate the structure of the front on the near-shore edge of the East Australian Current off northern New South Wales. Concurrent satellite data were also obtained. From this work it was found that the front could move in the east-west direction at speeds of order 10 to 20 km/day, that the surface mixed layer became very shallow near the surface front, and that the front's structure was at times affected by fresh water outflow from the Clarence River. It was also found that LANDSAT imagery could be useful in frontal investigations and that it is feasible to obtain depth - averaged currents with a geomagnetic electro-kinetograph (GEK). Author (GRA)

N 7-23104# Oregon State Univ., Corvallis. Coll. of Oceanography.

OPTICAL DYNAMICS EXPERIMENT (ODEX) DATA REPORT R/V ACANIA EXPEDITION 10 OCTOBER-17 NOVEMBER 1982. VOLUME 2: PARTICLE SIZE DISTRIBUTIONS. VOLUME 6: SCALAR SPECTRAL-RADIOMETER DATA

HASONG PAK, DAVID W. MENZIES, and JAMES C. KITCHEN Sep. 1986 408 p

(Contract N00014-84-C-0218)

(AD-A178535; DATA-124-VOL-2/6; REF-86-10-VOL-2/6) Avail: NTIS HC A18/MF A01 CSCL 08J

The Optical Dynamics Experiment (ODEX) was an interdisciplinary experiment to study the relation of physical forcing, biological processes, and the structure of optical parameters in the open ocean. This data report presents the data collected with the spectral radiometer package, and the particle size analysis of discrete water samples taken from CTD casts by the Oregon State Univ. Optical Oceanography Group. The ODEX cruise of Oct. and Nov. 1982 occupied 1984 stations along a transect from the California coast at 35 deg N to a study area covering the subtropical front near 32 deg N, 142 deg W. Plots are presented of hydrographic parameters, beam attenuation, percentage of surface irradiance at 9 wave-lengths, and diffuse attenuation at 5 wavelengths. Lists of the same parameters as well as discrete and total visible irradiance are presented. GRA

N87-24009# Massachusetts Inst. of Tech., Cambridge. Research Lab. of Electronics.

ACTIVE AND PASSIVE REMOTE SENSING OF ICE Semiannual Report, 1 Aug. 1986 - 31 Jan. 1987

JIN A. KONG 31 Jan. 1987 9 p

(Contract N00014-83-K-0258)

(AD-A179461) Avail: NTIS HC A02/MF A01 CSCL 17I

During the period August 1, 1986 to January 31, 1987, we have studied the volume scattering effects of snow-covered sea ice with a three-layer random medium model for microwave remote sensing. The strong fluctuation theory and the bilocal approximation are applied to calculate the effective permittivities for snow and sea ice. The wave scattering theory in conjunction with the distorted Born approximation is then used to compute bistatic coefficients and backscattering cross sections. Theoretical results are illustrated by matching experimental data for dry snow-covered thick first-year sea ice at Point Barrow. The radar backscattering cross sections are seen to increase with snow cover for snow-covered sea ice, due to the increased scattering effects in the snow layer. The results derived can also be applied to the passive remote sensing by calculating the emissivity from the bistatic scattering coefficients. GRA

N87-24012*# National Marine Fisheries Service, Miami, Fla. Southeast Fisheries Center.

UTILIZING REMOTE SENSING OF THEMATIC MAPPER DATA TO IMPROVE OUR UNDERSTANDING OF ESTUARINE PROCESSES AND THEIR INFLUENCE ON THE PRODUCTIVITY OF ESTUARINE-DEPENDENT FISHERIES Semiannual Progress Report

JOAN A. BROWDER, L. NELSON MAY, JR., ALAN ROSENTHAL, ROBERT H. BAUMANN, and JAMES G. GOSSELINK 10 Jun. 1987 21 p

(Contract NASA ORDER S-56107-D)

(NASA-CR-180984; NAS 1.26:180984; SAPR-4) Avail: NTIS HC A02/MF A01 CSCL 08B

A stochastic spatial computer model addressing coastal resource problems in Louisiana is being refined and validated using thematic mapper (TM) imagery. The TM images of brackish marsh sites were processed and data were tabulated on spatial parameters from TM images of the salt marsh sites. The Fisheries Image Processing Systems (FIPS) was used to analyze the TM scene. Activities were concentrated on improving the structure of the model and developing a structure and methodology for calibrating the model with spatial-pattern data from the TM imagery. B.G.

N87-24061# Naval Ocean Research and Development Activity, Bay St. Louis, Miss.

OCEAN WIND AND WAVE MODEL COMPARISONS WITH GEOSAT (GEODESY SATELLITE) SATELLITE DATA Final Report

R. L. PICKETT, D. A. BURNS, and R. D. BROOME Dec. 1986 11 p

(AD-A178302; NORDA-168) Avail: NTIS HC A02/MF A01 CSCL 08C

By comparing operational wind and wave models to GEOSAT, we found that on 10 March 1986, the Federal Republic of Germany had the best skill score for a regional wind analysis, NOAA had the best score for a global wind analysis, the Netherlands had the best score for a regional wave analysis and the U.S. Navy had the best score for a global wave analysis. GRA

N87-24731# Joint Publications Research Service, Arlington, Va. **HIGH RESOLUTION SEA SURFACE TEMPERATURE FIELD DERIVED**

SISONG ZHOU, WEIYING CHEN, and LIXIA ZHANG *In its* China Report: Science and Technology p 48-55 2 May 1986 Transl. into ENGLISH from Haiyang Kexue (Beijing, China), v. 9, no. 3, 9 May 1985 p 5-9

Avail: NTIS HC A05/MF A01

A procedure for deriving high resolution sea surface temperature field from digital AVHRR/HRPT data is described. For the purpose of reducing the processing time, only the reflective threshold or near infrared channel is used for selecting data over clear areas of ocean. The W.L. Smith single window channel sea surface temperature retrieval method is used for atmospheric attenuation correction for the area of Beihai Bay and the Yellow Sea during the cold half of the year. Compared with other measurements, the result is quite satisfactory. Author

N87-24766# Messerschmitt-Boelkow-Blohm G.m.b.H., Ottobrunn (West Germany). Space Systems Group.

ADVANCED IMAGING SPECTROMETER FOR OCEAN COLOR/FLUORESCENCE MEASUREMENTS AND FURTHER APPLICATIONS

B. KUNKEL, F. BLECHINGER, R. LUTZ, and H. WINKENBACH *In* ESA Proceedings of the International Symposium on Progress in Imaging Sensors p 237-246 Nov. 1986

Avail: NTIS HC A99/MF A01

A spaceborne chlorophyll fluorescence imaging spectrometer is proposed. The instrument is suitable also for a variety of other applications, especially as an airborne version. The technical concept is based on an all-reflective optics system and a 1024 sq matrix CCD detector array. The imaging spectrometer is designed to cover a spectral range from 425 to 960 nm in resolution

steps of 5 nm per channel at 0.06 % albedo resolution. It provides 108 spectral channels. The FOV amounts to + or - 16.2 deg at 300 m ground pixel size. This corresponds to 1024 pixels in the spatially scanned (cross track) direction. Since no frame-transfer matrix CCD array with 1024 sq pixels is available, the initiated airborne version uses 512 sq. ESA

N87-24816*# Ohio State Univ., Columbus. Dept. of Geodetic Science and Surveying.

RADIAL ORBIT ERROR REDUCTION AND SEA SURFACE TOPOGRAPHY DETERMINATION USING SATELLITE ALTIMETRY

THEODOSSIOS ENGELIS Jun. 1987 192 p

(Contract NAG5-519)

(NASA-CR-180570; NAS 1.26:180570; REPT-377) Avail: NTIS HC A09/MF A01 CSCL 08C

A method is presented in satellite altimetry that attempts to simultaneously determine the geoid and sea surface topography with minimum wavelengths of about 500 km and to reduce the radial orbit error caused by geopotential errors. The modeling of the radial orbit error is made using the linearized Lagrangian perturbation theory. Secular and second order effects are also included. After a rather extensive validation of the linearized equations, alternative expressions of the radial orbit error are derived. Numerical estimates for the radial orbit error and geoid undulation error are computed using the differences of two geopotential models as potential coefficient errors, for a SEASAT orbit. To provide statistical estimates of the radial distances and the geoid, a covariance propagation is made based on the full geopotential covariance. Accuracy estimates for the SEASAT orbits are given which agree quite well with already published results. Observation equations are developed using sea surface heights and crossover discrepancies as observables. A minimum variance solution with prior information provides estimates of parameters representing the sea surface topography and corrections to the gravity field that is used for the orbit generation. The simulation results show that the method can be used to effectively reduce the radial orbit error and recover the sea surface topography. Author

N87-24870* National Aeronautics and Space Administration. Goddard Space Flight Center, Greenbelt, Md.

ARCTIC SEA ICE, 1973-1976: SATELLITE PASSIVE-MICROWAVE OBSERVATIONS

CLAIRE L. PARKINSON, JOSEFINO C. COMISO, H. JAY ZWALLY, DONALD J. CAVALIERI, PER GLOERSEN, and WILLIAM J. CAMPBELL (Puget Sound Univ., Tacoma, Wash.) Jan. 1987 301 p Original contains color illustrations

(NASA-SP-489; NAS 1.21:489; LC-86-23876) Avail: NTIS HC A14 CSCL 08L

The Arctic region plays a key role in the climate of the earth. The sea ice cover affects the radiative balance of the earth and radically changes the fluxes of heat between the atmosphere and the ocean. The observations of the Arctic made by the Electrically Scanning Microwave Radiometer (ESMR) on board the Nimbus 5 research satellite are summarized for the period 1973 through 1976. B.G.

HYDROLOGY AND WATER MANAGEMENT

Includes snow cover and water runoff in rivers and glaciers, saline intrusion, drainage analysis, geomorphology of river basins, land uses, and estuarine studies.

A87-31409

NIMBUS 7 SMMR INVESTIGATION OF SNOWPACK PROPERTIES IN THE NORTHERN GREAT PLAINS FOR THE WINTER OF 1978-1979

MARSHALL J. MCFARLAND (Texas A & M University, College Station), GREGORY D. WILKE (USAF, Global Weather Central, Offutt AFB, NE), and PAUL H. HARDER, II (DBA Systems, Inc., Fairfax, VA) IEEE Transactions on Geoscience and Remote Sensing (ISSN 0196-2892), vol. GE-25, Jan. 1987, p. 35-46. refs

An investigation of the capabilities of remote sensing of snowpack properties was conducted with brightness temperatures from the Nimbus 7 Scanning Multichannel Microwave Radiometer (SMMR) and climatological data for the northern Great Plains for the winter of 1978-1979. The radiometer data included horizontally and vertically polarized brightness temperatures at the 0.81-, 1.66-, and 2.80-, and 4.54-cm wavelengths for both day and night overpasses, with a repeat coverage on the average of every two to three days. The brightness temperatures in each channel and the daily surface climatological elements of maximum and minimum air temperature, precipitation, snowfall, and snow depth were objectively analyzed to a 20-km grid with 35 rows and 42 columns. The analysis concentrated on temporal analyses of selected grid cells. Characteristic signatures were observed for initial snow accumulation, snow depth to about 20 cm, beginning of snow melting in the surface layers, and snow melt. The process of snow ripening was evident in the thawing and refreezing cycles of the snow surface layers. Discrimination of dry soil, wet soil, snow amount to 15 cm, and liquid water at the soil surface before runoff occurred was present with the use of both polarizations at the 0.81 and 1.66-cm wavelengths, although the longer wavelengths contained additional information on the state of the surface underlying the snow pack. Author

A87-32092

DETERMINING RAINFALL INTENSITY AND TYPE FROM GOES IMAGERY IN THE MIDLATITUDES

A. A. TSONIS (Wisconsin, University, Milwaukee) Remote Sensing of Environment (ISSN 0034-4257), vol. 21, Feb. 1987, p. 29-36. refs

Although a useful estimate of the areal extent of precipitation from visible and infrared satellite data can be made, the extraction of rainfall rates is still a problem. Earlier work by the author suggested that little, if any, correlation exists between rainfall rate and brightness or cloud top temperature individually. The results of this work indicate that by employing pattern matching techniques it may be possible to objectively define a satellite delineated rain area in terms of light-moderate and moderate-heavy. Further, convective and nonconvective precipitation areas can be separated. Author

A87-33295

ON THE RELATIVE ACCURACY OF SATELLITE AND RAINGAGE RAINFALL MEASUREMENTS OVER MIDDLE LATITUDES DURING DAYLIGHT HOURS

A. BELLON and G. L. AUSTIN (McGill Radar Weather Observatory, Sainte-Anne-de-Bellevue, Canada) Journal of Climate and Applied Meteorology (ISSN 0733-3021), vol. 25, Nov. 1986, p. 1712-1724. Research supported by the Canadian Forestry Service and NSERC. refs

Relationships between visible and/or IR data and the rainfall rate were derived by comparing raingage-calibrated radar data with colocated satellite information over Montreal, Canada. The comparison of the satellite estimates for 14 summertime rainfalls

was made with both the point gage measurements and with interpolated gage data. The overall absolute difference of 1739 point comparisons was found to be of the order of 85 percent at the 2-mm rain level. The rates of the rainfall rate were estimated from half-hourly point GOES measurements as a function of either (1) both visible and IR temperatures; (2) the normalized visible-only data; (3) the IR-only temperatures; or (4) the satellite rain area multiplied by a constant rainfall rate. The scores of the visible-IR and visible-only methods were found to be adequate (gamma = 0.56 and 0.50, respectively), but the IR-only method was judged inadequate. The satellite techniques were found to be better than gage-interpolated estimates at locations where the nearest gage was farther than 40 km, and thus to be most useful in the data-sparse regions. I.S.

A87-33297

AN EVALUATION OF SATELLITE-BASED INSOLATION ESTIMATES FOR OHIO

JOHN C. KLINK and KEVIN J. DOLLHOPF (Miami University, Oxford, OH) Journal of Climate and Applied Meteorology (ISSN 0733-3021), vol. 25, Nov. 1986, p. 1741-1751. refs

The accuracy of the estimates of daily insolation for Ohio produced by the National Environmental Satellite Data and Information Service (NESDIS) from GOES observations in 1982 was assessed through comparison with isolated measurements from eight ground-based stations. For the snow-free season, the mean errors (bias) of the estimates (positive for all days) are generally less than 0.75 MJ/sq m per day, and the correlation coefficients are above 0.95. Estimates are much less accurate when a snow cover existed. Generally, the bias is negative and exceeds -1.25 MJ/sq m per day, and correlation coefficients are less than 0.90. I.S.

A87-35311

DEVELOPMENT OF A SATELLITE REMOTE SENSING TECHNIQUE FOR THE STUDY OF ALPINE GLACIERS

ANNA DELLA VENTURA, ANNA RAMPINI (CNR, Istituto di Fisica Cosmica e Tecnologie Relative, Milan, Italy), RICCARDO RABAGLIATI (IBM Italia S.p.A., Mestre, Italy), and ROSSANA SERANDREI BARBERO (CNR, Istituto per lo Studio della Dinamica delle Grandi Masse, Venice, Italy) International Journal of Remote Sensing (ISSN 0143-1161), vol. 8, Feb. 1987, p. 203-215. refs

This paper presents an experiment in MSS image interpretation for the systematic observation of glacier surfaces in the Alps. The glacier monitoring potential of visible and near-infrared data is applied here to the surveying of mountain glaciers, characterized by small areas and strong shading because of their typical morphology. The method developed identifies glacier surfaces by evaluating the intensity values of visible images combined with clearness conditions related to exposure, slope and the surface homogeneity of the glacier. Conditions of clarity, in the absence of a digital terrain model, are estimated from the number of saturated pixels in the visible bands. At a higher level, the near-infrared data are used to identify snow and ice surfaces inside the glacier boundaries. The paper discusses the performance of the technique developed, as applied to the analysis of a temporal series concerning a group of 11 small glaciers with critical exposure conditions. The results are expressed as areas of glacier and snow-covered terrain in different years, thus enabling trends in regional mass balance to be estimated. Author

A87-35518

THE RELATION OF MILLIMETER-WAVELENGTH BACKSCATTER TO SURFACE SNOW PROPERTIES

LARRY D. WILLIAMS (Edinburgh, University, Scotland) and JOHN G. GALLAGHER (Royal Signals and Radar Establishment, Malvern, England) IEEE Transactions on Geoscience and Remote Sensing (ISSN 0196-2892), vol. GE-25, March 1987, p. 188-194. refs

Helicopter-mounted radar measurements of 94-GHz backscatter from snowcover, and ground-truth measurements of snow surface roughness, wetness, grain size, and porosity, are analyzed. For each of six polarization combinations, and separately for dry snow and wet snow, spatial mean values of the backscatter coefficient

are fit to linear combinations of the cosine of incidence angle and the snow variables. However, the significance of an included snow variable is considered questionable if the predicted response of the spatial mean values of the backscatter coefficient to that variable is small compared with the spatial standard deviation (typically 4-5 dB). This is the case for dry-snow grain size, porosity, and for some polarization combinations, wetness. Only the response to wet-snow surface roughness is consistently comparable in magnitude to the standard deviations of the spatial mean value of the backscatter coefficient. Author

A87-36102

CLOUD-COVER AND PRECIPITATION PATTERNS OVER THE REPUBLIC OF GUINEA ACCORDING TO GROUND-BASED AND SATELLITE OBSERVATIONS [REZHIM OBLACHNOSTI I OSADKOV NA TERRITORII GVINEISKOI RESPUBLIKI PO NAZEMNYM I SPUTNIKOVYM NABLIUDENIIAM]

N. A. TIMOFEEV, A. N. BOLSHAKOV, M. V. IVANCHIK, and A. I. SEVOSTIANOV (AN USSR, Morskoi Gidrofizicheskii Institut, Sevastopol, Ukrainian SSR) *Issledovanie Zemli iz Kosmosa* (ISSN 0205-9614), Nov.-Dec. 1986, p. 11-17. In Russian. refs

A87-36103

SURFACE MANIFESTATIONS OF HYDROPHYSICAL PROCESSES IN THE STRAIT OF GIBRALTAR ACCORDING TO 'SALYUT-6' PHOTOGRAPHS [POVERKHNOSTNYE PROIAVLENIIA GIDROFIZICHESKIKH PROTSESSOV V RAIONE GIBRALTARSKOGO PROLIVA PO MATERIALAM FOTOS'EMKI S ORBITAL'NOI STANTSII 'SALIUT-6']

A. S. KAZMIN (AN SSSR, Institut Okeanologii, Moscow, USSR) *Issledovanie Zemli iz Kosmosa* (ISSN 0205-9614), Nov.-Dec. 1986, p. 18-23. In Russian. refs

A87-36106

SATELLITE TECHNIQUES FOR STUDYING ICE CRUSTS AND UNDERGROUND WATERS IN THE EASTERN PAMIR [KOSMICHESKIE METODY IZUCHENIIA NALEDEI I PODZEMNYKH VOD VOSTOCHNOGO PAMIRA]

A. G. TOPCHIEV (Vsesoiuznyi Nauchno-Issledovatel'skii Tsentr AIUS-Agroresursy, Moscow, USSR) *Issledovanie Zemli iz Kosmosa* (ISSN 0205-9614), Nov.-Dec. 1986, p. 48-58. In Russian. refs

A87-39467* National Aeronautics and Space Administration. Goddard Space Flight Center, Greenbelt, Md.

MONSOON FLOOD BOUNDARY DELINEATION AND DAMAGE ASSESSMENT USING SPACE BORNE IMAGING RADAR AND LANDSAT DATA

MARC L. IMHOFF, C. VERMILLION (NASA, Goddard Space Flight Center, Greenbelt, MD), M. H. STORY (Science Applications Research Corp., Lanham, MD), A. M. CHOUDHURY, A. GAFOOR (Space Research and Remote Sensing Organization of Bangladesh, Dhaka) et al. *Photogrammetric Engineering and Remote Sensing* (ISSN 0099-1112), vol. 53, April 1987, p. 405-413. refs

Space-borne synthetic aperture radar (SAR) data acquired by the Shuttle Imaging Radar-B (SIR-B) Program and Landsat Multispectral Scanner Subsystem (MSS) Data from Landsat 4 were used to map flood boundaries for the assessment of flood damage in the Peoples Republic of Bangladesh. The cloud penetrating capabilities of the L-band radar provided a clear picture of the hydrologic conditions of the surface during a period of inclement weather at the end of the wet phase of the 1984 monsoon. The radar image data were digitally processed to geometrically rectify the pixel geometry and were filtered to subdue radar image speckle effects. Contrast enhancement techniques and density slicing were used to create discrete land-cover categories corresponding to surface conditions present at the time of the Shuttle overflight. The radar image classification map was digitally registered to a spectral signature classification map of the area derived from Landsat MSS data collected two weeks prior to the SIR-B mission. Classification accuracy comparisons were made between the radar and MSS classification maps, and flood boundary and flood damage assessment measurements were made with the merged data by

adding the classifications and inventorying the land-cover classes inundated at the time of flooding. Author

A87-40249* South Dakota School of Mines and Technology, Rapid City.

THE AREA-TIME-INTEGRAL TECHNIQUE TO ESTIMATE CONVECTIVE RAIN VOLUMES OVER AREAS APPLIED TO SATELLITE DATA - A PRELIMINARY INVESTIGATION

ANDRE A. DONEAUD, JAMES R. MILLER, JR., L. RONALD JOHNSON (South Dakota School of Mines and Technology, Rapid City), THOMAS H. VONDER HAAR, and PATRICK LAYBE (Colorado State University, Fort Collins) *Journal of Climate and Applied Meteorology* (ISSN 0733-3021), vol. 26, Jan. 1987, p. 156-169. refs

(Contract NAG5-386)

The use of the area-time-integral (ATI) technique, based only on satellite data, to estimate convective rain volume over a moving target is examined. The technique is based on the correlation between the radar echo area coverage integrated over the lifetime of the storm and the radar estimated rain volume. The processing of the GOES and radar data collected in 1981 is described. The radar and satellite parameters for six convective clusters from storm events occurring on June 12 and July 2, 1981 are analyzed and compared in terms of time steps and cluster lifetimes. Rain volume is calculated by first using the regression analysis to generate the regression equation used to obtain the ATI; the ATI versus rain volume relation is then employed to compute rain volume. The data reveal that the ATI technique using satellite data is applicable to the calculation of rain volume. I.F.

A87-40308#

REMOTE SENSING APPLICATIONS IN HYDROLOGY

THOMAS SCHMUGGE (USDA, Hydrology Laboratory, Beltsville, MD) *Reviews of Geophysics* (ISSN 8755-1209), vol. 25, March 1987, p. 148-152. refs

The physical basis of remote sensing depends on the inference of land-surface characteristics from the measurement of the emitted or reflected EM radiation from the earth. The hydrologically related parameters studied using this approach include: surface temperature, evapotranspiration, soil moisture, precipitation, snow, and components of the radiation balance. Significant progress has been made in determining these quantities using radiation at wavelengths from the microwave to gamma rays. The recent progress in several of these areas is documented in this review. Author

A87-40309* California Univ., Santa Barbara.

RECENT RESEARCH IN SNOW HYDROLOGY

JEFF DOZIER (California, University, Santa Barbara) *Reviews of Geophysics* (ISSN 8755-1209), vol. 25, March 1987, p. 153-161. Research supported by the California Air Resources Board. refs (Contract NAS5-28770)

Recent work on snow-pack energy exchange has involved detailed investigations on snow albedo and attempts to integrate energy-balance calculations over drainage basins. Along with a better understanding of the EM properties of snow, research in remote sensing has become more focused toward estimation of snow-pack properties. In snow metamorphism, analyses of the physical processes must now be coupled to better descriptions of the geometry of the snow microstructure. The dilution method now appears to be the best direct technique for measuring the liquid water content of snow; work on EM methods continues. Increasing attention to the chemistry of the snow pack has come with the general focus on acid precipitation in hydrology. Author

06 HYDROLOGY AND WATER MANAGEMENT

A87-42256

INLAND WETLAND CHANGE DETECTION USING AIRCRAFT MSS DATA

JOHN R. JENSEN, ELIJAH W. RAMSEY (South Carolina, University, Columbia), HALKARD E. MACKEY, JR. (DuPont de Nemours Savannah River Laboratory, Aiken, SC), ERIC J. CHRISTENSEN (EG&G Energy Measurements, Las Vegas, NV), and REBECCA R. SHARITZ (Georgia, University, Aiken, SC) Photogrammetric Engineering and Remote Sensing (ISSN 0099-1112), vol. 53, May 1987, p. 521-529. refs (Contract DE-AC09-76SR-00819; DE-AC09-76SR-00001)

Nontidal wetlands in a portion of the Savannah River swamp forest affected by reactor cooling water discharges were mapped using March 31, 1981 and April 29, 1985 high-resolution aircraft multispectral scanner (MSS) data. Due to the inherent distortion in the aircraft MSS data and the complex spectral characteristics of the wetland vegetation, it was necessary to implement several innovative techniques in the registration and classification of the MSS data of the Pen Branch Delta on each date. In particular, it was necessary to use a piecewise-linear registration process over relatively small regions to perform image-to-image registration. When performing unsupervised classification, an iterative 'cluster busting' technique was used which simplified the cluster labeling process. These procedures allowed important wetland vegetation categories to be identified on each date. The multiple-date classification maps were then evaluated using a post-classification comparison technique yielding estimates of change in the wetland classes. Author

N87-22364# Centre de Recherches en Physique de l'Environnement Terrestre et Planetaire, Orleans (France).

MEASUREMENT AND DETECTION OF PRECIPITATION. SATELLITE METHODS IN THE VISIBLE AND THE INFRARED [DETECTION ET MESURE DES PRECIPITATIONS. METHODES SATELLITAIRES EN VISIBLE ET EN INFRAROUGE]

MICHEL DESBOIS *In its* Energy Balance of the Tropical Systems (BEST). Conference on the Scientific Prospects of the Project p 5-10 1986 In FRENCH
Avail: NTIS HC A11/MF A01

The utilization of combined visible and infrared precipitation measurements is discussed. The application to the study of space-time distribution of large scale rain is reviewed, in particular the phenomena associated with El Nino. It is concluded that there is not a simple universal method that can be applied to any type of cloud, any region, any season. Local measurements are necessary in each case to calibrate the measuring system. ESA

N87-22373# Centre de Recherches en Physique de l'Environnement Terrestre et Planetaire, Orleans (France).

ENERGY BALANCE OF THE TROPICAL SYSTEMS (BEST): A SPACE EXPERIMENT PROPOSITION [PROJET D'EXPERIENCE SPATIALE 'BEST'. BILAN ENERGETIQUE DU SYSTEME TROPICAL]

P. AMAYENC, R. BERNARD, L. EYMARD, J. TESTUD, D. VIDAL-MADJAR, G. MEGIE, J. PELON, J. P. JEGOU, J. BARAT, P. FLAMANT (Ecole Polytechnique, Palaiseau, France) et al. *In its* Energy Balance of the Tropical Systems (BEST). Conference on the Scientific Prospects of the Project p 183-217 1986 In FRENCH

Avail: NTIS HC A11/MF A01

A satellite-borne system to measure tropical region atmospheric parameters is proposed. The instruments include active and passive microwave radars, optical radar, and infrared radiometry. The main parameters to be measured are precipitation intensity, ocean or ground interfaces, evaporation flow, water vapor distribution, and integrated suspended liquid water content. The vertical temperature profile is also measured. A project expansion to Doppler lidar wind velocity measurement is also discussed. Instrument technical characteristics are described. ESA

N87-24031*# National Aeronautics and Space Administration. Goddard Space Flight Center, Greenbelt, Md.

SPATIAL CHARACTERIZATION OF ACID RAIN STRESS IN CANADIAN SHIELD LAKES Progress Report, 1 Aug. 1985 - 1 Feb. 1986

FRED J. TANIS 1986 9 p

(Contract NAS5-28779)

(NASA-CR-180983; NAS 1.26:180983; ERIM-198400-19-L) Avail: NTIS HC A02/MF A01 CSCL 13B

The acidification of lake waters from airborne pollutants is of continental proportions both in North America and Europe. A major concern of the acid rain problem is the cumulative ecosystem damage to lakes and forest. The number of lakes affected in northeastern United States and on the Canadian Shield is thought to be enormous. The principle objective is to examine how seasonal changes in lake water transparency are related to annual acidic load. Further, the relationship between variations in lake acidification and ecophysical units is being examined. Finally, the utility of Thematic Mapper (TM) based observations to measure seasonal changes in the optical transparency in acid lakes is being investigated. Author

N87-24032*# National Aeronautics and Space Administration. Goddard Space Flight Center, Greenbelt, Md.

SPATIAL CHARACTERIZATION OF ACID RAIN STRESS IN CANADIAN SHIELD LAKES Progress Report, 1 Feb. - 1 Aug. 1986

FRED J. TANIS 1986 19 p

(Contract NAS5-28779)

(NASA-CR-180982; NAS 1.26:180982; ERIM-189400-21-L) Avail: NTIS HC A02/MF A01 CSCL 13B

A major concern of the acid rain problem is the cumulative ecosystem damage to lakes and forests. The number of lakes affected in northeastern United States and on the Canadian Shield is thought to be enormous. Seasonal changes in lake transparency are examined relative to annual acidic load. The relationship between variations in lake acidification and ecophysical units is being examined. Finally, the utility of Thematic Mapper (TM) based observations is being used to measure seasonal changes in the optical transparency in acid lakes. B.G.

07

DATA PROCESSING AND DISTRIBUTION SYSTEMS

Includes film processing, computer technology, satellite and aircraft hardware, and imagery.

A87-31412

INTERPRETATION OF THE POLARIMETRIC CO-POLARIZATION PHASE TERM IN RADAR IMAGES OBTAINED WITH THE JPL AIRBORNE L-BAND SAR SYSTEM

WOLFGANG-M. BOERNER, BING-YUEN FOO, and HYU J. EOM (Illinois, University, Chicago) IEEE Transactions on Geoscience and Remote Sensing (ISSN 0196-2892), vol. GE-25, Jan. 1987, p. 77-82. refs

The utilization of both polarimetric amplitude and relative phase terms of the polarization scattering matrix given for each pixel, is pursued for polarimetric SAR imagery interpretation. The existing amplitude-only backscattering approaches hitherto used are extended and modified to accommodate the interpretation of information contained in the amplitude and/or phase terms. Both a vector radiative transfer model for surface versus volume scattering from rough terrain with and without vegetation canopy and a high-frequency electrical curvature model for perfectly conducting surfaces are examined to come up with theoretical models that out-perform other hitherto known approaches. The developed models agree with the excellent polarimetric SAR imagery recently obtained with the JPL CV-990 dual-polarization

L-band (1.225 GHz) SAR system. Recommendations are made on how to further perfect the system for integration in the SIR-C and other future polarimetric SIR-SAR systems. Author

A87-32488

SPECTRAL CLASSIFICATION OF LANDSAT-5 THEMATIC MAPPER DATA

SUEO UENO, YOSHIYUKI KAWATA, and TAKASHI KUSAKA (Kanazawa Institute of Technology, Ishikawa, Japan) IN: International Symposium on Space Technology and Science, 15th, Tokyo, Japan, May 19-23, 1986, Proceedings. Volume 2. Tokyo, AGNE Publishing, Inc., 1986, p. 1577-1582. refs (Contract MOESC-60129032)

Image processing of TM data in a subscene site of 800 x 800 pixels over the Kanazawa area in Japan was performed using Landsat 5 TM computer-compatible tape (CCT) data preprocessed by NASDA. Based on the ground truth data with cartographic accuracy of 25-m span, classification was performed in both the supervised and the unsupervised schemes. The grey levels in the CCT were transformed into the principal components (PC) and the CCT and PC values were classified in both schemes. The supervised and unsupervised classifications of the TM data (summarized in terms of 16 cover types, such as water, urban area, rural area, rice fields, sand, cedar or mixed-conifer forests, etc.) have shown satisfactory statistical results for the grey levels in TM CCT and PC data. I.S.

A87-32489

CORRECTION FOR ATMOSPHERIC AND TOPOGRAPHIC EFFECTS ON THE LANDSAT MSS DATA

YOSHIYUKI KAWATA and SUEO UENO (Kanazawa Institute of Technology, Nonoichi, Japan) IN: International Symposium on Space Technology and Science, 15th, Tokyo, Japan, May 19-23, 1986, Proceedings. Volume 2. Tokyo, AGNE Publishing, Inc., 1986, p. 1583-1585. refs

A simple radiometric correction method is proposed for removing both the atmospheric and topographic effects from the Landsat MSS data. The application of the method proposed here to a real rugged-terrain image gives satisfactory results when the digital terrain data are available. The values of the necessary atmospheric parameters are computed from the LOWTRAN 5 Code. Lambert's law of reflection on the ground surface is assumed in this study. Author

A87-32506

SIMULATION SOFTWARE OF SYNTHETIC APERTURE RADAR

JIRO KOMAI, ITOSHI KOHNO (Earth Resources Satellite Data Analysis Center, Tokyo, Japan), MAKOTO ONO, and HIROKAZU TANAKA (Mitsubishi Electric Corp., Kamakura, Japan) IN: International Symposium on Space Technology and Science, 15th, Tokyo, Japan, May 19-23, 1986, Proceedings. Volume 2. Tokyo, AGNE Publishing, Inc., 1986, p. 1705-1710.

Synthetic aperture radar (SAR) simulation software with a high simulation capacity for various kinds of simulation parameters is described. The software consists of eight major blocks: (1) the terrain model generation block; (2) radar characteristics simulation block; (3) scattering characteristics simulation block; (4) theoretical image generation block; (5) hologram generation block; (6) image reconstruction block; (7) image display block; and (8) image analysis and evaluation block. Good coincidence is found between simulated and actual SAR images. R.R.

A87-35183

MIDAS - A NEW IMAGE-PROCESSING SYSTEM FOR REMOTE SENSING [MIDAS - EIN NEUES BILDBERARBEITUNGSSYSTEM FUER DIE FERNERKUNDUNG]

G. LOHMANN, H.-J. LOTZ-IWEN, W. MARKWITZ and R. WINTER (DFVLR, Hauptabteilung angewandte Datentechnik, Oberpfaffenhofen, West Germany) IN: DFVLR, Annual Report 1985 Cologne, West Germany, Deutsche Forschungs- und Versuchsanstalt fuer Luftund Raumfahrt, 1986, p. 70-74. In German.

MIDAS, a modular interactive decentralized computer interpretation system for second-generation satellite-remote-sensing images developed for use at the DFVLR remote-sensing data center, is described. In MIDAS, interactive workstations and a local image-processing (IP) computer (with display peripherals) are linked to the mainframe computer at DFVLR-Oberpfaffenhofen via a fast local-area network. The MIDAS software is essentially the UPSTAIRS system, comprising user software (utility programs, general IP programs, and sensor-specific and project-specific programs) and system-core software (database, computer interfaces, dialog manager, and virtual display system). The MIDAS structure and features are reviewed, and IHS and principal-components transformations of a Landsat TM image are presented as examples. T.K.

A87-35305

AUTOMATIC CLASSIFICATION OF POINTE D'ARCAIS LANDSCAPES USING THEMATIC MAPPER DATA WITH THE AID OF A TEXTURAL ANALYSIS [CLASSIFICATION AUTOMATIQUE ASSISTEE PAR UNE ANALYSE DE TEXTURE, DES PAYSAGES DE LA POINTE D'ARCAIS D'APRES DES DONNEES THEMATIC MAPPER]

DONG-CHEN HE (CNRS, Institut National des Sciences de l'Univers, Paris, France) and LI WANG (Ecole Normale Supérieure, Montrouge, France) International Journal of Remote Sensing (ISSN 0143-1161), vol. 8, Feb. 1987, p. 129-135. In French. refs

A method for the automatic classification of landscapes using Landsat-5 Thematic Mapper (TM) data is demonstrated with data of the Pointe d'Arcay (France) landscape obtained on April 12, 1984. A purely radiographic multispectral classification is first performed on the data of six TM bands (1, 2, 3, 4, 5, and 7) using an unsupervised algorithm of clustering around mobile centers. A textural analysis is then introduced to eliminate classification confusion between scene analysis classes, and an improvement over the purely radiographic classification is found. It is noted that because the textural analysis is based on a neighborhood of pixels, the resulting spatial resolution is decreased. R.R.

A87-35313

INTRODUCTION OF INITIAL CENTERS FOR THE ALGORITHM OF CLUSTERING AROUND MOBILE CENTERS [INTRODUCTION DE CENTRES INITIAUX POUR L'ALGORITHME D'AGREGATION AUTOUR DE CENTRES MOBILES]

DONG-CHEN HE (CNRS, Institut National des Sciences de l'Univers, Paris, France) and LI WANG (Ecole Normale Supérieure, Montrouge, France) International Journal of Remote Sensing (ISSN 0143-1161), vol. 8, Feb. 1987, p. 237-242. In French. refs

A method for the introduction of initial centers is proposed to improve the performance of the algorithm of clustering around mobile centers, eliminating the blind determination of the number of initial centers at the beginning of the algorithm. A simple histogram analysis permits the simultaneous determination of the number and optimum location of initial classes for an unsupervised classification. Using the example of a multispectral classification of Thematic Mapper data on the Arcachon basin, the present method is shown to be more accurate than the conventional method. R.R.

A87-35524

DERIVATION OF A FAST ALGORITHM TO ACCOUNT FOR DISTORTIONS DUE TO TERRAIN IN EARTH-VIEWING SATELLITE SENSOR IMAGES

JOHN W. MARVIN, MARK L. LABOVITZ, and ROBERT E. WOLFE (SASC Technologies, Inc., Lanham, MD) IEEE Transactions on Geoscience and Remote Sensing (ISSN 0196-2892), vol. GE-25, March 1987, p. 244-251. refs

Earth-viewing satellite sensors (e.g., the Landsat 4/5 Thematic Mapper) produce images with nontrivial amounts of geometric distortion due to local terrain variations. Although correction formulas are easy to derive, the high frequency of terrain variation relative to pixel size means that excessive computer time is required to process a large digital image. This paper derives approximations to the correction geometry that reduce computer time by orders of magnitude. A statistical sensitivity analysis shows that the approximations do not adversely affect the accuracy of the results even under a very demanding error budget. Author

A87-35925

PROBLEMS IN THE AUTOMATION OF MAP-COMPILATION PROCESSES ON THE BASIS OF REMOTE-SENSING DATA [PROBLEMY AVTOMATIZATSII SOZDANIYA KART NA OSNOVE AEROKOSMICHESKOI INFORMATSII]

A. P. VOROZHEIKIN, V. V. KISELEV, A. E. MENSHIKH, and M. E. SOLOMATIN Geodeziya i Kartografiya (ISSN 0016-7126), Dec. 1986, p. 31-34. In Russian.

A87-36359

REMOTE SENSING - HANDLING THE DATA

DAVID SLOGGETT and JONATHAN WILLIAMS (Software Sciences, Ltd., Farnborough, England) Space (ISSN 0267-954X), vol. 3, Mar.-Apr. 1987, p. 8-11.

The processing and interpretation of environmental and earth resource data are examined. The active and passive sensors on satellites which detect electromagnetic radiation that is converted to digital signals and photographic images are described. The on board processing and the real-time or playback transmission of data are discussed. The procedures for processing the data into digital or photographic forms involve bulk correction of the data and the use of an image processing system and image processing techniques. Consideration is given to archiving and dissemination of the data. Proposed developments in remote sensing are also discussed. I.F.

A87-36361

MAPPING FROM SPACE

ANDREW WESTWELL-ROPER and STEPHEN BECKOW (MacDonald, Dettwiler and Associates, Ltd., Richmond, Canada) Space (ISSN 0267-954X), vol. 3, Mar.-Apr. 1987, p. 24-28.

The use of satellite imagery to produce maps of the earth is examined. The advantages provided to map production by the SPOT satellite, which provides planimetric and elevation data, the Panchromatic Linear Array of the satellite, and operational geocoding, are discussed. A review of the techniques involved in traditional map production is presented. The automated image processing of satellite data to produce maps is described; it is determined that satellite map production is more economical than photogrammetry. The digital mapping and geographic information systems used for the storage of mapping information are considered. The application of AI to image processing and map production is proposed. I.F.

A87-36546

LANDFORM INVESTIGATION UTILIZING DIGITALLY PROCESSED SATELLITE THEMATIC MAPPER IMAGERY

ARWYN RHYS JONES (Reading, University, England) Earth, Moon, and Planets (ISSN 0167-9295), vol. 37, Feb. 1987, p. 171-185. refs

Thematic Mapper (TM) images obtained by Landsat 4 in January 1983 are used to demonstrate the additional geomorphological detail that can be extracted from TM imagery using computer-assisted digital image processing. Single-band

enhancement techniques include contrast stretching and edge enhancement, and multiband processing techniques include the application of an Intensity-Hue-Color transformation to false color composites, and the ratioing of two spectral bands. More complex multivariate techniques considered include unsupervised classification and principal component analysis. Best results are obtained when a specific relationship exists between the spectral response and the physical properties of the phenomena under investigation. R.R.

A87-36757

STEREOSCOPIC LINE SCAN IMAGING AND SATELLITE CONTROL

A. DRESCHER, G. MAYER, and J. PULS (DFVLR, Oberpfaffenhofen, West Germany) IN: Yearbook 1986 I; DGLR, Annual Meeting, Munich, West Germany, Oct. 8-10, 1986, Reports . Bonn, Deutsche Gesellschaft fuer Luft- und Raumfahrt, 1986, p. 45-48. refs (DGLR PAPER 86-106)

An interactive and semiautonomous attitude control concept for satellites is proposed. The concept uses on-board and ground-based processing intelligence via two-way exchange of raw and processed data. The use of ground truth for image correction is reviewed, and attitude requirements for stereoscopy in planned satellites are discussed. Attitude control characteristics and proposed attitude control changes are examined. C.D.

A87-37276

COMBINING PANCHROMATIC AND MULTISPECTRAL IMAGERY FROM DUAL RESOLUTION SATELLITE INSTRUMENTS

JOHN C. PRICE (USDA, Remote Sensing Research Laboratory, Beltsville, MD) Remote Sensing of Environment (ISSN 0034-4257), vol. 21, March 1987, p. 119-128. refs

A procedure is developed for combining high spatial resolution panchromatic data with lower resolution multispectral data in order to produce high spatial resolution digital data in multispectral form. Data simulating the French SPOT satellite were processed to resemble high altitude aerial photography, but image artifacts can hamper photointerpretative methods. Author

A87-37287

MERGING MULTIREOLUTION SPOT HRV AND LANDSAT TM DATA

R. WELCH and MANFRED EHLERS (Georgia, University, Athens) Photogrammetric Engineering and Remote Sensing (ISSN 0099-1112), vol. 53, March 1987, p. 301-303. refs

Methods for merging multisensor and multiresolution satellite data in digital formats to create composite images with improved interpretability are described. A merged multiresolution data set from a test site located in Atlanta, Georgia and imaged by the Landsat-5 Thematic Mapper on April 4, 1985 and by the SPOT High Resolution Visible cameras on May 4, 1986 is evaluated. The use of the intensity-hue-saturation (IHS) color transformation procedures of Haydn et al. (1982) to merge Landsat and SPOT images is discussed. It is noted that the IHS algorithm improves the quality of the SPOT and Landsat images, and the composites have spatial resolution properties similar to the reference panchromatic image and still retain the spectral discrimination qualities of the original multispectral data set. I.F.

A87-37288

THE DENALI IMAGE MAP

DOUGLAS R. BINNIE (USGS, EROS Data Center, Sioux Falls, SD) and ALDEN P. COLVOCORESSES (USGS, Reston, VA) Photogrammetric Engineering and Remote Sensing (ISSN 0099-1112), vol. 53, March 1987, p. 307-310. refs

Mt. McKinley in Denali National Park, AK has perhaps the greatest relief of any land mountain in the world in that it rises over 5000 meters (17,000 feet) above its surrounding base. Thus, it presents the ultimate challenge to the mapmaker to produce a satellite image map that will not be badly distorted by relief displacement. Moreover, the area presents a stark contrast

between the snow/ice and summer vegetation coverage. Although prospective purchasers of the Denali National Park map will decide if the information portrayal is worthwhile, it is up to the mapmaker to determine how well this mountain mass can be correctly positioned and cartographically displayed. Because summer seasons are short and cloud-prone, the mapmaker had to select and match nine images from 5 years of Landsat multispectral scanner (MSS) coverage. This work was carried out at the EROS Data Center (EDC) using the digital Large Area Mosaic System (LAMS). Other special features of this map are that it is printed on plastic, which should extend its life and versatility, and it carries an updated line map on the reverse side. Both maps are at 1:250,000 scale and carry a UTM grid to facilitate referencing.

Author

A87-37290

MEASUREMENTS ON DIGITIZED HARDCOPY IMAGES

J. C. TRINDER (New South Wales, University, Sydney, Australia) Photogrammetric Engineering and Remote Sensing (ISSN 0099-1112), vol. 53, March 1987, p. 315-321. refs

Aerial photographs, for which pointing precisions in the x, y, and z coordinates are known, have been digitized with effective square apertures ranging from 6.25 microns to 100 microns. The digitized data were reproduced as hardcopies and observed on a stereoplotter in order to determine precisions of observations. A comparison of these pointing precisions with those derived from the original aerial photographs reveals the magnitude of the aperture required for digitizing to ensure that the quality of the visual observations is maintained. Systematic errors in the positions of points observed in the images are determined by computer simulation and are related to pixel sizes. The studies indicate that visual observations to standard aerial photography are unaffected by digitizing if the pixel sizes are less than or equal to 25 microns; however, the rms of systematic errors in the digitized data attributed to the digitizing process can be about one-fifth of the pixel size.

Author

A87-37801

IMAGE PREPROCESSING FOR LINE DETECTION BASED ON LOCAL STRUCTURE ANALYSIS

ZHENG YU (Paris, Ecole Nationale Supérieure des Mines, Valbonne, France; Beijing University, People's Republic and C. BARDINET (Ecole Normale Supérieure; Paris, Ecole Nationale Supérieure des Mines, Valbonne, France) CODATA Bulletin (ISSN 0366-757X), no. 62, Oct. 1986, p. 9-25. refs

A local two-stage image processing method for image transformation or smoothing is proposed. The two stages of the method are learning and application. Local structure analysis begins with a computer-based simulation of all the local structures within a specific area of image points resulting in grey-level distributions, which are classified in order to produce a decision model based on yes and no operation orders. The construction of the decision model, and the procedures for applying a decision model to images are described. The capabilities and limitations of this method are discussed. The two-stage image processing method is applied to NOAA AVHRR and Landsat TM data on Tanzania. I.F.

A87-37802

THE GEOMULTI DATABASE MANAGEMENT SYSTEM

J. M. MONGET (Paris, Ecole Nationale Supérieure des Mines, Valbonne, France) CODATA Bulletin (ISSN 0366-757X), no. 62, Oct. 1986, p. 27-33.

The Geomulti system, which transforms remote sensing files into a geocoded data base, is described. The Geomulti system consists of: a multivariable coding system, a data base management system, supporting data structures, and a data query and manipulation package; the operations of each of these components are discussed. Data management is based on a geoparameter data base structure, which processes parameter files, peripheral data files, and output data files, and a geocode data structure, which processes tape or disk files. The data structures are implemented using an extension of the VIPS-MGO system to enable definition and handling of data structures as objects. The system

is applicable to multisatellite remote sensing, environmental cartography, and mineral inspection. A diagram of the system's global file organization is presented. I.F.

A87-37803

MULTISATELLITE DATA PROCESSING

C. BARDINET (Ecole Normale Supérieure, Paris, Ecole Nationale Supérieure des Mines, Valbonne, France) and J. M. MONGET (Paris, Ecole Nationale Supérieure des Mines, Valbonne, France) CODATA Bulletin (ISSN 0366-757X), no. 62, Oct. 1986, p. 35-49.

The use of multisatellite data processing in discriminating geographical and geological units or objects in different types of environments is examined. The efficiencies of Meteoros and Landsat, or NOAA6-7 and Tiros-N, or Meteoros and NOAA-Tiros N data in digital form are evaluated. The multisatellite digital image processing phases are: (1) geometric rectification of the graphic data set, (2) multispectral data classification, (3) smoothing and filtering processes, and (4) computer-aided mapping. The methodologies for geometric rectification and for classification are described. I.F.

A87-37922#

AVHRR DATA SERVICES IN EUROPE - THE EARTHNET APPROACH

L. FUSCO and K. MUIRHEAD (ESA, Earthnet Programme Office, Frascati, Italy) ESA Bulletin (ISSN 0376-4265), no. 49, Feb. 1987, p. 9-19.

Characteristics of the current AVHRR on the NOAA polar-orbiting meteorological satellites are described, and the ESA/Earthnet scheme for the coordinated acquisition, archiving, processing, and dissemination of its data is discussed. Extensive usage of AVHRR data for applications including regional and global vegetation monitoring and air and sea pollution monitoring is possible due to its low data costs, high radiometric resolution, and repetitive, large-area coverage. The Earthnet scheme will include a historical dataset for all areas of interest, an internationally-accessible on-line catalogue, and fully-annotated user products in raw form or preprocessed to geophysical values. Standardization of the tape format using the international Standard-Family Tape Format of the Landsat Technical Working Group is also discussed. R.R.

A87-38096*

THE FACTOR OF SCALE IN REMOTE SENSING

CURTIS E. WOODCOCK (Boston University, MA) and ALAN H. STRAHLER (Hunter College, NY) Remote Sensing of Environment (ISSN 0034-4257), vol. 21, April 1987, p. 311-332. refs (Contract NAS9-16664; NASA ORDER L-200080)

A method that measures the spatial structure of images as a function of spatial resolution is presented for selecting the appropriate scale for remote sensing. Graphs are obtained by imaging the scene at fine resolution and then collapsing the image to successively coarser resolutions while calculating the local variance. For the spatial resolution of SPOT and TM imagery, local image variance is relatively high for forested and urban/suburban environments, indicating that information-extraction techniques using texture, context, and mixture modeling are appropriate for these sensor systems. For agricultural environments where local variance is low, more traditional classifiers are appropriate. R.R.

A87-38098*

COMPARISON OF HCMM AND GOES SATELLITE TEMPERATURES AND EVALUATION OF SURFACE STATISTICS

E. CHEN (Florida, University, Gainesville) and L. H. ALLEN, JR. (Florida, University; USDA, Agricultural Research Station, Gainesville) Remote Sensing of Environment (ISSN 0034-4257), vol. 21, April 1987, p. 341-353. refs (Contract NAS5-26453)

Infrared data from GOES and HCMM satellites for areas in northern central and southern Florida were compared for February 1, 1979 to examine spatial variations of surface temperatures within

GOES pixels using nested HCMM pixel surface temperatures. Standard deviations of HCMM pixel temperatures associated with mean temperature of a GOES pixel temperature during this period were found to be smallest for homogeneous water surfaces (about 0.5 K), to be slightly larger for homogeneous land surfaces (about 0.1 K), and to range up as high as 3.5 K for mixed water-land surfaces. R.R.

A87-39184 RADIOMETRIC CORRECTION OF SAR IMAGES - A NEW CORRECTION ALGORITHM

DANIEL BEGIN, Q. H. J. GWYN, and FERDINAND BONN (Sherbrooke, Université, Canada) International Journal of Remote Sensing (ISSN 0143-1161), vol. 8, March 1987, p. 385-398. Research supported by the Ministère de l'Éducation du Québec. refs

Spatial variations of the backscatter coefficient result from synthetic aperture radar imaging systems and their platforms. An adaptive algorithm has been developed to correct the multiplicative variation of the backscatter in the longitudinal (parallel to flight line) and lateral (perpendicular to flight line) directions. The coefficient of variation along the parallel and lateral profiles, which consist of the means of the pixels along these lines perpendicular to the respective profiles, is constant. This implies that the radiometric variations are multiplicative. Because standard correction methods such as polynomial transfer functions give unsatisfactory results, an adaptive correction algorithm was developed to correct these images. The algorithm produces a transfer function by means of a filtering window which moves along the profile in what is essentially a moving mean procedure. However, the length of the window is automatically adjusted as a function of the variation of the profile. The adjustment is based on a calculation of the probability that values to be included or excluded from the window belong to the included population. The effects of the successive correction steps were monitored using several thematic test sites. The resultant images provide both increased quality and quantity of data without any degradation of the statistical properties of the data. Author

A87-39189 SURFACE MODELS INCLUDING DIRECT CROSS-RADIATION - A SIMPLE MODEL OF FURROWED SURFACES

CS. FERENCZ, D. HAMAR, J. LICHTENBERGER, GY. TARCSAI (Eotvos Lorand Tudományegyetem, Budapest, Hungary), and I. FERENCZ ARKOS (Budapesti, Muszaki Egyetem, Budapest, Hungary) International Journal of Remote Sensing (ISSN 0143-1161), vol. 8, March 1987, p. 449-465. Research supported by the Magyar Tudományos Akadémia, and FOMI Remote Sensing Centre. refs

In the interpretation of measured reflectance data it is important to consider those surface radiation effects which make a significant contribution to the overall irradiation pattern. A model, which includes the direct cross-radiation effect between the surface elements, was constructed for furrowed bare soil surfaces. According to the model computations performed, the direct cross-radiation plays a significant role in the measured, reflected signal intensity. The computational method developed is suitable for including the direct cross-radiation effect in surface radiation models in the optical region. Author

A87-39192* National Aeronautics and Space Administration. Goddard Space Flight Center, Greenbelt, Md. THEMATIC MAPPER BANDPASS SOLAR EXOATMOSPHERIC IRRADIANCES

B. L. MARKHAM and J. L. BARKER (NASA, Goddard Space Flight Center, Greenbelt, MD) International Journal of Remote Sensing (ISSN 0143-1161), vol. 8, March 1987, p. 517-523. refs

Based on solar irradiance data published by Neckel and Labs (1984) and Iqbal (1983), the solar exoatmospheric irradiances for Thematic Mapper (TM) bands 1, 2, 3, and 4 have been calculated. Results vary by up to 1 percent from previous published values, which were based on the earlier data of Neckel and Labs. For TM bands 5 and 7, integrated solar exoatmospheric irradiances

have also been recalculated using solar irradiance data published by Labs and Neckel (1968), Arvesen et al. (1969), and Iqbal (1983). These irradiances vary by up to 6 percent from previously published results, which were based on data published by Thekaekara (1972). Author

A87-41925 PHYSICAL PRINCIPLES OF IMAGE CONVERGENCE IN REMOTE SENSING [FIZICHESKIE PRINTSIPY SOVMESHCHENIIA IZOBRAZHENII, POLUCHAEMYKH PRI DISTANTSIONNOM ZONDIROVANII]

A. G. ERMOLAEV, S. V. KIREEV, and I. U. P. PYT'EV (Moskovskii Gosudarstvennyi Universitet, Moscow, USSR) Moskovskii Universitet, Vestnik, Seriya 3 - Fizika, Astronomiia (ISSN 0579-9392), vol. 27, Nov.-Dec. 1986, p. 95-97. In Russian.

The instability of the trajectory and attitude of the satellite at the moment of remote sensing leads to the fact that any two images of the same part of the earth surface are recorded from two different points of view and at different angles. An image-correction technique is proposed for the processing of images obtained at different times. The technique is based on a physical model of image recording and mathematical methods of morphological analysis. The processing of Landsat images is considered as an example. B.J.

A87-42628 AN EXPERT SYSTEM FOR LABELING SEGMENTS IN FORWARD LOOKING INFRARED (FLIR) IMAGERY

G. A. ROBERTS (Ford Aerospace and Communications Corp., Newport Beach, CA) IN: Applications of artificial intelligence III; Proceedings of the Meeting, Orlando, FL, Apr. 1-3, 1986. Bellingham, WA, Society of Photo-Optical Instrumentation Engineers, 1986, p. 50-57. refs

An expert system for labeling high priority potential targets, low priority potential targets, roads, trees, forests, and potential clearings in FLIR imagery is presented. This expert system consists of three stages: the initial labeling experts, initial label conflict resolution, and a final relaxation labeling stage. The techniques used in these stages are presented. Examples of segmentation and segment labeling are shown. Author

A87-42659* Jet Propulsion Lab., California Inst. of Tech., Pasadena.

OPTICAL IMAGE SUBTRACTION TECHNIQUES, 1975-1985

HUA-KUANG LIU and TIEN-HSIN CHAO (California Institute of Technology, Jet Propulsion Laboratory, Pasadena) IN: Hybrid image processing; Proceedings of the Meeting, Orlando, FL, Apr. 1, 2, 1986. Bellingham, WA, Society of Photo-Optical Instrumentation Engineers, 1986, p. 55-65. refs

Real- and nonreal-time optical image subtraction (OIS) techniques are reviewed. Real-time OIS techniques include source encoding, polarization modulation, pseudocolor image difference detection, the holographic shear lens technique, and nonlinear optics. Included in the nonreal-time category are speckle diffuser encoding, speckle-pattern encoding, halftone screen encoding, and polarization-shifted encoding. It is concluded that the most useful techniques are the real-time operations. It is noted that some nonreal-time optical techniques can be applied directly while others may be converted into real-time ones through the use of advance real-time spatial light modulators or electrooptic devices. K.K.

N87-20449*# Massachusetts Inst. of Tech., Cambridge. Research Lab. of Electronics.

RADAR SCENE GENERATION FOR TACTICAL DECISION AIDS Final Report, 15 Apr. 1986 - 14 Apr. 1987

J. A. KONG 28 Apr. 1987 7 p (Contract NAG5-769) (NASA-CR-180234; NAS 1.26:180234) Avail: NTIS HC A02/MF A01 CSCL 171

The Mueller matrix and polarization covariance matrix for polarimetric radar systems was studied. The clutter is modeled by a layer of random permittivity, described by a three-dimensional correlation function, with variance, and horizontal and vertical

correlation lengths. A general mixing formula was derived for discrete scatters immersed in a host medium. The results are applicable to general multiphase mixtures. The strong fluctuation theory was used to derive the backscattering cross sections, and was further extended to include higher order co-polarized and cross-polarized moments. A two-layer anisotropic random medium model was developed for the active and passive remote sensing of ice fields. A three-layer random medium model was adopted to study the volume scattering effects for the active and passive microwave remote sensing of snow-covered ice fields. The snow layer was simulated by an isotropic random medium and the ice layer by an anisotropic random medium. The vegetation canopy and snow-covered ice field were studied with a three-layer model, an isotropic random medium layer overlying an anisotropic random medium. The dyadic Green's function of the three-layer medium and the scattered electromagnetic intensities with Born approximation were calculated B.G.

N87-20554# Boeing Aerospace Co., Seattle, Wash.
NASA/MSFC LARGE STRETCH PRESS STUDY
 M. W. CHOATE, W. P. NEALSON, G. C. JAY, and W. D. BUSS
 Apr. 1985 138 p
 (Contract NAS8-35969)
 (NASA-CR-180376; NAS 1.26:180376; D180-27884-3) Avail:
 C A07/MF A01 CSCL 131

Mueller matrix and polarization covariance matrix for synthetic radar systems were studied. The clutter is modeled by a layer of random permittivity, described by a three-dimensional correlation function, with variance, and horizontal and vertical correlation lengths. Theoretical predictions were matched with experimental data for vegetation fields. A general mixing formula was derived for discrete scatters immersed in a host medium. The results are applicable to general multiphase mixtures. The strong fluctuation theory was used to derive the backscattering cross sections and was further extended to include higher order co-polarized and cross-polarized moments. A two-layer anisotropic random medium model was developed for the active and passive microwave remote sensing of ice fields. A three-layer random medium model was adopted to study the volume scattering effects for the active and passive microwave remote sensing of snow-covered fields. The snow layer was simulated by an isotropic random medium and the ice layer by an anisotropic random medium. The vegetation canopy and snow-covered ice field were studied with a three-layer model, an isotropic random medium layer overlying an anisotropic random medium. The dyadic Green's function of the three-layer medium and the scattered electromagnetic intensities with Born approximation were calculated. B.G.

N87-22278 Regione del Veneto, Mestre-Venezia (Italy).
COMPARATIVE EVALUATION AND GUIDE FOR THE INTEGRATED UTILIZATION OF LANDSAT (MSS AND TM) AND SPOT (HRV) SATELLITES REMOTELY SENSED DATA (VALUTAZIONE COMPARATA E GUIDA ALL'USO INTEGRATO DEI DATI TELERILEVATI DAI SATELLITI LANDSAT (MSS E TM) E SPOT (HRV))
 ALESSANDRO ANNONI and ENRICO ZINI 1986 149 p In ITALIAN Sponsored by the CIPE, and the Fondo di Investimenti (ETN-87-99356) Avail: Issuing Activity

A LANDSAT/SPOT user's manual is presented, including the description of both types of satellite, their performance, and the data characteristics. Data processing is illustrated, several procedures are explained, and useful parameters are given. ESA

N87-23014# Army Cold Regions Research and Engineering Lab., Hanover, N. H.
AN EVALUATION OF THE POLAR ICE PREDICTION SYSTEM Final Report
 W. B. TUCKER, III and W. D. HIBLER, III Feb. 1987 98 p
 (AD-A178522) Avail: NTIS HC A05/MF A01 CSCL 08L

The Polar Ice Prediction System (PIP) is a numerical ice forecasting system that has been implemented at the U.S. Navy Fleet Numerical Oceanographic Center (FNOC). The PIPS model

is run as a 24-hr timestep out to 144 hours (6 days) on a 47 x 25 grid at a resolution of 127 Km. This grid covers the entire Arctic basin as well as the Greenland and Norwegian Seas. Graphic forecast products are transmitted via the Naval Environmental Display Systems to the Naval Polar Oceanographic Center (NPOC) for guidance in preparation of weekly ice forecasts. Primary products are ice drift, thickness, concentration and divergence. A two-phased evaluation of PIPS was conducted. The first extended from 15 Nov 1985 until 15 March 1986 while the second phase ran from 15 June until 15 Oct 1986. As well as covering periods of ice growth and decay, the model was initialized differently for the two phases. During Phase I, the model self-generated its initial concentration field from analysis atmospheric forcing fields. For Phase II, the digitized ice analysis prepared by NPOC was used to update the model each week. GRA

N87-24011# Los Alamos National Lab., N. Mex.
AN ATMOSPHERIC CORRECTION ALGORITHM FOR REMOTE IDENTIFICATION OF NON-LAMBERTIAN SURFACES AND ITS RANGE OF VALIDITY
 A. GRATZKI and S. A. W. GERSTL 20 Feb. 1987 6 p Presented at IGARSS '87, Ann Arbor, Mich., 18 May 1987
 (Contract W-7405-ENG-36)
 (DE87-006059; LA-UR-87-571; CONF-870576-2) Avail: NTIS HC A02

The usefulness of remotely sensed surface data depends on the ability to correct for atmospheric perturbations on the image. An atmospheric correction algorithm has been proposed which removes atmospheric perturbations from off-nadir measured radiances at the top of the atmosphere in the visible and near-infrared wavelength region. The ability of the model to reproduce radiance distributions at the surface from radiances at the top of the atmosphere is tested and found to be better than 15%. The correction formalism requires as minimum information the total optical depth of the atmosphere and the surface albedo. In this study the accuracy of the model to assumptions about the aerosol phase function, the single-scattering albedo and the vertical profile of the optical depth is also tested. DOE

N87-24013# Geological Survey, Reston, Va. National Mapping Div.
RADAR AS A COMPLEMENT TO TOPOGRAPHIC MAPS FOR DELINEATING MARINE TERRACES Open File Report
 J. L. PLACE Dec. 1986 15 p
 (PB87-154597; USGS/OFR-86/010) Avail: NTIS HC A02/MF A01 CSCL 08B

In special situations, side-looking airborne radar images can be used to complement topographic maps for locating and mapping marine terraces on mountainous coasts. When a radar image and a topographic map are superimposed in a Zoom Transfer Scope, the two data sources enhance each other to provide more information than is available from either alone. For locating marine terraces on mountainous coasts, a radar view that is parallel with the coast of looking offshore apparently produces a more interpretable image than a view straight in toward the land. This technique has not proven to be equal to field work for terrace mapping, but it should be faster and less expensive for a preliminary terrace delineation. Radar images from the SEASAT satellite were also tested, but without notable success; the side-looking airborne radar images were generally superior for terrace delineation. GRA

N87-24014# Los Alamos National Lab., N. Mex.
MODELLING OF ATMOSPHERIC EFFECTS ON THE ANGULAR DISTRIBUTION OF A BACKSCATTERING PEAK
 B. J. POWERS and S. A. W. GERSTL 20 Feb. 1987 5 p Presented at the IGARSS '87, Ann Arbor, Mich., 18 May 1987
 (Contract W-7405-ENG-36)
 (DE87-006060; LA-UR-87-572; CONF-870576-1) Avail: NTIS HC A02/MF A01

If off-nadir satellite sensing of vegetative surfaces is considered, understanding the angular distribution of the radiance exiting the atmosphere in all upward directions is of interest. Of particular

07 DATA PROCESSING AND DISTRIBUTION SYSTEMS

interest is the discovery of those reflectance features which are invariant to atmospheric perturbations. When mono-directional radiation is incident on a vegetative scene a characteristic angular signature called the hot-spot is produced in the solar retro-direction. The remotely sensed hot-spot is modified by atmospheric extinction of the direct and reflected solar radiation, atmospheric backscattering, and the diffuse sky irradiance incident on the surface. It is demonstrated, however, by radiative transfer calculations through model atmospheres that at least one parameter which characterizes the canopy hot-spot, namely its angular half width, is invariant to atmospheric perturbations.

DOE

N87-24741# Stuttgart Univ. (West Germany).

IMPROVEMENT OF IMAGE QUALITY BY FORWARD MOTION COMPENSATION, A PRELIMINARY REPORT

FRIEDRICH ACKERMANN *In* ESA Proceedings of the International Symposium on Progress in Imaging Sensors p 25-32 Nov. 1986

Avail: NTIS HC A99/MF A01

Aerial photographs with and without forward motion compensation were compared. Measuring precision and geometrical accuracy in plan and height, and image quality as expressed by transfer functions were studied. Results confirm that air survey cameras with linear compensation of the forward motion during exposure permit longer exposure times and high resolution films. The direct result is visibly improved resolution, better image interpretation, and better measuring precision.

ESA

N87-24753# Khartoum Univ. (Sudan).

OPTICAL AND DIGITAL SAR PROCESSING TECHNIQUES: A STATISTICAL COMPARISON OF ACCURACY USING SEASAT IMAGERY

ABDALLA ELSADIG ALI *In* ESA Proceedings of the International Symposium on Progress in Imaging Sensors p 131-139 Nov. 1986

Avail: NTIS HC A99/MF A01

Geometric accuracy of SEASAT synthetic aperture orbital radar images was tested. Each of four images was processed using different SAR processing systems and methodologies. Image coordinates of selected points were measured and transformed to the terrain system using mathematical transformations. Comparison of the known terrain coordinates and the transformed image coordinates of these points on each image allowed various statistical characteristics to be derived and showed the capability of each of the processing systems tested in producing accurate SAR images. Results show that application of an affine transformation can substantially eliminate differential scale errors in optically processed images. Error magnitude in digitally processed images are much lower, and differential scale errors are eliminated.

ESA

N87-24754# Technische Univ., Hanover (West Germany). Inst. for Photogrammetry and Engineering Surveys.

INTRODUCTION OF GEOMETRIC INFORMATION TO RADAR IMAGE DATA

G. KONENCY and W. SCHUHR *In* ESA Proceedings of the International Symposium on Progress in Imaging Sensors p 141-147 Nov. 1986

Avail: NTIS HC A99/MF A01

To improve the geometric accuracy of initial radar image data, the introduction of additional geometric information to radar image data, e.g., ground control point coordinate values, terrain heights, and information about the behavior of the sensor is described. The derived formulas and practical results, especially for a more precise slant to groundrange conversion process, are suggested to serve the user with geometrically more precisely corrected basic SAR image data.

ESA

N87-24791# Xian Research Inst. of Surveying and Mapping (China).

ESTIMATING PHOTOGRAMMETRIC PRECISION AND CARTOGRAPHIC POTENTIAL OF SPACE IMAGERY

RENXIANG WANG *In* ESA Proceedings of the International Symposium on Progress in Imaging Sensors p 433-438 Nov. 1986

Avail: NTIS HC A99/MF A01

Photogrammetric precision and cartographic potential of metric photo and linear array images to be acquired from shuttle or satellite are assessed. The optional overlap of the metric photos for stereoploting is discussed. The 40% overlap may be the best option. The two categories of imagery for photogrammetry and remote sensing are reviewed.

ESA

N87-24799# Technische Univ., Vienna (Austria). Inst. fuer Vermessungswesen und Fernerkundung.

PHOTOGRAPHIC QUALITY OF COLOR IR AERIAL PHOTOS AS A FUNCTION OF ATMOSPHERIC PARAMETERS

W. SCHNEIDER *In* ESA Proceedings of the International Symposium on Progress in Imaging Sensors p 505-509 Nov. 1986 Sponsored by the Austrian Fonds zur Foerderung der Wissenschaftlichen Forschung

Avail: NTIS HC A99/MF A01

The relationship between the contrast of color CIR aerial photos, defined in terms of the image density range (width of density histogram) of a certain land cover type (spruce forest), and the atmospheric conditions during photo acquisition, defined in terms of the total normal optical thickness of the atmosphere as determined by simultaneous terrestrial spectroradiometric measurements, is analyzed. An empirical relationship between these quantities can be used to predict the contrast of aerial photos from terrestrial solar irradiance measurements prior to a planned photo flight.

ESA

N87-24804# Centre National d'Etudes Spatiales, Toulouse (France).

SPOT IMAGE QUALITY

G. BEGNI, B. BOISSIN, and M. LEROY *In* ESA Proceedings of the International Symposium on Progress in Imaging Sensors p 551-556 Nov. 1986

Avail: NTIS HC A99/MF A01

Postlaunch assessment tests of SPOT image quality are summarized. In geometric image quality, all specifications are fulfilled, most often with comfortable margins. Length distortion is 1 order of magnitude better than the specification, due in part to the excellent quality of the satellite attitude control system. The radiometric image quality is also very satisfactory, except for relatively minor problems in signal to noise ratio in the HRV2 panchromatic band.

ESA

N87-24808# Canada Centre for Remote Sensing, Ottawa (Ontario).

THE USE OF AUXILIARY DATA IN PHOTOGRAMMETRIC ADJUSTMENTS

J. R. GIBSON *In* ESA Proceedings of the International Symposium on Progress in Imaging Sensors p 583-588 Nov. 1986

Avail: NTIS HC A99/MF A01

Inertial Navigation System (INS) data were used in photogrammetric adjustments in an aerial hydrography project, photo inertial positioning project, laser profiler calibration project and stereo line imager project. The INS data provide an estimate of the aircraft position and attitude at specific time samples during a flight line. The INS data is known to be corrupted by long term drifts and offset errors, but provides relatively accurate differential data. The photogrammetric adjustment software models the low frequency error characteristics of the INS. Once the error model coefficients are determined, the derived INS error estimates may be computed and removed from the position and attitude data elements. The corrected INS data is then available for use in processing laser profiler data or for geometrically correcting line imager data.

ESA

N87-24814# Royal Inst. of Tech., Stockholm (Sweden). Dept. of Photogrammetry.

IMAGE QUALITY PROBLEMS IN PRACTICAL AERIAL PHOTOGRAPHY

ANDERS E. BOBERG / In ESA Proceedings of the International Symposium on Progress in Imaging Sensors p 627-634 Nov. 1986

Avail: NTIS HC A99/MF A01

Quality problems in land survey aerial photography are reviewed. The geometrical properties of the aerial cameras are checked yearly with the help of aerial photography of ice-covered lakes and stereoscopic height measurements in the images. Manual exposure determination with a correction table and automatic exposure calculation with a built-in integral or spot exposure meter are compared. Results of check measurements of the spectral transmission of color aerial filters are presented and quality problems related to color balance of color infrared film are discussed. Experiences of a subjective image assessment method are reported. ESA

N87-24817*# California Univ., Santa Barbara. Information Sciences Research Group.

REMOTE SENSING INFORMATION SCIENCES RESEARCH GROUP: SANTA BARBARA INFORMATION SCIENCES RESEARCH GROUP, YEAR 4 Final Report

JOHN E. ESTES, TERENCE SMITH, and JEFFREY L. STAR 1 Jun. 1987 17 p

(Contract NAGW-455)

(NASA-CR-181073; NAS 1.26:181073) Avail: NTIS HC A02/MF A01 CSCL 05B

Information Sciences Research Group (ISRG) research continues to focus on improving the type, quantity, and quality of information which can be derived from remotely sensed data. Particular focus is on the needs of the remote sensing research and application science community which will be served by the Earth Observing System (EOS) and Space Station, including associated polar and co-orbiting platforms. The areas of georeferenced information systems, machine assisted information extraction from image data, artificial intelligence and both natural and cultural vegetation analysis and modeling research will be expanded. E.R.

08

INSTRUMENTATION AND SENSORS

Includes data acquisition and camera systems and remote sensors.

A87-32210#

THE NETHERLANDS-INDONESIAN REMOTE-SENSING SATELLITE TERS [DE NEDERLANDS-INDONESISCHE REMOTE SENSING SATELLIET TERS]

J. H. DE KOOMEN (Fokker, Amsterdam, Netherlands) Ruimtevaart, vol. 35, Dec. 1986, p. 1-12. In Dutch.

The development history of the Tropical Earth Resources Satellite (TERS) is briefly traced, and the results of the technical feasibility study completed in 1984 are summarized. The factors weighed before selecting a single-satellite configuration with a 1680-km-altitude equatorial orbit are discussed, and the instrument requirements are considered, including 16 x 16-m color (540, 650, and 795 nm) and 8 x 8-m panchromatic resolution, image size 60 x 60 km, observation at least four times per day between 10 deg S and 10 deg N latitude, and 1-km-resolution 3000-km-swath CCD cloud sensing (directed about 10 deg ahead of the instrument). Consideration is given to the on-board data-handling and telemetry/telecommand subsystems, the 800-W solar-panel/rechargeable-battery power supply, altitude control, instrument-pointing options, and the use of 5-mm-thick Al-alloy sandwich plates in the

1.1 x 1.1 x 2-m primary structure (to provide adequate radiation shielding). T.K.

A87-32349

EARTH ROTATION, STATION COORDINATES AND ORBIT DETERMINATION FROM SATELLITE LASER RANGING

MASAAKI MURATA (National Aerospace Laboratory, Chofu, Japan) IN: International Symposium on Space Technology and Science, 15th, Tokyo, Japan, May 19-23, 1986, Proceedings. Volume 1. Tokyo, AGNE Publishing, Inc., 1986, p. 557-565. refs

The Project MERIT, a special program of international collaboration to Monitor Earth Rotation and Intercompare the Techniques of observation and analysis, has come to an end with great success. Its major objective was to evaluate the ultimate potential of space techniques such as VLBI and satellite laser ranging, in contrast with the other conventional techniques, in the determination of rotational dynamics of the earth. The National Aerospace Laboratory (NAL) has officially participated in the project as an associate analysis center for satellite laser technique for the period of the MERIT Main Campaign (September 1983-October 1984). In this paper, the NAL analysis center results are presented. Author

A87-32477

BALLOON-BORNE INFRARED MULTICHANNEL RADIOMETER FOR REMOTE SENSING OF HIGH RESOLUTION LOW-LEVEL WATER VAPOR FIELDS

VITO FRANCESCO POLCARO (CNR, Istituto di Astrofisica Spaziale, Frascati, Italy), CARLO ULIVIERI, ANTONIO CASTELLANI, and MAURIZIO DI RUSCIO (Roma, Universita, Rome, Italy) IN: International Symposium on Space Technology and Science, 15th, Tokyo, Japan, May 19-23, 1986, Proceedings. Volume 2. Tokyo, AGNE Publishing, Inc., 1986, p. 1495-1502. refs

Consideration is given to the possibility of determining the total water vapor content in the atmosphere from simultaneous measurements in three thermal infrared channels between 10 and 13 microns. The paper describes a fast algorithm for estimating the low-level precipitable water in clear air from these multisplit window measurements. A linear correlation is found between the atmospheric water vapor content and an appropriate combination of radiometric brightness temperatures. The stratospheric flight of a balloon-borne radiometer designed for operation in the proposed wavelengths over the Mediterranean Sea during the summer of 1987 is detailed. The total weight expected for the payload is 240 kg. A floating altitude of 5 mb should be reached through the use of a three million-cubic foot balloon. K.K.

A87-32491

A STUDY OF ELEVATION MEASUREMENT USING LFC PHOTOGRAPH

SOTARO TANAKA, TOSHIRO SUGIMURA (Remote Sensing Technology Center of Japan, Tokyo), and MITSUNORI YOSHIMURA (Hosei University, Koganei, Japan) IN: International Symposium on Space Technology and Science, 15th, Tokyo, Japan, May 19-23, 1986, Proceedings. Volume 2. Tokyo, AGNE Publishing, Inc., 1986, p. 1593-1600.

The capability of measuring the object point using large format camera (LFC) photographs acquired by the Space Shuttle STS-41 G was evaluated. From a set of films covering an area in Central Honshu, a stereo pair with a small area with mountains was selected, and the positions of the objects which could be identified on both photographs were determined. The steps of the procedure include earth curvature correction, determination of the projection center of the camera, angular orientation of the photograph, and finding the position of the object on the ground in the geodetic coordinate system. Target positions were determined with a positioning accuracy of 10 m in the horizontal direction and 20 m in the vertical direction. Factors that may cause deterioration of the positioning accuracy are discussed. I.S.

A87-32500

AIRBORNE OBSERVATION EXPERIMENTS FOR MOS-1 VERIFICATION PROGRAM (MVP)

KOREHIRO MAEDA, YOSHIO AZUMA (National Space Development Agency of Japan, Hatoyama), and MASAHIRO KOJIMA (National Space Development Agency of Japan, Tokyo) IN: International Symposium on Space Technology and Science, 15th, Tokyo, Japan, May 19-23, 1986, Proceedings. Volume 2. Tokyo, AGNE Publishing, Inc., 1986, p. 1659-1670.

The principal mission objectives of the Marine Observation Satellite-1 (MOS-1), scheduled for launch in February 1987, and the features and functions of the three radiometers (MESSR, VTIR, and MSR) to be carried by the MOS-1 are described. MVP, developed by NASDA to evaluate the total MOS-1 system by using the system's data obtained after launch, will evaluate the distortion correction method, the performance of the MOS-1 observation system, and the effectiveness of the MOS-1 observation parameter from the viewpoints of various utilizations. The evaluation results will be used in the development and operation of future earth observation systems. The results of the preliminary airborne observation experiments conducted by MVP using three radiometers equivalent to the MESSR, VTIR, and MSR, which yielded aerial photograph data over several test sites, are discussed. I.S.

A87-32501

EARTH RESOURCES SATELLITE-1 (ERS-1)

YOSHIHIRO ISHIZAWA, SHUNJI TAKAMURA, NORIO SAITO, and YOSHIHIRO HARADA (National Space Development Agency of Japan, Tokyo) IN: International Symposium on Space Technology and Science, 15th, Tokyo, Japan, May 19-23, 1986, Proceedings. Volume 2. Tokyo, AGNE Publishing, Inc., 1986, p. 1671-1676.

The ERS-1, designed for launch in FY 1990 by an H-I launch vehicle, is described. Its mission objectives include the establishment of a fundamental technology of remote sensing from space by synthetic aperture radar and optical sensors; the exploration of nonrenewable resources; and the monitoring of land-use, agriculture, forestry, etc. An outline is given of the ERS-1 system with emphasis placed on its configuration, mission and bus equipment, orbit, data acquisition, and developmental status. T.K.

A87-32505

SCIENTIFIC GOALS AND TECHNICAL LIMITATIONS OF THE SHUTTLEBORNE SYNTHETIC APERTURE EXPERIMENT X-SAR

HERWIG OETTL (DFVLR, Oberpfaffenhofen, West Germany) IN: International Symposium on Space Technology and Science, 15th, Tokyo, Japan, May 19-23, 1986, Proceedings. Volume 2. Tokyo, AGNE Publishing, Inc., 1986, p. 1699-1704. BMFT-CNR-supported research. refs

The capabilities and scientific goals of the X-band SAR being developed for a 1990 Shuttle flight are summarized. The X-SAR will draw 1.4 kW, have a maximum data rate under 46 Mbit/sec, and have a 12 x 0.4 m antenna. The X-SAR has linear vertical polarization with antenna gain exceeding 43 dBi, emit 40 microsec 9.6 GHz pulses, and have selectable slant range resolutions of 10 and 16 m. Azimuth resolution is to be 25 m and off-nadir viewing angles of 15-60 deg are to be available. From a 255 km altitude polar orbit, the X-SAR will be used to scan geologic formations, penetrate arid or semi-arid areas to detect different layers, and image layers of ice sheets, wet and dry snow status, and iceberg movements. Other goals are monitoring biomass density and waves, eddies, currents and pollution in the ocean. The X-SAR is eventually to be upgraded to include both copolarized and cross-polarized scanning. M.S.K.

A87-32507

OBSERVATION OF PRECIPITATION FROM SPACE BY THE WEATHER RADAR

KENICHI OKAMOTO, HARUNOBU MASUKO, SHIN YOSHIKADO (Ministry of Posts and Telecommunications, Radio Research Laboratory, Koganei, Japan), KENJI NAKAMURA, MASA HARU FUJITA (Ministry of Posts and Telecommunications, Radio Research Laboratory, Kashima, Japan) et al. IN: International Symposium on Space Technology and Science, 15th, Tokyo, Japan, May 19-23, 1986, Proceedings. Volume 2. Tokyo, AGNE Publishing, Inc., 1986, p. 1711-1720. refs

Progress to date on the development of a spaceborne active microwave weather radar by the Japan Radio Research Laboratory is summarized. The experiments have included joint operation with NASA of an airborne microwave rain scatterometer/radiometer functioning in the X- (9.86 GHz) and Ka-bands (34.45 GHz). Features and performance of the jointly operated system are described, including the scanning patterns explored, the principal characteristics of the radiometers, and data processing and display subsystems, which furnished quick-look color imagery for viewing within the aircraft. Results are reported from comparisons of the rainfall rate estimates obtained with a least-squares method with equivalent data from a ground-based C-band radar, and from measurements of rainfall over the ocean in terms of the attenuation coefficient. Preliminary specifications are provided for a spaceborne weather radar system. M.S.K.

A87-32952

APPLICATIONS OF SATELLITE MICROWAVE RADIOMETRY IN FINLAND

MARTTI T. HALLIKAINEN (Helsinki University of Technology, Espoo, Finland) and PETRI A. JOLMA (Nokia Telecommunications, Espoo, Finland) Geocarto International, no. 4, 1986, p. 17-25. refs

Data from the Scanning Multichannel Microwave Radiometer (SMMR) onboard the Nimbus-7 Satellite were applied to: (1) retrieval of the water equivalent of seasonal snow cover, (2) discrimination of forest and surface types, (3) determination of the near-surface wind speed, and (4) determination of sea ice concentration. Several retrieval algorithms were tested in each case by using an extensive SMMR data set. The brightness temperature difference between 18 GHz and 37 GHz, vertical polarization, was observed to give the highest correlation coefficient with the manually measured snow water equivalent. The 10.7 GHz horizontally polarized SMMR channel has the best capability to distinguish between different forest and land-cover categories. The same channel yields the near-surface wind speed in the Baltic Sea (width about 200 km) with reasonably good accuracy. Previously developed wind speed algorithms have been applied only to areas far away from land. The use of the 18-GHz horizontally polarized channel to determine the sea ice concentration provides higher accuracy than that of the 37-GHz channel. Author

A87-32985*# Atmospheric and Environmental Research, Inc., Cambridge, Mass.

IMPACT OF SATELLITE-BASED DATA ON FGGE GENERAL CIRCULATION STATISTICS

DAVID A. SALSTEIN, RICHARD D. ROSEN (Atmospheric and Environmental Research, Inc., Cambridge, MA), WAYMAN E. BAKER, and EUGENIA KALNAY (NASA, Goddard Space Flight Center, Greenbelt, MD) Royal Meteorological Society, Quarterly Journal (ISSN 0035-9009), vol. 113, Jan. 1987, p. 255-277. refs (Contract NAS5-26515; NAS5-27745)

The NASA Goddard Laboratory for Atmospheres (GLA) analysis/forecast system was run in two different parallel modes in order to evaluate the influence that data from satellites and other FGGE observation platforms can have on analyses of large scale circulation; in the first mode, data from all observation systems were used, while in the second only conventional upper air and surface reports were used. The GLA model was also integrated for the same period without insertion of any data; an independent objective analysis based only on rawinsonde and pilot balloon data is also performed. A small decrease in the vigor of

the general circulation is noted to follow from the inclusion of satellite observations. O.C.

A87-33122

APPLIED REMOTE SENSING

CHOR PONG LO (Georgia, University, Athens) Harlow, England, Longman Scientific and Technical, 1986, 404 p. refs

The application of remote sensing to the surveying, inventorying, and mapping of characteristic features of the terrestrial environment is examined. The principles of electromagnetic remote sensing, the characteristics of major imaging sensor systems, space platforms and imaging systems, and methods for interpreting the images are described. The mapping of the spatial distribution of the population, and the analysis of meteorological data using remotely sensed information are discussed. Consideration is given to the use of aerial photography, thermal IR imagery, radar imagery, and satellite imagery to study of the lithosphere, biosphere, land use, land cover mapping, and hydrosphere. Attention is given to the cartographic presentation of remote sensing data and geographic information systems. Specific case studies illustrating the uses of remotely sensed data are presented. I.F.

A87-33426* National Aeronautics and Space Administration. Langley Research Center, Hampton, Va.

OPERATIONAL OVERVIEW OF NASA GTE/CITE 1 AIRBORNE INSTRUMENT INTERCOMPARISONS - CARBON MONOXIDE, NITRIC OXIDE, AND HYDROXYL INSTRUMENTATION

SHERWIN M. BECK, RICHARD J. BENDURA, DAVID S. MCDOUGAL, JAMES M. HOELL, JR., GERALD L. GREGORY, GLEN W. SACHSE, GERALD F. HILL (NASA, Langley Research Center, Hampton, VA), HOWARD J. CURFMAN, JR. (Bionetics Corp., Hampton, VA), ARNOLD L. TORRES (NASA, Wallops Flight Center, Wallops Island, VA), ESTELLE P. CONDON (NASA, Ames Research Center, Moffett Field, CA) et al. Journal of Geophysical Research (ISSN 0148-0227), vol. 92, Feb. 20, 1987, p. 1977-1985. refs

An overview of the airborne intercomparisons of CO, NO, and OH instrumentation is presented in this first paper of the series on the NASA Global Tropospheric Experiment/Chemical Instrumentation Test and Evaluation (GTE/CITE 1). This paper provides the reader with background information about several important characteristics of the project. These include the overall objectives and approach, the measurements taken, the intercomparison protocol, aircraft platform, profiles of each aircraft flight, and the participants. A synopsis of the overall results of the CO, NO, and OH instrument intercomparisons is also included. Companion papers discuss the detailed results of the CO and NO intercomparison tests as well as pertinent scientific findings.

Author

A87-35306* California Univ., Santa Barbara.

THE REGRESSION INTERSECTION METHOD OF ADJUSTING IMAGE DATA FOR BAND RATIOING

ROBERT E. CRIPPEN (California, University, Santa Barbara) International Journal of Remote Sensing (ISSN 0143-1161), vol. 8, Feb. 1987, p. 137-155. refs
(Contract NAG5-177; NAGW-455)

Estimation of the combined path radiance and sensor offset terms is essential in adjusting multispectral image radiance measurements for band ratioing. Commonly applied techniques for making this estimate have required assumptions or ancillary information regarding the reflectance properties of surface materials. This paper presents a technique that is unique in that it provides absolute (not just relative) statistically-derived estimates without the use of ancillary information. It is termed the regression intersection method (RIM). RIM is based on contrasts between the spectral properties of various homogeneous areas in rugged terrain. These areas are selected by examination of the image data alone. Bispectral regression (first principal component) lines are determined for each area and are projected, in pairs, to intersection points. Ideally, the coordinates of these points must equal the measurements for zero ground radiance since that is the only condition under which spectrally different materials can

have the same radiance values. The median result from several site-pair and band-pair comparisons is used in order to statistically mitigate noise and minor variations due to natural variability. Tests show that the method is successful in determining correction values for the image data that result in maximum removal of the topographic effect in ratio images. Author

A87-35344

MODELS FOR RADAR SCATTERER DENSITY IN TERRAIN IMAGES

FRED W. SMITH (TAU Corp., Los Gatos, CA) and JANICE A. MALIN (Systems Control Technology, Inc., Palo Alto, CA) IEEE Transactions on Aerospace and Electronic Systems (ISSN 0018-9251), vol. AES-22, Sept. 1986, p. 642-647.
(Contract F33615-83-C-1071)

Statistical models for the density of strong scatterers detected in high resolution radar images of rural terrain are presented. The probability distribution of the density of these natural terrain detections was found to be a negative binomial. The variance of the negative binomial depended strongly on the window size used to measure the density. This dependence indicates that these detections, like those of a Poisson process, are locally uncorrelated, but have a slowly varying mean density whose correlation distance is 1 km or more. Negative binomial parameters were computed using over 200 sq km of terrain image for densities measured using windows sized from 75 m x 75 m to 375 m x 375 m. Average terrain detection densities of 0.001 and 0.0001 per resolution cell were evaluated on images with resolutions of 7 and 28 ft. Author

A87-35502

ATMOSPHERIC ENVIRONMENT MONITORING SYSTEM BASED ON AN EARTH-TO-SATELLITE HADAMARD TRANSFORM LASER LONG-PATH ABSORPTION SPECTROMETER - A PROPOSAL

NOBUO SUGIMOTO (National Institute for Environmental Studies, Tsukuba, Japan) Applied Optics (ISSN 0003-6935), vol. 26, March 1, 1987, p. 763, 764.

The Hadamard transform laser long-path absorption spectrometer (Hallpass) for monitoring trace gases in the global atmosphere is described. The measurement principal is based on laser long-path absorption between a ground-based laser station and a satellite-borne detector in a stationary orbit; the Hadamard transform method is utilized to make simultaneous measurements from multiple stations. The operation of Hallpass, and the advantages of using the Hadamard transform are discussed. The system is employed to evaluate the S/N of light detection. The Hallpass is effective for measuring trace gases in the troposphere and stratosphere and for regional and local pollution monitoring. I.F.

A87-36360

SENSORS FOR IMAGING

DOMINIC KING (Thomson-CSF, Division Tubes Electroniques, Boulogne-Billancourt, France) Space (ISSN 0267-954X), vol. 3, Mar.-Apr. 1987, p. 17-21. CNES-supported research.

Sensors for detecting radiation in the visible spectrum (0.4-0.8 micron) and short wave IR (SWIR) range of 1.55-1.70 microns are examined. The advantages of the SPOT pushbroom scanning system for earth observations and the implementation of a high resolution linear CCD into the SPOT-II satellite are discussed. The design and fabrication processes involved in developing a linear CCD with high sensitivity, low noise, good uniformity, resolution matching, and high reliability are described. A linear array of 3000 multiplexed InGaAs photodiodes for the SWIR channel on SPOT IV, which is to provide data applicable to agriculture, is proposed. The use of InGaAs for optical communications and of a two-dimensional matrix of photoelements for attitude control, and methods for improving CCD capabilities are studied. I.F.

A87-36933

ANALYSIS OF MODERATE AND INTENSE RAINFALL RATES CONTINUOUSLY RECORDED OVER HALF A CENTURY AND INFLUENCE ON MICROWAVE COMMUNICATIONS PLANNING AND RAIN-RATE DATA ACQUISITION

AUGUST BURGUENO, MANUEL PUIGSERVER (Barcelona Universidad, Spain), JOHN AUSTIN, and ENRIC VILAR (Portsmouth Polytechnic, England) IEEE Transactions on Communications (ISSN 0090-6778), vol. COM-35, April 1987, p. 382-395. refs

A87-37055

WHAT, WHERE, WHEN ..., WHY? EXTRACTING INFORMATION FROM REMOTE SENSING DATA

NANNO J. MULDER (International Institute for Aerospace Survey and Earth Sciences, Enschede, Netherlands) ITC Journal (ISSN 0303-2434), no. 2, 1986, p. 145-155. refs

A remote sensing system which will improve the extraction and interpretation of remote sensing data is proposed and a scenario for the development of this system is presented. The basic principles of remote sensing are reviewed. The properties of photon and microwave sensors, the use of a square grid cell on the surface of the earth as the spatial unit of measurement for each scene element, and the class membership, position, and time of a scene element are discussed. The use of information systems to extract information from remote sensing data and the application of expert systems to information processing are described. I.F.

A87-37289

AEROTRIANGULATION WITHOUT GROUND CONTROL

JAMES R. LUCAS (NOAA, Charting Research and Development Laboratory, Rockville, MD) Photogrammetric Engineering and Remote Sensing (ISSN 0099-1112), vol. 53, March 1987, p. 311-314. refs

Optimum accuracy in conventional aerotriangulation requires ground control around the perimeter of the area at intervals of seven airbases or less, and, if precise elevations are to be determined, there must also be elevation control in the center of the area. Recent investigations indicate that it may be possible to derive observations of the exposure station positions with submeter accuracy from a technique that uses one Navstar Global Positioning System (GPS) receiver in the aircraft and another on the ground. A method for employing these additional observation data in an aerotriangulation adjustment is presented, along with results of simulations which indicate that accurate aerotriangulation may be achievable without any ground control. Attempts at experimental verification have been hindered so far by weather, equipment problems, the limited satellite constellation, and competition for the use of available receivers. More experiments are planned for the fall of 1986. Author

A87-37421

DATA COMPRESSION SYSTEM FOR VIDEO IMAGES

P. S. RAJYALAKSHMI and R. K. RAJANGAM (Indian Space Research Organization, Digital Systems Div., Bangalore, India) IN: ITC/USA/'86; Proceedings of the International Telemetering Conference, Las Vegas, NV, Oct. 13-16, 1986. Research Triangle Park, NC, Instrument Society of America, 1986, p. 573-583.

The software and hardware for the data compression system, which compresses and transmits remote sensing satellite images, are described. The data compression technique exploits the statistical properties of the satellite imagery and thereby reduces the data transmission rate. The use of transform coding for image data compression is examined; the Walsh-Hadamard transform was employed as the transform coding technique in this study. The number of quantization levels is estimated using zonal and threshold samplings. A diagram of the compression system hardware is presented, and the functions of the arithmetic logic unit are discussed. Evaluation of the system's performance reveals that the Walsh-Hadamard transform technique is effective for the compression of satellite video imagery. I.F.

A87-38093* SASC Technologies, Inc., Lanham, Md

STOCHASTIC NATURE OF LANDSAT MSS DATA

M. L. LABOVITZ (SASC Technologies, Inc., Lanham, MD) and E. J. MASUOKA (NASA, Goddard Space Flight Center, Greenbelt, MD) Remote Sensing of Environment (ISSN 0034-4257), vol. 21, April 1987, p. 263-280. refs

A multiple series generalization of the ARIMA models is used to model Landsat MSS scan lines as sequences of vectors, each vector having four elements (bands). The purpose of this work is to investigate if Landsat scan lines can be described by a general multiple series linear stochastic model and if the coefficients of such a model vary as a function of satellite system and target attributes. To accomplish this objective, an exploratory experimental design was set up incorporating six factors, four representing target attributes - location, cloud cover, row (within location), and column (within location) - and two factors representing system attributes - satellite number and detector bank. Each factor was included in the design at two levels and, with two replicates per treatment, 128 scan lines were analyzed. The results of the analysis suggests that a multiple AR(4) model is an adequate representation across all scan lines. Furthermore, the coefficients of the AR(4) model vary with location, particularly changes in physiography (slope regimes), and with percent cloud cover, but are insensitive to changes in system attributes. Author

A87-38837* Jet Propulsion Lab., California Inst. of Tech., Pasadena.

SPACEBORNE IMAGING RADAR RESEARCH IN THE 1990S - AN OVERVIEW

CHARLES ELACHI (California Institute of Technology, Jet Propulsion Laboratory, Pasadena) (NASA, U.S. Navy, and Johns Hopkins University, Symposium on Measuring Ocean Waves from Space, Laurel, MD, Apr. 15-17, 1986) Johns Hopkins APL Technical Digest (ISSN 0270-5214), vol. 8, Jan.-Mar. 1987, p. 60-64. refs

Research and proposed experiments for improving the capabilities of spaceborne imaging radars are discussed. The development of multiparameter research sensors, long-term and global monitoring sensors, planetary mapping sensors, and topographic three-dimensional imagers is examined. The properties and functions of these proposed sensors are described; examples of these various types of sensors are provided. I.F.

A87-39183

THE TETHERED SATELLITE SYSTEM AS A NEW REMOTE SENSING PLATFORM

S. VETRELLA and A. MOCCIA (Napoli, Universita, Naples, Italy) International Journal of Remote Sensing (ISSN 0143-1161), vol. 8, March 1987, p. 369-383. Research supported by the Ministero della Pubblica Istruzione and CNR. refs

The characteristics and development of the Tethered Satellite (TS), which is to be a space platform that allows operation at different low altitudes, are described. Two experimental flights are proposed for the TS; the first mission involves deploying the tether 20 km upwards, and in the second mission the TS is to be deployed downwards to 100 km from the Shuttle. The attitude stability rates of the TS for along-track stereoscopic observations using linear arrays are analyzed. It is determined that an attitude stability rate of 10 to the -6th deg/sec is required for automatic correlation along epipolar planes during the proposed Mapsat mission and a rate of 0.00001 deg/sec is needed for the Stereosat mission. I.F.

A87-39190* Open Univ., Milton (England).

SYNERGISTIC USE OF MOMS-01 AND LANDSAT TM DATA

DAVID A. ROTHERY and PETER W. FRANCIS (Open University, Milton Keynes, England) International Journal of Remote Sensing (ISSN 0143-1161), vol. 8, March 1987, p. 501-508. Research supported by the Nuffield Foundation. refs (Contract NAS2-8759)

Imagery covering the Socompa volcano and debris avalanche deposit in northern Chile was acquired by MOMS-01 when the sun was low in the western sky. Illumination from the west shows many important topographic features to advantage. These are

inconspicuous or indistinguishable on Landsat TM images acquired at higher solar elevation. The effective spatial resolution of MOMS-01 is similar to that of the TM and its capacity for spectral discrimination is less. A technique has been developed to combine the multispectral information offered by TM with the topographic detail visible on MOMS-01 imagery recorded at a time of low solar elevation. Author

A87-39457
IMPACT OF RADIANCE VARIATIONS ON SATELLITE SENSOR CALIBRATION

MICHAEL J. DUGGIN (New York, State University, Syracuse) Applied Optics (ISSN 0003-6935), vol. 26, April 1, 1987, p. 1264-1271. refs
 (Contract USDA-58-319T-40238X)

The intercalibration of digital data from different sensors depends on systematic and random variations in factors controlling recorded radiance. Theoretical expressions are presented which describe the impact of random variations in those factors which control radiance incident on the sensor. Means of measuring or estimating the impact of random variations on intercalibration factors are discussed. Means of detecting and calibrating for systematic effects are also discussed. The optical-reflective, middle-infrared, and thermal infrared regions of the spectrum are considered. An example is presented whereby NOAA-7 and NOAA-8 advanced very high resolution radiometer (AVHRR) radiance data, obtained over the same test fields, are shown to depend on the differences in view angles used by the two satellites. Author

A87-40246
SATELLITE ESTIMATION OF A SOLAR IRRADIANCE AT THE SURFACE OF THE EARTH AND OF SURFACE ALBEDO USING A PHYSICAL MODEL APPLIED TO METEOSAT DATA

G. DEDIEU, P. Y. DESCHAMPS, and Y. H. KERR (CNES and CNRS, Laboratoire d'Etudes et de Recherches en Teledetection Spatiale, Toulouse, France) Journal of Climate and Applied Meteorology (ISSN 0733-3021), vol. 26, Jan. 1987, p. 79-87. CNES-CNRS-supported research. refs

A87-40379*# National Aeronautics and Space Administration, Washington, D.C.

SPACE REMOTE SENSORS

SAM KELLER (NASA, Office of Space Science and Applications, Washington, DC) IN: EASCON '86, Proceedings of the Nineteenth Annual Electronics and Aerospace Systems Conference, Washington, DC, Sept. 8-10, 1986. New York, Institute of Electrical and Electronics Engineers, Inc., 1986, p. 260-264.

Space remote sensors are analyzed as a component of a higher level 'robotic' system and the implications for sensor parameter selection and priority assignment are described. The EOS program and three of its particular sensor types are considered as examples of the principles discussed. Author

A87-40756
SIMULATIONS OF THE GOES VISIBLE SENSOR TO CHANGING SURFACE AND ATMOSPHERIC CONDITIONS

R. T. PINKER and J. A. EWING (Maryland, University, College Park) Journal of Geophysical Research (ISSN 0148-0227), vol. 92, April 20, 1987, p. 4001-4009. refs
 (Contract NOAA-NA-84AAH00026)

Numerical experiments have been conducted to simulate the GOES VISSR visible sensor's response under varying surface and atmospheric conditions, as a function of solar zenith angle. The possible bias in the information obtained with this limited spectral response sensor was assessed by comparing the narrow-band filtered clear-sky planetary albedo, as observable with the VISSR, with the broadband unfiltered planetary albedo under the same environmental conditions. Four cases of wavelength-dependent surface albedo and three atmospheric conditions have been simulated. It was demonstrated that the relationship between the filtered and the broadband planetary albedo depends primarily on the assumptions made about the magnitude and wavelength

dependence of the surface albedo and, to a lesser extent, on the atmospheric conditions. Author

A87-40768* Science Applications Research, Lanham, Md.
REFLECTIVITY OF EARTH'S SURFACE AND CLOUDS IN ULTRAVIOLET FROM SATELLITE OBSERVATIONS

T. F. ECK (Science Applications Research, Lanham, MD), P. K. BHARTIA (ST Systems Corp., Hyattsville, MD), P. H. HWANG (NASA, Goddard Space Flight Center, Greenbelt, MD), and L. L. STOWE (NOAA, National Environmental Satellite Data Information Service, Washington, DC) Journal of Geophysical Research (ISSN 0148-0227), vol. 92, April 20, 1987, p. 4287-4296. refs

The Total Ozone Mapping Spectrometer on board Nimbus 7 is used to infer the UV surface and cloud reflectance at 370 nm. Cloudless surface reflectivity was analyzed on a global basis for all surface types for several months. The UV surface reflectivity varies from 2 percent for some forest and grassland regions to 14 percent for some sandy desert areas. A notable exception is the large salt flats of Bolivia, which have a reflectivity of about 60 percent. Cloud reflectivity was also analyzed for clouds located at three levels in the atmosphere, as determined by the 11.5 micron channel of the Temperature Humidity Infrared Radiometer. Average cloud reflectivity at 370 nm ranges from 52 percent for low clouds (tops less than 2 km) to 76 percent for high clouds (tops greater than 7 km at the equator, decreasing to greater than 4 km at poles). Author

A87-40770* National Aeronautics and Space Administration, Goddard Space Flight Center, Greenbelt, Md.
SATELLITE SENSING OF AEROSOL ABSORPTION

YORAM J. KAUFMAN (NASA, Goddard Space Flight Center, Greenbelt, MD) Journal of Geophysical Research (ISSN 0148-0227), vol. 92, April 20, 1987, p. 4307-4317. refs

A method is developed for remote sensing of aerosol absorption from satellite images of the earth's surface. The method is based on the measurement of the change in the upward radiances between a clear and a hazy day over a varying surface reflectance. For a zero change balance between brightening due to scattering and darkening due to absorption and scattering is reached. This balance is utilized via a radiative transfer model to derive the aerosol single-scattering albedo. A sensitivity study is performed, and the method is tested against laboratory measurements. It is suggested that for the case of haze introduced on top of an existing background aerosol and with a fair estimate of the scattering phase function, the error in the remotely sensed single-scattering albedo is in the range of 0.03-0.05. The main errors in the method arise from variations in the surface reflectance between the clear and the hazy days, uncertainty in the scattering phase function, and variation of the aerosol and gaseous absorption between these two days. If the satellite calibration varies with time, the measurements of single-scattering albedo can be substantially affected. Author

A87-41432
RADIOMETRIC COMPARISON OF THE LANDSAT-5 TM AND MSS SENSORS

ALAIN ROYER, LISE CHARBONNEAU, RICHARD BROCHU (Sherbrooke, Universite, Canada), JENNIFER M. MURPHY, PHILIPPE M. TEILLET (Canada Centre for Remote Sensing, Ottawa) et al. International Journal of Remote Sensing (ISSN 0143-1161), vol. 8, April 1987, p. 579-591. Research supported by the Canada Centre for Remote Sensing and FCAR. refs
 (Contract NSERC-A-8643; NSERC-A-5252)

The radiometric accuracy of Landsat-5 TM data and MSS data is evaluated. The TM and MSS images employed in the study were recorded simultaneously over Montreal on August 4, 1984. The radiometric and geometric correction procedures of the Canada Centre for Remote Sensing are described. TM and MSS normalized and corrected apparent reflectances computed for 11 different cover types (four water areas, three urban areas having different densities, and four vegetative surfaces) are compared. It is observed that the normalized and corrected apparent reflectances

from TM and MSS correlate well; and the usefulness of the processing procedure is validated. I.F.

A87-41588

GROUND AND AERIAL USE OF AN INFRARED VIDEO CAMERA WITH A MID-INFRARED FILTER (1.45 TO 2.0 MICRONS)

J. H. EVERITT, D. E. ESCOBAR, P. R. NIXON (USDA, Remote Sensing Research Unit, Weslaco, TX), M. A. HUSSEY (Texas A&M University, Weslaco), and C. H. BLAZQUEZ (Florida, University, Lake Alfred) IN: Thermal imaging; Proceedings of the Meeting, Orlando, FL, Apr. 3, 4, 1986. Bellingham, WA, Society of Photo-Optical Instrumentation Engineers, 1986, p. 130-135. refs

A black-and-white infrared (0.9 to 2.2 micron) video camera, filtered to record radiation within the 1.45 to 2.0 microns midinfrared water absorption region, was evaluated with ground and aerial studies. Imagery of single leaves of seven plant species (four succulent; three nonsucculent) showed that succulent leaves were easily distinguishable from nonsucculent leaves. Spectrophotometric leaf reflectance measurements made over the 1.45 to 2.0 microns confirmed the imagery results. Ground-based video recordings also showed that severely drought-stressed buffelgrass (*Cenchrus ciliaris* L.) plants were distinguishable from the nonstressed and moderately stressed plants. Moreover, the camera provided airborne imagery that clearly differentiated between irrigated and nonirrigated grass plots. Due to the lower radiation intensity in the mid-infrared spectral region and the low sensitivity response of the camera's tube, these video images were not as sharp as those obtained by visible or visible/near-infrared sensitive video cameras. Nevertheless, these results showed that a video camera with midinfrared sensitivity has potential for use in remote sensing research and applications. Author

A87-42254* Jet Propulsion Lab., California Inst. of Tech., Pasadena.

RECTIFICATION OF TERRAIN INDUCED DISTORTIONS IN RADAR IMAGERY

RONALD KWOK, JOHN C. CURLANDER, and SHIRLEY S. PANG (California Institute of Technology, Jet Propulsion Laboratory, Pasadena) Photogrammetric Engineering and Remote Sensing (ISSN 0099-1112), vol. 53, May 1987, p. 507-513. refs

This paper describes a technique to generate geocoded synthetic aperture radar (SAR) imagery corrected for terrain induced geometric distortions. This algorithm transforms the raw slant range image, generated by the signal processor, into a map registered product, resampled to either Universal Transverse Mercator (UTM) or Polar Stereographic projections, and corrected for foreshortening. The technique utilizes the space platform trajectory information in conjunction with a digital elevation map (DEM) of the target area to generate an ortho-radar map with near-autonomous operation. The current procedure requires only two to three tie-points to compensate for the platform position uncertainty that results in translational error between the image and the DEM. This approach is unique in that it does not require generation of a simulated radar image from the DEM or a grid of tie-points to characterize the image-to-map distortions. Rather, it models the inherent distortions based on knowledge of the radar data collection characteristics, the signal Doppler parameters, and the local terrain height to automatically predict the registration transformation. This algorithm has been implemented on a minicomputer system equipped with an array processor and a large random-access memory to optimize the throughput. Author

A87-42257

COMPARISON BETWEEN DIGITAL AND MANUAL INTERPRETATION OF HIGH ALTITUDE AERIAL PHOTOGRAPHS

PAUL W. SNOOK, NORMAN E. MERRITT, RAYMOND L. CZAPLEWSKI (USDA, Forest Service, Fort Collins, CO), and KENNETH C. WINTERBERGER (USDA, Forest Service, Anchorage, AK) Photogrammetric Engineering and Remote Sensing (ISSN 0099-1112), vol. 53, May 1987, p. 531-534. refs

Second generation color infrared transparencies of the Tanana River Basin in Alaska were digitized using a scanning microdensitometer. Unsupervised clustering was performed independently on each of 20 digital images. Area estimates from 20 8-hectare sample plots were obtained by manual and computer aided interpretations. Manual interpretation of large-scale (1:3000) photographs and ground truth served as reference. Computer-aided interpretation was consistently more accurate than the manual interpretation when compared to reference. However, the time and cost for digital processing was much higher than manual interpretation if information for only a small portion (e.g., an 8-ha plot) of the digital image is required. Author

A87-42639* California Univ., Davis.

POLARIZED VIEWS OF THE EARTH FROM ORBITAL ALTITUDE

KINSELL L. COULSON (California, University, Davis), VICTOR S. WHITEHEAD (NASA, Johnson Space Center, Houston, TX), and CHARLES CAMPBELL (NASA, Johnson Space Center; Lockheed Engineering and Management Services Co., Houston, TX) IN: Ocean optics VIII; Proceedings of the Meeting, Orlando, FL, Mar. 31-Apr. 2, 1986. Bellingham, WA, Society of Photo-Optical Instrumentation Engineers, 1986, p. 35-41. NASA-supported research. refs

By means of a pair of boresighted and synchronized cameras fitted with orthogonally oriented polarizing filters and carried aboard the Space Shuttle, a large number of polarized images of the earth's surface have been obtained from orbital altitude. Selected pairs of images, both in color and in black and white, have been digitized and computer processed to yield analogous images in each of the three Stokes parameters necessary for characterizing the state of linear polarization of the emergent light. Many of the images show surface properties more distinctly in degree and plane of polarization than in simple intensity alone. However, the maximum information content as well as noise suppression and minimization of atmospheric interference, is achieved by proper combinations of the Stokes parameters. It is believed that these are the first, and certainly the most extensive, set of polarized images of the earth ever obtained from space. Author

N87-20621# European Space Agency, Paris (France).

PROCEEDINGS OF THE EUROPEAN SYMPOSIUM ON POLAR PLATFORM OPPORTUNITIES AND INSTRUMENTATION FOR REMOTE-SENSING (ESPOIR)

E. J. ROLFE, ed. and B. BATTRICK, ed. Nov. 1986 127 p Symposium held in Avignon, France, 16-18 Jun. 1986 (ESA-SP-266; ISSN-0379-6566; ETN-87-99434) Avail: NTIS HC A07/MF A01

European activities in preparing the Columbus polar platforms; United States cooperation with Europe; atmosphere, land, ocean/ice, and solid Earth missions; and platform instruments, calibrating, data management, orbit configuration, and servicing were discussed.

ESA

N87-20622# European Space Agency. European Space Research and Technology Center, ESTEC, Noordwijk (Netherlands).

THE EARTH OBSERVATION ACTIVITIES OF THE EUROPEAN SPACE AGENCY AND THE USE OF THE POLAR PLATFORM OF THE INTERNATIONAL SPACE STATION

B. PFEIFFER *In its Proceedings of the European Symposium on Polar platform Opportunities and Instrumentation for Remote-sensing (ESPOIR)* p 7-10 Nov. 1986

Avail: NTIS HC A07/MF A01

The Meteosat, ERS-1, and Earthnet programs are reviewed. The long term follow-on programs are outlined. Space infrastructure elements of ESA and their use for Earth observation are described. User requirements and ESA policy for a polar Earth observations platform are discussed. ESA

N87-20624# Deutsche Forschungs- und Versuchsanstalt fuer Luft- und Raumfahrt, Oberpfaffenhofen (West Germany).

EUROPEAN UTILIZATION ASPECTS STUDIES

F. SCHLUDE *In ESA Proceedings of the European Symposium on Polar platform Opportunities and Instrumentation for Remote-sensing (ESPOIR)* p 21-27 Nov. 1986

Avail: NTIS HC A07/MF A01

Starting from a synthesis of space station user data needs, a minimum instrumentation scenario was derived. Grouping of these instruments gave application oriented missions which led to two model missions that can be realized on an international two polar platform system. ESA

N87-20634# Deutsche Forschungs- und Versuchsanstalt fuer Luft- und Raumfahrt, Oberpfaffenhofen (West Germany).

LAND PANEL REPORT

J. BODECHTEL and F. LANZL *In ESA Proceedings of the European Symposium on Polar platform Opportunities and Instrumentation for Remote-sensing (ESPOIR)* p 79-83 Nov. 1986

Avail: NTIS HC A07/MF A01

International Space Station polar platform sensor configurations and missions are suggested. The platforms should maintain the capability for operational land remote sensing using optical sensors; improve the capability of optical sensors in terms of radiometric and spatial resolution, coverage, stereoscopic capability, etc.; improve experimental capabilities for allweather remote sensing of land with microwave sensors, to provide an operational capability similar to that of optical sensors; optimize the integration of microwave and optical data; set up demonstration programs in renewable resources, achieve operational status in the 1990s; and promote fundamental research activities. ESA

N87-20642# Air/Ocean Remote Sensing Co., San Diego, Calif. **SIMULATION OF WIND GRADIENT ERRORS IN NROSS (NAVY REMOTE OCEAN SENSING SYSTEM) RADAR SCATTEROMETER DATA IN A SIMPLIFIED GEOMETRY Final Report, May - Sep. 1986**

JAMES L. MUELLER Aug. 1986 48 p

(Contract N62271-86-M-0235)

(AD-A175754; AO1-1(ST1); NEPRF-CR-86-05) Avail: NTIS HC A03/MF A01 CSCL 171

A set of simplified case studies is used to illuminate the effect of spatial gradients in normalized radar cross section (NRCS) on the accuracy of NRCS at NROSS (Navy Remote Ocean Sensing System) scatterometer (NSCAT) cell centroids, and at wind vector retrieval grid points displaced from the centroid. Values of linear and quadratic variables $s(x,y)$ are estimated at the centroid and at a point displaced from the centroid of a parallelogram cell, using first the mean value (S) over the cell (a nearest neighbor or binning approach) and then a bilinear interpolation estimator $Si(x,y)$. Isoparametric finite elements are used to take cell shape into account in the interpolation. At cell centroids with linear fields $s(x,y)$, errors are negligible using either (S) or $Si(x,y)$. At cell centroids with nonlinear fields $s(x,y)$, errors using (S) and $Si(x,y)$ both approach 0.5% (with interpolation errors being slightly less) at spatial gradients of 0.1 dB/km. At displaced points with linear

fields $s(x,y)$, errors using interpolation $Si(x,y)$ are negligible at all gradients, but error using cell means (S) exceeds 6% at gradients of 0.1 dB/km. At displaced points with nonlinear fields $s(x,y)$, error using interpolation $Si(x,y)$ approaches 2%, while error using cell means (S) exceeds 7%, near spatial gradients of 0.1 dB/km. The simulated errors associated with binning are large, and interpolation yields much better accuracy. GRA

N87-21474# International Meteorological Inst., Stockholm (Sweden). Arrhenius Lab.

THE OBSERVATIONAL OBJECTIVES AND THE IMPLEMENTATION OF THE GLOBAL WEATHER EXPERIMENT

B. R. DOEOES *In WMO Proceedings of the International Conference on the Results of the Global Weather Experiment and their Implications for the World Weather Watch, Volume 1* p 47-74 Apr. 1986

Avail: NTIS MF A01; print copy available from WMO, Geneva, Switzerland

The transformation of the main scientific objectives of the Global Weather Experiment into observational requirements and the design of the FGGE composite global observing system as eventually implemented are described. In addition to the surface based World Weather Watch Global Observing System it included geostationary and polar orbiting meteorological satellites, dedicated ships and long range aircraft making soundings in the equatorial tropics, constant level balloons drifting at 14 km providing observations of the atmospheric flow in the tropics, and buoys drifting in the southern ocean making observations at the sea surface. Meteorological data were obtained using a large number of commercial aircraft equipped with special observing systems. It is concluded that the observations obtained during the 2 Intensive Special Observing Periods (15 January to 20 February, and 10 May to 8 June, 1979) provided nearly all the data stated in the requirements for the Experiment. ESA

N87-21521# World Climate Programme, Geneva (Switzerland).

REPORT OF THE WORKSHOP ON ASSIMILATION OF SATELLITE WIND AND WAVE DATA IN NUMERICAL WEATHER AND WAVE PREDICTION MODELS

Sep. 1986 69 p Workshop held in Shinfield Park, England, 25-26 Mar. 1986 Prepared in cooperation with ICSU, Rome, Italy

(WCP-122; WMO-TD-148; ETN-87-99183) Avail: NTIS MF A01; print copy available from WMO, Geneva, Switzerland

The assimilation of microwave data in atmospheric and wave models, and the relation between on-line data assimilation systems and quick-look and off-line analysis facilities were discussed. The assimilation system should provide gridded data of surface winds, surface stresses, surface fluxes of sensible and latent heat, and surface waves, using all the sensor data of oceanographic satellites with all other available conventional and (meteorological) satellite data. The generation of a multiyear, continuous time sequence of gridded surface stress and heat flux fields is essential for climatological studies. Since the data assimilation requirements of climate and forecasting applications are essentially identical, and most of the required data are routinely collected at forecasting centers, it is practical to implement the data assimilation system at global weather forecasting centers. Numerical experiments which can be carried out with SEASAT data to develop and test integrated data assimilation methods were identified. ESA

N87-22281*# National Aeronautics and Space Administration. Langley Research Center, Hampton, Va.

SURFACE BIDIRECTIONAL REFLECTANCE PROPERTIES OF TWO SOUTHWESTERN ARIZONA DESERTS FOR WAVELENGTHS BETWEEN 0.4 AND 2.2 MICROMETERS

CHARLES H. WHITLOCK, G. CARLTON PURGOLD, and STUART R. LECROY (PRC Kentron, Inc., Hampton, Va.) May 1987 48 p

(NASA-TP-2643; L-16159; NAS 1.60:2643) Avail: NTIS HC A03/MF A01 CSCL 20F

Surface bidirectional reflectance characteristics are presented for the Sonora Desert and the Mohawk Valley at solar zenith

angles of 13, 31, and 57 degs at wavelengths between 0.4 and 1.6 microns. Nadir reflectance values are presented for wavelengths between 0.4 and 2.2 microns for solar zenith angles of 13, 17.5, 27, 31, 45, 57, and 62 degs. Data were taken from a helicopter during May 1985 in support of an Earth Radiation Budget Experiment (ERBE), a Stratospheric Aerosol Gas Experiment (SAGE II), and an Advanced Very High Resolution Radiometer (AVHRR) satellite validation experiment. Author

N87-22457* National Aeronautics and Space Administration. Goddard Space Flight Center, Greenbelt, Md.
PROBLEMS IN MERGING EARTH SENSING SATELLITE DATA SETS

PAUL H. SMITH and MICHAEL J. GOLDBERG Mar. 1987 15 p
(NASA-TM-87820; REPT-87B0275; NAS 1.15:87820) Avail: NTIS HC A02/MF A01 CSCL 12B

Satellite remote sensing systems provide a tremendous source of data flow to the Earth science community. These systems provide scientists with data of types and on a scale previously unattainable. Looking forward to the capabilities of Space Station and the Earth Observing System (EOS), the full realization of the potential of satellite remote sensing will be handicapped by inadequate information systems. There is a growing emphasis in Earth science research to ask questions which are multidisciplinary in nature and global in scale. Many of these research projects emphasize the interactions of the land surface, the atmosphere, and the oceans through various physical mechanisms. Conducting this research requires large and complex data sets and teams of multidisciplinary scientists, often working at remote locations. A review of the problems of merging these large volumes of data into spatially referenced and manageable data sets is presented. Author

N87-23012# Air Force Geophysics Lab., Hanscom AFB, Mass.
ATMOSPHERIC REMOTE SENSING IN ARCTIC REGIONS
GERALD W. FELDE, JAMES T. BUNTING, and KENNETH R. HARDY 1986 10 p Reprinted from the Department of Defense Symposium and Workshop on Arctic and Arctic-Related Environmental Sciences, 1986 p 1-8
(AD-A179550; AFGL-TR-87-0128) Avail: NTIS HC A02/MF A01 CSCL 08L

The particular features which must be considered when sensing arctic regions from space platforms include a generally dry atmosphere, thin and low water content clouds which often cover large areas, a highly reflective snow or ice background in the visible spectrum, and weak thermal contrast between snow and cloud in the thermal infrared spectrum. In recent years, more attention has been given to the problem of identifying clouds in arctic regions. An investigation of operational cloud analysis programs for arctic regions has been initiated; results from this study have shown that clouds are often specified in regions which turn out to be generally cloud-free and vice versa. Some possible reasons for this error will be presented. Results of discriminating clouds from a snow background using multi spectral visible and near infrared sensors will also be given. A new Special Sensor Microwave/Imager (SSM/I) operating at four frequencies from 19 to 85 GHz is designed to provide estimates of several surface and atmospheric characteristics. Several parameters which will be estimated from SSM/I data are of particular interest to arctic regions. These include snow parameters, sea ice attributes, cloud amount over snow, cloud liquid water content, soil moisture, and land surface temperature. GRA

N87-23558* Geological Survey, Flagstaff, Ariz.
ENHANCED LANDSAT IMAGES OF ANTARCTICA AND PLANETARY EXPLORATION

B. K. LUCCHITTA, J. A. BOWELL, K. EDWARDS, E. M. ELIASON, and H. M. FERGUSON /n NASA, Washington Reports of Planetary Geology and Geophysics Program, 1986 p 554 May 1987 Submitted for publication

Avail: NTIS HC A24/MF A01 CSCL 08B

Since early in the LANDSAT program, black-and-white paper prints of band 7 (near infrared) of the LANDSAT multispectral scanner have been used extensively to prepare semicontrolled maps of Antarctica. Image-processing techniques are now employed to enhance fine detail and to make controlled image-mosaic maps in color. LANDSAT multispectral images of Antarctica help to expand our knowledge of extraterrestrial bodies by showing bare-ice areas as bright blue patches; on such patches meteorites tend to be concentrated and are collected. Many subtle flow features in Antarctic ice streams resemble features at the mouths of Martian outflow channels, which suggests that the channels also contained ice. Furthermore, flow lines in Antarctic ice sheets that merge with ice shelves resemble Martian flow features associated with dissected terrain along the Martian northern highland margin, and support the concept that ice was involved in the transport of material from the southern highlands to the northern lowland plains. In Antarctica, as on Mars, the virtual absence of fluvial activity over millions of years has permitted the growth of glacial and eolian features to unusually large sizes. Author

N87-24734# Defense Mapping Agency Aerospace Center, St. Louis, Mo.

PRELIMINARY RESULTS OBTAINED BY DMAAC FROM THE PROCESSING OF A LIMITED SET OF GEOSAT SATELLITE RADAR ALTIMETER DATA

DENNIS H. VANHEE 19 Nov. 1986 15 p
(AD-A179081) Avail: NTIS HC A02/MF A01 CSCL 17I

Details of the activities associated with the processing of GEOSAT satellite radar altimetry data are discussed. Summary statistics and observations obtained during the processing of a limited set of GEOSAT altimeter data are presented. Statistics from comparisons of GEOSAT-derived mean gravity anomalies with those obtained from available survey data are shown. Future plans and directions for the continued processing and exploitations of this data are indicated. GRA

N87-24738# European Space Agency, Paris (France).
PROCEEDINGS OF THE INTERNATIONAL SYMPOSIUM ON PROGRESS IN IMAGING SENSORS

B. BATTRICK, ed. and E. J. ROLFE, ed. Nov. 1986 663 p In ENGLISH, FRENCH, and GERMAN Proceedings held in Stuttgart, West Germany, 1-5 Sep. 1985; sponsored by the International Society for Photogrammetry and Remote Sensing, the Deutsche Gesellschaft fuer Photogrammetrie und Fernerkundung, DGLR, ESA, and DFVLR Submitted for publication Original contains color illustrations
(ESA-SP-252; ISSN-0379-6566; ETN-87-99861) Avail: NTIS HC A99/MF A01

The complete proceedings of the symposium are presented. Some topics of interest were: Remote sensing image quality; camera calibration; optical data from space; sensor orientation and navigation; microwave data; and imaging spectrometers. Also discussed were: Aerial photography; microwave sensors; acquisition and use of space photographic data; and photogrammetry. ESA

N87-24739*# Jet Propulsion Lab., California Inst. of Tech., Pasadena.

EARTH SURFACE SENSING IN THE '90'S

CHARLES ELACHI *In* ESA Proceedings of the International Symposium on Progress in Imaging Sensors p 1-11 Nov. 1986
Original document contains color illustrations Sponsored by NASA

Avail: NTIS HC A99/MF A01 CSCL 08B

Advances in Earth sensor technology and data handling techniques are reviewed. These will allow the acquisition of high resolution images over a wide range of the electromagnetic spectrum (from microwave to optical) with sufficient spectral resolution to permit detailed analysis of the surface chemical, thermal, and physical properties. When combined with the topography, this will allow the user to analyze the full data set in a perspective view that enhances interpretation capability. ESA

N87-24740# Stuttgart Univ. (West Germany). Inst. for Navigation.

SMART SENSORS: AN OVERVIEW AND SELECTED EXAMPLES

M. J. NAHVI and PH. HARTL *In* ESA Proceedings of the International Symposium on Progress in Imaging Sensors p 13-22 Nov. 1986

Avail: NTIS HC A99/MF A01

Smart sensors are reviewed and three conceptual levels are recognized, defining a functional hierarchy: data improvement, to increase accuracy; information extraction, to reduce data rate, and decision, to produce autonomy. Applications in measurement, control, remote sensing, and autonomous systems are illustrated, and advantages are quantified. Onboard processing for data reduction and autonomy is the trend in remote sensing and space missions, requiring intelligence, a knowledge base, and models of the external world. The role of smart sensors in an intelligent system is discussed and the extent of its operation is defined. Parallels with living compound lens and eye are observed. ESA

N87-24742# Physikalisch-Technische Bundesanstalt, Brunswick (West Germany).

OPTICAL TRANSFER FUNCTION (OTF)-BASED QUALITY CRITERIA FOR AERIAL CAMERAS AND IMAGING SYSTEMS

K.-J. ROSENBRUCH *In* ESA Proceedings of the International Symposium on Progress in Imaging Sensors p 33-37 Nov. 1986

Avail: NTIS HC A99/MF A01

It is demonstrated how for optical systems and imaging sensors, the optical transfer function can be reduced and used in practical application. For an image quality criterion (IQC) and data reduction, instead of the modulation transfer function (MTF) curve, the integral value is a reasonable data reduction. This integral should be extended up to the intersecting point of the total MTF curve of the receiver. If a correlation between quality numbers and the subjective impression of photographs is required, the just recognizable quality steps are proportional to the logarithm of a given integral. For the evaluation of the information content and digital image processing, the total MTF and relevant threshold modulation curves are important but not the integrals or log of integrals. The kind of object or its spatial frequency spectrum is not to be taken into account in an IQC evaluation. ESA

N87-24743# National Research Council of Canada, Ottawa (Ontario). Photogrammetric Research Section.

THOUGHTS ON A STANDARD ALGORITHM FOR CAMERA CALIBRATION

HARTMUT ZIEMANN *In* ESA Proceedings of the International Symposium on Progress in Imaging Sensors p 41-48 Nov. 1986

Avail: NTIS HC A99/MF A01

Starting from concerns related to the calibration of aerial cameras, aspects of standardization of camera calibration procedures are discussed. These include standardization activities and a possible role of the International Society for Photogrammetry and Remote Sensing in such activities, a definition of the term

camera calibration, and a mathematical model and an algorithm for camera calibration. The mathematical model includes special considerations for cameras with adjustable focus. ESA

N87-24744# Xian Research Inst. of Surveying and Mapping (China).

APPLIED FORMULAE FOR CALIBRATION OF AERIAL PHOTOGRAMMETRIC CAMERAS

WANG YUWEI *In* ESA Proceedings of the International Symposium on Progress in Imaging Sensors p 49-54 Nov. 1986

Avail: NTIS HC A99/MF A01

Formulas for calibrating the inner orientation of aerial photogrammetric cameras, and to estimate its accuracy are given. The calculation accuracy is enhanced in determining principal point position and focal length by iteration in which the influences of distortion and scale line errors of calibration plate are taken into consideration. There are no restrictions on scale line errors of calibration plate. Theoretically, any calibration plates with low accuracy of scale lines in terms of nominal sizes can be used, if they are calibrated accurately. The obtained principal point and focal length agree with those in the literature. Their values are the weighted averages of those determined by pairs of points on the axes of image plane, so that photogrammetric accuracy benefits from the application of the parameters. Each calculated parameter has its own error estimate. ESA

N87-24745# Bonn Univ. (West Germany). Inst. of Photogrammetry.

GEOMETRICAL SYSTEM CALIBRATION, ESPECIALLY FOR METRIC AERIAL CAMERAS

G. KUPFER *In* ESA Proceedings of the International Symposium on Progress in Imaging Sensors p 55-62 Nov. 1986

Avail: NTIS HC A99/MF A01

Geometrical system calibration is defined and its history is reviewed. Practical considerations and desirable capabilities of a calibration algorithm are discussed. Problems of full and partial system calibration are shown and recommendations for geometrical system calibration are given. Possibilities of the procedure are shown by examples. ESA

N87-24746# Deutsche Forschungs- und Versuchsanstalt fuer Luft- und Raumfahrt, Oberpfaffenhofen (West Germany).

COMPARATIVE ANALYSIS OF THEMATIC MAPPER AND SPOT IMAGE DATA FOR LAND USE INVESTIGATION

W. KIRCHHOF, W. MAUSER, and H. J. STIBIG *In* ESA Proceedings of the International Symposium on Progress in Imaging Sensors p 65-71 Nov. 1986 Prepared in cooperation with Freiburg Univ. (West Germany). Original document contains color illustrations

Avail: NTIS HC A99/MF A01

Data records including 10, 20, 30, 50, and 80 m pixels from a Thematic Mapper (TM) simulation were analyzed regarding information content. Discrimination of objects, structures, and textures as a function of pixel size and combination of spectral bands is investigated by visual interpretation and supervised classification for applications in agriculture and forestry. New TM bands bring extensive improvement in separating areas of vegetation and built-up areas and in delimiting growth and moisture states. The TM is suited for extracting thematic information of surface areas of 1 hectare or more, 3 to 4 spectral bands are normally sufficient. The information content of the 20 m SPOT multiband data does not differ from that of comparable TM bands (TM2, TM3, TM4). Structural and textural contents of the panchromatic 10 m SPOT band form a substantial complement to the TM information. ESA

N87-24748# Deutsche Forschungs- und Versuchsanstalt fuer Luft- und Raumfahrt, Cologne (West Germany).

APPLICATION OF MODULAR OPTOELECTRONIC MULTISPECTRAL SCANNER (MOMS) DATA TO HYDROLOGY AND VEGETATION STUDIES. TEST SITE: PANTANAL REGION (BRAZIL/ PARAGUAY)

HERMANN J. H. KUX, MARTIN HAUCK, and KONRAD HILLER
In ESA Proceedings of the International Symposium on Progress in Imaging Sensors p 87-90 Nov. 1986 Prepared in cooperation with Instituto de Pesquisas Espaciais, Sao Jose dos Campos (Brazil)

Avail: NTIS HC A99/MF A01

A section of Brazil/Paraguay/Bolivia imaged by MOMS was digitally classified and merged with a Thematic Mapper scene from the same region. A test of consistency and correctness was applied to the digital classifications of both sensors using kappa (κ) statistics. Considering that the κ value obtained is very low (0.1202), there is no agreement between the results of MOMS and TM classifications. The classification matrix shows a high confusion among the classes dense vegetation and wetlands. Areas covered by dense vegetation were interspersed with and/or overlaid with areas of wetlands with different water content. This great variation of soil moisture seems to be the principal environmental factor responsible for the high confusion found in these thematic classes.

ESA

N87-24749# Stuttgart Univ. (West Germany).

THE USE OF CAMERA ORIENTATION DATA IN PHOTOGRAMMETRY: A REVIEW

FRIEDRICH ACKERMANN In ESA Proceedings of the International Symposium on Progress in Imaging Sensors p 93-99 Nov. 1986

Avail: NTIS HC A99/MF A01

It is shown that precise camera orientation data obtained from flight navigation systems are of greatest importance to aerial photogrammetry, with regard to geometrical accuracy and economy. The first application of navigation systems concerns real time flight navigation and pinpoint photography to obtain regular overlap. The requirements can be met by any high precision navigation system. The most immediate use of recorded and postprocessed orientation data is in combination with aerial triangulation which would become practically independent of ground control points. Only position data are needed. The accuracy requirements are high but can potentially be met by GPS phase measurements. The accuracy requirements for direct setting of orientation parameters of photographs or pairs of photographs, avoiding aerial triangulation of reference to ground control, are extremely high and cannot yet be met by navigation systems.

ESA

N87-24750# Stuttgart Univ. (West Germany).

THE EFFECTS OF CAMERA POSITION AND ATTITUDE DATA IN AERIAL TRIANGULATION, A SIMULATION STUDY

PETER FRIESS In ESA Proceedings of the International Symposium on Progress in Imaging Sensors p 101-111 Nov. 1986

Avail: NTIS HC A99/MF A01

Accuracy attainable in aerial triangulation using navigation data in joint block adjustment was studied in simulations. The influence of camera position data on the accuracy of photogrammetric blocks is considerable. They always allow reduction of control to the minimum case with four ground control points in the corners of the block. Camera position coordinates observed with low accuracy (10 m) allow aerial triangulation with minimum ground control and provide ground point position accuracies which could otherwise only be reached with quite dense ground control. Precise attitude data combined with camera position data provide an additional improvement of block adjustment. The use of precise measured rotations alone combined with sparse ground control (two control point chains) is also possible.

ESA

N87-24751# National Aerospace Lab., Amsterdam (Netherlands).

A MODULAR AND VERSATILE ACQUISITION, RECORDING AND PREPROCESSING SYSTEM FOR AIRBORNE REMOTE SENSING

H. POUWELS and L. J. AARTMAN In ESA Proceedings of the International Symposium on Progress in Imaging Sensors p 113-121 Nov. 1986

Avail: NTIS HC A99/MF A01

An aircraft which can be equipped with either a SLAR, a multispectral scanner, or a TV-based scanner is described. The airborne recording equipment is designed to accommodate these various sensors. The general airborne system setup is: the sensor, a dedicated digitizing unit, and an interface to a high density digital tape recorder. Aircraft parameters like position, attitude, and time are recorded on the same tape. Flight tapes are replayed on existing equipment as used for PCM encoded telemetry data; only a high bit rate decoding unit is added. Raw remote sensing data and flight data are transferred to computer tapes. The software system Preprocessing Airborne Remote Sensing performs radiometric and geometric corrections for aircraft motion and for sensor characteristics.

ESA

N87-24752# Deutsche Forschungs- und Versuchsanstalt fuer Luft- und Raumfahrt, Wesseling (West Germany). Inst. for Optoelectronics.

INFRARED EARTH HORIZON SENSOR CONCEPTS IN VARIOUS SPECTRAL BANDS

SIEGFRIED CRAUBNER and RUDOLF RICHTER In ESA Proceedings of the International Symposium on Progress in Imaging Sensors p 123-127 Nov. 1986

Avail: NTIS HC A99/MF A01

Concepts for infrared Earth horizon sensors operating in different spectral bands are presented. Besides the 14 to 16 micron CO₂ band currently used, the 9.4 to 9.8 micron ozone band and the 20 to 22 micron water vapor band are suitable for horizon detection. Measurements in the ozone band would allow a smaller optics aperture than in the CO₂ band. The advantage of the water vapor band is a horizon nearer to the Earth's rim and a lower variation of the horizon radiance profile for the different standard atmospheres. Using commercially available metal/thermistor bolometers or pyroelectric detectors, the signal to noise ratio in the bands 9.4 to 9.8, 14 to 16, and 20 to 22 microns can be made sufficient. Thus there is no need to use cooled detectors in this application.

ESA

N87-24755# Marconi Co. Ltd., Great Baddow (England).

THE EFFECT OF RECEIVER AMPLIFIER NON-LINEARITY ON ERS-1 SYNTHETIC APERTURE RADAR IMAGERY

J. J. W. WILSON In ESA Proceedings of the International Symposium on Progress in Imaging Sensors p 149-155 Nov. 1986 Sponsored by ESA

Avail: NTIS HC A99/MF A01

The effect of a nonlinear active microwave instrument (AMI) receiver system gain characteristic on ERS-1 synthetic aperture radar imagery is assessed by feeding the signal from a point target on a distributed target background together with thermal noise into the receiver system. The output from the receiver system is then subjected to range and azimuth compression in order to generate the image intensity at the point in the image corresponding to the peak of the point target response function. The impact of nonlinearity and saturation in the AMI receiver system transfer characteristic are assessed by comparing the image intensity arising from passing the input signal through the AMI receiver system with the image intensity arising from passing the same input through a similar but completely linear receiver system.

ESA

N87-24756* Jet Propulsion Lab., California Inst. of Tech., Pasadena.

RADIOMETRIC CALIBRATION OF THE SHUTTLE IMAGING RADAR (SIR-C) SYSTEM

JOHN C. CURLANDER *In* ESA Proceedings of the International Symposium on Progress in Imaging Sensors p 157-160 Nov. 1986 Sponsored by NASA

Avail: NTIS HC A99/MF A01 CSCL 17E

The radiometric calibration accuracy of the Shuttle Imaging Radar (SIR-C) sensor is discussed. The analysis includes the antenna, RF electronics, the digital data handling system, the platform attitude control, attitude determination accuracy, and orbit effects. The radiometric distortion of the image products by the ground processing system used for the image formation is also considered. Since the SIR-C system is a dual-frequency quad-polarized system (i.e., 8 channels), the amplitude and phase error is considered over all possible operating modes and environments for absolute and relative (long-term and short-term) calibration within a channel and across channels. ESA

N87-24757# National Research Council of Canada, Ottawa (Ontario). Photogrammetric Research Div. of Physics.

PROPOSED CHANGES TO THE CANADIAN CAMERA CALIBRATION REPORT

H. ZIEMANN, M. L. LANDREVILLE, and J. E. W. PLUMMER *In* ESA Proceedings of the International Symposium on Progress in Imaging Sensors p 163-169 Nov. 1986

Avail: NTIS HC A99/MF A01

The requirements for an aerial survey camera are discussed, and Canadian camera calibration reports are reviewed. The reports are based on the requirements stated in the Canadian federal Specification for Aerial Survey Photography; changes in the Specification resulted at a number of times in changes to the calibration report. A large number of items included at one time or another are explained. A proposal indicating which items should be retained during a major revision of the calibration report, and which new items should be added, is made. ESA

N87-24761# Institut Geographique National, Paris (France).

APPLICATIONS OF LASER AIRBORNE TELEMETRY AT INSTITUT GEOGRAPHIQUE NATIONAL (IGN), FRANCE

R. BROSSIER *In* ESA Proceedings of the International Symposium on Progress in Imaging Sensors p 193-199 Nov. 1986

Avail: NTIS HC A99/MF A01

An airborne system on pressurized aircraft for the determination of ground profiles to provide an altimetric network for small scale photogrammetric surveys was developed. The system includes a laser telemeter for measuring the distance between aircraft and ground, and a pressure sensor for obtaining an isobaric reference. From this initial version, a system was developed to synchronize laser emission with photograph exposures. Another application concerns determination of ground profiles in wooded areas, which implies a modification of laser reception, for receiving all the echos coming from the ground. The ground profile itself is determined by sampling of the data. ESA

N87-24763# Stuttgart Univ. (West Germany). Inst. for Navigation.

APPLICATION OF GLOBAL POSITIONING SYSTEM (GPS) RECEIVERS FOR EARTH OBSERVATION

PH. HARTL and W. SCHOELLER *In* ESA Proceedings of the International Symposium on Progress in Imaging Sensors p 207-214 Nov. 1986

Avail: NTIS HC A99/MF A01

Use of the Global Positioning System (GPS) to acquire navigational information is proposed. The extremely high relative accuracy of a few dm over several hundred kilometers can be achieved in positioning, if the carrier phase measurement is applied in connection with the differential mode. The carrier phase signals can be used for attitude measurements. Here an interferometer system must be used, which consists of at least three antennas and corresponding receivers. They must constitute a pair of orthogonal interferometers. Relative accuracies on the order of

fractions of a degree down to several arcseconds might be achieved. ESA

N87-24765# European Space Agency. European Space Research and Technology Center, ESTEC, Noordwijk (Netherlands).

DEFINITION OF A THERMAL INFRARED PUSHBROOM IMAGER FOR EARTH OBSERVATION

M. RAST, M. L. REYNOLDS, and P. HOLLIER (MATRA Espace, Toulouse, France) *In its* Proceedings of the International Symposium on Progress in Imaging Sensors p 229-234 Nov. 1986

Avail: NTIS HC A99/MF A01

The feasibility of a thermal IR pushbroom camera design to satisfy the high resolution, multispectral imaging requirement corresponding to Earth observation mission objectives was assessed. In view of the state of the art, it seems that such an instrument is feasible within the next decade. According to a scientific and user requirement inquiry, the suggested ground resolution of 30 m could be reduced to 50 m while maintaining the main mission objectives and requirements. This reduction would relax the technical and cost problems for a spaceborne instrument. For example, it is estimated that the mass would reduce from 320 kg to 120 kg and diminish the maximum dimensions from 3.0 m to 1.7 m due to an entrance aperture reduction from 500 mm to 250 mm. ESA

N87-24767# Canada Centre for Remote Sensing, Ottawa (Ontario).

THE MULTIDETECTOR ELECTRO-OPTICAL IMAGING SENSOR (MEIS) 2 PUSHBROOM IMAGER: FOUR YEARS OF OPERATION

S. M. TILL, R. A. NEVILLE, W. D. MCCOLL, and R. P. GAUTHIER *In* ESA Proceedings of the International Symposium on Progress in Imaging Sensors p 247-253 Nov. 1986

Avail: NTIS HC A99/MF A01

A linear array multispectral airborne imager was designed to provide remote sensing data with improved radiometric and geometric characteristics, and with spectral selectivity for specific applications. Four years of operation, acquiring digital imagery for 50 airborne missions per year, provided unique data from this state-of-the-art imager, for application research and for sensor evaluation. Ongoing sensor development includes optics for continuous fore-aft stereo data acquisition, calibrated narrow band (3 nm) spectral filter sets, integration of downwelling irradiance and radiance spectral data, interference filters free from spectral blue shift, and an automated laboratory calibration facility. ESA

N87-24768# Messerschmitt-Boelkow-Blohm G.m.b.H., Munich (West Germany).

THE STEREO PUSHBROOM SCANNER SYSTEM DIGITAL PHOTOGRAMMETRY SYSTEM (DPS) AND ITS ACCURACY

OTTO HOFMANN *In* ESA Proceedings of the International Symposium on Progress in Imaging Sensors p 257-264 Nov. 1986 Previously announced as N87-17167

Avail: NTIS HC A99/MF A01

A digital stereoscanner with three line sensor arrays working on the pushbroom principle and a suitable rigorous compilation process, was designed. It delivers the orientation data of the camera in selectable update points along the flight path of aircraft, spacecraft, or missiles, the three-dimensional coordinates of the digital elevation model, ortho and stereo-orthophotos, digital elements for line maps and rectified multispectral images. By computer simulated operational models the influence of the camera and flight parameters on the accuracy of the models was tested. ESA

N87-24769# Technische Univ., Hanover (West Germany). Inst. for Photogrammetry and Engineering Surveys.

AERIAL TRIANGULATION OF CCD LINE-SCANNER IMAGES

E. KRUCK and P. LOHMANN *In* ESA Proceedings of the International Symposium on Progress in Imaging Sensors p 265-270 Nov. 1986

Avail: NTIS HC A99/MF A01

A method for the evaluation of CCD line scanner imagery is presented. The mathematical formulation considers central perspective geometry within a single line and allows easy implementation on analytical photogrammetric systems. The adjustment allows the use of additional frame camera images as well as other measurements. An anchor point file for the generation of orthophotos may be generated whenever digital terrain model data are available. Results using a combined adjustment of Spacelab Metric Camera photographs and MOMS data are presented. ESA

N87-24771# Deutsche Forschungs- und Versuchsanstalt fuer Luft- und Raumfahrt, Oberpfaffenhofen (West Germany).

INVESTIGATION OF SIMULATED MONOCULAR ELECTRO-OPTICAL STEREO SCANNER (MEOSS)-IMAGERY FOR SENSOR NAVIGATION AND TERRAIN DERIVATION

J. WU *In* ESA Proceedings of the International Symposium on Progress in Imaging Sensors p 279-284 Nov. 1986

Avail: NTIS HC A99/MF A01

Rectification of Monocular Electro-Optical Stereo Scanner images for distortions due to perturbations of position and attitude parameters and elevation differences in the terrain is discussed. Analytical photogrammetry is applied to evaluations of the stereoscopic image data. Primary results are the sensor orientation and the terrain model. The digital image processing system includes a photogrammetric aerial triangulation program based on collinearity conditions and weight constraints. Numerical simulation reveals the potential usage of such a sensor system concerning sensor navigation and terrain derivation. ESA

N87-24773# Xian Research Inst. of Surveying and Mapping (China).

ON THE MATCHING OF RESOLUTION IN AERIAL PHOTOGRAPHIC SYSTEMS

JUNLIANG CAI and HUIPING CHEN *In* ESA Proceedings of the International Symposium on Progress in Imaging Sensors p 295-302 Nov. 1986

Avail: NTIS HC A99/MF A01

Matching of lens and film resolutions and image motion is discussed. A matching when the resolution of film is 3 to 4 times higher than that of lens with the image motion less than 2/3 to 3/4 of line pair width of static resolution is best. In order to improve the dynamic resolution, it is more effective to limit the image motion than to improve the static resolution. Therefore, the use of image motion compensation is necessary. In this case, the static resolution 3 to 4 times higher than the resolution corresponding to residual image motion is preferable. ESA

N87-24775# Deutsche Forschungs- und Versuchsanstalt fuer Luft- und Raumfahrt, Oberpfaffenhofen (West Germany).

EXPOSURE TEST WITH HIGH RESOLUTION FILMS FROM HIGH ALTITUDE

M. SCHROEDER and C. DUDA *In* ESA Proceedings of the International Symposium on Progress in Imaging Sensors p 311-316 Nov. 1986

Avail: NTIS HC A99/MF A01

High altitude (10 km) aerial photographs on high resolution films (3412 b/w; SO-131 (CIR); SO-242 (Co) taken at various illumination conditions and with different exposure settings were analyzed by densitometric measurements in order to find the influence of exposure and illumination on film density. From these measurements, formulas for exposure settings as function of the Sun elevation were derived. ESA

N87-24776# Firma Maps G.m.b.H., Munich (West Germany).

VERY HIGH RESOLUTION AERIAL FILMS

ROLF BECKER *In* ESA Proceedings of the International Symposium on Progress in Imaging Sensors p 317-326 Nov. 1986

Avail: NTIS HC A99/MF A01

The use of very high resolution aerial films in aerial photography is evaluated. Commonly used panchromatic, color, and CIR films and their high resolution equivalents are compared. Based on practical experience and systematic investigations, the very high image quality and improved height accuracy that can be achieved using these films are demonstrated. Advantages to be gained from this improvement and operational restrictions encountered when using high resolution film are discussed. ESA

N87-24781# Zeiss (Carl), Oberkochen (West Germany).

THE RMK AERIAL CAMERA SYSTEM: PERFORMANCE POTENTIAL OF AERIAL PHOTOGRAPHY WITH FORWARD MOTION COMPENSATION

W. LORCH *In* ESA Proceedings of the International Symposium on Progress in Imaging Sensors p 363-366 Nov. 1986

Avail: NTIS HC A99/MF A01

It is shown that the use of forward motion compensation (FMC) in aerial survey cameras increases the image quality significantly. Medium-resolution films are mostly being used with FMC. Another considerable image quality increase can be achieved by the use of high-resolution films which were not very suited for large-scale photography because of their high contrast. Performance is optimum with the lens stepped down 1 stop. Experience shows that an adverse residual image motion due to unfavorable external influences does not occur if exposure times of 1/300 sec or less are used. ESA

N87-24782# Wild Heerbrugg Ltd. (Switzerland).

WILD AVIOPHOT (TM) RC20 AERIAL CAMERA SYSTEM. THE OTHER APPROACH TO IMAGE MOTION COMPENSATION IN AERIAL PHOTOGRAPHY

ARTHUR ROHRBACH and ROLAND SCHLIENGER *In* ESA Proceedings of the International Symposium on Progress in Imaging Sensors p 367-373 Nov. 1986

Avail: NTIS HC A99/MF A01

It is shown that the integration of forward motion compensation (FMC) in the Wild Aviophot RC20 aerial camera system, allows a better exploitation of the high inherent optical performance of the Wild lenses. The main practical benefits are: an increase in image quality and resolution when combining the FMC device of the EC20 with high-resolution emulsions; as well as a better use and exploitation of the standard film types, in connection with large-scale and very-large-scale photographs, under less than ideal light conditions (low light-level). Given the high investment and running costs involved in aerial photography, features like an increase in image resolution, additional flying hours, high product reliability, and flexible connection to aircraft navigation systems are highly significant for overall mapping economy. ESA

N87-24785# Technische Univ., Berlin (West Germany). Dept. of Photogrammetry and Cartography.

DIGITAL DATA ACQUISITION FOR CLOSE-RANGE PHOTOGRAMMETRY

JOERG ALBERTZ and ALFRED MEHLBREUER *In* ESA Proceedings of the International Symposium on Progress in Imaging Sensors p 385-390 Nov. 1986

Avail: NTIS HC A99/MF A01

A digital close-range photogrammetric data acquisition system, suitable for mobile operation and designed to take stereo-images simultaneously is presented. A proposal is made for a high resolution digital acquisition system. By this approach the limited geometrical resolution of CCD-arrays can be improved. Applications with a scanning electron microscope are shown. ESA

N87-24788# Technische Univ., Dresden (East Germany). Dept. of Geodesy and Cartography.

THE PRODUCTION OF PHOTOGRAPHS OF THE EARTH'S SURFACE TAKEN FROM SATELLITES AND THEIR APPLICATION IN MAP PRODUCTION AND MAP REVISION

KLAUS SZANGOLIES /In ESA Proceedings of the International Symposium on Progress in Imaging Sensors p 411-413 Nov. 1986

Avail: NTIS HC A99/MF A01

It is shown that photographs taken from space by a camera with 6 spectral channels meet the requirements of most mapping tasks at the scales 1:50,000 to 1:200,000 (and smaller) with regard to the interpretation capability and the geometric accuracy. Advantages compared with the large format aerial cameras lie in the fact that photographs of six different spectral channels are simultaneously obtained, and that the resolving power of the single cameras is considerably higher because of the narrow spectral ranges. ESA

N87-24789# Technische Univ., Munich (West Germany). Inst. fuer Geographie.

LARGE FORMAT CAMERA IMAGE ANALYSIS FOR MAPPING OF LAND USE PATTERNS IN THE REGION NOALE - MUSONE, PO-RIVER-PLAIN, NORTH ITALY

H.-G. GIERLOFF-EMDEN /In ESA Proceedings of the International Symposium on Progress in Imaging Sensors p 415-426 Nov. 1986

Avail: NTIS HC A99/MF A01

Large Format Camera (LFC)-photography was analyzed to test the applicability of LFC-photographs for topographic and thematic maps. Scales of 1:100,000, 1:50,000 and 1:25,000 were assessed concerning the information and the interpretability of the object-categories, point-shape, line-shape, plane-shape, and the objects in the real world and the discreet signatures in the maps. The minimum visible is analyzed according to ground truth in the test areas. Stereoscopic techniques are not used. Results show that LFC-photography is qualified for topographic maps on the scale of 1:100,000 and 1:50,000 (selected purpose) and for thematic maps up to the scale of 1:25,000 for land use pattern and land surface features. ESA

N87-24792# Ludwig-Maximilians-Universitaet, Munich (West Germany). Inst. fuer Geographie.

LARGE FORMAT CAMERA PHOTOGRAPHS OF THE BLACK HILLS, USA, AND THEIR SUITABILITY FOR TOPOGRAPHIC AND THEMATIC MAPPING

KLAUS R. DIETZ /In ESA Proceedings of the International Symposium on Progress in Imaging Sensors p 439-448 Nov. 1986 In GERMAN; ENGLISH summary

Avail: NTIS HC A99/MF A01

Large Format Camera (LFC) photos of the Black Hills, taken on Space Shuttle Mission 41-G, were compared with Metric Camera (MC) photos from the same area, as well as with maps and with high altitude photos. The use of high resolution film, forward motion compensation, and better illumination conditions and base height ratios of the LFC photos give a distinct improvement compared to the MC data. The LFC images seem suitable for mapping on the scale of 1:100,000, if supported by field work. Due to the moderate image quality provided by the EROS Data Center, the production of maps on the scale of 1:50,000 does not seem possible. ESA

N87-24798# National Research Council of Canada, Ottawa (Ontario). Photogrammetric Research Div. of Physics.

SPECTROPHOTOMETRIC MEASUREMENTS ON COLOR AERIAL PHOTOGRAPHS

H. ZIEMANN, J. C. CROTEAU, J. R. HANDY, and E. NAGY /In ESA Proceedings of the International Symposium on Progress in Imaging Sensors p 491-503 Nov. 1986

Avail: NTIS HC A99/MF A01

It is shown that a microdensitometer can be calibrated to carry out spectrophotometric measurements on aerial photographs. In spite of several approximations necessary to extend the measured PDS 1010M data to the full photometric range and to use available

integration tables for the CIE color-matching functions, the results appear to be accurate enough to indicate known characteristics of the used color-emulsions. The used experimental color panels were rather small resulting in relatively noisy PDS 1010M measurements; more accurate results would be obtained with larger panels. The saturation for the used panels is small; higher saturation would be desirable. Results indicate that color panels of the same quality and size as the available neutral density (ND) reflectance panels are desirable for further test photography; color panels provide additional information about the response of color emulsions not available from the ND reflectance panels. ESA

N87-24811# Deutsche Forschungs- und Versuchsanstalt fuer Luft- und Raumfahrt, Oberpfaffenhofen (West Germany). Inst. for Optoelectronics.

EARTH OBSERVATION EXPERIMENTS ON THE GERMAN SPACELAB MISSION D2

F. LANZL /In ESA Proceedings of the International Symposium on Progress in Imaging Sensors p 609-616 Nov. 1986

Avail: NTIS HC A99/MF A01

The Spacelab D2 remote sensing mission applications and equipment are summarized. The Mapping Experiment from Space involves topographic and thematic mapping with an improved Metric Camera. Modular Optoelectronic Multispectral Scanner 2 studies correlation of multispectral and terrain information. The Spacelab Atmospheric Lidar Experiment is designed for determination of atmospheric data for weather forecasts. ESA

N87-24812# Deutsche Forschungs- und Versuchsanstalt fuer Luft- und Raumfahrt, Oberpfaffenhofen (West Germany). Inst. for Optoelectronics.

THE MONOCULAR ELECTRO-OPTICAL STEREO SCANNER (MEOSS) SATELLITE EXPERIMENT

F. LANZL /In ESA Proceedings of the International Symposium on Progress in Imaging Sensors p 617-620 Nov. 1986

Avail: NTIS HC A99/MF A01

An along track spaceborne threefold scanner flight on the SROSS satellite is introduced. It includes investigation and test of different evaluation methods for threefold stereo scan systems for the planning of future higher resolution systems, and angular dependent reflectance information and frequent coverage of same test area. Applications include meteorology, mapping, environmental monitoring, and geological and forestry surveys. ESA

N87-24813# Deutsche Forschungs- und Versuchsanstalt fuer Luft- und Raumfahrt, Oberpfaffenhofen (West Germany). Inst. for Optoelectronics.

MODERN CCD SENSORS AND THEIR APPLICATIONS IN EARTH OBSERVATION AND PLANETARY MISSIONS

P. SEIGE /In ESA Proceedings of the International Symposium on Progress in Imaging Sensors p 621-625 Nov. 1986

Avail: NTIS HC A99/MF A01

The characteristics of CCD's are listed. Trends in CCD technology are outlined. ESA

N87-24815# Technische Univ., Munich (West Germany). Faculty of Geosciences.

THE MODULAR OPTOELECTRONIC MULTISPECTRAL SCANNER (MOMS) PROGRAM OF THE BUNDESMINISTERIUM FUER FORSCHUNG UND TECHNOLOGIE (BMFT). MILESTONES IN THE DEVELOPMENT OF AN OPERATIONAL EARTH OBSERVATION SYSTEM

J. BODECHTEL, D. MEISSNER, P. SEIGE, H. WINKENBACH (Deutsche Forschungs- und Versuchsanstalt fuer Luft- und Raumfahrt, Oberpfaffenhofen, West Germany), and J. ZILGER /In ESA Proceedings of the International Symposium on Progress in Imaging Sensors p 635-639 Nov. 1986

Avail: NTIS HC A99/MF A01

The mission of the Modular Optoelectronic Multispectral Scanner (MOMS) aboard two flights of the Space Transportation System demonstrated the feasibility of the concept with regard to technical and scientific objectives. On account of the successful

09 GENERAL

missions a cooperation was agreed for comparing MOMS observations with operational Landsat-Thematic Mapper data over selected test sites as a means of obtaining relative measure of performance. The results obtained and aspects of MOMS instrument development aiming at the realization of an operational system are presented. ESA

09

GENERAL

Includes economic analysis.

A87-32502

UNITED STATES REMOTE SENSING SATELLITES (RSSS) PAST, PRESENT, AND FUTURE

LOUIS GOMBERG (RCA, Astro-Electronics Div., Princeton, NJ) IN: International Symposium on Space Technology and Science, 15th, Tokyo, Japan, May 19-23, 1986, Proceedings. Volume 2. Tokyo, AGNE Publishing, Inc., 1986, p. 1677-1688.

The current operational remote sensing satellite programs in the United States are described. These include the DMSP, supplying the Armed Forces with meteorological and other environmental data; the TIROS system, which is the civilian analog of the DMSP, and is the original remote sensing satellite; the GOES, which provides NOAA with large-area cloud-cover data and wind direction; and the Landsat system, used to evaluate and manage earth resources. The salient features of the satellites in each system, the sensors carried, and the new developments introduced into these systems are presented. The Naval Remote Ocean Sensing Satellite being planned by the U.S. Navy for development is briefly discussed. I.S.

A87-32955

INDIAN REMOTE SENSING PROGRAMME

B. L. DEEKSHATULU and S. ADIGA (National Remote Sensing Agency, Hyderabad, India) Geocarto International, no. 4, 1986, p. 49-59. refs

India's remote sensing program is reviewed. India has developed facilities for the design, development, and management of remote sensing satellites and sensors, the acquisition, processing, dissemination, and analysis of the data, and the training of users. The characteristics and capabilities of India's satellites, earth station, and platforms are described. Consideration is given to the Indian Remote Sensing Satellite (IRSS) mission, the National Natural Resources Management System, IRSS utilization projects, user training and education, and international remote sensing projects. India's remote sensing capabilities have been applied to the study of agriculture, soils, forestry, ecology/morphology, minerals, land use, hydrology, and urban planning. Specific examples of Indian remote sensing projects are provided. I.F.

A87-33125

WORLD-WIDE WEATHER

KOICHIRO TAKAHASHI, ED. Rotterdam and Accord, MA, A. A. Balkema, 1986, 263 p. Translation. No individual items are abstracted in this volume.

Various global meteorological phenomena are examined. Attention is placed on the changing world climate, solar energy and the world climate, the water of the world, and wind systems of the world. Consideration is given to seasonal winds, rain and drought in India and Pakistan, plum rains and the Tibetan Plateau, the climate of the Mediterranean region, coastal deserts, the arid zone of Brazil, tropical rain and the intertropical convergence zone, the changing water level of Lake Victoria, tropical cold waves, typhoons, cyclones, hurricanes, winter storms, bora and foehn, windspouts and tornadoes, blizzards, the weather of the South Pole, the weather of the North Pole and the Arctic cold wave, tundra, icefloes and icebergs, and the ice age. The effect of human

activity, in particular air pollution and aircraft routes, on the climate is discussed. I.F.

A87-34208

OPTIMIZATION OF A PROGRAM OF EXPERIMENTS IN CONNECTION WITH THE OPERATIONAL PLANNING OF STUDIES CARRIED OUT WITH A SPACECRAFT (OPTIMIZATSIYA PROGRAMMY EKSPERIMENTOV PRI OPERATIVNOM PLANIROVANII ISSLEDOVANII, VYPOLNIAE-MYKH S KA)

M. I. U. BELIAEV and D. N. RULEV Kosmicheskie Issledovaniia (ISSN 0023-4206), vol. 25, Jan.-Feb. 1987, p. 30-36. In Russian. refs

An approach to the optimal planning of experiments for the Salyut orbital station is described. The problem of operational experiment planning is reduced to an integer problem of linear programming. A set of programs for the BESM-6 computer has been developed for implementing the proposed method. The remote sensing of earth resources is considered as an example. B.J.

A87-34600

FRENCH SPOT AND THE U.S. LANDSAT JOCKEY FOR POSITION IN THE RACE FOR A MULTIMILLION-DOLLAR REMOTE SENSING MARKET

DAVID S. MEYER Commercial Space (ISSN 8756-4831), vol. 2, no. 4, Winter 1987, p. 62-66.

Spot and Landsat 4 and 5 images are the basis of an industry taking remote sensing technology to the market place. Landsat thematic mapper images are produced by combining data from bands in the visible and near infrared ranges of the electromagnetic spectrum; the images provide more information about vegetation than Spot images do. Overall detail, at only 30-m resolution, is lower than that provided by Spot, which can merge 20-m-resolution multispectral and 10-m-resolution panchromatic data. The data products (tapes and film) are used by companies and government agencies in such diverse areas as mapping, petroleum and mineral exploration, crop analysis, coastal studies, hydrology and hazardous waste monitoring. Eosat took over the operation of NASA Landsat satellites in 1985, but the agreed-on transitional funding to cover five years has not been forthcoming from the U.S. government. A new Landsat cannot be launched until 1989 and there is a good chance that Eosat will have to buy Spot data from their competitor to supplement their data archive. Spot is a joint venture of the French CNES space agency with Sweden and Belgium. The Japanese, Canadians and ESA, meanwhile, are planning their own entries into the remote sensing data markets. The rapidly expanding personal computer industry, making image and data processing easier and cheaper, will lead the remote sensing industry to gross more than \$1 billion by the year 2000. D.H.

A87-34799

INTELSAT'S SMALL EARTH STATIONS - IMPACT ON THE DEVELOPING WORLD

PATRICK MCDUGAL (Intelsat, Washington, DC) Space Communication and Broadcasting (ISSN 0167-9368), vol. 4, Dec. 1986, p. 455-462.

This article offers a brief historical look at the progress in the use of small earth stations in the developing world, and a present status report on Intelsat's new service offerings, especially in the use of smaller earth station technology. Three experiments or series of experiments are discussed: those conducted on NASA's ATS (Applications Technology Satellite) series of satellites, India's SITE (Satellite Instructional Television Experiment), and the Rural Satellite Project sponsored by the U.S. Agency for International Development. Intelsat's contributions to the growth of telecommunications in the developing world include: domestic leases, VISTA and INTELNET services, Project SHARE, and some new strategies for the financing of telecommunications projects. The article concludes that it is only recently that some of the true benefits of satellite communications have been realized in the developing countries because of improvements in technology, reduction in costs, and diversity of service offerings. Author

N87-41435

THE APPLICATION OF REMOTE SENSING TECHNIQUES IN CHINA

SHI-REN YANG (Chinese Academy of Sciences, Institute of Remote Sensing Application, Beijing, People's Republic of International Journal of Remote Sensing (ISSN 0143-1161), vol. 8, April 1987, p. 651-658.

The current status of the application of remote sensing techniques in China is described. The Chinese Landsat ground station was recently put into operation, and more than thirty low and medium altitude aircraft for remote sensing applications are now operational. Digital image processing systems are now widely used in remote sensing applications, while new instruments and sensors have been developed and are now in use. Applications of remote sensing in China for land resource surveys, urban pollution detection and environmental monitoring, agriculture, forestry, hydrology, geology, coal mining, uranium exploration, glaciology and cryopedology are discussed. Author

N87-20626# Centre National d'Etudes Spatiales, Toulouse (France). SPOT IMAGE.

REMOTE SENSING APPLICATIONS: COMMERCIAL ISSUES AND OPPORTUNITIES FOR SPACE STATION

G. BRACHET /In ESA Proceedings of the European Symposium on Polar platform Opportunities and Instrumentation for Remote-sensing (ESPOIR) p 35-37 Nov. 1986

Avail: NTIS HC A07/MF A01

The SPOT program is reviewed and the long term prospects beyond SPOT-4 are assessed. Management, legal, and commercial aspects are emphasized. ESA

N87-24493# Joint Publications Research Service, Arlington, Va.

ARIANESPACE TOP PERFORMANCE BENEFITS ESA

REIMAR LUEST /In its Europe Report: Science and Technology p 2-5 19 Jun. 1986 Transl. into ENGLISH from Frankfurter Zeitung/Blick Durch die Wirtschaft (Frankfurt/Main, West Germany), 29 Apr. 1986 p 5

Avail: NTIS HC A08/MF A01

The economic exploitation of space is growing in importance. The achievements in telecommunication satellites are reviewed. There are also numerous practical applications of earth reconnaissance from space which are also of considerable significance economically. Examples of these are the monitoring of pollution, sea and coastal surveillance, geological reconnaissance, cartography, and weather forecasting. The exploitation of zero gravity could also be of increasing significance in the areas of materials research and process engineering; chemical processes; liquid and gas physics; pharmacology; and biosciences. The role of the Arianespace is discussed in terms of economic and political impact on Europe. B.G.

N87-24777# Dornier-Werke G.m.b.H., Friedrichshafen (West Germany).

THE FIRST ESA REMOTE SENSING SATELLITE (STATUS AND OUTLOOK)

HANS MARTIN BRAUN and ERICH H. VELTEN /In ESA Proceedings of the International Symposium on Progress in Imaging Sensors p 329-334 Nov. 1986

Avail: NTIS HC A99/MF A01

The ERS-1 satellite design and development status are outlined. Mission objectives concentrate on ocean monitoring for scientific and economic purposes. The core payload consists of the active microwave instrumentation containing a synthetic aperture radar and a microwave scatterometer, and a radar altimeter. Supplementary instruments are an along track scanning radiometer, a microwave sounder, a precise range and range rate experiment, and a laser retroreflector. ESA

N87-24780# National Research Council of Canada, Ottawa (Ontario). Photogrammetric Research Section.

THE ROLE OF GOVERNMENT SPECIFICATIONS IN AERIAL PHOTOGRAPHY

HARTMUT ZIEMANN /In ESA Proceedings of the International Symposium on Progress in Imaging Sensors p 351-353 Nov. 1986

Avail: NTIS HC A99/MF A01

It is indicated that the introduction and periodic review of a Specification for Aerial Survey Photography is helpful in achieving a fairly high and consistent quality in the aerial photography acquired by contractors for the needs of the Canadian federal government by forcing good contractor performance and by occasionally requiring modifications to or the replacement of aerial survey cameras. The interaction between the Canadian regulating and controlling agency, the camera manufacturers, and contractors proves beneficial to all parties. ESA

N87-24797# Tokyo Univ. (Japan). Inst. of Industrial Science.

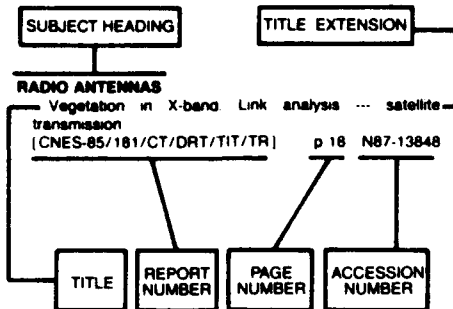
EARTH RESOURCES SATELLITE (ERS-1) PROJECT IN JAPAN

SHUNJI MURAI /In ESA Proceedings of the International Symposium on Progress in Imaging Sensors p 487-488 Nov. 1986

Avail: NTIS HC A99/MF A01

The ERS-1 (Japanese spacecraft) sensor system including a synthetic aperture radar, four-band visible/near infrared CCD sensor with stereo mode and a four-band short wave infrared sensor (1.65, 2.10, 2.20 and 2.35 micrometers) is introduced. Applications include monitoring of natural resources as well as agriculture, forestry, fishery, environmental protection, natural disasters, and surveillance of coastal regions. ESA

Typical Subject Index Listing



The subject heading is a key to the subject content of the document. The title is used to provide a description of the subject matter. When the title is insufficiently descriptive of the document content, the title extension is added, separated from the title by three hyphens. The (NASA or AIAA) accession number and the page number are included in each entry to assist the user in locating the abstract in the abstract section. If applicable, a report number is also included as an aid in identifying the document. Under any one subject heading, the accession numbers are arranged in sequence with the AIAA accession numbers appearing first.

A

ABSORPTION SPECTROSCOPY

Atmospheric environment monitoring system based on an earth-to-satellite Hadamard transform laser long-path absorption spectrometer - A proposal p 45 A87-35502

ACID RAIN

Spatial characterization of acid rain stress in Canadian Shield lakes [NASA-CR-180983] p 36 A87-24031
Spatial characterization of acid rain stress in Canadian Shield lakes [NASA-CR-180982] p 36 A87-24032

AERIAL PHOTOGRAPHY

A comparison of optical bar, high-altitude, and black-and-white photography in land classification p 4 A87-35122
Statistical evaluation of forest characteristics from aerial and space photographs p 5 A87-36109
Aerial and space investigations of soils and vegetation --- Russian book p 6 A87-36579
Aircraft radiopositioning for airborne photography during hydrographic coastal surveys p 23 A87-36945
An application of low altitude multispectral photography to agricultural field trials p 6 A87-37054
Testing the consistency for mapping urban vegetation with high-altitude aerial photographs and Landsat MSS data p 13 A87-37277
Aerotriangulation without ground control p 46 A87-37289
Measurements on digitized hardcopy images p 39 A87-37290
Strategies and technologies for monitoring the environment p 14 A87-38593
Use of maps, aerial photographs, and other remote sensor data for practical evaluations of hazardous waste sites p 14 A87-42255
Comparison between digital and manual interpretation of high altitude aerial photographs p 48 A87-42257

Proceedings of the International Symposium on Progress in Imaging Sensors [ESA-SP-252] p 50 N87-24738
Improvement of image quality by forward motion compensation, a preliminary report p 42 N87-24741
Optical Transfer Function (OTF)-based quality criteria for aerial cameras and imaging systems p 51 N87-24742

Thoughts on a standard algorithm for camera calibration p 51 N87-24743
Applied formulae for calibration of aerial photogrammetric cameras p 51 N87-24744
Geometrical system calibration, especially for metric aerial cameras p 51 N87-24745
The effects of camera position and attitude data in aerial triangulation, a simulation study p 52 N87-24750
Proposed changes to the Canadian camera calibration report p 53 N87-24757
Applications of laser airborne telemetry at Institut Geographique National (IGN), France p 53 N87-24761

On the matching of resolution in aerial photographic systems p 54 N87-24773
Exposure test with high resolution films from high altitude p 54 N87-24775
Very high resolution aerial films p 54 N87-24776
The role of government specifications in aerial photography p 57 N87-24780
The RMK aerial camera system: Performance potential of aerial photography with forward motion compensation p 54 N87-24781
Wild Aviophot (TM) RC20 aerial camera system. The other approach to image motion compensation in aerial photography p 54 N87-24782
Spectrophotometric measurements on color aerial photographs p 55 N87-24798
Photographic quality of color IR aerial photos as a function of atmospheric parameters p 42 N87-24799
Determination of spectral reflectance of crops during growth from calibrated multispectral small format aerial photography p 12 N87-24801
The use of auxiliary data in photogrammetric adjustments p 42 N87-24808
Image quality problems in practical aerial photography p 43 N87-24814

AEROSOLS

Sea surface temperature measurement from space allowing for the effect of the stratospheric aerosols p 22 A87-35148
Satellite sensing of aerosol absorption p 47 A87-40770

Optical properties of the marine atmospheric boundary layer - Aerosol profiles p 28 A87-42638

AFRICA

The use of AVHRR data in operational agricultural assessment in Africa p 9 A87-40304
Real-time crop assessment using color theory and satellite data p 10 N87-20619

AGRICULTURE

Workshop on Space Remote Sensing for Agricultural and Thematic Mapping, Budapest, Hungary, Apr. 18, 1986, Proceedings p 1 A87-32007
Remote sensing research in global agricultural productivity p 2 A87-32008
Remote sensing methods of yield forecasting p 2 A87-32009
The application of remote sensing in agricultural meteorology at the Meteorological Service of the HPR p 2 A87-32010
The topographic effect on Landsat data in gently undulating terrain in southern Sweden p 4 A87-35307
An application of low altitude multispectral photography to agricultural field trials p 6 A87-37054
Procedures for the description of agricultural crops and soils in optical and microwave remote sensing studies p 8 A87-39187
Rice crop identification and area estimation using remotely-sensed data from Indian cropping patterns p 9 A87-41434
Foundations and applications of multispectral scanning in agriculture [NLR-MP-85015-U] p 10 N87-21408

A crop condition and crop yield estimation method based on NOAA/AVHRR satellite data p 10 N87-22280
The impact of climate change from increased atmospheric carbon dioxide on American agriculture [DOE/NBB-0077] p 11 N87-23032

AGROCLIMATOLOGY

The use of AVHRR data in operational agricultural assessment in Africa p 9 A87-40304

AGROMETEOROLOGY

The application of remote sensing in agricultural meteorology at the Meteorological Service of the HPR p 2 A87-32010

AIR NAVIGATION

Aircraft radiopositioning for airborne photography during hydrographic coastal surveys p 23 A87-36945
Application of Global Positioning System (GPS) receivers for Earth observation p 53 N87-24763

AIR POLLUTION

Lidar observation of elevated pollution layers over Los Angeles p 13 A87-33292
A review of national and international activities on modeling the effects of increased CO2 concentrations on the simulation of regional crop production: A report on linkage between climate and crop models [DE87-005994] p 10 N87-22336
Spatial characterization of acid rain stress in Canadian Shield lakes [NASA-CR-180983] p 36 A87-24031

AIR QUALITY

Lidar observation of elevated pollution layers over Los Angeles p 13 A87-33292

AIR SEA ICE INTERACTIONS

Feedback between ice flow, barotropic flow, and baroclinic flow in the presence of bottom topography p 27 A87-40289
Remote sensing of the Fram Strait marginal ice zone p 27 A87-40433
Mesoscale oceanographic processes beneath the ice of Fram Strait p 28 A87-40434
Remote sensing as a research tool --- sea ice surveillance from aircraft and spacecraft p 28 A87-40648
An evaluation of the polar ice prediction system [AD-A176522] p 41 N87-23014
Arctic Sea ice, 1973-1976: Satellite passive-microwave observations [NASA-SP-489] p 33 N87-24870

AIR WATER INTERACTIONS

The dependence of sea-surface microwave emission on wind speed, frequency, incidence angle, and polarization over the frequency range from 1 to 40 GHz p 22 A87-35515
Satellite measurements of sea surface cooling during hurricane Gloria p 24 A87-37886
Possibilities of using artificial Earth satellite data for computing heat exchange between the ocean and atmosphere in Newfoundland energy-active zone during winter p 31 N87-21980
The 1982-1983 El Nino Atlas: Nimbus-7 microwave radiometer data [NASA-CR-180914] p 31 N87-22386

AIRBORNE EQUIPMENT

Interpretation of the polarimetric co-polarization phase term in radar images obtained with the JPL airborne L-band SAR system p 36 A87-31412
Airborne observation experiments for MOS-1 verification program (MVP) p 44 A87-32500
Operational overview of NASA GTE/CITE 1 airborne instrument intercomparisons - Carbon monoxide, nitric oxide, and hydroxyl instrumentation --- Global Tropospheric Experiment/Chemical Instrumentation Test and Evaluation p 45 A87-33426
Measurements of nitric oxide in the boundary layer and free troposphere over the Pacific Ocean p 21 A87-33431
Carbon monoxide measurements over the eastern Pacific during GTE/CITE 1 --- Chemical Instrumentation Test and Evaluation p 21 A87-33435
Measurement of the spatial spectrum of ocean waves using a two-frequency scatterometer p 23 A87-36107
Nadir looking airborne radar and possible applications to forestry p 7 A87-38095

- Airborne remote sensing of forest biomes p 9 A87-40301
- Ground and aerial use of an infrared video camera with a mid-infrared filter (1.45 to 2.0 microns) p 48 A87-41588
- The Multidetector Electro-optical Imaging Sensor (MEIS) 2 pushbroom imager Four years of operation p 53 N87-24767
- AIRBORNE LASERS**
- Wind and nadir angle effects on airborne lidar water 'surface' returns p 29 A87-42641
- AIRBORNE SURVEILLANCE RADAR**
- Strategies and technologies for monitoring the environment p 14 A87-39593
- AIRBORNE/SPACEBORNE COMPUTERS**
- The integration of spectral and spatial analysis for land use classification [AD-A178703] p 14 N87-23015
- A modular and versatile acquisition, recording and preprocessing system for airborne remote sensing p 52 N87-24751
- ALBEDO**
- Recent research in snow hydrology p 35 A87-40309
- Surface bidirectional reflectance properties of two southwestern Arizona deserts for wavelengths between 0.4 and 2.2 micrometers [NASA-TP-2643] p 49 N87-22281
- An atmospheric correction algorithm for remote identification of non-Lambertian surfaces and its range of validity [DE87-006059] p 41 N87-24011
- ALGORITHMS**
- Introduction of initial centers for the algorithm of clustering around mobile centers ... in multispectral image classification p 37 A87-35313
- Derivation of a fast algorithm to account for distortions due to terrain in earth-viewing satellite sensor images p 38 A87-35524
- Radiometric correction of SAR images - A new correction algorithm p 40 A87-39184
- An expert system for labeling segments in forward looking infrared (FLIR) imagery p 40 A87-42628
- A technique to estimate the ocean surface energy flux using VAS multispectral data p 30 N87-20710
- An atmospheric correction algorithm for remote identification of non-Lambertian surfaces and its range of validity [DE87-006059] p 41 N87-24011
- Thoughts on a standard algorithm for camera calibration p 51 N87-24743
- ALPINE METEOROLOGY**
- Remotely sensed sea surface temperature for the Alpine Experiment (ALPEX) ... AVHRR-2 data p 30 N87-21497
- ALPS MOUNTAINS (EUROPE)**
- Development of a satellite remote sensing technique for the study of alpine glaciers p 34 A87-35311
- ALTIMETERS**
- Spectrasat instrument design using maximum heritage p 26 A87-38847
- ALTIMETRY**
- Applications of laser airborne telemetry at Institut Geographique National (IGN), France p 53 N87-24761
- AMAZON REGION (SOUTH AMERICA)**
- Trace gas exchanges and transports over the Amazonian rain forest p 12 A87-32196
- AMPLIFICATION**
- The effect of receiver amplifier non-linearity on ERS-1 synthetic aperture radar imagery p 52 N87-24755
- ANGULAR DISTRIBUTION**
- Modelling of atmospheric effects on the angular distribution of a backscattering peak [DE87-006060] p 41 N87-24014
- ANGULAR VELOCITY**
- Determination of the velocity of ocean gyres through Synthetic Aperture Radar p 22 A87-35314
- ANNUAL VARIATIONS**
- Remote-sensing method for determining monthly precipitation sums using Meteor-satellite data on the Atlantic Ocean p 21 A87-34447
- Seasonal and regional variations of active/passive microwave signatures of sea ice p 22 A87-35516
- Analysis of moderate and intense rainfall rates continuously recorded over half a century and influence on microwave communications planning and rain-rate data acquisition p 46 A87-36933
- Variations in the polarized leaf reflectance of Sorghum bicolor p 7 A87-38097
- Comparison of HCMM and GOES satellite temperatures and evaluation of surface statistics p 39 A87-38098
- Regional and seasonal variations of surface reflectance from satellite observations at 0.6 micron p 27 A87-40250

- The 1982-1983 El Nino Atlas Nimbus-7 microwave radiometer data [NASA-CR-180914] p 31 N87-22386
- Arctic Sea ice, 1973-1976 Satellite passive-microwave observations [NASA-SP-489] p 33 N87-24870
- ANOMALOUS TEMPERATURE ZONES**
- The impact of initial conditions and SST Anomalies on extended range predictions for the El Nino period ... sea surface temperature (SST) p 32 N87-23046
- ANTARCTIC REGIONS**
- West Antarctic ice streams draining into the Ross Ice Shelf Configuration and mass balance p 19 A87-31592
- Recurring polynyas over the Cosmonaut Sea and the Maud Rise p 23 A87-37563
- Enhanced LANDSAT images of Antarctica and planetary exploration p 50 N87-23558
- AQUIFERS**
- Satellite techniques for studying ice crusts and underground waters in the eastern Pamir p 35 A87-36106
- ARCTIC OCEAN**
- Coastal zone color scanner imagery of phytoplankton pigment distribution in Icelandic waters p 29 A87-42645
- An evaluation of the polar ice prediction system [AD-A178522] p 41 N87-23014
- ARCTIC REGIONS**
- Atmospheric remote sensing in arctic regions [AD-A179550] p 50 N87-23012
- Arctic Sea ice, 1973-1976 Satellite passive-microwave observations [NASA-SP-489] p 33 N87-24870
- ARIANE LAUNCH VEHICLE**
- Arianespace top performance benefits ESA p 57 N87-24493
- ARTIFICIAL INTELLIGENCE**
- Smart sensors: An overview and selected examples p 51 N87-24740
- ASTROMETRY**
- International Conference on Earth Rotation and the Terrestrial Reference Frame, Columbus, OH, July 31-Aug. 2, 1985, Proceedings. Volumes 1 & 2 p 15 A87-36126
- ATLANTIC OCEAN**
- Remote-sensing method for determining monthly precipitation sums using Meteor-satellite data on the Atlantic Ocean p 21 A87-34447
- Long waves in the equatorial Atlantic Ocean during 1983 p 23 A87-37564
- Quick look Atlantic Ocean rain maps for gale [NASA-CR-180511] p 30 N87-21533
- Tidal estimation in the Atlantic and Indian Oceans, 3 deg x 3 deg solution [NASA-TM-87812] p 30 N87-21534
- Possibilities of using artificial Earth satellite data for computing heat exchange between the ocean and atmosphere in Newfoundland energy-active zone during winter p 31 N87-21980
- An evaluation of the polar ice prediction system [AD-A178522] p 41 N87-23014
- ATMOSPHERIC ATTENUATION**
- Analysis of moderate and intense rainfall rates continuously recorded over half a century and influence on microwave communications planning and rain-rate data acquisition p 46 A87-36933
- A two-look technique for studying atmospheric effects in optical scanner data for the ocean p 26 A87-39178
- High resolution sea surface temperature field derived p 33 N87-24731
- ATMOSPHERIC BOUNDARY LAYER**
- Observations of intermittent cumulus convection in the boundary layer p 20 A87-32976
- Evaluation of a surface/vegetation parameterization using satellite measurements of surface temperature p 3 A87-33298
- Measurements of nitric oxide in the boundary layer and free troposphere over the Pacific Ocean p 21 A87-33431
- Free tropospheric and boundary layer measurements of NO over the central and eastern North Pacific Ocean p 21 A87-33432
- Optical properties of the marine atmospheric boundary layer - Aerosol profiles p 28 A87-42638
- ATMOSPHERIC CHEMISTRY**
- Operational overview of NASA GTE/CITE 1 airborne instrument intercomparisons - Carbon monoxide, nitric oxide, and hydroxyl instrumentation ... Global Tropospheric Experiment/Chemical Instrumentation Test and Evaluation p 45 A87-33426
- OH measurement near the intertropical convergence zone in the Pacific p 21 A87-33430
- Free tropospheric and boundary layer measurements of NO over the central and eastern North Pacific Ocean p 21 A87-33432

- Carbon monoxide measurements over the eastern Pacific during GTE/CITE 1 ... Chemical Instrumentation Test and Evaluation p 21 A87-33435
- ATMOSPHERIC CIRCULATION**
- Trace gas exchanges and transports over the Amazonian rain forest p 12 A87-32196
- Impact of satellite-based data on FGGE general circulation statistics p 44 A87-32985
- The observational objectives and the implementation of the Global Weather Experiment p 49 N87-21474
- ATMOSPHERIC COMPOSITION**
- Operational overview of NASA GTE/CITE 1 airborne instrument intercomparisons - Carbon monoxide, nitric oxide, and hydroxyl instrumentation ... Global Tropospheric Experiment/Chemical Instrumentation Test and Evaluation p 45 A87-33426
- Atmospheric environment monitoring system based on an earth-to-satellite Hadamard transform laser long-path absorption spectrometer - A proposal p 45 A87-35502
- The possibility of using satellite measurements of methane in the atmosphere to study the global-distribution characteristics of its sources p 13 A87-36125
- ATMOSPHERIC CORRECTION**
- The AVHRR/HIRS operational method for satellite based sea surface temperature determination [NOAA-TR-NESDIS-28] p 31 N87-22388
- An atmospheric correction algorithm for remote identification of non-Lambertian surfaces and its range of validity [DE87-006059] p 41 N87-24011
- High resolution sea surface temperature field derived p 33 N87-24731
- ATMOSPHERIC EFFECTS**
- Correction for atmospheric and topographic effects on the Landsat MSS data p 37 A87-32489
- Simulations of the GOES visible sensor to changing surface and atmospheric conditions p 47 A87-40756
- Photographic quality of color IR aerial photos as a function of atmospheric parameters p 42 N87-24799
- ATMOSPHERIC HEAT BUDGET**
- Convective heating and precipitation estimates for the tropical South Pacific during FGGE, 10-18 January 1979 p 21 A87-32982
- ATMOSPHERIC MODELS**
- The impact of initial conditions and SST Anomalies on extended range predictions for the El Nino period ... sea surface temperature (SST) p 32 N87-23046
- Modelling of atmospheric effects on the angular distribution of a backscattering peak [DE87-006060] p 41 N87-24014
- Ocean wind and wave model comparisons with GEOSAT (GEOSATellite) satellite data [AD-A178302] p 33 N87-24061
- ATMOSPHERIC MOISTURE**
- Balloon-borne infrared multichannel radiometer for remote sensing of high resolution low-level water vapor fields p 43 A87-32477
- The 1982-1983 El Nino Atlas Nimbus-7 microwave radiometer data [NASA-CR-180914] p 31 N87-22386
- ATMOSPHERIC OPTICS**
- Photographic quality of color IR aerial photos as a function of atmospheric parameters p 42 N87-24799
- ATMOSPHERIC PHYSICS**
- Atmospheric remote sensing in arctic regions [AD-A179550] p 50 N87-23012
- ATMOSPHERIC SCATTERING**
- Inversion of canopy reflectance models for estimation of vegetation parameters [NASA-CR-181059] p 12 N87-24737
- ATMOSPHERIC SOUNDING**
- Carbon monoxide measurements over the eastern Pacific during GTE/CITE 1 ... Chemical Instrumentation Test and Evaluation p 21 A87-33435
- Atmospheric environment monitoring system based on an earth-to-satellite Hadamard transform laser long-path absorption spectrometer - A proposal p 45 A87-35502
- Atmospheric remote sensing in arctic regions [AD-A179550] p 50 N87-23012
- ATMOSPHERIC TEMPERATURE**
- Observations of intermittent cumulus convection in the boundary layer p 20 A87-32976
- ATTENUATION COEFFICIENTS**
- The relationship between phytoplankton concentration and light attenuation in ocean waters p 29 A87-42642
- ATTITUDE (INCLINATION)**
- The effects of camera position and attitude data in aerial triangulation, a simulation study p 52 N87-24750
- AUSTRALIA**
- Habitat mapping by Landsat for aerial census of kangaroos p 2 A87-32094
- Australian utilization and research into remote sensing p 20 A87-32490

AUTOMATION

- Problems in the automation of map-compilation processes on the basis of remote-sensing data p 38 A87-35925

AVIONICS

- The integration of spectral and spatial analysis for land use classification [AD-A178703] p 14 N87-23015

AXES OF ROTATION

- Polar motion-induced gravity p 15 A87-36176

B**BACKSCATTERING**

- The relation of millimeter-wavelength backscatter to surface snow properties p 34 A87-35518
Radiometric correction of SAR images - A new correction algorithm p 40 A87-39184
Two-color short-pulse laser altimeter measurements of ocean surface backscatter p 27 A87-39462
Radar scene generation for tactical decision aids [NASA-CR-180234] p 40 N87-20449
NASA/MSFC large stretch press study [NASA-CR-180376] p 41 N87-20554
Modeling of atmospheric effects on the angular distribution of a backscattering peak [DE87-006060] p 41 N87-24014

BALLOON SOUNDING

- Exploration of geomagnetic field anomaly with balloon for geophysical research p 17 A87-32478

BALLOON-BORNE INSTRUMENTS

- Balloon-borne infrared multichannel radiometer for remote sensing of high resolution low-level water vapor fields p 43 A87-32477

BAND RATIOING

- The regression intersection method of adjusting image data for band ratioing p 45 A87-35306
A software defoliant for geological analysis of band ratios p 18 A87-39193

BANDWIDTH

- Data Compression System for video images p 46 A87-37421

BARLEY

- Influence of different nitrogen and irrigation treatments on the spectral reflectance of barley p 2 A87-32090

BAROCLINIC INSTABILITY

- Feedback between ice flow, barotropic flow, and baroclinic flow in the presence of bottom topography p 27 A87-40289

BAROTROPIC FLOW

- Feedback between ice flow, barotropic flow, and baroclinic flow in the presence of bottom topography p 27 A87-40289

BATHYMETERS

- Potential of laser remote sensing of oil below water surface [FOA-C-30435-3.1] p 30 N87-20659

BAYES THEOREM

- Landsat as an aid in evaluating the adequacy of a grain silo network p 7 A87-37282

BAYS (TOPOGRAPHIC FEATURES)

- Aircraft radiopositioning for airborne photography during hydrographic coastal surveys p 23 A87-36945

BIOMASS

- Forest biomass, canopy structure, and species composition relationships with multipolarization L-band synthetic aperture radar data p 4 A87-35121
Error analysis of leaf area estimates made from allometric regression models [NASA-TM-89220] p 11 N87-24010
New dimension analyses with error analysis for quaking aspen and black spruce [NASA-TM-89219] p 11 N87-24735
Inversion of canopy reflectance models for estimation of vegetation parameters [NASA-CR-181059] p 12 N87-24737

BIOPHYSICS

- Canopy reflectance, photosynthesis, and transpiration. II - The role of biophysics in the linearity of their interdependence p 6 A87-37278

BIOSPHERE

- Applied remote sensing --- Book p 45 A87-33122

BISTATIC REFLECTIVITY

- Active and passive remote sensing of ice [AD-A179461] p 32 N87-24009

BLACK AND WHITE PHOTOGRAPHY

- A comparison of optical bar, high-altitude, and black-and-white photography in land classification p 4 A87-35122

BORN APPROXIMATION

- Radar scene generation for tactical decision aids [NASA-CR-180234] p 40 N87-20449

BOUNDARY VALUE PROBLEMS

- Introduction of initial centers for the algorithm of clustering around mobile centers --- in multispectral image classification p 37 A87-35313
The impact of initial conditions and SST Anomalies on extended range predictions for the El Nino period --- sea surface temperature (SST) p 32 N87-23046

BRIGHTNESS

- Relation between precipitation and brightness of earth surface in the NOAA/GVIP data p 3 A87-32498

BRIGHTNESS DISTRIBUTION

- Phase portraits of vegetation development trajectories in a multidimensional spectral attribute space p 10 A87-41771

BRIGHTNESS TEMPERATURE

- Quantifying spatial and temporal variabilities of microwave brightness temperature over the U.S. Southern Great Plains p 5 A87-35309

C**CADAstral MAPPING**

- The VICOM system for digital image processing at the Institute of Cartography of Technical University, Hanover (West Germany) p 16 N87-22290

CALIBRATING

- Deriving surface albedo measurements from narrow band satellite data p 13 A87-39182
Impact of radiance variations on satellite sensor calibration p 47 A87-39457
Thoughts on a standard algorithm for camera calibration p 51 N87-24743
Applied formulae for calibration of aerial photogrammetric cameras p 51 N87-24744
Geometrical system calibration, especially for metric aerial cameras p 51 N87-24745
Radiometric calibration of the Shuttle Imaging Radar (SIR-C) system p 53 N87-24756
Proposed changes to the Canadian camera calibration report p 53 N87-24757
The role of government specifications in aerial photography p 57 N87-24780
Determination of spectral reflectance of crops during growth from calibrated multispectral small format aerial photography p 12 N87-24801
Image quality problems in practical aerial photography p 43 N87-24814

CALIFORNIA

- Radar as a complement to topographic maps for delineating marine terraces [PB87-154597] p 41 N87-24013

CAMERAS

- Thoughts on a standard algorithm for camera calibration p 51 N87-24743
Applied formulae for calibration of aerial photogrammetric cameras p 51 N87-24744
Geometrical system calibration, especially for metric aerial cameras p 51 N87-24745
The use of camera orientation data in photogrammetry: A review p 52 N87-24749
The effects of camera position and attitude data in aerial triangulation, a simulation study p 52 N87-24750
Proposed changes to the Canadian camera calibration report p 53 N87-24757
Wild AvioPhot (TM) RC20 aerial camera system: The other approach to image motion compensation in aerial photography p 54 N87-24782

CANADA

- On the relative accuracy of satellite and rain gauge rainfall measurements over middle latitudes during daylight hours p 34 A87-33295

CANADIAN SHIELD

- Shuttle Imaging Radar (SIR-B) investigations of the Canadian shield - Initial Report p 17 A87-31410
Spatial characterization of acid rain stress in Canadian Shield lakes [NASA-CR-180983] p 36 N87-24031
Spatial characterization of acid rain stress in Canadian Shield lakes [NASA-CR-180982] p 36 N87-24032

CANOPIES (VEGETATION)

- Estimation of canopy parameters of row planted vegetation canopies using reflectance data for only four view directions p 2 A87-32093
Forest biomass, canopy structure, and species composition relationships with multipolarization L-band synthetic aperture radar data p 4 A87-35121
Canopy reflectance, photosynthesis, and transpiration. II - The role of biophysics in the linearity of their interdependence p 6 A87-37278
Computation of diffuse sky irradiance from multidirectional radiance measurements p 6 A87-37279

- Inferring spectral reflectances of plant elements by simple inversion of bidirectional reflectance measurements p 7 A87-37281

Airborne remote sensing of forest biomes

- p 9 A87-40301

- Error analysis of leaf area estimates made from allometric regression models [NASA-TM-89220] p 11 N87-24010

- New dimension analyses with error analysis for quaking aspen and black spruce [NASA-TM-89219] p 11 N87-24735

- Inversion of canopy reflectance models for estimation of vegetation parameters [NASA-CR-181059] p 12 N87-24737

CARBON DIOXIDE

- A review of national and international activities on modeling the effects of increased CO2 concentrations on the simulation of regional crop production: A report on linkage between climate and crop models [DE87-005994] p 10 N87-22336
The impact of climate change from increased atmospheric carbon dioxide on American agriculture [DOE/NBB-0077] p 11 N87-23032

CARBON MONOXIDE

- Carbon monoxide measurements over the eastern Pacific during GTE/CITE 1 --- Chemical Instrumentation Test and Evaluation p 21 A87-33435

CELESTIAL GEODESY

- The determination of earth-rotation parameters from satellite laser ranging p 15 A87-34186
GINFEST - Geodetic intercomparison network for evaluating space techniques p 15 A87-36164
Creation of a global geodetic network using Mark III VLBI p 15 A87-36166
GPS-based geodesy in California, Mexico and the Caribbean p 16 A87-41386

CHANGE DETECTION

- Landcover change in Hiroshima during 1979/1984 detected by Landsat MSS and TM data p 12 A87-32494

CHARGE COUPLED DEVICES

- Aerial triangulation of CCD line-scanner images p 54 N87-24769
Modern CCD sensors and their applications in Earth observation and planetary missions p 55 N87-24813

CHLOROPHYLLS

- A two-look technique for studying atmospheric effects in optical scanner data for the ocean p 26 A87-39178
The relationship between phytoplankton concentration and light attenuation in ocean waters p 29 A87-42642
Remote sensing of chlorophyll concentrations in the northern Gulf of Mexico p 29 A87-42643
A model for the use of satellite remote sensing for the measurement of primary production in the ocean p 29 A87-42644
Sunlight induced 685 nm fluorescence imagery p 30 A87-42646

CHRONOLOGY

- LANDSAT-based lineament analysis, East Texas Basin, and structural history of the Sabine Uplift area, East Texas and North Louisiana [PB87-176327] p 19 N87-24043

CHUKCHI SEA

- Statistical description of the summertime ice edge in the Chukchi Sea, task 2 [DE87-001056] p 31 N87-22387

CITIES

- Polarization, land use type and intraurban location as variables in SAR mapping accuracy p 12 A87-32953
Comparison of Landsat MSS and TM data for urban land-use classification p 13 A87-35523
Testing the consistency for mapping urban vegetation with high-altitude aerial photographs and Landsat MSS data p 13 A87-37277
An assessment of Landsat MSS and TM data for urban and near-urban land-cover digital classification p 13 A87-37280
Urban land use separability as a function of radar polarization p 14 A87-39188
Towards an automatic identification of urban textures p 14 N87-24747

CLASSIFICATIONS

- Landsat classification of Argentina summer crops p 3 A87-32098
Comparison of Landsat MSS and TM data for urban land-use classification p 13 A87-35523
An assessment of Landsat MSS and TM data for urban and near-urban land-cover digital classification p 13 A87-37280

CLIMATE

- The impact of climate change from increased atmospheric carbon dioxide on American agriculture [DOE/NBB-0077] p 11 N87-23032

CLIMATOLOGY

- World-wide weather --- Book p 56 A87-33125

CLOUD COVER

The impact of climate change from increased atmospheric carbon dioxide on American agriculture [DOE/NBB-0077] p 11 N87-23032

CLOUD COVER

Remote-sensing method for determining monthly precipitation sums using Meteor-satellite data on the Atlantic Ocean p 21 A87-34447

Cloud-cover and precipitation patterns over the Republic of Guinea according to ground-based and satellite observations p 35 A87-36102

Reflectivity of earth's surface and clouds in ultraviolet from satellite observations p 47 A87-40768

CLOUD PHYSICS

Atmospheric remote sensing in arctic regions [AD-A179550] p 50 N87-23012

COAL

High resolution remote sensing of spatially and spectrally complex coal surface mines of central Pennsylvania - A comparison between simulated SPOT MSS and Landsat-5 thematic mapper p 18 A87-39468

COASTAL CURRENTS

DUCK '85 nearshore waves and currents experiment data summary report [AD A177419] p 31 N87-22382

COASTAL WATER

Remote-sensed tracers for hydrodynamic surface flow estimation p 26 A87-39176

A two-look technique for studying atmospheric effects in optical scanner data for the ocean p 26 A87-39178

Continental shelf processes affecting the oceanography of the South Atlantic Bight [DE87-005303] p 30 N87-20716

COASTAL ZONE COLOR SCANNER

The interaction of light with phytoplankton in the marine environment p 29 A87-42640

Remote sensing of chlorophyll concentrations in the northern Gulf of Mexico p 29 A87-42643

A model for the use of satellite remote sensing for the measurement of primary production in the ocean p 29 A87-42644

Coastal zone color scanner imagery of phytoplankton pigment distribution in Icelandic waters p 29 A87-42645

COASTS

Geochronological studies of strandlines of Saurashtra, India, detected by remote sensing techniques p 15 A87-35308

Remote sensing of coastal wetlands p 9 A87-40944

DUCK '85 nearshore waves and currents experiment data summary report [AD-A177419] p 31 N87-22382

Studies of the east Australian current off northern New South Wales [AD-A178461] p 32 N87-23103

Utilizing remote sensing of thematic mapper data to improve our understanding of estuarine processes and their influence on the productivity of estuarine-dependent fisheries [NASA-CR-180984] p 33 N87-24012

Radar as a complement to topographic maps for delineating marine terraces [PB87-154597] p 41 N87-24013

COLLOCATION

Reports on cartography and geodesy, series 1, number 96 [ISSN-0469-4236] p 16 N87-22286

COLOR INFRARED PHOTOGRAPHY

A comparison of optical bar, high-altitude, and black-and-white photography in land classification p 4 A87-35122

Comparison between digital and manual interpretation of high altitude aerial photographs p 48 A87-42257

Real-time crop assessment using color theory and satellite data p 10 N87-20619

Photographic quality of color IR aerial photos as a function of atmospheric parameters p 42 N87-24799

COLOR PHOTOGRAPHY

Spectrophotometric measurements on color aerial photographs p 55 N87-24798

COMMERCE

Remote sensing applications Commercial issues and opportunities for space station - SPOT p 57 N87-20626

COMMUNICATION SATELLITES

Anaspace top performance benefits ESA p 57 N87-24493

COMPUTATIONAL GRIDS

Tidal estimation in the Atlantic and Indian Oceans, 3 deg x 3 deg solution [NASA-TM-87812] p 30 N87-21534

COMPUTER AIDED MAPPING

Problems in the automation of map-compilation processes on the basis of remote-sensing data p 38 A87-35925

Mapping from space p 38 A87-36361

Reports on cartography and geodesy, series 1, number 97 [ISSN-0469-4236] p 16 N87-22286

The VICOM system for digital image processing at the Institute of Cartography of Technical University, Hanover (West Germany) p 16 N87-22290

COMPUTER GRAPHICS

Reports on cartography and geodesy, series 1, number 97 [ISSN-0469-4236] p 16 N87-22286

The VICOM system for digital image processing at the Institute of Cartography of Technical University, Hanover (West Germany) p 16 N87-22290

CHART A computer plotting package for the display of position-dependent marine data [PB87-148607] p 31 N87-22297

COMPUTER PROGRAMS

CHART A computer plotting package for the display of position-dependent marine data [PB87-148607] p 31 N87-22297

COMPUTER VISION

The integration of spectral and spatial analysis for land use classification [AD-A178703] p 14 N87-23015

Smart sensors An overview and selected examples p 51 N87-24740

COMPUTERIZED SIMULATION

Simulation software of synthetic aperture radar p 37 A87-32506

CONFERENCES

Workshop on Space Remote Sensing for Agricultural and Thematic Mapping, Budapest, Hungary, Apr. 18, 1986, Proceedings p 1 A87-32007

International Conference on Earth Rotation and the Terrestrial Reference Frame, Columbus, OH, July 31-Aug. 2, 1985, Proceedings, Volumes 1 & 2 p 15 A87-36126

Measuring ocean waves from space, Proceedings of the Symposium, Johns Hopkins University, Laurel, MD, Apr. 15-17, 1986 p 24 A87-36826

Ocean optics VIII, Proceedings of the Meeting, Orlando, FL, Mar. 31-Apr. 2, 1986 [SPIE-637] p 28 A87-42637

Proceedings of the European Symposium on Polar platform Opportunities and Instrumentation for Remote-Sensing (ESPOIR) [ESA-SP-266] p 48 N87-20621

Proceedings of the International Symposium on Progress in Imaging Sensors [ESA-SP-252] p 50 N87-24738

CONIFERS

New dimension analyses with error analysis for quaking aspen and black spruce [NASA-TM-89219] p 11 N87-24735

CONTINENTAL SHELVES

Continental shelf processes affecting the oceanography of the South Atlantic Bight [DE87-005303] p 30 N87-20716

CONVECTION CLOUDS

Observations of intermittent cumulus convection in the boundary layer p 20 A87-32976

The area-time-integral technique to estimate convective rain volumes over areas applied to satellite data - A preliminary investigation p 35 A87-40249

CONVECTIVE HEAT TRANSFER

Convective heating and precipitation estimates for the tropical South Pacific during FGGE, 10-18 January 1979 p 21 A87-32982

CONVERGENCE

Physical principles of image convergence in remote sensing p 40 A87-41925

COOLING

Satellite measurements of sea surface cooling during hurricane Gloria p 24 A87-37886

CORAL REEFS

Coral reef remote sensing applications p 20 A87-32951

COVARIANCE

A new covariance model for inertial gravimetry and gradiometry p 14 A87-31591

CRITERIA

Optical Transfer Function (OTF)-based quality criteria for aerial cameras and imaging systems p 51 N87-24742

CROP GROWTH

Remote sensing methods of yield forecasting p 2 A87-32009

Procedures for the description of agricultural crops and soils in optical and microwave remote sensing studies p 8 A87-39187

Phase portraits of vegetation development trajectories in a multidimensional spectral attribute space p 10 A87-41771

Foundations and applications of multispectral scanning in agriculture [NLR-MP-85015-U] p 10 N87-21408

A crop condition and crop yield estimation method based on NOAA/AVHRR satellite data p 10 N87-22280

A review of national and international activities on modeling the effects of increased CO2 concentrations on the simulation of regional crop production. A report on linkage between climate and crop models [DE87-005994] p 10 N87-22336

The impact of climate change from increased atmospheric carbon dioxide on American agriculture [DOE/NBB-0077] p 11 N87-23032

Determination of spectral reflectance of crops during growth from calibrated multispectral small format aerial photography p 12 N87-24801

CROP IDENTIFICATION

Signature-extendable technology - Global space-based crop recognition p 1 A87-31414

Workshop on Space Remote Sensing for Agricultural and Thematic Mapping, Budapest, Hungary, Apr. 18, 1986, Proceedings p 1 A87-32007

Identifying vegetable crops with Landsat Thematic Mapper data p 4 A87-35120

Some observations on crop profile modelling p 5 A87-35310

A comparison of supervised maximum likelihood and decision tree classification for crop cover estimation from multitemporal Landsat MSS data p 5 A87-35312

Landsat as an aid in evaluating the adequacy of a grain silo network p 7 A87-37282

Rice crop identification and area estimation using remotely-sensed data from Indian cropping patterns p 9 A87-41434

Real-time crop assessment using color theory and satellite data p 10 N87-20619

Foundations and applications of multispectral scanning in agriculture [NLR-MP-85015-U] p 10 N87-21408

CROP INVENTORIES

Landsat classification of Argentine summer crops p 3 A87-32098

CROP VIGOR

Real-time crop assessment using color theory and satellite data p 10 N87-20619

A crop condition and crop yield estimation method based on NOAA/AVHRR satellite data p 10 N87-22280

CRUSTAL FRACTURES

Quick-look guide to the crustal dynamics project's data information system [NASA-TM-87818] p 16 N87-23018

CUMULUS CLOUDS

Observations of intermittent cumulus convection in the boundary layer p 20 A87-32976

Optical properties of the marine atmospheric boundary layer - Aerosol profiles p 28 A87-42638

D

DAMAGE ASSESSMENT

Monsoon flood boundary delineation and damage assessment using space borne imaging radar and Landsat data p 35 A87-39467

Spatial characterization of acid rain stress in Canadian Shield lakes [NASA-CR-180982] p 36 N87-24032

DATA ACQUISITION

Analysis of moderate and intense rainfall rates continuously recorded over half a century and influence on microwave communications planning and rain-rate data acquisition p 46 A87-36933

Report of the workshop on Assimilation of Satellite Wind and Wave Data in Numerical Weather and Wave Prediction Models [WCP-122] p 49 N87-21521

A modular and versatile acquisition, recording and preprocessing system for airborne remote sensing p 52 N87-24751

Digital data acquisition for close-range photogrammetry p 54 N87-24785

Remote Sensing Information Sciences Research Group Santa Barbara Information Sciences Research Group, year 4 [NASA-CR-181073] p 43 N87-24817

DATABASE MANAGEMENT SYSTEMS

The Geomulti database management system p 39 A87-37802

Reports on cartography and geodesy, series 1, number 97 [ISSN-0469-4236] p 16 N87-22286

The VICOM system for digital image processing at the Institute of Cartography of Technical University, Hanover (West Germany) p 16 N87-22290

Problems in merging Earth sensing satellite data sets [NASA-TM-87820] p 50 N87-22457

Quick-look guide to the crustal dynamics project's data information system [NASA-TM-87818] p 16 N87-23018

DATA COMPRESSION

- Data Compression System for video images
p 46 A87-37421

DATA PROCESSING

- Remote sensing - Handling the data
p 38 A87-36359
- What, where, when, why? Extracting information from remote sensing data
p 46 A87-37055
- Montane vegetation stratification through digital processing of Landsat MSS data
p 9 A87-40302
- Report of the workshop on Assimilation of Satellite Wind and Wave Data in Numerical Weather and Wave Prediction Models
[WCP-122] p 49 A87-21521

DATA RETRIEVAL

- Applications of satellite microwave radiometry in Finland
p 44 A87-32952

DATA SIMULATION

- High resolution remote sensing of spatially and spectrally complex coal surface mines of central Pennsylvania - A comparison between simulated SPOT MSS and Landsat-5 thematic mapper
p 18 A87-39468
- Simulations of the GOES visible sensor to changing surface and atmospheric conditions
p 47 A87-40756

DATA SMOOTHING

- Bi-harmonic spline interpolation of GEOS-3 and Seasat altimeter data
p 20 A87-32770

DECIDUOUS TREES

- Error analysis of leaf area estimates made from allometric regression models
[NASA-TM-89220] p 11 A87-24010
- New dimension analyses with error analysis for quaking aspen and black spruce
[NASA-TM-89219] p 11 A87-24735

DECISION THEORY

- A comparison of supervised maximum likelihood and decision tree classification for crop cover estimation from multitemporal Landsat MSS data
p 5 A87-35312

DEFORESTATION

- Relation between precipitation and brightness of earth surface in the NOAA/GVIP data
p 3 A87-32498
- Deforestation in the tropics - New measurements in the Amazon Basin using Landsat and NOAA advanced very high resolution radiometer imagery
p 4 A87-33441

DESERTIFICATION

- Relation between precipitation and brightness of earth surface in the NOAA/GVIP data
p 3 A87-32498
- Reconnaissance of vegetal formations in a Guinean forest sector by means of Landsat images
p 6 A87-36946

DESERTS

- Surface bidirectional reflectance properties of two southwestern Arizona deserts for wavelengths between 0.4 and 2.2 micrometers
[NASA-TP-2643] p 49 A87-22281

DEVELOPING NATIONS

- Intelsat's small earth stations - Impact on the developing world
p 56 A87-34799

DIFFUSE RADIATION

- Computation of diffuse sky irradiance from multidirectional radiance measurements
p 6 A87-37279

DIGITAL DATA

- Combining panchromatic and multispectral imagery from dual resolution satellite instruments
p 38 A87-37276
- Measurements on digitized hardcopy images
p 39 A87-37290
- Montane vegetation stratification through digital processing of Landsat MSS data
p 9 A87-40302

DIGITAL RADAR SYSTEMS

- Simulation software of synthetic aperture radar
p 37 A87-32506

DIGITAL SYSTEMS

- Reports on cartography and geodesy, series 1, number 97
[ISSN-0469-4236] p 16 A87-22286
- The stereo pushbroom scanner system Digital Photogrammetry System (DPS) and its accuracy
p 53 A87-24768

DIGITAL TECHNIQUES

- MIDAS - A new image-processing system for remote sensing
p 37 A87-35183
- Merging multiresolution SPOT HRV and Landsat TM data
p 38 A87-37287
- Comparison between digital and manual interpretation of high altitude aerial photographs
p 48 A87-42257
- Optical and digital SAR processing techniques: A statistical comparison of accuracy using SEASAT imagery
p 42 A87-24753
- Digital data acquisition for close-range photogrammetry
p 54 A87-24785

DIRECTIVITY

- Some approaches for comparing remote and in-situ estimates of directional wave spectra
p 24 A87-38835

- The microwave measurement of ocean-wave directional spectra
p 24 A87-38836
- Surface bidirectional reflectance properties of two southwestern Arizona deserts for wavelengths between 0.4 and 2.2 micrometers
[NASA-TP-2643] p 49 A87-22281

DISTANCE MEASURING EQUIPMENT

- Reports on cartography and geodesy, series 1, number 96
[ISSN-0469-4236] p 16 A87-22282

DIURNAL VARIATIONS

- An evaluation of satellite-based insolation estimates for Ohio
p 34 A87-33297

DMSP SATELLITES

- United States remote sensing satellites (RSSs) past, present, and future
p 56 A87-32502

DOPPLER RADAR

- Airborne microwave Doppler measurements of ocean wave directional spectra
p 26 A87-39180

DUNES

- Landsat image enhancement study of possible submerged sand-dunes in the Arabian Gulf
p 22 A87-35315

DYNAMIC CHARACTERISTICS

- Optical dynamics experiment (ODEX) data report R/V acacia expedition 10 October-17 November 1982. Volume 2: Particle size distributions. Volume 6: Scalar spectral-radiometer data
[AD-A178535] p 32 A87-23104

DYNAMIC MODELS

- Use of satellite altimetry for ocean monitoring
p 23 A87-36101

DYNAMICAL SYSTEMS

- Quick-look guide to the crustal dynamics project's data information system
[NASA-TM-87818] p 16 A87-23018

E**EARTH ALBEDO**

- Deriving surface albedo measurements from narrow band satellite data
p 13 A87-39182
- Satellite estimation of a solar irradiance at the surface of the earth and of surface albedo using a physical model applied to Meteosat data
p 47 A87-40246

EARTH ATMOSPHERE

- Applied remote sensing - Book
p 45 A87-33122
- Modelling of atmospheric effects on the angular distribution of a backscattering peak
[DE87-096060] p 41 A87-24014

EARTH CORE

- Global images of the earth's interior
p 15 A87-37918

EARTH CRUST

- Global images of the earth's interior
p 15 A87-37918

EARTH OBSERVATIONS (FROM SPACE)

- Marine Observation Satellite-1 (MOS-1)
p 20 A87-32499
- United States remote sensing satellites (RSSs) past, present, and future
p 56 A87-32502
- Applied remote sensing - Book
p 45 A87-33122
- Derivation of a fast algorithm to account for distortions due to terrain in earth-viewing satellite sensor images
p 38 A87-35524
- Measuring ocean waves from space: Proceedings of the Symposium, Johns Hopkins University, Laurel, MD, Apr. 15-17, 1986
p 24 A87-38826
- Spaceborne imaging radar research in the 1990s - An overview
p 46 A87-38837
- Space remote sensors
p 47 A87-40379
- Polarized views of the earth from orbital altitude
p 48 A87-42639

- Proceedings of the European Symposium on Polar platform Opportunities and Instrumentation for Remote-Sensing (ESPOIR)
[ESA-SP-266] p 48 A87-20621

- The Earth observation activities of the European Space Agency and the use of the polar platform of the International Space Station
p 49 A87-20622
- Land panel report - International Space Station
p 49 A87-20634

- Ocean-ice panel report - International Space Station
p 30 A87-20635

- Proceedings of the International Symposium on Progress in Imaging Sensors
[ESA-SP-252] p 50 A87-24738

- Earth surface sensing in the '90's
p 51 A87-24739
- Smart sensors: An overview and selected examples
p 51 A87-24740

- Application of Global Positioning System (GPS) receivers for Earth observation
p 53 A87-24763

- Definition of a thermal infrared pushbroom imager for Earth observation
p 53 A87-24765

- The production of photographs of the Earth's surface taken from satellites and their application in map production and map revision
p 55 A87-24788

- Earth Resources Satellite (ERS-1) project in Japan
p 57 A87-24797

- Earth observation experiments on the German Spacelab mission D2
p 55 A87-24811

- The Monocular Electro-Optical Stereo Scanner (MEOSS) satellite experiment
p 55 A87-24812

- Modern CCD sensors and their applications in Earth observation and planetary missions
p 55 A87-24813

- The Modular Optoelectronic Multispectral Scanner (MOMS) program of the Bundesministerium fuer Forschung und Technologie (BMFT). Milestones in the development of an operational Earth Observation system
p 55 A87-24815

EARTH OBSERVING SYSTEM (EOS)

- Problems in merging Earth sensing satellite data sets [NASA-TM-87820] p 50 A87-22457

- Remote Sensing Information Sciences Research Group Santa Barbara Information Sciences Research Group, year 4
[NASA-CR-181073] p 43 A87-24817

EARTH PLANETARY STRUCTURE

- Exploration of geomagnetic field anomaly with balloon for geophysical research
p 17 A87-32478

EARTH RESOURCES

- The Netherlands-Indonesian remote-sensing satellite TERS
p 43 A87-32210
- Indian remote sensing programme
p 56 A87-32955
- Statistical evaluation of forest characteristics from aerial and space photographs
p 5 A87-36109
- Aerial and space investigations of soils and vegetation - Russian book
p 6 A87-36579
- The Geomulti database management system
p 39 A87-37802

- The application of remote sensing techniques in China
p 57 A87-41435

- Land panel report - International Space Station
p 49 A87-20634

- Earth Resources Satellite (ERS-1) project in Japan
p 57 A87-24797

EARTH ROTATION

- Earth rotation, station coordinates and orbit determination from satellite laser ranging
p 43 A87-32349

- The determination of earth-rotation parameters from satellite laser ranging
p 15 A87-34186

- International Conference on Earth Rotation and the Terrestrial Reference Frame, Columbus, OH, Jul. 31-Aug. 2, 1985, Proceedings. Volumes 1 & 2
p 15 A87-36126

- Polar motion-induced gravity
p 15 A87-36176

EARTH SURFACE

- Estimation of roughness of the earth's surface using Landsat MSS data on the assumption of reciprocity on light scattering
p 12 A87-32493
- Polar motion-induced gravity
p 15 A87-36176
- Mapping from space
p 38 A87-36361
- Computation of diffuse sky irradiance from multidirectional radiance measurements
p 6 A87-37279

- Temporal observations of surface soil moisture using a passive microwave sensor
p 7 A87-38094

- Comparison of HCMM and GOES satellite temperatures and evaluation of surface statistics
p 39 A87-38098

- Surface models including direct cross-radiation - A simple model of furrowed surfaces
p 40 A87-39189

- Thematic Mapper bandpass solar exoatmospheric irradiances
p 40 A87-39192

- Satellite estimation of a solar irradiance at the surface of the earth and of surface albedo using a physical model applied to Meteosat data
p 47 A87-40246

- Simulations of the GOES visible sensor to changing surface and atmospheric conditions
p 47 A87-40756

- Reflectivity of earth's surface and clouds in ultraviolet from satellite observations
p 47 A87-40768

- Satellite sensing of aerosol absorption
p 47 A87-40770

- Physical principles of image convergence in remote sensing
p 40 A87-41925

- Polarized views of the earth from orbital altitude
p 48 A87-42639

- Earth surface sensing in the '90's
p 51 A87-24739

- Remote Sensing Information Sciences Research Group Santa Barbara Information Sciences Research Group, year 4
[NASA-CR-181073] p 43 A87-24817

EARTH TERMINALS

- Intelsat's small earth stations - Impact on the developing world
p 56 A87-34799

EARTH TIDES

- Tidal estimation in the Atlantic and Indian Oceans, 3 deg x 3 deg solution
[NASA-TM-87812] p 30 A87-21534

EARTHNET

AVHRR data services in Europe - The Earthnet approach p 39 A87-37922

ECOLOGY

Spectral classification of Landsat-5 Thematic Mapper data p 37 A87-32488
Ten year change in forest succession and composition measured by remote sensing [NASA-CR-180948] p 11 N87-24736

ECONOMIC IMPACT

The impact of climate change from increased atmospheric carbon dioxide on American agriculture [DOE/NBB-0077] p 11 N87-23032

ECONOMY

Antarespace top performance benefits ESA p 57 N87-24493

ECOSYSTEMS

Spatial characterization of acid rain stress in Canadian Shield lakes [NASA-CR-180982] p 36 N87-24032

EDGES

Studies of the east Australian current off northern New South Wales [AD-A178461] p 32 N87-23103

EL NINO

A technique to estimate the ocean surface energy flux using VAS multispectral data p 30 N87-20710
Measurement and detection of precipitation. Satellite methods in the visible and the infrared p 36 N87-22364

The 1982-1983 El Nino Atlas: Nimbus-7 microwave radiometer data [NASA-CR-180914] p 31 N87-22386
The impact of initial conditions and SST Anomalies on extended range predictions for the El Nino period - sea surface temperature (SST) p 32 N87-23046

ELECTRO-OPTICAL PHOTOGRAPHY

Investigation of simulated Monocular Electro-Optical Stereo Scanner (MEOSS)-imagery for sensor navigation and terrain derivation p 54 N87-24771
Earth observation experiments on the German Spacelab mission D2 p 55 N87-24811
The Monocular Electro-Optical Stereo Scanner (MEOSS) satellite experiment p 55 N87-24812
The Modular Optoelectronic Multispectral Scanner (MOMS) program of the Bundesministerium fuer Forschung und Technologie (BMFT). Milestones in the development of an operational Earth Observation system p 55 N87-24815

ELECTRO-OPTICS

The stereo pushbroom scanner system Digital Photogrammetry System (DPS) and its accuracy p 53 N87-24768

ELEVATION

A study of elevation measurement using LFC photograph - Large Format Camera p 43 A87-32491

EMISSIONIVITY

Measurement of the surface emissivity of turbid waters p 19 A87-32097
Salinity effects on the microwave emission of soils p 5 A87-35520

ENERGY TRANSFER

Possibilities of using artificial Earth satellite data for computing heat exchange between the ocean and atmosphere in Newfoundland energy-active zone during winter p 31 N87-21980

ENVIRONMENT POLLUTION

Continental shelf processes affecting the oceanography of the South Atlantic Bight [DE87-005303] p 30 N87-20716

ENVIRONMENTAL PROTECTION

Environmental protection from space p 13 A87-36363

ENVIRONMENTAL MONITORING

Remote sensing research in global agricultural productivity p 2 A87-32008
The Netherlands-Indonesian remote-sensing satellite TERS p 43 A87-32210
The possibility of using satellite measurements of methane in the atmosphere to study the global-distribution characteristics of its sources p 13 A87-36125
Strategies and technologies for monitoring the environment p 14 A87-39593

ENVIRONMENTAL SURVEYS

Spectral classification of Landsat-5 Thematic Mapper data p 37 A87-32488

EPIDEMIOLOGY

Detection of Rift Valley fever viral activity in Kenya by satellite remote sensing imagery p 7 A87-37827

EQUATORIAL REGIONS

Long waves in the equatorial Atlantic Ocean during 1983 p 23 A87-37564

ERROR ANALYSIS

Polarization, land use type and intraurban location as variables in SAR mapping accuracy p 12 A87-32953

A software defoliant for geological analysis of band ratios p 18 A87-39193

Error analysis of leaf area estimates made from allometric regression models [NASA-TM-89220] p 11 N87-24010

New dimension analyses with error analysis for quaking aspen and black spruce [NASA-TM-89219] p 11 N87-24735

ERRORS

Simulation of wind gradient errors in NROSS (Navy Remote Ocean Sensing System) radar scatterometer data in a simplified geometry [AD-A175754] p 49 N87-20642

Radial orbit error reduction and sea surface topography determination using satellite altimetry [NASA-CR-180570] p 33 N87-24816

ERS-1 (ESA SATELLITE)

Earth resources satellite-1 (ERS-1) p 44 A87-32501
The effect of receiver amplifier non-linearity on ERS-1 synthetic aperture radar imagery p 52 N87-24755
The first ESA remote sensing satellite (status and outlook) p 57 N87-24777

ESTIMATES

A crop condition and crop yield estimation method based on NOAA/VHRR satellite data p 10 N87-22280

EUROPEAN SPACE AGENCY

The Earth observation activities of the European Space Agency and the use of the polar platform of the International Space Station p 49 N87-20622

EUROPEAN SPACE PROGRAMS

The Earth observation activities of the European Space Agency and the use of the polar platform of the International Space Station p 49 N87-20622
European utilization aspects studies - space stations p 49 N87-20624

EVALUATION

An evaluation of the polar ice prediction system [AD-A178522] p 41 N87-23014

EVAPOTRANSPIRATION

Concerning the relationship between evapotranspiration and soil moisture p 8 A87-40244

EXPERIMENT DESIGN

Balloon-borne infrared multichannel radiometer for remote sensing of high resolution low-level water vapor fields p 43 A87-32477
Optimization of a program of experiments in connection with the operational planning of studies carried out with a spacecraft p 56 A87-34208
The observational objectives and the implementation of the Global Weather Experiment p 49 N87-21474

EXPERT SYSTEMS

An expert system for labeling segments in forward looking infrared (FLIR) imagery p 40 A87-42628

EXPOSURE

Exposure test with high resolution films from high altitude p 54 N87-24775

F

FARM CROPS

Signature-extendable technology - Global space-based crop recognition p 1 A87-31414
Workshop on Space Remote Sensing for Agricultural and Thematic Mapping, Budapest, Hungary, Apr. 18, 1986. Proceedings p 1 A87-32007
Remote sensing research in global agricultural productivity p 2 A87-32008
Remote sensing methods of yield forecasting p 2 A87-32009
Evaluation of a surface/vegetation parameterization using satellite measurements of surface temperature p 3 A87-33298
Determination of spectral reflectance of crops during growth from calibrated multispectral small format aerial photography p 12 N87-24801

FARMLANDS

Some observations on crop profile modelling p 5 A87-35310

FINLAND

Applications of satellite microwave radiometry in Finland p 44 A87-32952

FLIGHT TESTS

The Tethered Satellite System as a new remote sensing platform p 46 A87-39183

FLIR DETECTORS

An expert system for labeling segments in forward looking infrared (FLIR) imagery p 40 A87-42628

FLOOD DAMAGE

Monsoon flood boundary delineation and damage assessment using space borne imaging radar and Landsat data p 35 A87-39467

FLOW DISTRIBUTION

Remotely-sensed tracers for hydrodynamic surface flow estimation p 26 A87-39176

Continental shelf processes affecting the oceanography of the South Atlantic Bight [DE87-005303] p 30 N87-20716

FLOW GEOMETRY

West Antarctic ice streams draining into the Ross Ice Shelf Configuration and mass balance p 19 A87-31592

FLUORESCENCE

Sunlight induced 685 nm fluorescence imagery p 30 A87-42646
Advanced imaging spectrometer for ocean color/fluorescence measurements and further applications p 33 N87-24766

FLUX DENSITY

A technique to estimate the ocean surface energy flux using VAS multispectral data p 30 N87-20710

FOLIAGE

Error analysis of leaf area estimates made from allometric regression models [NASA-TM-89220] p 11 N87-24010

FORECASTING

An evaluation of the polar ice prediction system [AD-A178522] p 41 N87-23014

FOREST FIRE DETECTION

Satellite detection of tropical burning in Brazil p 8 A87-39191

FOREST MANAGEMENT

Nadir looking airborne radar and possible applications to forestry p 7 A87-38095
Ten year change in forest succession and composition measured by remote sensing [NASA-CR-180948] p 11 N87-24736

FORESTS

Multipolarization SAR data for surface feature delineation and forest vegetation characterization p 1 A87-31411
Continental land cover assessment using Landsat MSS data p 3 A87-32095
Forest biomass, canopy structure, and species composition relationships with multipolarization L-band synthetic aperture radar data p 4 A87-35121
A comparison of optical bar, high-altitude, and black-and-white photography in land classification p 4 A87-35122
Statistical evaluation of forest characteristics from aerial and space photographs p 5 A87-36109
Reconnaissance of vegetal formations in a Guinean forest sector by means of Landsat images p 6 A87-36946

Airborne remote sensing of forest biomes p 9 A87-40301

Evaluation of the airborne imaging spectrometer for remote sensing of forest stand conditions [NASA-CR-180918] p 10 N87-22296

Error analysis of leaf area estimates made from allometric regression models [NASA-TM-89220] p 11 N87-24010

Measured radar return at the near vertical from forested terrains [DE87-009384] p 11 N87-24593

Earth science research [NASA-CR-180512] p 11 N87-24733

New dimension analyses with error analysis for quaking aspen and black spruce [NASA-TM-89219] p 11 N87-24735

Ten year change in forest succession and composition measured by remote sensing [NASA-CR-180948] p 11 N87-24736

FREE ATMOSPHERE

Measurements of nitric oxide in the boundary layer and free troposphere over the Pacific Ocean p 21 A87-33431

FRENCH SPACE PROGRAMS

The French Space Oceanography Program p 20 A87-32503

FREQUENCY MODULATION

Multilook images of ocean waves by synthetic aperture radars p 28 A87-41068

G

GAS EXCHANGE

Trace gas exchanges and transports over the Amazonian rain forest p 12 A87-32196

GAS TRANSPORT

Trace gas exchanges and transports over the Amazonian rain forest p 12 A87-32196

GAS-LIQUID INTERACTIONS

Wind and nadir angle effects on airborne lidar water 'surface' returns p 29 A87-42641

GEOCHRONOLOGY

Geochronological studies of strandlines of Saurashtra, India, detected by remote sensing techniques p 15 A87-35308

H

GEODESY

- Report on the Special Program 78 satellite geodesy of the Technical University of Munich
[ASTRON-GEODAET-ARB-48] p 16 N87-20618
- Reports on cartography and geodesy, series 1, number 96
[ISSN-0469-4236] p 16 N87-22282
- Reports on cartography and geodesy, series 1, number 97
[ISSN-0469-4236] p 16 N87-22286

GEODETTIC COORDINATES

- Investigation of tectonic deformations using global satellite laser ranging data p 14 A87-33375
- Report on the Special Program 78 satellite geodesy of the Technical University of Munich
[ASTRON-GEODAET-ARB-48] p 16 N87-20618

GEODETTIC SATELLITES

- The Geosat altimeter mission - A milestone in satellite oceanography p 27 A87-40281
- Using the Global Positioning System (GPS) for high precision geodetic surveys - Highlights and problem areas p 16 A87-41383

GEODETTIC SURVEYS

- Investigation of tectonic deformations using global satellite laser ranging data p 14 A87-33375
- GINFEST - Geodetic intercomparison network for evaluating space techniques p 15 A87-36164
- Creation of a global geodetic network using Mark III VLBI p 15 A87-36166
- Using the Global Positioning System (GPS) for high precision geodetic surveys - Highlights and problem areas p 16 A87-41383
- Altitude measurements for the determination of the Earth's gravity field
[NASA-CR-180520] p 17 N87-23033

GEODYNAMICS

- Global images of the earth's interior p 15 A87-37918

GEOGRAPHIC INFORMATION SYSTEMS

- Preliminary report on the development of marine geographic information systems p 23 A87-37056
- The Geomulti database management system p 39 A87-37802

GEOIDS

- Altitude measurements for the determination of the Earth's gravity field
[NASA-CR-180520] p 17 N87-23033
- Radial orbit error reduction and sea surface topography determination using satellite altimetry
[NASA-CR-180570] p 33 N87-24816

GEOLOGICAL FAULTS

- The geostructural characteristics of the rift zone on the Lambert glacier (Antarctica) according to space images p 18 A87-36105
- Fault patterns by space remote sensing and the rotation of western Oregon during Cenozoic times p 18 A87-36525
- LANDSAT-based lineament analysis, East Texas Basin, and structural history of the Sabine Uplift area, East Texas and North Louisiana
[PB87-176327] p 19 N87-24043

GEOLOGICAL SURVEYS

- Shuttle Imaging Radar (SIR-B) investigations of the Canadian shield - Initial Report p 17 A87-31410
- The geometry of the intersections of tectonic structures detected on satellite images p 17 A87-36104
- A software defoliant for geological analysis of band ratios p 18 A87-39193
- Spacelab data - A new contribution for structural interpretations of remotely sensed data in geology p 18 A87-39790
- Radar as a complement to topographic maps for delineating marine terraces
[PB87-154597] p 41 N87-24013

GEOMAGNETISM

- Exploration of geomagnetic field anomaly with balloon for geophysical research p 17 A87-32478

GEOMETRIC ACCURACY

- Introduction of geometric information to radar image data p 42 N87-24754

GEOMETRIC RECTIFICATION (IMAGERY)

- Derivation of a fast algorithm to account for distortions due to terrain in earth-viewing satellite sensor images p 38 A87-35524
- Stereoscopic line scan imaging and satellite control
[DGLR PAPER 86-106] p 38 A87-36757
- Multisatellite data processing p 39 A87-37803
- Rectification of terrain induced distortions in radar imagery p 48 A87-42254
- Aerial triangulation of CCD line-scanner images p 54 N87-24769

GEOMETRICAL OPTICS

- Geometrical system calibration, especially for metric aerial cameras p 51 N87-24745

GEOMORPHOLOGY

- Geochronological studies of strandlines of Saurashtra, India, detected by remote sensing techniques p 15 A87-35308
- A soil map through Landsat satellite imagery in a part of the Auranga catchment in the Ranchi and Palamou districts of Bihar, India p 9 A87-41428

GEOPOTENTIAL

- A new covariance model for inertial gravimetry and gradiometry p 14 A87-31591

GLACIERS

- Development of a satellite remote sensing technique for the study of alpine glaciers p 34 A87-35311
- The geostructural characteristics of the rift zone on the Lambert glacier (Antarctica) according to space images p 18 A87-36105

GLOBAL ATMOSPHERIC RESEARCH PROGRAM

- Convective heating and precipitation estimates for the tropical South Pacific during FGGE, 10-18 January 1979 p 21 A87-32982
- Impact of satellite-based data on FGGE general circulation statistics p 44 A87-32985
- The observational objectives and the implementation of the Global Weather Experiment p 49 N87-21474
- Remotely sensed sea surface temperature for the Alpine Experiment (ALPEX) --- AVHRR-2 data p 30 N87-21497

GLOBAL POSITIONING SYSTEM

- Aerotriangulation without ground control p 46 A87-37289
- GPS-based geodesy in California, Mexico and the Caribbean p 16 A87-41380
- Using the Global Positioning System (GPS) for high precision geodetic surveys - Highlights and problem areas p 16 A87-41383
- Application of Global Positioning System (GPS) receivers for Earth observation p 53 N87-24763

GOES SATELLITES

- Determining rainfall intensity and type from GOES imagery in the midlatitudes p 34 A87-32092
- Soil moisture estimation using GOES-VISSR infrared data - A case study with a simple statistical method p 8 A87-40248
- Simulations of the GOES visible sensor to changing surface and atmospheric conditions p 47 A87-40756

GOVERNMENT/INDUSTRY RELATIONS

- The role of government specifications in aerial photography p 57 N87-24780

GRASSLANDS

- Reflectance characteristics and its application in the classification of Nigerian Savanna soils p 3 A87-32954
- Some observations on crop profile modelling p 5 A87-35310

GRAVIMETRY

- A new covariance model for inertial gravimetry and gradiometry p 14 A87-31591

GRAVITATIONAL FIELDS

- Altitude measurements for the determination of the Earth's gravity field
[NASA-CR-180520] p 17 N87-23033

GRAVITY ANOMALIES

- Polar motion-induced gravity p 15 A87-36176

GRAVITY GRADIOMETERS

- A new covariance model for inertial gravimetry and gradiometry p 14 A87-31591

GRAVITY WAVES

- The propagation of short surface waves on longer gravity waves p 28 A87-40835

GREENLAND

- An evaluation of the polar ice prediction system
[AD-A178522] p 41 N87-23014

GROUND STATIONS

- GINFEST - Geodetic intercomparison network for evaluating space techniques p 15 A87-36164
- Creation of a global geodetic network using Mark III VLBI p 15 A87-36166

GROUND TRUTH

- Operational overview of NASA GTE/CITE 1 airborne instrument intercomparisons - Carbon monoxide, nitric oxide, and hydroxyl instrumentation --- Global Tropospheric Experiment/Chemical Instrumentation Test and Evaluation p 45 A87-33426
- Cloud-cover and precipitation patterns over the Republic of Guinea according to ground-based and satellite observations p 35 A87-36102
- Earth science research
[NASA-CR-180512] p 11 N87-24733

GROUND WATER

- Satellite techniques for studying ice crusts and underground waters in the eastern Pamir p 35 A87-36106

GYRES

- Determination of the velocity of ocean gyres through Synthetic Aperture Radar p 22 A87-35314

HABITATS

- Habitat mapping by Landsat for aerial census of kangaroos p 2 A87-32094

HARMONIC FUNCTIONS

- Biharmonic spline interpolation of GEOS-3 and Seasat altimeter data p 20 A87-32770

HAZE

- Satellite sensing of aerosol absorption p 47 A87-40770

HEAT CAPACITY MAPPING MISSION

- Comparison of HCMM and GOES satellite temperatures and evaluation of surface statistics p 39 A87-38098

HEAT FLUX

- A technique to estimate the ocean surface energy flux using VAS multispectral data p 30 N87-20710

HEAT TRANSFER

- Possibilities of using artificial Earth satellite data for computing heat exchange between the ocean and atmosphere in Newfoundland energy-active zone during winter p 31 N87-21980

HELICOPTERS

- Measured radar return at the near vertical from forested terrains
[DE87-009384] p 11 N87-24593

HIGH ALTITUDE

- Comparison between digital and manual interpretation of high altitude aerial photographs p 48 A87-42257

HIGH ALTITUDE TESTS

- Exposure test with high resolution films from high altitude p 54 N87-24775

HIGH RESOLUTION

- Exposure test with high resolution films from high altitude p 54 N87-24775
- Very high resolution aerial films p 54 N87-24776

HISTOGRAMS

- Introduction of initial centers for the algorithm of clustering around mobile centers --- in multispectral image classification p 37 A87-35313

HORIZON SCANNERS

- Infrared Earth horizon sensor concepts in various spectral bands p 52 N87-24752

HURRICANES

- Satellite measurements of sea surface cooling during hurricane Gloria p 24 A87-37886
- The age and source of ocean swell observed in Hurricane Josephine p 25 A87-38843

HYDROGRAPHY

- Aircraft radiopositioning for airborne photography during hydrographic coastal surveys p 23 A87-36945
- Optical dynamics experiment (ODEX) data report R/V acania expedition 10 October-17 November 1982. Volume 2: Particle size distributions. Volume 6: Scalar spectral-radiometer data
[AD-A178535] p 32 N87-23104

HYDROLOGY

- Surface manifestations of hydrophysical processes in the Strait of Gibraltar according to 'Salyut-6' photographs p 35 A87-36103
- Satellite techniques for studying ice crusts and underground waters in the eastern Pamir p 35 A87-36106
- Remote sensing applications in hydrology p 35 A87-40308
- Recent research in snow hydrology p 35 A87-40309
- Application of Modular Optoelectronic Multispectral Scanner (MOMS) data to hydrology and vegetation studies
Test site: Pantanal Region (Brazil/Paraguay) p 52 N87-24748

HYDROXYL RADICALS

- OH measurement near the intertropical convergence zone in the Pacific p 21 A87-33430

ICE ENVIRONMENTS

- An evaluation of the polar ice prediction system
[AD-A178522] p 41 N87-23014

ICE FORMATION

- An evaluation of the polar ice prediction system
[AD-A178522] p 41 N87-23014

ICE MAPPING

- Remote sensing as a research tool --- sea ice surveillance from aircraft and spacecraft p 28 A87-40648
- Statistical description of the summertime ice edge in the Chukchi Sea, task 2
[DE87-001056] p 31 N87-22387
- Arctic Sea ice, 1973-1976: Satellite passive-microwave observations
[NASA-SP-489] p 33 N87-24870

ICE REPORTING

- Ocean-ice panel report ... International Space Station p 30 N87-20635
- An evaluation of the polar ice prediction system [AD-A178522] p 41 N87-23014
- IMAGE ANALYSIS**
- Reflectance characteristics and its application in the classification of Nigerian Savanna soils p 3 A87-32954
- Development of a satellite remote sensing technique for the study of alpine glaciers p 34 A87-35311
- Introduction of initial centers for the algorithm of clustering around mobile centers ... in multispectral image classification p 37 A87-35313
- Rapid analysis of satellite radar images of sea ice p 22 A87-35873
- What, where, when ... why? Extracting information from remote sensing data p 46 A87-37055
- Measurements on digitized hardcopy images p 39 A87-37290
- Surface models including direct cross-radiation ... A simple model of furrowed surfaces p 40 A87-39189
- Comparative analysis of Thematic Mapper and SPOT image data for land use investigation p 51 N87-24746
- Large format camera image analysis for mapping of land use patterns in the region Noale - Musone, Po-River-Plain, North Italy p 55 N87-24789
- IMAGE ENHANCEMENT**
- Landsat image enhancement study of possible submerged sand-dunes in the Arabian Gulf p 22 A87-35315
- A software defoliant for geological analysis of band ratios p 18 A87-39193
- Improvement of image quality by forward motion compensation, a preliminary report p 42 N87-24741
- IMAGE MOTION COMPENSATION**
- Improvement of image quality by forward motion compensation, a preliminary report p 42 N87-24741
- On the matching of resolution in aerial photographic systems p 54 N87-24773
- The RMK aerial camera system Performance potential of aerial photography with forward motion compensation p 54 N87-24781
- Wild Aviophot (TM) RC20 aerial camera system The other approach to image motion compensation in aerial photography p 54 N87-24782
- IMAGE PROCESSING**
- MIDAS - A new image-processing system for remote sensing p 37 A87-35183
- The regression intersection method of adjusting image data for band ratioing p 45 A87-35306
- The topographic effect on Landsat data in gently undulating terrain in southern Sweden p 4 A87-35307
- Some observations on crop profile modelling p 5 A87-35310
- Landform investigation utilizing digitally processed satellite Thematic Mapper imagery p 38 A87-36546
- Merging multiresolution SPOT HRV and Landsat TM data p 38 A87-37287
- Image preprocessing for line detection based on local structure analysis p 39 A87-37801
- Multisatellite data processing p 39 A87-37803
- Physical principles of image convergence in remote sensing p 40 A87-41925
- Optical image subtraction techniques, 1975-1985 p 40 A87-42659
- Reports on cartography and geodesy, series 1, number 97 [ISSN-0469-4236] p 16 N87-22286
- The VICOM system for digital image processing at the Institute of Cartography of Technical University, Hanover (West Germany) p 16 N87-22290
- The integration of spectral and spatial analysis for land use classification [AD-A178703] p 14 N87-23015
- An atmospheric correction algorithm for remote identification of non-Lambertian surfaces and its range of validity [DE87-006059] p 41 N87-24011
- Utilizing remote sensing of thematic mapper data to improve our understanding of estuarine processes and their influence on the productivity of estuarine-dependent fisheries [NASA-CR-180984] p 33 N87-24012
- Earth science research [NASA-CR-180512] p 11 N87-24733
- Optical Transfer Function (OTF)-based quality criteria for aerial cameras and imaging systems p 51 N87-24742
- Towards an automatic identification of urban textures p 14 N87-24747
- A modular and versatile acquisition, recording and preprocessing system for airborne remote sensing p 52 N87-24751

- Optical and digital SAR processing techniques A statistical comparison of accuracy using SEASAT imagery p 42 N87-24753
- Introduction of geometric information to radar image data p 42 N87-24754
- Investigation of simulated Monocular Electro-Optical Stereo Scanner (MEOSS)-imagery for sensor navigation and terrain derivation p 54 N87-24771
- The use of auxiliary data in photogrammetric adjustments p 42 N87-24808
- IMAGE RECONSTRUCTION**
- Determination of the velocity of ocean gyres through Synthetic Aperture Radar p 22 A87-35314
- Stereoscopic line scan imaging and satellite control [DGLR PAPER 86-106] p 38 A87-36757
- IMAGE RESOLUTION**
- On the matching of resolution in aerial photographic systems p 54 N87-24773
- Very high resolution aerial films p 54 N87-24776
- The RMK aerial camera system Performance potential of aerial photography with forward motion compensation p 54 N87-24781
- SPOT image quality p 42 N87-24804
- Image quality problems in practical aerial photography p 43 N87-24814
- IMAGING RADAR**
- Wave-measurement capabilities of the surface contour radar and the airborne oceanographic lidar p 25 A87-38840
- IMAGING SPECTROMETERS**
- The Radar Ocean-Wave Spectrometer p 25 A87-38846
- Remote sensing of coastal wetlands p 9 A87-40944
- Evaluation of the airborne imaging spectrometer for remote sensing of forest stand conditions [NASA-CR-180918] p 10 N87-22296
- IMAGING TECHNIQUES**
- Sensors for imaging p 45 A87-36360
- NASA/MSC large stretch press study [NASA-CR-180376] p 41 N87-20554
- Optical Transfer Function (OTF)-based quality criteria for aerial cameras and imaging systems p 51 N87-24742
- INDIA**
- Indian remote sensing programme p 56 A87-32955
- INDIAN OCEAN**
- Tidal estimation in the Atlantic and Indian Oceans, 3 deg x 3 deg solution [NASA-TM-87812] p 30 N87-21534
- INDONESIAN SPACE PROGRAM**
- The Netherlands-Indonesian remote-sensing satellite TERS p 43 A87-32210
- INERTIA**
- A new covariance model for inertial gravimetry and gradiometry p 14 A87-31591
- INERTIAL NAVIGATION**
- The use of camera orientation data in photogrammetry A review p 52 N87-24749
- The use of auxiliary data in photogrammetric adjustments p 42 N87-24808
- INFORMATION SYSTEMS**
- Reports on cartography and geodesy, series 1, number 97 [ISSN-0469-4236] p 16 N87-22286
- Quick-look guide to the crustal dynamics project's data information system [NASA-TM-87818] p 16 N87-23018
- Remote Sensing Information Sciences Research Group Santa Barbara Information Sciences Research Group, year 4 [NASA-CR-181073] p 43 N87-24817
- INFORMATION THEORY**
- A crop condition and crop yield estimation method based on NOAA-AVHRR satellite data p 10 N87-22280
- INFRARED DETECTORS**
- Atmospheric remote sensing in arctic regions [AD-A179550] p 50 N87-23012
- INFRARED FILTERS**
- Ground and aerial use of an infrared video camera with a mid-infrared filter (1.45 to 2.0 microns) p 48 A87-41588
- INFRARED IMAGERY**
- Remote sensing as a research tool ... sea ice surveillance from aircraft and spacecraft p 28 A87-40648
- An expert system for labeling segments in forward looking infrared (FLIR) imagery p 40 A87-42628
- Definition of a thermal infrared pushbroom imager for Earth observation p 53 N87-24765
- INFRARED PHOTOGRAPHY**
- A comparison of optical bar, high-altitude, and black-and-white photography in land classification p 4 A87-35122

INFRARED RADIATION

- GLAI estimation using measurements of red near infrared, and middle infrared radiance p 4 A87-35119
- Mid-infrared remote sensing systems and their application to lithologic mapping p 17 A87-35522
- Polarized views of the earth from orbital altitude p 48 A87-42639

INFRARED RADIOMETERS

- Measurement of the surface emissivity of turbid waters p 19 A87-32097
- Balloon-borne infrared multichannel radiometer for remote sensing of high resolution low level water vapor fields p 43 A87-32477
- Deforestation in the tropics - New measurements in the Amazon Basin using Landsat and NOAA advanced very high resolution radiometer imagery p 4 A87-33441
- Soil moisture estimation using GOES VISSR infrared data - A case study with a simple statistical method p 8 A87-40248

INFRARED SCANNERS

- Infrared Earth horizon sensor concepts in various spectral bands p 52 N87-24752

INFRARED SPECTRA

- Measurement and detection of precipitation Satellite methods in the visible and the infrared p 36 N87-22364

INLAND WATERS

- Inland wetland change detection using aircraft MSS data p 36 A87-42256

INSOLATION

- An evaluation of satellite-based insolation estimates for Ohio p 34 A87-33297

INSTRUMENT ORIENTATION

- The use of camera orientation data in photogrammetry A review p 52 N87-24749
- The effects of camera position and altitude data in aerial triangulation, a simulation study p 52 N87-24750

INTELSAT SATELLITES

- Intelsat's small earth stations - Impact on the developing world p 56 A87-34799

INTERNAL WAVES

- Surface manifestations of hydrophysical processes in the Strait of Gibraltar according to 'Salyut-6' photographs p 35 A87-36103
- The SIR-B mission Towards an understanding of internal waves in the ocean [ARE-TR-86122] p 32 N87-23102

INTERNATIONAL COOPERATION

- Proceedings of the European Symposium on Polar platform Opportunities and Instrumentation for Remote Sensing (ESPOIR) [ESA-SP-266] p 48 N87-20621

INTERPLANETARY SPACECRAFT

- Modern CCD sensors and their applications in Earth observation and planetary missions p 55 N87-24813

INTERPOLATION

- Biharmonic spline interpolation of GEOS-3 and Seasat altimeter data p 20 A87-32770
- Simulation of wind gradient errors in NROSS (Navy Remote Ocean Sensing System) radar scatterometer data in a simplified geometry [AD-A175754] p 49 N87-20642

INTERTROPICAL CONVERGENT ZONES

- Convective heating and precipitation estimates for the tropical South Pacific during FGGE, 10-18 January 1979 p 21 A87-32982
- OH measurement near the intertropical convergence zone in the Pacific p 21 A87-33430

IRRADIANCE

- Computation of diffuse sky irradiance from multidirectional radiance measurements p 6 A87-37279

IRRIGATION

- Influence of different nitrogen and irrigation treatments on the spectral reflectance of barley p 2 A87-32090

ITERATIVE SOLUTION

- Introduction of initial centers for the algorithm of clustering around mobile centers ... in multispectral image classification p 37 A87-35313

J

JAPAN

- Monitoring of snow and ice in Hokkaido Island using multitemporal NOAA-AVHRR data p 20 A87-32497

JAPANESE SPACECRAFT

- Marine Observation Satellite-1 (MOS-1) p 20 A87-32499
- Airborne observation experiments for MOS-1 verification program (MVP) p 44 A87-32500
- Earth Resources Satellite (ERS-1) project in Japan p 57 N87-24797

K

KENYA

- Detection of Rift Valley fever viral activity in Kenya by satellite remote sensing imagery p 7 A87-37827

L

LAGEOS (SATELLITE)

- Earth rotation, station coordinates and orbit determination from satellite laser ranging p 43 A87-32349

- The determination of earth-rotation parameters from satellite laser ranging p 15 A87-34186

LAKES

- Spatial characterization of acid rain stress in Canadian Shield lakes [NASA-CR-180983] p 36 N87-24031

- Spatial characterization of acid rain stress in Canadian shield lakes [NASA-CR-180982] p 36 N87-24032

LAND ICE

- West Antarctic ice streams draining into the Ross Ice Shelf Configuration and mass balance p 19 A87-31592

- Satellite techniques for studying ice crusts and underground waters in the eastern Pamir p 35 A87-36106

LAND USE

- Remote sensing research in global agricultural productivity p 2 A87-32008

- Calibration of satellite radiometers and the comparison of vegetation indices p 2 A87-32091

- Polarization, land use type and intraurban location as variables in SAR mapping accuracy p 12 A87-32953

- Applied remote sensing --- Book p 45 A87-33122

- A comparison of optical bar, high-altitude, and black-and-white photography in land classification p 4 A87-35122

- Comparison of Landsat MSS and TM data for urban land-use classification p 13 A87-35523

- An assessment of Landsat MSS and TM data for urban and near-urban land-cover digital classification p 13 A87-37280

- Remote sensing of vegetation change near Inco's Sudbury mining complexes p 8 A87-39185

- Urban land use separability as a function of radar polarization p 14 A87-39188

- Comparative analysis of Thematic Mapper and SPOT image data for land use investigation p 51 N87-24746

- Large format camera image analysis for mapping of land use patterns in the region Noale - Musone, Po-River-Plain, North Italy p 55 N87-24789

- Image quality problems in practical aerial photography p 43 N87-24814

LANDFORMS

- Landform investigation utilizing digitally processed satellite Thematic Mapper imagery p 38 A87-36546

LANDSAT SATELLITES

- Habitat mapping by Landsat for aerial census of kangaroos p 2 A87-32094

- Continental land cover assessment using Landsat MSS data p 3 A87-32095

- Landsat classification of Argentina summer crops p 3 A87-32098

- Correction for atmospheric and topographic effects on the Landsat MSS data p 37 A87-32489

- Estimation of roughness of the earth's surface using Landsat MSS data on the assumption of reciprocity on light scattering p 12 A87-32493

- Landcover change in Hiroshima during 1979/1984 detected by Landsat MSS and TM data p 12 A87-32494

- Fundamental study on systematization of selecting new development area with Landsat data and topographic informations p 12 A87-32496

- United States remote sensing satellites (RSSs) past, present, and future p 56 A87-32502

- French spot and the U.S. Landsat jockey for position in the race for a multimillion-dollar remote sensing market --- commercial prospects for Landsat and Spot imagery p 56 A87-34600

- Identifying vegetable crops with Landsat Thematic Mapper data p 4 A87-35120

- The topographic effect on Landsat data in gently undulating terrain in southern Sweden p 4 A87-35307

- Landsat image enhancement study of possible submerged sand-dunes in the Arabian Gulf p 22 A87-35315

- Comparison of Landsat MSS and TM data for urban land-use classification p 13 A87-35523

- Fault patterns by space remote sensing and the rotation of western Oregon during Cenozoic times p 18 A87-36525

- Reconnaissance of vegetal formations in a Guinean forest sector by means of Landsat images p 6 A87-36946

- Testing the consistency for mapping urban vegetation with high-altitude aerial photographs and Landsat MSS data p 13 A87-37277

- An assessment of Landsat MSS and TM data for urban and near-urban land-cover digital classification p 13 A87-37280

- Landsat as an aid in evaluating the adequacy of a grain silo network p 7 A87-37282

- The Denali image map p 38 A87-37288

- Data Compression System for video images p 46 A87-37421

- Multisatellite data processing p 39 A87-37803

- Remote sensing of coastal wetlands p 9 A87-40944

- A soil map through Landsat satellite imagery in a part of the Auranga catchment in the Ranchi and Palamou districts of Bihar, India p 9 A87-41428

- Comparative evaluation and guide for the integrated utilization of LANDSAT (MSS and TM) and SPOT (HRV) satellites remotely sensed data p 41 N87-22278

- Enhanced LANDSAT images of Antarctica and planetary exploration p 50 N87-23558

- LANDSAT 2 Geochronological studies of strandlines of Saurashtra, India, detected by remote sensing techniques p 15 A87-35308

- LANDSAT 4 Landform investigation utilizing digitally processed satellite Thematic Mapper imagery p 38 A87-36546

- Monsoon flood boundary delineation and damage assessment using space borne imaging radar and Landsat data p 35 A87-39467

- LANDSAT 5 Spectral classification of Landsat-5 Thematic Mapper data p 37 A87-32488

- High resolution remote sensing of spatially and spectrally complex coal surface mines of central Pennsylvania - A comparison between simulated SPOT MSS and Landsat-5 thematic mapper p 18 A87-39468

- Radiometric comparison of the Landsat-5 TM and MSS sensors p 47 A87-41432

- Towards an automatic identification of urban textures p 14 N87-24747

- LASER ALTIMETERS Two-color short-pulse laser altimeter measurements of ocean surface backscatter p 27 A87-39462

- Laser reflectance as a function of rough water glitter profile [AD-A178774] p 32 N87-23016

- Applications of laser airborne telemetry at Institut Geographique National (IGN), France p 53 N87-24761

- LASER APPLICATIONS Potential of laser remote sensing of oil below water surface [FOA-C-30435-3.1] p 30 N87-20659

- Applications of laser airborne telemetry at Institut Geographique National (IGN), France p 53 N87-24761

- LASER INDUCED FLUORESCENCE Free tropospheric and boundary layer measurements of NO over the central and eastern North Pacific Ocean p 21 A87-33432

- Potential of laser remote sensing of oil below water surface [FOA-C-30435-3.1] p 30 N87-20659

- LASER OUTPUTS Laser reflectance as a function of rough water glitter profile [AD-A178774] p 32 N87-23016

- LASER RANGE FINDERS Earth rotation, station coordinates and orbit determination from satellite laser ranging p 43 A87-32349

- Investigation of tectonic deformations using global satellite laser ranging data p 14 A87-33375

- The determination of earth-rotation parameters from satellite laser ranging p 15 A87-34186

- International Conference on Earth Rotation and the Terrestrial Reference Frame, Columbus, OH, July 31-Aug. 2, 1985, Proceedings. Volumes 1 & 2 p 15 A87-36126

- GINFEST - Geodetic intercomparison network for evaluating space techniques p 15 A87-36164

- Report on the Special Program 78 satellite geodesy of the Technical University of Munich [ASTRON-GEODAET-ARB-48] p 16 N87-20618

- Reports on cartography and geodesy, series 1, number 96 [ISSN-0469-4236] p 16 N87-22282

- Applications of laser airborne telemetry at Institut Geographique National (IGN), France p 53 N87-24761

LASER SPECTROMETERS

- Atmospheric environment monitoring system based on an earth-to-satellite Hadamard transform laser long-path absorption spectrometer - A proposal p 45 A87-35502

- Mid-infrared remote sensing systems and their application to lithologic mapping p 17 A87-35522

LATERITES

- First results of latentic cover mapping with SPOT images The Kangaba region (South-Mali) p 18 A87-36925

LEAVES

- Variations in the polarized leaf reflectance of Sorghum bicolor p 7 A87-38097

- Error analysis of leaf area estimates made from allometric regression models [NASA-TM-89220] p 11 N87-24010

- New dimension analyses with error analysis for quaking aspen and black spruce [NASA-TM-89219] p 11 N87-24735

- Inversion of canopy reflectance models for estimation of vegetation parameters [NASA-CR-181059] p 12 N87-24737

LENSES

- On the matching of resolution in aerial photographic systems p 54 N87-24773

LIGHT SCATTERING

- Estimation of roughness of the earth's surface using Landsat MSS data on the assumption of reciprocity on light scattering p 12 A87-32493

- The interaction of light with phytoplankton in the marine environment p 29 A87-42640

LIGHT SOURCES

- Optical image subtraction techniques, 1975-1985 p 40 A87-42659

LIMESTONE

- Geochronological studies of strandlines of Saurashtra, India, detected by remote sensing techniques p 15 A87-35308

LINEAR POLARIZATION

- Polarized views of the earth from orbital altitude p 48 A87-42639

LINEAR PROGRAMMING

- Optimization of a program of experiments in connection with the operational planning of studies carried out with a spacecraft p 56 A87-34208

LITHOLOGY

- Mid-infrared remote sensing systems and their application to lithologic mapping p 17 A87-35522

LITHOSPHERE

- Applied remote sensing --- Book p 45 A87-33122

LOUISIANA

- Utilizing remote sensing of thematic mapper data to improve our understanding of estuarine processes and their influence on the productivity of estuarine-dependent fisheries [NASA-CR-180984] p 33 N87-24012

LOW GRAVITY MANUFACTURING

- Arianespace top performance benefits ESA [ETN-87-99356] p 41 N87-22278

M

MAGNETIC AMPLIFIERS

- The effect of receiver amplifier non-linearity on ERS-1 synthetic aperture radar imagery p 52 N87-24755

MAGNETIC ANOMALIES

- Exploration of geomagnetic field anomaly with balloon for geophysical research p 17 A87-32478

MAGNETIC MEASUREMENT

- Exploration of geomagnetic field anomaly with balloon for geophysical research p 17 A87-32478

MANUALS

- Comparative evaluation and guide for the integrated utilization of LANDSAT (MSS and TM) and SPOT (HRV) satellites remotely sensed data [ETN-87-99356] p 41 N87-22278

MAPPING

- Mid-infrared remote sensing systems and their application to lithologic mapping p 17 A87-35522

- First results of latentic cover mapping with SPOT images The Kangaba region (South-Mali) p 18 A87-36925

- Testing the consistency for mapping urban vegetation with high-altitude aerial photographs and Landsat MSS data p 13 A87-37277

- Quick look Atlantic Ocean rain maps for gale [NASA-CR-180511] p 30 N87-21533

- Possibilities of using artificial Earth satellite data for computing heat exchange between the ocean and atmosphere in Newfoundland energy-active zone during winter p 31 N87-21980

- Reports on cartography and geodesy, series 1, number 96
[ISSN-0469-4236] p 16 N87-22282
- Altitude measurements for the determination of the Earth's gravity field
[NASA-CR-180520] p 17 N87-23033
- MARINE ENVIRONMENTS**
Measurements of nitric oxide in the boundary layer and free troposphere over the Pacific Ocean
p 21 A87-33431
- Preliminary report on the development of marine geographic information systems p 23 A87-37056
- The interaction of light with phytoplankton in the marine environment p 29 A87-42640
- CHART A computer plotting package for the display of position-dependent marine data
[PB87-148607] p 31 N87-22297
- High resolution sea surface temperature field derived p 33 N87-24731
- MARINE METEOROLOGY**
Convective heating and precipitation estimates for the tropical South Pacific during FGGE, 10-18 January 1979
p 21 A87-32982
- The present status of operational wave forecasting ... for ocean surface p 24 A87-38831
- Optical properties of the marine atmospheric boundary layer - Aerosol profiles p 28 A87-42638
- MARINE TECHNOLOGY**
Optical dynamics experiment (ODEX) data report R/V acania expedition 10 October-17 November 1982. Volume 2. Particle size distributions. Volume 6. Scalar spectral-radiometer data
[AD-A178535] p 32 N87-23104
- MARITIME SATELLITES**
Marine Observation Satellite-1 (MOS-1)
p 20 A87-32499
- Airborne observation experiments for MOS-1 verification program (MVP) p 44 A87-32500
- MARKETING**
French spot and the U.S. Landsat jockey for position in the race for a multimillion-dollar remote sensing market ... commercial prospects for Landsat and Spot imagery p 56 A87-34600
- MARS SURFACE**
Enhanced LANDSAT images of Antarctica and planetary exploration p 50 N87-23558
- MARSHLANDS**
Utilizing remote sensing of thematic mapper data to improve our understanding of estuarine processes and their influence on the productivity of estuarine-dependent fisheries
[NASA-CR-180984] p 33 N87-24012
- MASS FLOW**
West Antarctic ice streams draining into the Ross Ice Shelf Configuration and mass balance p 19 A87-31592
- MATHEMATICAL MODELS**
A new covariance model for inertial gravimetry and gradiometry p 14 A87-31591
- A soil thermal model for remote sensing p 5 A87-35521
- Stochastic nature of Landsat MSS data p 46 A87-38093
- Surface models including direct cross-radiation - A simple model of furrowed surfaces p 40 A87-39189
- An atmospheric correction algorithm for remote identification of non-Lambertian surfaces and its range of validity
[DE87-006059] p 41 N87-24011
- Inversion of canopy reflectance models for estimation of vegetation parameters
[NASA-CR-181059] p 12 N87-24737
- Radial orbit error reduction and sea surface topography determination using satellite altimetry
[NASA-CR-180570] p 33 N87-24816
- MAXIMUM LIKELIHOOD ESTIMATES**
A comparison of supervised maximum likelihood and decision tree classification for crop cover estimation from multitemporal Landsat MSS data p 5 A87-35312
- Landsat as an aid in evaluating the adequacy of a grain silo network p 7 A87-37282
- MEASURING INSTRUMENTS**
Reports on cartography and geodesy, series 1, number 96
[ISSN-0469-4236] p 16 N87-22282
- MELTING**
Microwave sea-ice signatures near the onset of melt p 22 A87-35517
- MESOSCALE PHENOMENA**
Mesoscale oceanographic processes beneath the ice of Fram Strait p 28 A87-40434
- METEOROLOGICAL PARAMETERS**
Energy Balance of the Tropical Systems (BEST): A space experiment proposition p 36 N87-22373

- Arctic Sea ice, 1973-1976. Satellite passive-microwave observations
[NASA-SP-489] p 33 N87-24870
- METEOROLOGICAL RADAR**
VHF radar for ocean surface current and sea state remote sensing p 19 A87-31631
- Observation of precipitation from space by the weather radar p 44 A87-32507
- METEOROLOGICAL SATELLITES**
Impact of satellite-based data on FGGE general circulation statistics p 44 A87-32985
- Remote-sensing method for determining monthly precipitation sums using Meteor-satellite data on the Atlantic Ocean p 21 A87-34447
- AVHRR data services in Europe - The Earthnet approach p 39 A87-37922
- Satellite estimation of a solar irradiance at the surface of the earth and of surface albedo using a physical model applied to Meteosat data p 47 A87-40246
- Atmospheric remote sensing in arctic regions
[AD-A179550] p 50 N87-23012
- Arianespace top performance benefits ESA p 57 N87-24493
- METEOROLOGICAL SERVICES**
The application of remote sensing in agricultural meteorology at the Meteorological Service of the HPR p 2 A87-32010
- METEOSAT SATELLITE**
A curious sea-surface-temperature phenomenon observed by Meteosat p 19 A87-31572
- Multisatellite data processing p 39 A87-37803
- METHANE**
The possibility of using satellite measurements of methane in the atmosphere to study the global-distribution characteristics of its sources p 13 A87-36125
- METRIC PHOTOGRAPHY**
Geometrical system calibration, especially for metric aerial cameras p 51 N87-24745
- Large Format Camera photographs of the Black Hills, USA, and their suitability for topographic and thematic mapping p 55 N87-24792
- MICROWAVE EMISSION**
The dependence of sea-surface microwave emission on wind speed, frequency, incidence angle, and polarization over the frequency range from 1 to 40 GHz
p 22 A87-35515
- Salinity effects on the microwave emission of soils p 5 A87-35520
- MICROWAVE EQUIPMENT**
Atmospheric remote sensing in arctic regions
[AD-A179550] p 50 N87-23012
- MICROWAVE IMAGERY**
Remote sensing as a research tool ... sea ice surveillance from aircraft and spacecraft p 28 A87-40648
- MICROWAVE RADIOMETERS**
Nimbus 7 SMMR investigation of snowpack properties in the northern Great Plains for the winter of 1978-1979 p 34 A87-31409
- Applications of satellite microwave radiometry in Finland p 44 A87-32952
- Seasonal and regional variations of active/passive microwave signatures of sea ice p 22 A87-35516
- Microwave sea-ice signatures near the onset of melt p 22 A87-35517
- Salinity effects on the microwave emission of soils p 5 A87-35520
- Recurring polynyas over the Cosmonaut Sea and the Maud Rise p 23 A87-37563
- Monitoring vegetation using Nimbus-7 scanning multichannel microwave radiometer's data p 8 A87-39194
- Remotely sensed sea surface temperature for the Alpine Experiment (ALPEX) ... AVHRR-2 data p 30 N87-21497
- MICROWAVE SENSORS**
Temporal observations of surface soil moisture using a passive microwave sensor p 7 A87-38094
- Nadir looking airborne radar and possible applications to forestry p 7 A87-38095
- MICROWAVE SOUNDING**
Airborne microwave Doppler measurements of ocean wave directional spectra p 26 A87-39180
- MICROWAVE SPECTRA**
The microwave measurement of ocean-wave directional spectra p 24 A87-38836
- Procedures for the description of agricultural crops and soils in optical and microwave remote sensing studies p 8 A87-39187
- MICROWAVE SPECTROMETERS**
The physical basis for estimating wave-energy spectra with the radar ocean-wave spectrometer p 25 A87-38839
- Advanced imaging spectrometer for ocean color/fluorescence measurements and further applications p 33 N87-24766

MICROWAVE TRANSMISSION

- Analysis of moderate and intense rainfall rates continuously recorded over half a century and influence on microwave communications planning and rain-rate data acquisition p 46 A87-36933

MICROWAVES

- Quantifying spatial and temporal variabilities of microwave brightness temperature over the U.S. Southern Great Plains p 5 A87-35309

MIDLATITUDE ATMOSPHERE

- Determining rainfall intensity and type from GOES imagery in the midlatitudes p 34 A87-32092
- On the relative accuracy of satellite and raingage rainfall measurements over middle latitudes during daylight hours p 34 A87-33295

MILLET

- A crop condition and crop yield estimation method based on NOAA/AVHRR satellite data p 10 N87-22280

MILLIMETER WAVES

- The relation of millimeter-wavelength backscatter to surface snow properties p 34 A87-35518

MINERAL DEPOSITS

- First results of lateritic cover mapping with SPOT images The Kangaba region (South Mali) p 18 A87-36925
- Predicting the location of kimberlite from a probability analysis of linear structure on remote sensing data p 18 A87-39186

MINERAL EXPLORATION

- Mid-infrared remote sensing systems and their application to lithologic mapping p 17 A87-35522

MINES

- High resolution remote sensing of spatially and spectrally complex coal surface mines of central Pennsylvania - A comparison between simulated SPOT MSS and Landsat-5 thematic mapper p 18 A87-39468

MINING

- Remote sensing of vegetation change near Inco's Sudbury mining complexes p 8 A87-39185

MINNESOTA

- Earth science research
[NASA-CR-180512] p 11 N87-24733
- Ten year change in forest succession and composition measured by remote sensing
[NASA-CR-180948] p 11 N87-24736

MISSION PLANNING

- Airborne observation experiments for MOS-1 verification program (MVP) p 44 A87-32500
- Scientific goals and technical limitations of the shuttleborne synthetic aperture experiment X-SAR p 44 A87-32505

MIXING

- Studies of the east Australian current off northern New South Wales
[AD-A178461] p 32 N87-23103

MODULATION TRANSFER FUNCTION

- Improvement of image quality by forward motion compensation, a preliminary report p 42 N87-24741
- Optical Transfer Function (OTF)-based quality criteria for aerial cameras and imaging systems p 51 N87-24742

MONSOONS

- Monsoon flood boundary delineation and damage assessment using space borne imaging radar and Landsat data p 35 A87-39467

MOUNTAINS

- Montane vegetation stratification through digital processing of Landsat MSS data p 9 A87-40302
- Radar as a complement to topographic maps for delineating marine terraces
[PB87-154597] p 41 N87-24013

MULTISENSOR APPLICATIONS

- Merging multiresolution SPOT HRV and Landsat TM data p 38 A87-37287

MULTISPECTRAL BAND CAMERAS

- The production of photographs of the Earth's surface taken from satellites and their application in map production and map revision p 55 N87-24788
- Determination of spectral reflectance of crops during growth from calibrated multispectral small format aerial photography p 12 N87-24801

MULTISPECTRAL BAND SCANNERS

- Continental land cover assessment using Landsat MSS data p 3 A87-32095
- Correction for atmospheric and topographic effects on the Landsat MSS data p 37 A87-32489
- Estimation of roughness of the earth's surface using Landsat MSS data on the assumption of reciprocity on light scattering p 12 A87-32493
- Temperature change in Hiroshima during 1979/1984 Landsat MSS and TM data p 12 A87-32494

- Intersection method of adjusting image and rationing p 45 A87-35306
- Development of a satellite remote sensing technique for the study of alpine glaciers p 34 A87-35311

- A comparison of supervised maximum likelihood and decision tree classification for crop cover estimation from multitemporal Landsat MSS data p 5 A87-35312
- Landsat image enhancement study of possible submerged sand-dunes in the Arabian Gulf p 22 A87-35315
- Combining panchromatic and multispectral imagery from dual resolution satellite instruments p 38 A87-37276
- Testing the consistency for mapping urban vegetation with high-altitude aerial photographs and Landsat MSS data p 13 A87-37277
- An assessment of Landsat MSS and TM data for urban and near-urban land-cover digital classification p 13 A87-37280
- Stochastic nature of Landsat MSS data p 46 A87-38093
- Synergistic use of MOMS-01 and Landsat TM data --- Modular Optoelectronic Multispectral Scanner p 46 A87-39190
- Radiometric comparison of the Landsat-5 TM and MSS sensors p 47 A87-41432
- Inland wetland change detection using aircraft MSS data p 36 A87-42256
- Application of Modular Optoelectronic Multispectral Scanner (MOMS) data to hydrology and vegetation studies. Test site: Pantanal Region (Brazil/Paraguay) p 52 N87-24748
- The Multidetector Electro-optical Imaging Sensor (MEIS) 2 pushbroom imager: Four years of operation p 53 N87-24767
- The Modular Optoelectronic Multispectral Scanner (MOMS) program of the Bundesministerium fuer Forschung und Technologie (BMFT). Milestones in the development of an operational Earth Observation system p 55 N87-24815
- MULTISPECTRAL PHOTOGRAPHY**
- An application of low altitude multispectral photography to agricultural field trials p 6 A87-37054
- Foundations and applications of multispectral scanning in agriculture p 10 N87-21408
- Enhanced LANDSAT images of Antarctica and planetary exploration p 50 N87-23558
- N**
- NARROWBAND**
- Deriving surface albedo measurements from narrow band satellite data p 13 A87-39182
- NASA PROGRAMS**
- Operational overview of NASA GTE/CITE 1 airborne instrument intercomparisons - Carbon monoxide, nitric oxide, and hydroxyl instrumentation --- Global Tropospheric Experiment/Chemical Instrumentation Test and Evaluation p 45 A87-33426
- NATIONAL PARKS**
- The Denali image map p 38 A87-37288
- NAVIGATION**
- CHART: A computer plotting package for the display of position-dependent marine data [PB87-148607] p 31 N87-22297
- NAVIGATION AIDS**
- Application of Global Positioning System (GPS) receivers for Earth observation p 53 N87-24763
- Investigation of simulated Monocular Electro-Optical Stereo Scanner (MEOSS)-imagery for sensor navigation and terrain derivation p 54 N87-24771
- NAVIGATION INSTRUMENTS**
- The use of camera orientation data in photogrammetry: A review p 52 N87-24749
- NEARSHORE WATER**
- Surface manifestations of hydrophysical processes in the Strait of Gibraltar according to 'Salyut-6' photographs p 35 A87-36103
- NIGERIA**
- Reflectance characteristics and its application in the classification of Nigerian Savanna soils p 3 A87-32954
- NIMBUS 7 SATELLITE**
- Nimbus 7 SMMR investigation of snowpack properties in the northern Great Plains for the winter of 1978-1979 p 34 A87-31409
- Reflectivity of earth's surface and clouds in ultraviolet from satellite observations p 47 A87-40768
- NITRIC OXIDE**
- Measurements of nitric oxide in the boundary layer and free troposphere over the Pacific Ocean p 21 A87-33431
- Free tropospheric and boundary layer measurements of NO over the central and eastern North Pacific Ocean p 21 A87-33432
- NITROGEN**
- Influence of different nitrogen and irrigation treatments on the spectral reflectance of barley p 2 A87-32090

NOAA SATELLITES

- Global vegetation monitoring using NOAA vegetation index data p 3 A87-32495
- Monitoring of snow and ice in Hokkaido island using multitemporal NOAA-AVHRR data p 20 A87-32497
- Relation between precipitation and brightness of earth surface in the NOAA/GVIP data p 3 A87-32498
- A crop condition and crop yield estimation method based on NOAA-AVHRR satellite data p 10 N87-22280

NONLINEARITY

- The effect of receiver amplifier non-linearity on ERS-1 synthetic aperture radar imagery p 52 N87-24755

NORTH AMERICA

- Comparison of North and South American biomes from AVHRR observations p 9 A87-40303

NORWAY

- An evaluation of the polar ice prediction system [AD-A178522] p 41 N87-23014

NUMERICAL ANALYSIS

- High resolution sea surface temperature field derived [AD-A178522] p 33 N87-24731

NUMERICAL WEATHER FORECASTING

- The present status of operational wave forecasting --- for ocean surface p 24 A87-38831
- The operational performance of the fleet numerical oceanography center global spectral ocean-wave model p 24 A87-38832
- Recent results with a third-generation ocean-wave model p 24 A87-38833
- The impact of initial conditions and SST anomalies on extended range predictions for the El Nino period --- sea surface temperature (SST) p 32 N87-23046

O**OCEAN BOTTOM**

- Feedback between ice flow, barotropic flow, and baroclinic flow in the presence of bottom topography p 27 A87-40289
- Tidal estimation in the Atlantic and Indian Oceans, 3 deg x 3 deg solution [NASA-TM-87812] p 30 N87-21534

OCEAN COLOR SCANNER

- The relationship between phytoplankton concentration and light attenuation in ocean waters p 29 A87-42642
- Advanced imaging spectrometer for ocean color/fluorescence measurements and further applications p 33 N87-24766

OCEAN CURRENTS

- VHF radar for ocean surface current and sea state remote sensing p 19 A87-31631
- Determination of the velocity of ocean gyres through Synthetic Aperture Radar p 22 A87-35314
- Tidal estimation in the Atlantic and Indian Oceans, 3 deg x 3 deg solution [NASA-TM-87812] p 30 N87-21534
- DUCK '85 nearshore waves and currents experiment data summary report [AD-A177419] p 31 N87-22382
- Studies of the ocean current off northern New South Wales [AD-A178461] p 32 N87-23103

OCEAN DATA ACQUISITION SYSTEMS

- A Spectrasat system design based on the Geosat experiment p 26 A87-38848
- Ocean-ice panel report --- International Space Station p 30 N87-20635
- Simulation of wind gradient errors in NROSS (Navy Remote Ocean Sensing System) radar scatterometer data in a simplified geometry [AD-A175754] p 49 N87-20642
- Report of the workshop on Assimilation of Satellite Wind and Wave Data in Numerical Weather and Wave Prediction Models [WCP-122] p 49 N87-21521
- Advanced imaging spectrometer for ocean color/fluorescence measurements and further applications p 33 N87-24766
- The first ESA remote sensing satellite (status and outlook) p 57 N87-24777

OCEAN DYNAMICS

- Use of satellite altimetry for ocean monitoring p 23 A87-36101
- The age and source of ocean swell observed in Hurricane Josephine p 25 A87-38843
- Spectrasat - A hybrid ROWS/SAR approach to monitor ocean waves from space p 25 A87-38845
- The Geosat altimeter mission - A milestone in satellite oceanography p 27 A87-40281
- Feedback between ice flow, barotropic flow, and baroclinic flow in the presence of bottom topography p 27 A87-40289
- Mesoscale oceanographic processes beneath the ice of Fram Strait p 28 A87-40434

OCEAN MODELS

- The present status of operational wave forecasting --- for ocean surface p 24 A87-38831
- The operational performance of the fleet numerical oceanography center global spectral ocean-wave model p 24 A87-38832
- Recent results with a third-generation ocean-wave model p 24 A87-38833
- A practical methodology for estimating wave spectra from the SIR-B p 25 A87-38841
- The age and source of ocean swell observed in Hurricane Josephine p 25 A87-38843
- The effect of a non-Gaussian point target response function on radar altimeter returns from the sea surface p 26 A87-39179
- Ocean wind and wave model comparisons with GEOSAT (GEOdesy SATEllite) satellite data [AD-A178302] p 33 N87-24061

OCEAN SURFACE

- Bi-harmonic spline interpolation of GEOS-3 and Seasat altimeter data p 20 A87-32770
- The dependence of sea-surface microwave emission on wind speed, frequency, incidence angle, and polarization over the frequency range from 1 to 40 GHz p 22 A87-35515
- Surface manifestations of hydrophysical processes in the Strait of Gibraltar according to 'Salyut-6' photographs p 35 A87-36103
- Measurement of the spatial spectrum of ocean waves using a two-frequency scatterometer p 23 A87-36107
- Some approaches for comparing remote and in-situ estimates of directional wave spectra p 24 A87-38835
- The microwave measurement of ocean-wave directional spectra p 24 A87-38836
- The physical basis for estimating wave-energy spectra with the radar ocean-wave spectrometer p 25 A87-38839
- Wave-measurement capabilities of the surface contour radar and the airborne oceanographic lidar p 25 A87-38840
- The Radar Ocean-Wave Spectrometer p 25 A87-38846
- A Spectrasat system design based on the Geosat experiment p 26 A87-38848
- The effect of a non-Gaussian point target response function on radar altimeter returns from the sea surface p 26 A87-39179
- Airborne microwave Doppler measurements of ocean wave directional spectra p 26 A87-39180
- Two-color short-pulse laser altimeter measurements of ocean surface backscatter p 27 A87-39462
- The propagation of short surface waves on longer gravity waves p 28 A87-40835
- Multilook images of ocean waves by synthetic aperture radars p 28 A87-41068
- Wind and nadir angle effects on airborne lidar wave 'surface' returns p 29 A87-42641
- A technique to estimate the ocean surface energy flux using VAS multispectral data p 30 N87-20710
- Laser reflectance as a function of rough water glitter profile [AD-A178774] p 32 N87-23016
- Altimeter measurements for the determination of the Earth's gravity field [NASA-CR-180520] p 17 N87-23033
- The SIR-B mission: Towards an understanding of internal waves in the ocean [ARE-TR-86122] p 32 N87-23102
- Ocean wind and wave model comparisons with GEOSAT (GEOdesy SATEllite) satellite data [AD-A178302] p 33 N87-24061
- Radial orbit error reduction and sea surface topography determination using satellite altimetry [NASA-CR-180570] p 33 N87-24816
- OCEANOGRAPHIC PARAMETERS**
- Optical dynamics experiment (ODEX) data report R/V *Acadia* expedition 10 October-17 November 1982. Volume 2: Particle size distributions. Volume 6: Scalar spectral-radiometer data [AD-A178535] p 32 N87-23104
- Arctic Sea ice, 1973-1976. Satellite passive-microwave observations [NASA-SP-489] p 33 N87-24870
- OCEANOGRAPHY**
- Marine Observation Satellite-1 (MOS-1) p 20 A87-32499
- The French Space Oceanography Program p 20 A87-32503
- Measuring ocean waves from space. Proceedings of the Symposium, Johns Hopkins University, Laurel, MD, Apr. 15-17, 1986 p 24 A87-38826
- Remote sensing as a research tool --- sea ice surveillance from aircraft and spacecraft p 28 A87-40648

- Ocean optics VIII; Proceedings of the Meeting, Orlando, FL, Mar. 31-Apr. 2, 1986
[SPIE-637] p 28 A87-42637
- A model for the use of satellite remote sensing for the measurement of primary production in the ocean p 29 A87-42644
- Continental shelf processes affecting the oceanography of the South Atlantic Bight
[DE87-005303] p 30 N87-20716
- Report of the workshop on Assimilation of Satellite Wind and Wave Data in Numerical Weather and Wave Prediction Models
[WCP-122] p 49 N87-21521
- An evaluation of the polar ice prediction system
[AD-A178522] p 41 N87-23014
- The SIR-B mission: Towards an understanding of internal waves in the ocean
[ARE-TR-86122] p 32 N87-23102
- OHIO**
- An evaluation of satellite-based insolation estimates for Ohio p 34 A87-33297
- OIL POLLUTION**
- Potential of laser remote sensing of oil below water surface
[FOA-C-30435-3.1] p 30 N87-20659
- ONBOARD DATA PROCESSING**
- A modular and versatile acquisition, recording and preprocessing system for airborne remote sensing p 52 N87-24751
- OPTICAL DATA PROCESSING**
- Ocean optics VIII; Proceedings of the Meeting, Orlando, FL, Mar. 31-Apr. 2, 1986
[SPIE-637] p 28 A87-42637
- Optical image subtraction techniques, 1975-1985 p 40 A87-42659
- Optical and digital SAR processing techniques: A statistical comparison of accuracy using SEASAT imagery p 42 N87-24753
- OPTICAL DENSITY**
- Spectrophotometric measurements on color aerial photographs p 55 N87-24798
- OPTICAL EQUIPMENT**
- Ocean optics VIII; Proceedings of the Meeting, Orlando, FL, Mar. 31-Apr. 2, 1986
[SPIE-637] p 28 A87-42637
- OPTICAL POLARIZATION**
- Variations in the polarized leaf reflectance of Sorghum bicolor p 7 A87-38097
- OPTICAL PROPERTIES**
- Optical properties of the marine atmospheric boundary layer - Aerosol profiles p 28 A87-42638
- Optical dynamics experiment (ODEX) data report R/V acania expedition 10 October-17 November 1982. Volume 2: Particle size distributions. Volume 6: Scalar spectral-radiometer data
[AD-A178535] p 32 N87-23104
- OPTICAL RADAR**
- Lidar observation of elevated pollution layers over Los Angeles p 13 A87-33292
- OH measurement near the intertropical convergence zone in the Pacific p 21 A87-33430
- Wave-measurement capabilities of the surface contour radar and the airborne oceanographic lidar p 25 A87-38840
- Wind and nadir angle effects on airborne lidar water 'surface' returns p 29 A87-42641
- Energy Balance of the Tropical Systems (BEST): A space experiment proposition p 36 N87-22373
- Laser reflectance as a function of rough water glitter profile
[AD-A178774] p 32 N87-23016
- OPTICAL SCANNERS**
- A two-look technique for studying atmospheric effects in optical scanner data for the ocean p 26 A87-39178
- The Monocular Electro-Optical Stereo Scanner (MEOSS) satellite experiment p 55 N87-24812
- OPTICAL TRANSFER FUNCTION**
- Optical Transfer Function (OTF)-based quality criteria for aerial cameras and imaging systems p 51 N87-24742
- OPTIMIZATION**
- Optimization of a program of experiments in connection with the operational planning of studies carried out with a spacecraft p 56 A87-34208
- OPTOELECTRONIC DEVICES**
- Synergistic use of MOMS-01 and Landsat TM data --- Modular Optoelectronic Multispectral Scanner p 46 A87-39190
- ORBIT CALCULATION**
- Earth rotation, station coordinates and orbit determination from satellite laser ranging p 43 A87-32349

ORBITAL SPACE STATIONS

- Proceedings of the European Symposium on Polar platform Opportunities and Instrumentation for Remote-Sensing (ESPOIR)
[ESA-SP-266] p 48 N87-20621
- The Earth observation activities of the European Space Agency and the use of the polar platform of the International Space Station p 49 N87-20622
- European utilization aspects studies --- space stations p 49 N87-20624
- Land panel report --- International Space Station p 49 N87-20634
- Ocean-ice panel report --- International Space Station p 30 N87-20635

OROGRAPHY

- The Denali image map p 38 A87-37288

ORTHOPHOTOGRAPHY

- Introduction of geometric information to radar image data p 42 N87-24754

OZONE

- Trace gas exchanges and transports over the Amazonian rain forest p 12 A87-32196

OZONOMETRY

- Reflectivity of earth's surface and clouds in ultraviolet from satellite observations p 47 A87-40768

P**PACIFIC OCEAN**

- Free tropospheric and boundary layer measurements of NO over the central and eastern North Pacific Ocean p 21 A87-33432
- Carbon monoxide measurements over the eastern Pacific during GTE/CITE 1 --- Chemical Instrumentation Test and Evaluation p 21 A87-33435

PARAMETER IDENTIFICATION

- Inversion of canopy reflectance models for estimation of vegetation parameters
[NASA-CR-181059] p 12 N87-24737

PARTICLE SIZE DISTRIBUTION

- Optical dynamics experiment (ODEX) data report R/V acania expedition 10 October-17 November 1982. Volume 2: Particle size distributions. Volume 6: Scalar spectral-radiometer data
[AD-A178535] p 32 N87-23104

PAYLOAD INTEGRATION

- Optimization of a program of experiments in connection with the operational planning of studies carried out with a spacecraft p 56 A87-34208

PERFORMANCE PREDICTION

- The operational performance of the fleet numerical oceanography center global spectral ocean-wave model p 24 A87-38832
- The Tethered Satellite System as a new remote sensing platform p 46 A87-39183

PERIODIC VARIATIONS

- Recurring polynyas over the Cosmonaut Sea and the Maud Rise p 23 A87-37563

PERMITTIVITY

- Radar scene generation for tactical decision aids
[NASA-CR-180234] p 40 N87-20449
- NASA/MSFC large stretch press study
[NASA-CR-180376] p 41 N87-20554

PERSIAN GULF

- Landsat image enhancement study of possible submerged sand-dunes in the Arabian Gulf p 22 A87-35315

PERTURBATION

- An atmospheric correction algorithm for remote identification of non-Lambertian surfaces and its range of validity
[DE87-006059] p 41 N87-24011

PERTURBATION THEORY

- Radial orbit error reduction and sea surface topography determination using satellite altimetry
[NASA-CR-180570] p 33 N87-24816

PHASE DEVIATION

- Relating polarization phase difference of SAR signals to scene properties p 1 A87-31413

PHOTOCHEMICAL REACTIONS

- OH measurement near the intertropical convergence zone in the Pacific p 21 A87-33430
- Measurements of nitric oxide in the boundary layer and free troposphere over the Pacific Ocean p 21 A87-33431

PHOTO GEOLOGY

- The geometry of the intersections of tectonic structures detected on satellite images p 17 A87-36104
- The geosstructural characteristics of the rift zone on the Lambert glacier (Antarctica) according to space images p 18 A87-36105
- Fault patterns by space remote sensing and the rotation of western Oregon during Cenozoic times p 18 A87-36525

- Spacelab data - A new contribution for structural interpretations of remotely sensed data in geology p 18 A87-39790

PHOTOGRAMMETRY

- Aerotriangulation without ground control p 46 A87-37289
- Measurements on digitized hardcopy images p 39 A87-37290
- Proceedings of the International Symposium on Progress in Imaging Sensors
[ESA-SP-252] p 50 N87-24738
- The use of camera orientation data in photogrammetry A review p 52 N87-24749
- Applications of laser airborne telemetry at Institut Geographique National (IGN), France p 53 N87-24761
- The stereo pushbroom scanner system Digital Photogrammetry System (DPS) and its accuracy p 53 N87-24768
- Aerial triangulation of CCD line-scanner images p 54 N87-24769
- The role of government specifications in aerial photography p 57 N87-24780
- Digital data acquisition for close-range photogrammetry p 54 N87-24785
- Estimating photogrammetric precision and cartographic potential of space imagery p 42 N87-24791
- The use of auxiliary data in photogrammetric adjustments p 42 N87-24808

PHOTOGRAPHIC FILM

- On the matching of resolution in aerial photographic systems p 54 N87-24773
- Exposure test with high resolution films from high altitude p 54 N87-24775
- Very high resolution aerial films p 54 N87-24776
- The RMK aerial camera system: Performance potential of aerial photography with forward motion compensation p 54 N87-24781

PHOTOGRAPHIC MEASUREMENT

- A study of elevation measurement using LFC photograph --- Large Format Camera p 43 A87-32491

PHOTOINTERPRETATION

- Image preprocessing for line detection based on local structure analysis p 39 A87-37801
- Spacelab data - A new contribution for structural interpretations of remotely sensed data in geology p 18 A87-39790
- Comparison between digital and manual interpretation of high altitude aerial photographs p 48 A87-42257
- Improvement of image quality by forward motion compensation, a preliminary report p 42 N87-24741

PHOTOMAPPING

- Problems in the automation of map-compilation processes on the basis of remote-sensing data p 38 A87-35925
- The Denali image map p 38 A87-37288
- Proposed changes to the Canadian camera calibration report p 53 N87-24757
- Wild Aviophot (TM) RC20 aerial camera system. The other approach to image motion compensation in aerial photography p 54 N87-24782
- The production of photographs of the Earth's surface taken from satellites and their application in map production and map revision p 55 N87-24788
- Large format camera image analysis for mapping of land use patterns in the region Noale - Musone, Po-River-Plain, North Italy p 55 N87-24789
- Estimating photogrammetric precision and cartographic potential of space imagery p 42 N87-24791
- Large Format Camera photographs of the Black Hills, USA, and their suitability for topographic and thematic mapping p 55 N87-24792
- Earth observation experiments on the German Spacelab mission D2 p 55 N87-24811

PHOTOSYNTHESIS

- Canopy reflectance, photosynthesis, and transpiration. II - The role of biophysics in the linearity of their interdependence p 6 A87-37278

PIGMENTS

- Coastal zone color scanner imagery of phytoplankton pigment distribution in Icelandic waters p 29 A87-42645

PLANKTON

- The interaction of light with phytoplankton in the marine environment p 29 A87-42640
- The relationship between phytoplankton concentration and light attenuation in ocean waters p 29 A87-42642
- Remote sensing of chlorophyll concentrations in the northern Gulf of Mexico p 29 A87-42643
- Coastal zone color scanner imagery of phytoplankton pigment distribution in Icelandic waters p 29 A87-42645
- Sunlight induced 685 nm fluorescence imagery p 30 A87-42646

PLANT STRESS

Evaluation of the airborne imaging spectrometer for remote sensing of forest stand conditions
[NASA-CR-180918] p 10 N87-22296

PLANTS (BOTANY)

Inferring spectral reflectances of plant elements by simple inversion of bidirectional reflectance measurements p 7 A87-37281

PLOTTING

CHART: A computer plotting package for the display of position-dependent marine data
[PB87-148607] p 31 N87-22297

POLAR ORBITS

AVHRR data services in Europe - The Earthnet approach p 39 A87-37922

A polar platform for the remote sensing needs of ecology and agriculture - A view from the U.K. p 9 A87-41430

Proceedings of the European Symposium on Polar platform Opportunities and Instrumentation for Remote-Sensing (ESPOIR)
[ESA-SP-266] p 48 N87-20621

Land panel report --- International Space Station p 49 N87-20634

Ocean-ice panel report --- International Space Station p 30 N87-20635

POLAR REGIONS

An evaluation of the polar ice prediction system
[AD-A178522] p 41 N87-23014

POLAR WANDERING (GEOLOGY)

Polar motion-induced gravity p 15 A87-36176

POLARIMETRY

Interpretation of the polarimetric co-polarization phase term in radar images obtained with the JPL airborne L-band SAR system p 36 A87-31412

POLARIZATION (WAVES)

Radar scene generation for tactical decision aids
[NASA-CR-180234] p 40 N87-20449

NASA/MSFC large stretch press study
[NASA-CR-180376] p 41 N87-20554

POLARIZATION CHARACTERISTICS

Relating polarization phase difference of SAR signals to scene properties p 1 A87-31413

Polarization, land use type and intraurban location as variables in SAR mapping accuracy p 12 A87-32953

Urban land use separability as a function of radar polarization p 14 A87-39188

POLLUTION MONITORING

Lidar observation of elevated pollution layers over Los Angeles p 13 A87-33292

Environmental protection from space p 13 A87-36363

Use of maps, aerial photographs, and other remote sensor data for practical evaluations of hazardous waste sites p 14 A87-42255

POLLUTION TRANSPORT

Continental shelf processes affecting the oceanography of the South Atlantic Bight
[DE87-005303] p 30 N87-20716

POSEIDON SATELLITE

The French Space Oceanography Program p 20 A87-32503

POSITION (LOCATION)

CHART: A computer plotting package for the display of position-dependent marine data
[PB87-148607] p 31 N87-22297

POSITION INDICATORS

Application of Global Positioning System (GPS) receivers for Earth observation p 53 N87-24763

POSITIONING

A study of elevation measurement using LFC photograph --- Large Format Camera p 43 A87-32491

POSTLAUNCH REPORTS

SPOT image quality p 42 N87-24804

PRECIPITATION (METEOROLOGY)

Relation between precipitation and brightness of earth surface in the NOAA/GVIP data p 3 A87-32498

Observation of precipitation from space by the weather radar p 44 A87-32507

Convective heating and precipitation estimates for the tropical South Pacific during FGGE, 10-18 January 1979 p 21 A87-32982

Remote-sensing method for determining monthly precipitation sums using Meteor-satellite data on the Atlantic Ocean p 21 A87-34447

PREDICTION ANALYSIS TECHNIQUES

New dimension analyses with error analysis for quaking aspen and black spruce
[NASA-TM-89219] p 11 N87-24735

PREPROCESSING

Utilizing remote sensing of thematic mapper data to improve our understanding of estuarine processes and their influence on the productivity of estuarine-dependent fisheries
[NASA-CR-180984] p 33 N87-24012

A modular and versatile acquisition, recording and preprocessing system for airborne remote sensing p 52 N87-24751

PRINCIPAL COMPONENTS ANALYSIS

A software defoliant for geological analysis of band ratios p 18 A87-39193

PROBABILITY THEORY

Predicting the location of kimberlite from a probability analysis of linear structure on remote sensing data p 18 A87-39186

PRODUCT DEVELOPMENT

The first ESA remote sensing satellite (status and outlook) p 57 N87-24777

PRODUCTIVITY

A review of national and international activities on modeling the effects of increased CO₂ concentrations on the simulation of regional crop production. A report on linkage between climate and crop models
[DE87-005994] p 10 N87-22336

PROVING

DUCK '85 nearshore waves and currents experiment data summary report
[AD-A177419] p 31 N87-22382

PULSED LASERS

Two-color short-pulse laser altimeter measurements of ocean surface backscatter p 27 A87-39462

PUSHBROOM SENSOR MODES

Synergistic use of MOMS-01 and Landsat TM data --- Modular Optoelectronic Multispectral Scanner p 46 A87-39190

Definition of a thermal infrared pushbroom imager for Earth observation p 53 N87-24765

The Multidetector Electro-optical Imaging Sensor (MEIS) 2 pushbroom imager: Four years of operation p 53 N87-24767

The stereo pushbroom scanner system Digital Photogrammetry System (DPS) and its accuracy p 53 N87-24768

Q

Q FACTORS

Optical Transfer Function (OTF)-based quality criteria for aerial cameras and imaging systems p 51 N87-24742

QUALITY CONTROL

SPOT image quality p 42 N87-24804

Image quality problems in practical aerial photography p 43 N87-24814

R

RADAR DATA

Forest biomass, canopy structure, and species composition relationships with multipolarization L-band synthetic aperture radar data p 4 A87-35121

Simulation of wind gradient errors in NROSS (Navy Remote Ocean Sensing System) radar scatterometer data in a simplified geometry
[AD-A175754] p 49 N87-20642

RADAR ECHOES

VHF radar for ocean surface current and sea state remote sensing p 19 A87-31631

The area-time-integral technique to estimate convective rain volumes over areas applied to satellite data - A preliminary investigation p 35 A87-40249

RADAR EQUIPMENT

Preliminary results obtained by DMAAC from the processing of a limited set of GEOSAT satellite radar altimeter data
[AD-A179081] p 50 N87-24734

RADAR IMAGERY

Shuttle Imaging Radar (SIR-B) investigations of the Canadian shield - Initial Report p 17 A87-31410

Multipolarization SAR data for surface feature delineation and forest vegetation characterization p 1 A87-31411

Interpretation of the polarimetric co-polarization phase term in radar images obtained with the JPL airborne L-band SAR system p 36 A87-31412

Relating polarization phase difference of SAR signals to scene properties p 1 A87-31413

Simulation software of synthetic aperture radar p 37 A87-32506

Models for radar scatterer density in terrain images p 45 A87-35344

Rapid analysis of satellite radar images of sea ice p 22 A87-35873

Some approaches for comparing remote and in-situ estimates of directional wave spectra p 24 A87-38835

Spaceborne imaging radar research in the 1990s - An overview p 46 A87-38837

A practical methodology for estimating wave spectra from the SIR-B p 25 A87-38841

Radiometric correction of SAR images - A new correction algorithm p 40 A87-39184

Urban land use separability as a function of radar polarization p 14 A87-39188

The propagation of short surface waves on longer gravity waves p 28 A87-40835

Multilook images of ocean waves by synthetic aperture radars p 28 A87-41068

Rectification of terrain induced distortions in radar imagery p 48 A87-42254

Radar scene generation for tactical decision aids
[NASA-CR-180234] p 40 N87-20449

NASA/MSFC large stretch press study
[NASA-CR-180376] p 41 N87-20554

Radar as a complement to topographic maps for delineating marine terraces
[PB87-154597] p 41 N87-24013

The effect of receiver amplifier non-linearity on ERS-1 synthetic aperture radar imagery p 52 N87-24755

RADAR MAPS

Introduction of geometric information to radar image data p 42 N87-24754

RADAR MEASUREMENT

Nadir looking airborne radar and possible applications to forestry p 7 A87-38095

Airborne microwave Doppler measurements of ocean wave directional spectra p 26 A87-39180

Measured radar return at the near vertical from forested terrains
[DE87-009384] p 11 N87-24593

RADAR SCANNING

The Radar Ocean-Wave Spectrometer p 25 A87-38846

RADAR SCATTERING

Models for radar scatterer density in terrain images p 45 A87-35344

RADAR TRACKING

West Antarctic ice streams draining into the Ross Ice Shelf Configuration and mass balance p 19 A87-31592

Lidar observation of elevated pollution layers over Los Angeles p 13 A87-33292

RADIANCE

GLAI estimation using measurements of red, near infrared, and middle infrared radiance p 4 A87-35119

Impact of radiance variations on satellite sensor calibration p 47 A87-39457

RADIATION ABSORPTION

Satellite sensing of aerosol absorption p 47 A87-40770

RADIATION DISTRIBUTION

Surface models including direct cross-radiation - A simple model of furrowed surfaces p 40 A87-39189

RADIATION EFFECTS

Impact of radiance variations on satellite sensor calibration p 47 A87-39457

RADIATIVE TRANSFER

Canopy reflectance, photosynthesis, and transpiration. II - The role of biophysics in the linearity of their interdependence p 6 A87-37278

The AVHRR/IRS operational method for satellite based sea surface temperature determination
[NOAA-TR-NESDIS-28] p 31 N87-22388

Modelling of atmospheric effects on the angular distribution of a backscattering peak
[DE87-006060] p 41 N87-24014

RADIO ALTIMETERS

The effect of a non-Gaussian point target response function on radar altimeter returns from the sea surface p 26 A87-39179

Preliminary results obtained by DMAAC from the processing of a limited set of GEOSAT satellite radar altimeter data
[AD-A179081] p 50 N87-24734

RADIO NAVIGATION

Aircraft radiopositioning for airborne photography during hydrographic coastal surveys p 23 A87-36945

RADIO TELESCOPES

GINFEST - Geodetic intercomparison network for evaluating space techniques p 15 A87-36164

RADIOMETERS

AVHRR data services in Europe - The Earthnet approach p 39 A87-37922

Radiometric comparison of the Landsat-5 TM and MSS sensors p 47 A87-41432

A crop condition and crop yield estimation method based on NOAA/AVHRR satellite data p 10 N87-22280

RADIOMETRIC CORRECTION

Calibration of satellite radiometers and the comparison of vegetation indices p 2 A87-32091

Correction for atmospheric and topographic effects on the Landsat MSS data p 37 A87-32489

Radiometric correction of SAR images - A new correction algorithm p 40 A87-39184

RADIOMETRIC RESOLUTION

- Deforestation in the tropics - New measurements in the Amazon Basin using Landsat and NOAA advanced very high resolution radiometer imagery p 4 A87-33441
- Satellite detection of tropical burning in Brazil p 8 A87-39191
- Monitoring vegetation using Nimbus-7 scanning multichannel microwave radiometer's data p 8 A87-39194
- Comparison of North and South American biomes from AVHRR observations p 9 A87-40303
- The use of AVHRR data in operational agricultural assessment in Africa p 9 A87-40304
- Radiometric calibration of the Shuttle Imaging Radar (SIR-C) system p 53 N87-24756

RAIN

- Determining rainfall intensity and type from GOES imagery in the midlatitudes p 34 A87-32092
- On the relative accuracy of satellite and raingage rainfall measurements over middle latitudes during daylight hours p 34 A87-33295
- Cloud-cover and precipitation patterns over the Republic of Guinea according to ground-based and satellite observations p 35 A87-36102
- Analysis of moderate and intense rainfall rates continuously recorded over half a century and influence on microwave communications planning and rain-rate data acquisition p 46 A87-36933
- The area-time-integral technique to estimate convective rain volumes over areas applied to satellite data - A preliminary investigation p 35 A87-40249
- Quick look Atlantic Ocean rain maps for gale [NASA-CR-180511] p 30 N87-21533
- Measurement and detection of precipitation. Satellite methods in the visible and the infrared p 36 N87-22364

RAIN FORESTS

- Trace gas exchanges and transports over the Amazonian rain forest p 12 A87-32196

RAIN GAGES

- On the relative accuracy of satellite and raingage rainfall measurements over middle latitudes during daylight hours p 34 A87-33295

REAL TIME OPERATION

- Optical image subtraction techniques, 1975-1985 p 40 A87-42659
- Real-time crop assessment using color theory and satellite data p 10 N87-20619

RED SEA

- Tectonic evaluation of the Nubian Shield of northeastern Sudan using Thematic Mapper imagery [NASA-CR-180575] p 19 N87-22319

REFLECTANCE

- Surface bidirectional reflectance properties of two southwestern Arizona deserts for wavelengths between 0.4 and 2.2 micrometers [NASA-TP-2643] p 49 N87-22281
- Inversion of canopy reflectance models for estimation of vegetation parameters [NASA-CR-181059] p 12 N87-24737

REFLECTED WAVES

- Wind and nadir angle effects on airborne lidar water 'surface' returns p 29 A87-42641

REGRESSION ANALYSIS

- The regression intersection method of adjusting image data for band rationing p 45 A87-35306
- A technique to estimate the ocean surface energy flux using VAS multispectral data p 30 N87-20710
- Error analysis of leaf area estimates made from allometric regression models [NASA-TM-89220] p 11 N87-24010

RELIEF MAPS

- Spaceborne imaging radar research in the 1990s - An overview p 46 A87-38837

REMOTE SENSING

- Signature-extendable technology - Global space-based crop recognition p 1 A87-31414
- VHF radar for ocean surface current and sea state remote sensing p 19 A87-31631
- Workshop on Space Remote Sensing for Agricultural and Thematic Mapping, Budapest, Hungary, Apr. 18, 1986, Proceedings p 1 A87-32007
- Remote sensing research in global agricultural productivity p 2 A87-32008
- Remote sensing methods of yield forecasting p 2 A87-32009
- The application of remote sensing in agricultural meteorology at the Meteorological Service of the HPR p 2 A87-32010
- Influence of different nitrogen and irrigation treatments on the spectral reflectance of barley p 2 A87-32090
- Calibration of satellite radiometers and the comparison of vegetation indices p 2 A87-32091
- Estimation of canopy parameters of row planted vegetation canopies using reflectance data for only four view directions p 2 A87-32093

- Habitat mapping by Landsat for aerial census of kangaroos p 2 A87-32094
- Measurement of the surface emissivity of turbid waters p 19 A87-32097
- The Netherlands-Indonesian remote-sensing satellite TERS p 43 A87-32210
- Balloon-borne infrared multichannel radiometer for remote sensing of high resolution low-level water vapor fields p 43 A87-32477
- Australian utilization and research into remote sensing p 20 A87-32490
- Landcover change in Hiroshima during 1979/1984 detected by Landsat MSS and TM data p 12 A87-32494
- Global vegetation monitoring using NOAA vegetation index data p 3 A87-32495
- Fundamental study on systematization of selecting new development area with Landsat data and topographic information p 12 A87-32496
- Earth resources satellite-1 (ERS-1) p 44 A87-32501
- United States remote sensing satellites (RSSs) past, present, and future p 56 A87-32502
- Coral reef remote sensing applications p 20 A87-32951
- Applications of satellite microwave radiometry in Finland p 44 A87-32952
- Indian remote sensing programme p 56 A87-32955
- Applied remote sensing - Book p 45 A87-33122
- Remote-sensing method for determining monthly precipitation sums using Meteor-satellite data on the Atlantic Ocean p 21 A87-34447
- French spot and the U.S. Landsat jockey for position in the race for a multimillion-dollar remote sensing market - commercial prospects for Landsat and Spot imagery p 56 A87-34600
- GLAI estimation using measurements of red, near infrared, and middle infrared radiance p 4 A87-35119
- Identifying vegetable crops with Landsat Thematic Mapper data p 4 A87-35120
- MIDAS - A new image-processing system for remote sensing p 37 A87-35183
- Quantifying spatial and temporal variabilities of microwave brightness temperature over the U.S. Southern Great Plains p 5 A87-35309
- Development of a satellite remote sensing technique for the study of alpine glaciers p 34 A87-35311
- The dependence of sea-surface microwave emission on wind speed, frequency, incidence angle, and polarization over the frequency range from 1 to 40 GHz p 22 A87-35515
- Seasonal and regional variations of active/passive microwave signatures of sea ice p 22 A87-35516
- Microwave sea-ice signatures near the onset of melt p 22 A87-35517
- The relation of millimeter-wavelength backscatter to surface snow properties p 34 A87-35518
- A soil thermal model for remote sensing p 5 A87-35521
- Comparison of Landsat MSS and TM data for urban land-use classification p 13 A87-35523
- Problems in the automation of map-compilation processes on the basis of remote-sensing data p 38 A87-35925
- Measurement of the spatial spectrum of ocean waves using a two-frequency scatterometer p 23 A87-36107
- Remote sensing - Handling the data p 38 A87-36359
- Mapping from space p 38 A87-36361
- Environmental protection from space p 13 A87-36363
- Fault patterns by space remote sensing and the rotation of western Oregon during Cenozoic times p 18 A87-36525
- An application of low altitude multispectral photography to agricultural field trials p 6 A87-37054
- What, where, when why? Extracting information from remote sensing data p 46 A87-37055
- Inferring spectral reflectances of plant elements by simple inversion of bidirectional reflectance measurements p 7 A87-37281
- Landsat as an aid in evaluating the adequacy of a grain silo network p 7 A87-37282
- Data Compression System for video images p 46 A87-37421
- Image preprocessing for line detection based on local structure analysis p 39 A87-37801
- The Geomult database management system p 39 A87-37802
- Detection of Rift Valley fever viral activity in Kenya by satellite remote sensing imagery p 7 A87-37827
- AVHRR data services in Europe - The Earthnet approach p 39 A87-37922
- Stochastic nature of Landsat MSS data p 46 A87-38093
- Temporal observations of surface soil moisture using a passive microwave sensor p 7 A87-38094

- Nadir looking airborne radar and possible applications to forestry p 7 A87-38095
- The factor of scale in remote sensing p 39 A87-38096
- Variations in the polarized leaf reflectance of Sorghum bicolor p 7 A87-38097
- Measuring ocean waves from space. Proceedings of the Symposium, Johns Hopkins University, Laurel, MD, Apr 15-17, 1986 p 24 A87-38826
- Some approaches for comparing remote and in-situ estimates of directional wave spectra p 24 A87-38835
- Wave-measurement capabilities of the surface contour radar and the airborne oceanographic lidar p 25 A87-38840
- The Radar Ocean-Wave Spectrometer p 25 A87-38846
- Remotely-sensed tracers for hydrodynamic surface flow estimation p 26 A87-39176
- A two-look technique for studying atmospheric effects in optical scanner data for the ocean p 26 A87-39178
- Airborne microwave Doppler measurements of ocean wave directional spectra p 26 A87-39180
- Deriving surface albedo measurements from narrow band satellite data p 13 A87-39182
- The Tethered Satellite System as a new remote sensing platform p 46 A87-39183
- Remote sensing of vegetation change near Inco's Sudbury mining complexes p 8 A87-39185
- Predicting the location of kimberlite from a probability analysis of linear structure on remote sensing data p 18 A87-39186
- Procedures for the description of agricultural crops and soils in optical and microwave remote sensing studies p 8 A87-39187
- Surface models including direct cross-radiation - A simple model of furrowed surfaces p 40 A87-39189
- Synergistic use of MOMS-01 and Landsat TM data - Modular Optoelectronic Multispectral Scanner p 46 A87-39190
- Satellite detection of tropical burning in Brazil p 8 A87-39191
- Thematic Mapper bandpass solar exoatmospheric irradiances p 40 A87-39192
- Monitoring vegetation using Nimbus-7 scanning multichannel microwave radiometer's data p 8 A87-39194
- High resolution remote sensing of spatially and spectrally complex coal surface mines of central Pennsylvania - A comparison between simulated SPOT MSS and Landsat-5 thematic mapper p 18 A87-39468
- Strategies and technologies for monitoring the environment p 14 A87-39593
- Spacelab data - A new contribution for structural interpretations of remotely sensed data in geology p 18 A87-39790
- Concerning the relationship between evapotranspiration and soil moisture p 8 A87-40244
- Airborne remote sensing of forest biomes p 9 A87-40301
- Comparison of North and South American biomes from AVHRR observations p 9 A87-40303
- The use of AVHRR data in operational agricultural assessment in Africa p 9 A87-40304
- Remote sensing applications in hydrology p 35 A87-40308
- Recent research in snow hydrology p 35 A87-40309
- Ice-edge eddies in the Fram Strait marginal ice zone p 27 A87-40432
- Remote sensing of the Fram Strait marginal ice zone p 27 A87-40433
- Remote sensing as a research tool - sea ice surveillance from aircraft and spacecraft p 28 A87-40648
- Satellite sensing of aerosol absorption p 47 A87-40770
- Remote sensing of coastal wetlands p 9 A87-40944
- Rice crop identification and area estimation using remotely-sensed data from Indian cropping patterns p 9 A87-41434
- The application of remote sensing techniques in China p 57 A87-41435
- Physical principles of image convergence in remote sensing p 40 A87-41925
- Use of maps, aerial photographs, and other remote sensor data for practical evaluations of hazardous waste sites p 14 A87-42255
- Remote sensing of chlorophyll concentrations in the northern Gulf of Mexico p 29 A87-42643
- A model for the use of satellite remote sensing for the measurement of primary production in the ocean p 29 A87-42644
- Sunlight induced 685 nm fluorescence imagery p 30 A87-42646

- Radar scene generation for tactical decision aids
[NASA-CR-180234] p 40 N87-20449
- NASA/MSFC large stretch press study
[NASA-CR-180376] p 41 N87-20554
- Real-time crop assessment using color theory and satellite data p 10 N87-20619
- Proceedings of the European Symposium on Polar platform Opportunities and instrumentation for Remote-Sensing (ESPOIR)
[ESA-SP-266] p 48 N87-20621
- Remote sensing applications: Commercial issues and opportunities for space station --- SPOT p 57 N87-20626
- Land panel report --- International Space Station p 49 N87-20634
- Potential of laser remote sensing of oil below water surface
[FOA-C-30435-3.1] p 30 N87-20659
- Foundations and applications of multispectral scanning in agriculture p 30 N87-20659
- [NLR-MP-85015-U] p 10 N87-21408
- Remotely sensed sea surface temperature for the Alpine Experiment (ALPEX) --- AVHRR-2 data p 30 N87-21497
- Comparative evaluation and guide for the integrated utilization of LANDSAT (MSS and TM) and SPOT (HRV) satellites remotely sensed data p 30 N87-21497
- [ETN-87-99356] p 41 N87-22278
- Problems in merging Earth sensing satellite data sets
[NASA-TM-87820] p 50 N87-22457
- Active and passive remote sensing of ice
[AD-A179461] p 32 N87-24009
- Error analysis of leaf area estimates made from allometric regression models
[NASA-TM-89220] p 11 N87-24010
- Proceedings of the International Symposium on Progress in Imaging Sensors p 50 N87-24738
- [ESA-SP-252] p 51 N87-24739
- Earth surface sensing in the '90's p 51 N87-24739
- Smart sensors: An overview and selected examples p 51 N87-24740
- A modular and versatile acquisition, recording and preprocessing system for airborne remote sensing p 52 N87-24751
- The Multidetector Electro-optical Imaging Sensor (MEIS) 2 pushbroom imager: Four years of operation p 53 N87-24767
- Estimating photogrammetric precision and cartographic potential of space imagery p 42 N87-24791
- Earth observation experiments on the German Spacelab mission D2 p 55 N87-24811
- Modern CCD sensors and their applications in Earth observation and planetary missions p 55 N87-24813
- Remote Sensing Information Sciences Research Group: Santa Barbara Information Sciences Research Group, year 4
[NASA-CR-181073] p 43 N87-24817
- REMOTE SENSORS**
- Coral reef remote sensing applications p 20 A87-32951
- Mid-infrared remote sensing systems and their application to lithologic mapping p 17 A87-35522
- Derivation of a fast algorithm to account for distortions due to terrain in earth-viewing satellite sensor images p 38 A87-35524
- Sensors for imaging p 45 A87-36360
- Space remote sensors p 47 A87-40379
- Simulations of the GOES visible sensor to changing surface and atmospheric conditions p 47 A87-40756
- Ground and aerial use of an infrared video camera with a mid-infrared filter (1.45 to 2.0 microns) p 48 A87-41588
- Laser reflectance as a function of rough water glitter profile
[AD-A178774] p 32 N87-23016
- Proceedings of the International Symposium on Progress in Imaging Sensors p 50 N87-24738
- [ESA-SP-252] p 51 N87-24739
- Earth surface sensing in the '90's p 51 N87-24739
- Smart sensors: An overview and selected examples p 51 N87-24740
- Earth Resources Satellite (ERS-1) project in Japan p 57 N87-24797
- RESEARCH AND DEVELOPMENT**
- Indian remote sensing programme p 56 A87-32955
- RICE**
- Rice crop identification and area estimation using remotely-sensed data from Indian cropping patterns p 9 A87-41434
- ROBOTICS**
- Space remote sensors p 47 A87-40379
- ROSS ICE SHELF**
- West Antarctic ice streams draining into the Ross Ice Shelf Configuration and mass balance p 19 A87-31592

RUN TIME (COMPUTERS)

- Rapid analysis of satellite radar images of sea ice p 22 A87-35873

S**SALINITY**

- Salinity effects on the microwave emission of soils p 5 A87-35520
- Continental shelf processes affecting the oceanography of the South Atlantic Bight
[DE87-005303] p 30 N87-20716

SAMPLING

- A crop condition and crop yield estimation method based on NOAA/AVHRR satellite data p 10 N87-22280
- Optical dynamics experiment (ODEX) data report R/V acania expedition 10 October-17 November 1982 Volume 2 Particle size distributions Volume 6 Scalar spectral-radiometer data
[AD-A178535] p 32 N87-23104

SATELLITE ALTIMETRY

- Biharmonic spline interpolation of GEOS-3 and Seasat altimeter data p 20 A87-32770
- Use of satellite altimetry for ocean monitoring p 23 A87-36101
- Spectrasat instrument design using maximum heritage p 26 A87-38847
- The Geosat altimeter mission - A milestone in satellite oceanography p 27 A87-40281
- Altimeter measurements for the determination of the Earth's gravity field
[NASA-CR-180520] p 17 N87-23033
- Ocean wind and wave model comparisons with GEOSAT (GEOSAT Satellite) satellite data
[AD-A178302] p 33 N87-24061
- Preliminary results obtained by DMAAC from the processing of a limited set of GEOSAT satellite radar altimeter data
[AD-A179081] p 50 N87-24734
- Radial orbit error reduction and sea surface topography determination using satellite altimetry
[NASA-CR-180570] p 33 N87-24816

SATELLITE ATTITUDE CONTROL

- Stereoscopic line scan imaging and satellite control
[DGLR PAPER 86-106] p 38 A87-36757
- Infrared Earth horizon sensor concepts in various spectral bands p 52 N87-24752

SATELLITE COMMUNICATION

- Analysis of moderate and intense rainfall rates continuously recorded over half a century and influence on microwave communications planning and rain-rate data acquisition p 46 A87-36933

SATELLITE DESIGN

- A Spectrasat system design based on the Geosat experiment p 26 A87-38848
- The first ESA remote sensing satellite (status and outlook) p 57 N87-24777
- Earth Resources Satellite (ERS-1) project in Japan p 57 N87-24797

SATELLITE IMAGERY

- Nimbus 7 SMMR investigation of snowpack properties in the northern Great Plains for the winter of 1978-1979 p 34 A87-31409
- Signature-extendable technology - Global space-based crop recognition p 1 A87-31414
- The application of remote sensing in agricultural meteorology at the Meteorological Service of the HPR p 2 A87-32010
- Determining rainfall intensity and type from GOES imagery in the midlatitudes p 34 A87-32092
- Habitat mapping by Landsat for aerial census of kangaroos p 2 A87-32094
- Continental land cover assessment using Landsat MSS data p 3 A87-32095
- Landsat classification of Argentina summer crops p 3 A87-32098
- The Netherlands-Indonesian remote-sensing satellite TERS p 43 A87-32210
- Spectral classification of Landsat-5 Thematic Mapper data p 37 A87-32488
- Correction for atmospheric and topographic effects on the Landsat MSS data p 37 A87-32489
- Australian utilization and research into remote sensing p 20 A87-32490
- Landcover change in Hiroshima during 1979/1984 detected by Landsat MSS and TM data p 12 A87-32494
- Global vegetation monitoring using NOAA vegetation index data p 3 A87-32495
- Monitoring of snow and ice in Hokkaido Island using multitemporal NOAA-AVHRR data p 20 A87-32497
- Relation between precipitation and brightness of earth surface in the NOAA/GVIP data p 3 A87-32498
- Coral reef remote sensing applications p 20 A87-32951

- Applications of satellite microwave radiometry in Finland p 44 A87-32952
- Reflectance characteristics and its application in the classification of Nigerian Savanna soils p 3 A87-32954
- Impact of satellite-based data on FGGE general circulation statistics p 44 A87-32985
- Deforestation in the tropics - New measurements in the Amazon Basin using Landsat and NOAA advanced very high resolution radiometer imagery p 4 A87-33441
- French spot and the U.S. Landsat jockey for position in the race for a multimillion-dollar remote sensing market --- commercial prospects for Landsat and Spot imagery p 56 A87-34600
- MIDAS - A new image-processing system for remote sensing p 37 A87-35183
- Automatic classification of Pointe d'Arcy landscapes using Thematic Mapper data with the aid of a textural analysis p 37 A87-35305
- The topographic effect on Landsat data in gently undulating terrain in southern Sweden p 4 A87-35307
- Development of a satellite remote sensing technique for the study of alpine glaciers p 34 A87-35311
- A comparison of supervised maximum likelihood and decision tree classification for crop cover estimation from multitemporal Landsat MSS data p 5 A87-35312
- A soil thermal model for remote sensing p 5 A87-35521
- Comparison of Landsat MSS and TM data for urban land-use classification p 13 A87-35523
- Derivation of a fast algorithm to account for distortions due to terrain in earth-viewing satellite sensor images p 38 A87-35524
- Rapid analysis of satellite radar images of sea ice p 22 A87-35873
- Satellite techniques for studying ice crusts and underground waters in the eastern Pamir p 35 A87-36106
- Remote sensing - Handling the data p 38 A87-36359
- Mapping from space p 38 A87-36361
- Environmental protection from space p 13 A87-36363
- Landform investigation utilizing digitally processed satellite Thematic Mapper imagery p 38 A87-36546
- Stereoscopic line scan imaging and satellite control
[DGLR PAPER 86-106] p 38 A87-36757
- Reconnaissance of vegetal formations in a Guinean forest sector by means of Landsat images p 6 A87-36946
- Preliminary report on the development of marine geographic information systems p 23 A87-37056
- Combining panchromatic and multispectral imagery from dual resolution satellite instruments p 38 A87-37276
- Merging multiresolution SPOT HRV and Landsat TM data p 38 A87-37287
- The Denali image map p 38 A87-37288
- Data Compression System for video images p 46 A87-37421
- Multisatellite data processing p 39 A87-37803
- Detection of Rift Valley fever viral activity in Kenya by satellite remote sensing imagery p 7 A87-37827
- Stochastic nature of Landsat MSS data p 46 A87-38093
- The factor of scale in remote sensing p 39 A87-38096
- A two-look technique for studying atmospheric effects in optical scanner data for the ocean p 26 A87-39178
- Deriving surface albedo measurements from narrow band satellite data p 13 A87-39182
- Remote sensing of vegetation change near Inco's Sudbury mining complexes p 8 A87-39185
- Predicting the location of kimberlite from a probability analysis of linear structure on remote sensing data p 18 A87-39186
- Synergistic use of MOMS-01 and Landsat TM data --- Modular Optoelectronic Multispectral Scanner p 46 A87-39190
- Monsoon flood boundary delineation and damage assessment using space borne imaging radar and Landsat data p 35 A87-39467
- High resolution remote sensing of spatially and spectrally complex coal surface mines of central Pennsylvania - A comparison between simulated SPOT MSS and Landsat-5 thematic mapper p 18 A87-39468
- Concerning the relationship between evapotranspiration and soil moisture p 8 A87-40244
- Soil moisture estimation using GOES-VISSR infrared data - A case study with a simple statistical method p 8 A87-40248
- The area-time-integral technique to estimate convective rain volumes over areas applied to satellite data - A preliminary investigation p 35 A87-40249
- The Geosat altimeter mission - A milestone in satellite oceanography p 27 A87-40281

Montane vegetation stratification through digital processing of Landsat MSS data p 9 A87-40302

The use of AVHRR data in operational agricultural assessment in Africa p 9 A87-40304

Ice-edge eddies in the Fram Strait marginal ice zone p 27 A87-40432

A soil map through Landsat satellite imagery in a part of the Auranga catchment in the Ranchi and Palamou districts of Bihar, India p 9 A87-41428

The application of remote sensing techniques in China p 57 A87-41435

Physical principles of image convergence in remote sensing p 40 A87-41925

A model for the use of satellite remote sensing for the measurement of primary production in the ocean p 29 A87-42644

Quick look Atlantic Ocean rain maps for gale [NASA-CR-180511] p 30 N87-21533

Possibilities of using artificial Earth satellite data for computing heat exchange between the ocean and atmosphere in Newfoundland energy-active zone during winter p 31 N87-21980

Tectonic evaluation of the Nubian Shield of northeastern Sudan using Thematic Mapper imagery [NASA-CR-180575] p 19 N87-22319

Enhanced LANDSAT images of Antarctica and planetary exploration p 50 N87-23558

Utilizing remote sensing of thematic mapper data to improve our understanding of estuarine processes and their influence on the productivity of estuarine-dependent fisheries [NASA-CR-180984] p 33 N87-24012

LANDSAT-based lineament analysis, East Texas Basin, and structural history of the Sabine Uplift area, East Texas and North Louisiana [PB87-176327] p 19 N87-24043

High resolution sea surface temperature field derived p 33 N87-24731

Comparative analysis of Thematic Mapper and SPOT image data for land use investigation p 51 N87-24746

Application of Modular Optoelectronic Multispectral Scanner (MOMS) data to hydrology and vegetation studies. Test site: Pantanal Region (Brazil/Paraguay) p 52 N87-24748

Optical and digital SAR processing techniques: A statistical comparison of accuracy using SEASAT imagery p 42 N87-24753

The stereo pushbroom scanner system Digital Photogrammetry System (DPS) and its accuracy p 53 N87-24768

SPOT image quality p 42 N87-24804

Arctic Sea ice, 1973-1976: Satellite passive-microwave observations [NASA-SP-489] p 33 N87-24870

SATELLITE INSTRUMENTS

A Spectrasat system design based on the Geosat experiment p 26 A87-38848

Impact of radiance variations on satellite sensor calibration p 47 A87-39457

SATELLITE NETWORKS

Multisatellite data processing p 39 A87-37803

SATELLITE OBSERVATION

A curious sea-surface-temperature phenomenon observed by Meteosat p 19 A87-31572

The French Space Oceanography Program p 20 A87-32503

On the relative accuracy of satellite and rain gauge rainfall measurements over middle latitudes during daylight hours p 34 A87-33295

An evaluation of satellite-based insolation estimates for Ohio p 34 A87-33297

Evaluation of a surface/vegetation parameterization using satellite measurements of surface temperature p 3 A87-33298

Recurring polynyas over the Cosmonaut Sea and the Maud Rise p 23 A87-37563

Comparison of satellite-derived sea surface temperatures with in situ skin measurements p 23 A87-37565

Detection of Rift Valley fever viral activity in Kenya by satellite remote sensing imagery p 7 A87-37827

Satellite measurements of sea surface cooling during hurricane Gloria p 24 A87-37886

Comparison of HCMM and GOES satellite temperatures and evaluation of surface statistics p 39 A87-38098

The operational performance of the fleet numerical oceanography center global spectral ocean-wave model p 24 A87-38832

Recent results with a third-generation ocean-wave model p 24 A87-38833

The microwave measurement of ocean-wave directional spectra p 24 A87-38836

Satellite detection of tropical burning in Brazil p 8 A87-39191

Strategies and technologies for monitoring the environment p 14 A87-39593

Regional and seasonal variations of surface reflectance from satellite observations at 0.6 micron p 27 A87-40250

Comparison of North and South American biomes from AVHRR observations p 9 A87-40303

Satellite sensing of aerosol absorption p 47 A87-40770

Report on the Special Program 78 satellite geodesy of the Technical University of Munich [ASTRON-GEODAET-ARB-48] p 16 N87-20618

Report of the workshop on Assimilation of Satellite Wind and Wave Data in Numerical Weather and Wave Prediction Models [WCP-122] p 49 N87-21521

A crop condition and crop yield estimation method based on NOAA/AVHRR satellite data p 10 N87-22280

Measurement and detection of precipitation: Satellite methods in the visible and the infrared p 36 N87-22364

Problems in merging Earth sensing satellite data sets [NASA-TM-87820] p 50 N87-22457

SATELLITE SOUNDING

Shuttle Imaging Radar (SIR-B) investigations of the Canadian shield - Initial Report p 17 A87-31410

Cloud-cover and precipitation patterns over the Republic of Guinea according to ground-based and satellite observations p 35 A87-36102

The possibility of using satellite measurements of methane in the atmosphere to study the global-distribution characteristics of its sources p 13 A87-36125

Monitoring vegetation using Nimbus-7 scanning multichannel microwave radiometer's data p 8 A87-39194

SATELLITE TRACKING

Earth rotation, station coordinates and orbit determination from satellite laser ranging p 43 A87-32349

Investigation of tectonic deformations using global satellite laser ranging data p 14 A87-33375

Reports on cartography and geodesy, series 1, number 96 [ISSN-0469-4236] p 16 N87-22282

SATELLITE-BORNE INSTRUMENTS

Calibration of satellite radiometers and the comparison of vegetation indices p 2 A87-32091

Derivation of a fast algorithm to account for distortions due to terrain in earth-viewing satellite sensor images p 38 A87-35524

GINFEST - Geodetic intercomparison network for evaluating space techniques p 15 A87-36164

Sensors for imaging p 45 A87-36360

Combining panchromatic and multispectral imagery from dual resolution satellite instruments p 38 A87-37276

Energy Balance of the Tropical Systems (BEST): A space experiment proposition p 36 N87-22373

Definition of a thermal infrared pushbroom imager for Earth observation p 53 N87-24765

Advanced imaging spectrometer for ocean color/fluorescence measurements and further applications p 33 N87-24766

The first ESA remote sensing satellite (status and outlook) p 57 N87-24777

The Monocular Electro-Optical Stereo Scanner (MEOSS) satellite experiment p 55 N87-24812

SATELLITE-BORNE PHOTOGRAPHY

The geostructural characteristics of the rift zone on the Lambert glacier (Antarctica) according to space images p 18 A87-36105

Statistical evaluation of forest characteristics from aerial and space photographs p 5 A87-36109

Aerial and space investigations of soils and vegetation - Russian book p 6 A87-36579

SATELLITE-BORNE RADAR

Spaceborne imaging radar research in the 1990s - An overview p 46 A87-38837

The physical basis for estimating wave-energy spectra with the radar ocean-wave spectrometer p 25 A87-38839

Monsoon flood boundary delineation and damage assessment using space borne imaging radar and Landsat data p 35 A87-39467

SCALE (RATIO)

The factor of scale in remote sensing p 39 A87-38096

SCATTERING COEFFICIENTS

Active and passive remote sensing of ice [AD-A179461] p 32 N87-24009

SCATTEROMETERS

Observation of precipitation from space by the weather radar p 44 A87-32507

Seasonal and regional variations of active/passive microwave signatures of sea ice p 22 A87-35516

Measurement of the spatial spectrum of ocean waves using a two-frequency scatterometer p 23 A87-36107

Simulation of wind gradient errors in NROSS (Navy Remote Ocean Sensing System) radar scatterometer data in a simplified geometry [AD-A175754] p 49 N87-20642

SCENE ANALYSIS

Relating polarization phase difference of SAR signals to scene properties p 1 A87-31413

Automatic classification of Pointe d'Arcay landscapes using Thematic Mapper data with the aid of a textural analysis p 37 A87-35305

SEA ICE

Monitoring of snow and ice in Hokkaido Island using multitemporal NOAA-AVHRR data p 20 A87-32497

Seasonal and regional variations of active/passive microwave signatures of sea ice p 22 A87-35516

Microwave sea-ice signatures near the onset of melt p 22 A87-35517

Rapid analysis of satellite radar images of sea ice p 22 A87-35873

Recurring polynyas over the Cosmonaut Sea and the Maud Rise p 23 A87-37563

Ice-edge eddies in the Fram Strait marginal ice zone p 27 A87-40432

Remote sensing of the Fram Strait marginal ice zone p 27 A87-40433

Statistical description of the summertime ice edge in the Chukchi Sea, task 2 [DE87-001056] p 31 N87-22387

Active and passive remote sensing of ice [AD-A179461] p 32 N87-24009

SEA ROUGHNESS

The present status of operational wave forecasting - for ocean surface p 24 A87-38831

SEA STATES

VHF radar for ocean surface current and sea state remote sensing p 19 A87-31631

Laser reflectance as a function of rough water glitter profile [AD-A178774] p 32 N87-23016

SEA SURFACE TEMPERATURE

A curious sea-surface-temperature phenomenon observed by Meteosat p 19 A87-31572

Measurement of the surface emissivity of turbid waters p 19 A87-32097

Sea surface temperature measurement from space allowing for the effect of the stratospheric aerosols p 22 A87-35148

Long waves in the equatorial Atlantic Ocean during 1983 p 23 A87-37564

Comparison of satellite-derived sea surface temperatures with in situ skin measurements p 23 A87-37565

Satellite measurements of sea surface cooling during hurricane Gloria p 24 A87-37886

Remotely sensed sea surface temperature for the Alpine Experiment (ALPEX) - AVHRR-2 data p 30 N87-21497

The 1982-1983 El Nino Atlas: Nimbus-7 microwave radiometer data [NASA-CR-180914] p 31 N87-22386

The AVHRR/HIRS operational method for satellite based sea surface temperature determination p 31 N87-22388

The impact of initial conditions and SST anomalies on extended range predictions for the El Nino period - sea surface temperature (SST) p 32 N87-23046

High resolution sea surface temperature field derived p 33 N87-24731

SEA TRUTH

Comparison of satellite-derived sea surface temperatures with in situ skin measurements p 23 A87-37565

The SIR-B mission: Towards an understanding of internal waves in the ocean [ARE-TR-86122] p 32 N87-23102

SEA WATER

Recurring polynyas over the Cosmonaut Sea and the Maud Rise p 23 A87-37563

The relationship between phytoplankton concentration and light attenuation in ocean waters p 29 A87-42642

Optical dynamics experiment (ODEX) data report R/V acania expedition 10 October-17 November 1982. Volume 2: Particle size distributions. Volume 6: Scalar spectral-radiometer data [AD-A178535] p 32 N87-23104

SEASAT SATELLITES

Spectrasat - A hybrid ROWS/SAR approach to monitor ocean waves from space p 25 A87-38845

SEGMENTS

An expert system for labeling segments in forward looking infrared (FLIR) imagery p 40 A87-42628

SHUTTLE IMAGING RADAR

Shuttle Imaging Radar (SIR-B) investigations of the Canadian shield - Initial Report p 17 A87-31410

Spaceborne imaging radar research in the 1990s - An overview p 46 A87-38837

- A practical methodology for estimating wave spectra from the SIR-B p 25 A87-38841
- The age and source of ocean swell observed in Hurricane Josephine p 25 A87-38843
- Spectrasat - A hybrid ROWS/SAR approach to monitor ocean waves from space p 25 A87-38845
- The SIR-B mission: Towards an understanding of internal waves in the ocean [ARE-TR-86122] p 32 N87-23102
- Radiometric calibration of the Shuttle Imaging Radar (SIR-C) system p 53 N87-24756
- SIDE-LOOKING RADAR**
- Rectification of terrain induced distortions in radar imagery p 48 A87-42254
- SIGNAL ANALYSIS**
- Relating polarization phase difference of SAR signals to scene properties p 1 A87-31413
- The effect of a non-Gaussian point target response function on radar altimeter returns from the sea surface p 26 A87-39179
- SIGNAL DETECTION**
- Active and passive remote sensing of ice [AD-A179461] p 32 N87-24009
- SIGNAL DISTORTION**
- Rectification of terrain induced distortions in radar imagery p 48 A87-42254
- SIGNAL TO NOISE RATIOS**
- Polarized views of the earth from orbital altitude p 48 A87-42639
- SIGNATURE ANALYSIS**
- Signature-extendable technology - Global space-based crop recognition p 1 A87-31414
- SIMULATION**
- Simulation of wind gradient errors in NROSS (Navy Remote Ocean Sensing System) radar scatterometer data in a simplified geometry [AD-A175754] p 49 N87-20642
- A review of national and international activities on modeling the effects of increased CO2 concentrations on the simulation of regional crop production: A report on linkage between climate and crop models [DE87-005994] p 10 N87-22336
- SKY RADIATION**
- Computation of diffuse sky irradiance from multidirectional radiance measurements p 6 A87-37279
- SNOW COVER**
- Nimbus 7 SMMR investigation of snowpack properties in the northern Great Plains for the winter of 1978-1979 p 34 A87-31409
- Monitoring of snow and ice in Hokkaido Island using multitemporal NOAA-AVHRR data p 20 A87-32497
- The relation of millimeter-wavelength backscatter to surface snow properties p 34 A87-35518
- Recent research in snow hydrology p 35 A87-40309
- Active and passive remote sensing of ice [AD-A179461] p 32 N87-24009
- SOFTWARE TOOLS**
- Simulation software of synthetic aperture radar p 37 A87-32506
- SOIL MAPPING**
- Aerial and space investigations of soils and vegetation --- Russian book p 6 A87-36579
- Global images of the earth's interior p 15 A87-37918
- A soil map through Landsat satellite imagery in a part of the Auranga catchment in the Ranchi and Palamou districts of Bihar, India p 9 A87-41428
- SOIL MOISTURE**
- Evaluation of a surface/vegetation parameterization using satellite measurements of surface temperature p 3 A87-33298
- Quantifying spatial and temporal variabilities of microwave brightness temperature over the U.S. Southern Great Plains p 5 A87-35309
- Salinity effects on the microwave emission of soils p 5 A87-35520
- A soil thermal model for remote sensing p 5 A87-35521
- Temporal observations of surface soil moisture using a passive microwave sensor p 7 A87-38094
- Concerning the relationship between evapotranspiration and soil moisture p 8 A87-40244
- Soil moisture estimation using GOES-VISSR infrared data - A case study with a simple statistical method p 8 A87-40248
- Evaluation of the airborne imaging spectrometer for remote sensing of forest stand conditions [NASA-CR-180918] p 10 N87-22296
- SOIL SCIENCE**
- Reflectance characteristics and its application in the classification of Nigerian Savanna soils p 3 A87-32954
- Salinity effects on the microwave emission of soils p 5 A87-35520

- Procedures for the description of agricultural crops and soils in optical and microwave remote sensing studies p 8 A87-39187
- SOILS**
- Salinity effects on the microwave emission of soils p 5 A87-35520
- SOLAR POSITION**
- Surface bidirectional reflectance properties of two southwestern Arizona deserts for wavelengths between 0.4 and 2.2 micrometers [NASA-TP-2643] p 49 N87-22281
- SOLAR RADIATION**
- Computation of diffuse sky irradiance from multidirectional radiance measurements p 6 A87-37279
- Thematic Mapper bandpass solar exoatmospheric irradiances p 40 A87-39192
- Satellite estimation of a solar irradiance at the surface of the earth and of surface albedo using a physical model applied to Meteosat data p 47 A87-40246
- A model for the use of satellite remote sensing for the measurement of primary production in the ocean p 29 A87-42644
- Modelling of atmospheric effects on the angular distribution of a backscattering peak [DE87-006060] p 41 N87-24014
- SORGHUM**
- A crop condition and crop yield estimation method based on NOAA-AVHRR satellite data p 10 N87-22280
- SOUTH AMERICA**
- Comparison of North and South American biomes from AVHRR observations p 9 A87-40303
- SOUTHERN CALIFORNIA**
- Lidar observation of elevated pollution layers over Los Angeles p 13 A87-33292
- SPACE BASED RADAR**
- Observation of precipitation from space by the weather radar p 44 A87-32507
- SPACE COMMERCIALIZATION**
- Anaspace top performance benefits ESA p 57 N87-24493
- SPACE EXPLORATION**
- Enhanced LANDSAT images of Antarctica and planetary exploration p 50 N87-23558
- SPACE PLATFORMS**
- A polar platform for the remote sensing needs of ecology and agriculture - A view from the U.K. p 9 A87-41430
- Proceedings of the European Symposium on Polar Platform Opportunities and Instrumentation for Remote Sensing (ESPOIR) [ESA-SP-266] p 48 N87-20621
- The Earth observation activities of the European Space Agency and the use of the polar platform of the International Space Station p 49 N87-20622
- Land panel report --- International Space Station p 49 N87-20634
- Ocean-ice panel report --- International Space Station p 30 N87-20635
- SPACE SHUTTLE PAYLOADS**
- Scientific goals and technical limitations of the shuttleborne synthetic aperture experiment X-SAR p 44 A87-32505
- Large format camera image analysis for mapping of land use patterns in the region Noale - Musone, Po-River-Plan, North Italy p 55 N87-24789
- Large Format Camera photographs of the Black Hills, USA, and their suitability for topographic and thematic mapping p 55 N87-24792
- SPACE STATIONS**
- Problems in merging Earth sensing satellite data sets [NASA-TM-87820] p 50 N87-22457
- SPACEBORNE EXPERIMENTS**
- Scientific goals and technical limitations of the shuttleborne synthetic aperture experiment X-SAR p 44 A87-32505
- Optimization of a program of experiments in connection with the operational planning of studies carried out with a spacecraft p 56 A87-34208
- SPACEBORNE PHOTOGRAPHY**
- A study of elevation measurement using LFC photograph --- Large Format Camera p 43 A87-32491
- Surface manifestations of hydrophysical processes in the Strait of Gibraltar according to 'Salyut-6' photographs p 35 A87-36103
- The geometry of the intersections of tectonic structures detected on satellite images p 17 A87-36104
- Spacelab data - A new contribution for structural interpretations of remotely sensed data in geology p 18 A87-39790
- Phase portraits of vegetation development trajectories in a multidimensional spectral attribute space p 10 A87-41771
- Proceedings of the International Symposium on Progress in Imaging Sensors [ESA-SP-252] p 50 N87-24738

- Investigation of simulated Monocular Electro-Optical Stereo Scanner (MEOSS)-imagery for sensor navigation and terrain derivation p 54 N87-24771
- The production of photographs of the Earth's surface taken from satellites and their application in map production and map revision p 55 N87-24788
- Large format camera image analysis for mapping of land use patterns in the region Noale - Musone, Po-River-Plan, North Italy p 55 N87-24789
- Estimating photogrammetric precision and cartographic potential of space imagery p 42 N87-24791
- Large Format Camera photographs of the Black Hills, USA, and their suitability for topographic and thematic mapping p 55 N87-24792
- The Monocular Electro-Optical Stereo Scanner (MEOSS) satellite experiment p 55 N87-24812
- The Modular Optoelectronic Multispectral Scanner (MOMS) program of the Bundesministerium fuer Forschung und Technologie (BMFT) Milestones in the development of an operational Earth Observation system p 55 N87-24815
- SPACELAB**
- Spacelab data - A new contribution for structural interpretations of remotely sensed data in geology p 18 A87-39790
- SPACELAB PAYLOADS**
- Earth observation experiments on the German Spacelab mission D2 p 55 N87-24811
- The Modular Optoelectronic Multispectral Scanner (MOMS) program of the Bundesministerium fuer Forschung und Technologie (BMFT) Milestones in the development of an operational Earth Observation system p 55 N87-24815
- SPATIAL DISTRIBUTION**
- Quantifying spatial and temporal variabilities of microwave brightness temperature over the U.S. Southern Great Plains p 5 A87-35309
- Comparison of HCMA' and GOES satellite temperatures and evaluation of surface statistics p 39 A87-38098
- Ten year change in forest succession and composition measured by remote sensing [NASA-CR-180948] p 11 N87-24736
- SPATIAL RESOLUTION**
- The factor of scale in remote sensing p 39 A87-38096
- SPECIFICATIONS**
- The role of government specifications in aerial photography p 57 N87-24780
- SPECTRAL BANDS**
- Thematic Mapper bandpass solar exoatmospheric irradiances p 40 A87-39192
- Comparative analysis of Thematic Mapper and SPOT image data for land use investigation p 51 N87-24746
- Infrared Earth horizon sensor concepts in various spectral bands p 52 N87-24752
- SPECTRAL ENERGY DISTRIBUTION**
- The physical basis for estimating wave-energy spectra with the radar ocean-wave spectrometer p 25 A87-38839
- Phase portraits of vegetation development trajectories in a multidimensional spectral attribute space p 10 A87-41771
- SPECTRAL REFLECTANCE**
- Influence of different nitrogen and irrigation treatments on the spectral reflectance of barley p 2 A87-32090
- Estimation of canopy parameters of row planted vegetation canopies using reflectance data for only four view directions p 2 A87-32093
- Reflectance characteristics and its application in the classification of Nigerian Savanna soils p 3 A87-32954
- Canopy reflectance, photosynthesis, and transpiration II - The role of biophysics in the linearity of their interdependence p 6 A87-37278
- Inferring spectral reflectances of plant elements by simple inversion of bidirectional reflectance measurements p 7 A87-37281
- Variations in the polarized leaf reflectance of Sorghum bicolor p 7 A87-38097
- Thematic Mapper bandpass solar exoatmospheric irradiances p 40 A87-39192
- Regional and seasonal variations of surface reflectance from satellite observations at 0.6 micron p 27 A87-40250
- Reflectivity of earth's surface and clouds in ultraviolet from satellite observations p 4 A87-40768
- Evaluation of the airborne imaging spectrometer for remote sensing of forest stand conditions [NASA-CR-180918] p 10 N87-22296
- Determination of spectral reflectance of crops during growth from calibrated multispectral small format aerial photography p 12 N87-24801
- SPECTROPHOTOMETRY**
- Spectrophotometric measurements on color aerial photographs p 55 N87-24798

SPECTROHADIOMETERS

- SPECTROHADIOMETERS**
Influence of different nitrogen and irrigation treatments on the spectral reflectance of barley p 2 A87-32090
Evaluation of the airborne imaging spectrometer for remote sensing of forest stand conditions [NASA-CR-180918] p 10 N87-22296
- SPECTRUM ANALYSIS**
A Spectrasat system design based on the Geosat experiment p 26 A87-38848
- SPECULAR REFLECTION**
Laser reflectance as a function of rough water glitter profile [AD-A178774] p 32 N87-23016
- SPLINE FUNCTIONS**
Biharmonic spline interpolation of GEOS-3 and Seasat altimeter data p 20 A87-32770
- SPOT (FRENCH SATELLITE)**
French spot and the U.S. Landsat jockey for position in the race for a multimillion-dollar remote sensing market ... commercial prospects for Landsat and Spot imagery p 56 A87-34600
First results of latent cover mapping with SPOT images The Kangaba region (South-Mali) p 18 A87-36925
Combining panchromatic and multispectral imagery from dual resolution satellite instruments p 38 A87-37276
Remote sensing of coastal wetlands p 9 A87-40944
Remote sensing applications. Commercial issues and opportunities for space station ... SPOT p 57 N87-20626
Comparative evaluation and guide for the integrated utilization of LANDSAT (MSS and TM) and SPOT (HRV) satellites remotely sensed data [ETN-87-99356] p 41 N87-22278
Comparative analysis of Thematic Mapper and SPOT image data for land use investigation p 51 N87-24746
SPOT image quality p 42 N87-24804
- STANDARDIZATION**
Thoughts on a standard algorithm for camera calibration p 51 N87-24743
- STATISTICAL ANALYSIS**
Some observations on crop profile modelling p 5 A87-35310
Predicting the location of kimberlite from a probability analysis of linear structure on remote sensing data p 18 A87-39186
Earth science research [NASA-CR-180512] p 11 N87-24733
- STATISTICAL WEATHER FORECASTING**
Impact of satellite-based data on FGGE general circulation statistics p 44 A87-32985
- STEREOPHOTOGRAPHY**
The stereo pushbroom scanner system Digital Photogrammetry System (DPS) and its accuracy p 53 N87-24768
- STEREOSCOPY**
Stereoscopic line scan imaging and satellite control [DGLR PAPER 86-106] p 38 A87-36757
Investigation of simulated Monocular Electro-Optical Stereo Scanner (MEOSS)-imagery for sensor navigation and terrain derivation p 54 N87-24771
- STOCHASTIC PROCESSES**
Stochastic nature of Landsat MSS data p 46 A87-38093
- STRAITS**
Surface manifestations of hydrophysical processes in the Strait of Gibraltar according to "Salyut-6" photographs p 35 A87-36103
Ice-edge eddies in the Fram Strait marginal ice zone p 27 A87-40432
Remote sensing of the Fram Strait marginal ice zone p 27 A87-40433
Mesoscale oceanographic processes beneath the ice of Fram Strait p 28 A87-40434
- STRATIFICATION**
Montane vegetation stratification through digital processing of Landsat MSS data p 9 A87-40302
- STRATOSPHERE**
Sea surface temperature measurement from space allowing for the effect of the stratospheric aerosols p 22 A87-35148
- STRUCTURAL ANALYSIS**
LANDSAT-based lineament analysis, East Texas Basin, and structural history of the Sabine Uplift area, East Texas and North Louisiana [PB87-176327] p 19 N87-24043
- STRUCTURAL PROPERTIES (GEOLOGY)**
Fault patterns by space remote sensing and the rotation of western Oregon during Cenozoic times p 18 A87-36525
Image preprocessing for line detection based on local structure analysis p 39 A87-37801
Spacelab data - A new contribution for structural interpretations of remotely sensed data in geology p 18 A87-39790

- Tectonic evaluation of the Nubian Shield of northeastern Sudan using Thematic Mapper imagery [NASA-CR-180575] p 19 N87-22319
Radar as a complement to topographic maps for delineating marine terraces [PB87-154597] p 41 N87-24013
LANDSAT-based lineament analysis, East Texas Basin, and structural history of the Sabine Uplift area, East Texas and North Louisiana [PB87-176327] p 19 N87-24043
- SUBTRACTION**
Optical image subtraction techniques, 1975-1985 p 40 A87-42659
- SUDAN**
Tectonic evaluation of the Nubian Shield of northeastern Sudan using Thematic Mapper imagery [NASA-CR-180575] p 19 N87-22319
- SUNLIGHT**
Sunlight induced 665 nm fluorescence imagery p 30 A87-42646
- SUPERHIGH FREQUENCIES**
Scientific goals and technical limitations of the shuttleborne synthetic aperture experiment X-SAR p 44 A87-32505
- SURFACE DISTORTION**
Rectification of terrain induced distortions in radar imagery p 48 A87-42254
- SURFACE LAYERS**
Remotely-sensed tracers for hydrodynamic surface flow estimation p 26 A87-39176
Studies of the east Australian current off northern New South Wales [AD-A178461] p 32 N87-23103
- SURFACE NAVIGATION**
Application of Global Positioning System (GPS) receiver for Earth observation p 53 N87-24763
- SURFACE PROPERTIES**
Deriving surface albedo measurements from narrow band satellite data p 13 A87-39182
- SURFACE ROUGHNESS**
Estimation of roughness of the earth's surface using Landsat MSS data on the assumption of reciprocity on light scattering p 12 A87-32493
Surface models including direct cross-radiation - A simple model of furrowed surfaces p 40 A87-39189
Laser reflectance as a function of rough water glitter profile [AD-A178774] p 32 N87-23016
- SURFACE TEMPERATURE**
Evaluation of a surface/vegetation parameterization using satellite measurements of surface temperature p 3 A87-33298
A soil thermal model for remote sensing p 5 A87-35521
Comparison of HCMM and GOES satellite temperatures and evaluation of surface statistics p 39 A87-38098
- SURFACE WAVES**
The present status of operational wave forecasting ... for ocean surface p 24 A87-38831
A practical methodology for estimating wave spectra from the SIR-B p 25 A87-38841
The propagation of short surface waves on longer gravity waves p 28 A87-40835
- SYNOPTIC MEASUREMENT**
Use of satellite altimetry for ocean monitoring p 23 A87-36101
- SYNOPTIC METEOROLOGY**
World-wide weather ... Book p 56 A87-33125
- SYNTHETIC APERTURE RADAR**
Multipolarization SAR data for surface feature delineation and forest vegetation characterization p 1 A87-31411
Interpretation of the polarimetric co-polarization phase term in radar images obtained with the JPL airborne L-band SAR system p 36 A87-31412
Relating polarization phase difference of SAR signals to scene properties p 1 A87-31413
Scientific goals and technical limitations of the shuttleborne synthetic aperture experiment X-SAR p 44 A87-32505
Simulation software of synthetic aperture radar p 37 A87-32506
Polarization, land use type and intraurban location as variables in SAR mapping accuracy p 12 A87-32953
Forest biomass, canopy structure, and species composition relationships with multipolarization L-band synthetic aperture radar data p 4 A87-35121
Determination of the velocity of ocean gyres through Synthetic Aperture Radar p 22 A87-35314
Spectrasat instrument design using maximum heritage p 26 A87-38847
Radiometric correction of SAR images - A new correction algorithm p 40 A87-39184
Urban land use separability as a function of radar polarization p 14 A87-39188

- Multilook images of ocean waves by synthetic aperture radars p 28 A87-41068
The effect of receiver amplifier non-linearity on ERS-1 synthetic aperture radar imagery p 52 N87-24755
- T**
- TARGET ACQUISITION**
An expert system for labeling segments in forward looking infrared (FLIR) imagery p 40 A87-42628
- TARGET RECOGNITION**
The integration of spectral and spatial analysis for land use classification [AD-A178703] p 14 N87-23015
- TECHNOLOGICAL FORECASTING**
Earth surface sensing in the 90's p 51 N87-24739
- TECHNOLOGY ASSESSMENT**
Very high resolution aerial films p 54 N87-24776
- TECHNOLOGY UTILIZATION**
European utilization aspects studies ... space stations p 49 N87-20624
- TECTONICS**
Investigation of tectonic deformations using global satellite laser ranging data p 14 A87-33375
The geometry of the intersections of tectonic structures detected on satellite images p 17 A87-38104
GPS-based geodesy in California, Mexico and the Caribbean p 16 A87-41380
Tectonic evaluation of the Nubian Shield of northeastern Sudan using Thematic Mapper imagery [NASA-CR-180575] p 19 N87-22319
- TELEVISION CAMERAS**
Ground and aerial use of an infrared video camera with a long-infrared filter (1.45 to 2.0 microns) p 48 A87-41588
- TEMPERATURE DISTRIBUTION**
Continental shelf processes affecting the oceanography of the South Atlantic Bight [DE87-005303] p 30 N87-20716
High resolution sea surface temperature field derived p 33 N87-24731
- TEMPERATURE MEASUREMENT**
Measurement of the surface emissivity of turbid waters p 19 A87-32097
Sea surface temperature measurement from space allowing for the effect of the stratospheric aerosols p 22 A87-35148
- TEMPORAL DISTRIBUTION**
Quantifying spatial and temporal variabilities of microwave brightness temperature over the U.S. Southern Great Plains p 5 A87-35309
- TEMPORAL RESOLUTION**
Temporal observations of surface soil moisture using a passive microwave sensor p 7 A87-38094
- TERRAIN**
Measured radar return at the near vertical from forested terrains [DE87-009384] p 11 N87-24593
- TERRAIN ANALYSIS**
Models for radar scatterer density in terrain images p 45 A87-35344
Phase portraits of vegetation development trajectories in a multidimensional spectral attribute space p 10 A87-41771
Investigation of simulated Monocular Electro-Optical Stereo Scanner (MEOSS)-imagery for sensor navigation and terrain derivation p 54 N87-24771
- TETHERED SATELLITES**
The Tethered Satellite System as a new remote sensing platform p 46 A87-39183
- TEXAS**
LANDSAT-based lineament analysis, East Texas Basin, and structural history of the Sabine Uplift area, East Texas and North Louisiana [PB87-176327] p 19 N87-24043
- TEXTURES**
Automatic classification of Pointe d'Arcay landscapes using Thematic Mapper data with the aid of a textural analysis p 37 A87-35305
The integration of spectral and spatial analysis for land use classification [AD-A178703] p 14 N87-23015
- THEMATIC MAPPING**
Workshop on Space Remote Sensing for Agricultural and Thematic Mapping, Budapest, Hungary, Apr. 18, 1986, Proceedings p 1 A87-32007
Spectral classification of Landsat-5 Thematic Mapper data p 37 A87-32488
Landcover change in Hiroshima during 1979/1984 detected by Landsat MSS and TM data p 12 A87-32494
Polarization, land use type and intraurban location as variables in SAR mapping accuracy p 12 A87-32953
Identifying vegetable crops with Landsat Thematic Mapper data p 4 A87-35120

Automatic classification of Pointe d'Arcay landscapes using Thematic Mapper data with the aid of a textural analysis p 37 A87-35305

The topographic effect on Landsat data in gently undulating terrain in southern Sweden p 4 A87-35307

Landform investigation utilizing digitally processed satellite Thematic Mapper imagery p 38 A87-36546

Combining panchromatic and multispectral imagery from dual resolution satellite instruments p 38 A87-37276

An assessment of Landsat MSS and TM data for urban and near-urban land-cover digital classification p 13 A87-37280

Merging multiresolution SPOT HRV and Landsat TM data p 38 A87-37287

Global images of the earth's interior p 15 A87-37918

Remote sensing of vegetation change near Inco's Sudbury mining complexes p 8 A87-39185

Thematic Mapper bandpass solar exoatmospheric irradiances p 40 A87-39192

Radiometric comparison of the Landsat-5 TM and MSS sensors p 47 A87-41432

Reports on cartography and geodesy, series 1, number 97 [ISSN-0469-4236] p 16 A87-22286

Tectonic evaluation of the Nubian Shield of northeastern Sudan using Thematic Mapper imagery [NASA-CR-180575] p 19 A87-22219

Utilizing remote sensing of thematic mapper data to improve our understanding of estuarine processes and their influence on the productivity of estuarine-dependent fisheries [NASA-CR-180984] p 33 A87-24012

Spatial characterization of acid rain stress in Canadian Shield lakes [NASA-CR-180983] p 36 A87-24031

Earth science research [NASA-CR-180512] p 11 A87-24733

Comparative analysis of Thematic Mapper and SPOT image data for land use investigation p 51 A87-24746

Towards an automatic identification of urban textures p 14 A87-24747

Application of Modular Optoelectronic Multispectral Scanner (MOMS) data to hydrology and vegetation studies. Test site: Pantanal Region (Brazil/Paraguay) p 52 A87-24748

TIROS SATELLITES

United States remote sensing satellites (RSSs) past, present, and future p 56 A87-32502

TOPEX

The French Space Oceanography Program p 20 A87-32503

Spectrasat instrument design using maximum heritage p 26 A87-38847

TOPOGRAPHY

Correction for atmospheric and topographic effects on the Landsat MSS data p 37 A87-32489

Fundamental study on systematization of selecting new development area with Landsat data and topographic information p 12 A87-32496

The topographic effect on Landsat data in gently undulating terrain in southern Sweden p 4 A87-35307

Wave-measurement capabilities of the surface contour radar and the airborne oceanographic lidar p 25 A87-38840

Feedback between ice flow, barotropic flow, and baroclinic flow in the presence of bottom topography p 27 A87-40289

Reports on cartography and geodesy, series 1, number 97 [ISSN-0469-4236] p 16 A87-22286

Radar as a complement to topographic maps for delineating marine terraces [PB87-154597] p 41 A87-24013

Large Format Camera photographs of the Black Hills, USA and their suitability for topographic and thematic mapping p 55 A87-24792

Radial orbit error reduction and sea surface topography determination using satellite altimetry [NASA CR 180570] p 33 A87-24816

TOXIC HAZARDS

Use of maps, aerial photographs and other remote sensor data for practical evaluations of hazardous waste sites p 14 A87-42255

TRACERS

Remotely-sensed tracers for hydrodynamic surface flow estimation p 26 A87-39176

TRACKING STATIONS

Earth rotation station coordinates and orbit determination from satellite laser ranging p 43 A87-32349

TRANSFER FUNCTIONS

The AVHRR HIRS operational method for satellite based sea surface temperature determination NOAA TR NCEP-28 p 31 A87-22388

TRANSPIRATION

Canopy reflectance, photosynthesis, and transpiration II - The role of biophysics in the linearity of their interdependence p 6 A87-37278

TREES (PLANTS)

Earth science research [NASA-CR-180512] p 11 A87-24733

TRIANGULATION

Aerotriangulation without ground control p 46 A87-37289

The effects of camera position and attitude data in aerial triangulation, a simulation study p 52 A87-24750

Aerial triangulation of CCD line-scanner images p 54 A87-24769

TROPICAL METEOROLOGY

Cloud-cover and precipitation patterns over the Republic of Guinea according to ground-based and satellite observations p 35 A87-36102

Measurement and detection of precipitation. Satellite methods in the visible and the infrared p 36 A87-22364

TROPICAL REGIONS

Deforestation in the tropics - New measurements in the Amazon Basin using Landsat and NOAA advanced very high resolution radiometer imagery p 4 A87-33441

Satellite detection of tropical burning in Brazil p 8 A87-39191

Measurement and detection of precipitation. Satellite methods in the visible and the infrared p 36 A87-22364

Energy Balance of the Tropical Systems (BEST): A space experiment proposition p 36 A87-22373

TROPOSPHERE

Operational overview of NASA GTE/CITE 1 airborne instrument intercomparisons - Carbon monoxide, nitric oxide, and hydroxyl instrumentation - Global Tropospheric Experiment/Chemical Instrumentation Test and Evaluation p 45 A87-33426

OH measurement near the intertropical convergence zone in the Pacific p 21 A87-33430

Measurements of nitric oxide in the boundary layer and free troposphere over the Pacific Ocean p 21 A87-33431

Free tropospheric and boundary layer measurements of NO over the central and eastern North Pacific Ocean p 21 A87-33432

Carbon monoxide measurements over the eastern Pacific during GTE/CITE 1 - Chemical Instrumentation Test and Evaluation p 21 A87-33435

TURBIDITY

Measurement of the surface emissivity of turbid waters p 19 A87-32097

U

UK SPACE PROGRAM

A polar platform for the remote sensing needs of ecology and agriculture - A view from the UK p 9 A87-41430

ULTRAVIOLET RADIATION

Reflectivity of earth's surface and clouds in ultraviolet from satellite observations p 47 A87-40768

UNDERWATER OPTICS

Ocean optics VIII, Proceedings of the Meeting, Orlando, FL, Mar. 31-Apr 2, 1986 [SPIE-637] p 28 A87-42637

UNITED STATES

Continental land cover assessment using Landsat MSS data p 3 A87-32095

Spatial characterization of acid rain stress in Canadian Shield lakes [NASA-CR-180992] p 36 A87-24032

USER MANUALS (COMPUTER PROGRAMS)

Quick-look guide to the crustal dynamics project's data information system [NASA-TM-87818] p 16 A87-23018

USER REQUIREMENTS

European utilization aspects studies - space stations p 49 A87-20624

Comparative evaluation and guide for the integrated utilization of LANDSAT (MSS and TM) and SPOT (HRV) satellites remotely sensed data [ETN-87-99356] p 41 A87-22278

V

VEGETABLES

Identifying vegetable crops with Landsat Thematic Mapper data p 4 A87-35120

VEGETATION

Multipolarization SAR data for surface feature delineation and forest vegetation characterization p 1 A87-31411

Aerial and space investigations of soils and vegetation - Russian book p 6 A87-36579

Reconnaissance of vegetal formations in a Guinean forest sector by means of Landsat images p 6 A87-36946

Testing the consistency for mapping urban vegetation with high-altitude aerial photographs and Landsat MSS data p 13 A87-37277

Application of Modular Optoelectronic Multispectral Scanner (MOMS) data to hydrology and vegetation studies. Test site: Pantanal Region (Brazil/Paraguay) p 52 A87-24748

VEGETATION GROWTH

Variations in the polarized leaf reflectance of Sorghum bicolor p 7 A87-38097

Remote sensing of vegetation change near Inco's Sudbury mining complexes p 8 A87-39185

A software defoliant for geological analysis of band ratios p 18 A87-39193

Monitoring vegetation using Nimbus-7 scanning multichannel microwave radiometer's data p 8 A87-39194

Montane vegetation stratification through digital processing of Landsat MSS data p 9 A87-40302

Comparison of North and South American biomes from AVHRR observations p 9 A87-40303

Ten year change in forest succession and composition measured by remote sensing [NASA-CR-180948] p 11 A87-24736

VEGETATIVE INDEX

Calibration of satellite radiometers and the comparison of vegetation indices p 2 A87-32091

Estimation of canopy parameters of row planted vegetation canopies using reflectance data for only four view directions p 2 A87-32093

Global vegetation monitoring using NOAA vegetation index data p 3 A87-32495

Relation between precipitation and brightness of earth surface in the NOAA/GVIP data p 3 A87-32498

Evaluation of a surface/vegetation parameterization using satellite measurements of surface temperature p 3 A87-33298

GLAI estimation using measurements of red, near infrared, and middle infrared radiance p 4 A87-35119

VERTICAL AIR CURRENTS

Observations of intermittent cumulus convection in the boundary layer p 20 A87-32976

VERTICAL DISTRIBUTION

Optical properties of the marine atmospheric boundary layer - Aerosol profiles p 28 A87-42638

VERTICAL ORIENTATION

Measured radar return at the near vertical from forested terrains [DE87-009384] p 11 A87-24593

VERY HIGH FREQUENCIES

VHF radar for ocean surface current and sea state remote sensing p 19 A87-31631

VERY LONG BASE INTERFEROMETRY

Creation of a global geodetic network using Mark III VLBI p 15 A87-36166

VIDEO DATA

Data Compression System for video images p 46 A87-37421

VIDEO EQUIPMENT

Ground and aerial use of an infrared video camera with a mid-infrared filter (1.45 to 2.0 microns) p 48 A87-41588

VIDEO SIGNALS

Laser reflectance as a function of rough water glitter profile [AD-A178774] p 32 A87-23016

VIEW EFFECTS

Impact of radiance variations on satellite sensor calibration p 47 A87-39457

VIRUSES

Detection of Rift Valley fever viral activity in Kenya by satellite remote sensing imagery p 7 A87-37827

VISIBLE INFRARED SPIN SCAN RADIOMETER

Simulations of the GOES visible sensor to changing surface and atmospheric conditions p 47 A87-40756

VISIBLE SPECTRUM

Procedures for the description of agricultural crops and soils in optical and microwave remote sensing studies p 8 A87-39187

Optical dynamics experiment (ODEX) data report R-V acania expedition 10 October-17 November 1982 - Volume 2 - Particle size distributions. Volume 6 - Scalar spectral-radiometer data [AD-A178535] p 32 A87-23104

VISUAL OBSERVATION

Temporal observations of surface soil moisture using a passive microwave sensor p 7 A87-38094

VISUAL PERCEPTION

The integration of spectral and spatial analysis for land use classification [AD-A178703] p 14 A87-23015

VOLCANOES

VOLCANOES

- Synergistic use of MOMS-01 and Landsat TM data ---
Modular Optoelectronic Multispectral Scanner p 46 A87-39190

VORTICES

- Ice-edge eddies in the Fram Strait marginal ice zone p 27 A87-40432

W

WASTE DISPOSAL

- Use of maps, aerial photographs, and other remote sensor data for practical evaluations of hazardous waste sites p 14 A87-42255

WATER

- Laser reflectance as a function of rough water glitter profile [AD-A178774] p 32 N87-23016

WATER BALANCE

- Energy Balance of the Tropical Systems (BEST): A space experiment proposition p 36 N87-22373

WATER CIRCULATION

- Long waves in the equatorial Atlantic Ocean during 1983 p 23 A87-37564
Remotely-sensed tracers for hydrodynamic surface flow estimation p 26 A87-39176

WATER COLOR

- The relationship between phytoplankton concentration and light attenuation in ocean waters p 29 A87-42642
Remote sensing of chlorophyll concentrations in the northern Gulf of Mexico p 29 A87-42643
Coastal zone color scanner imagery of phytoplankton pigment distribution in Icelandic waters p 29 A87-42645

WATER POLLUTION

- Inland wetland change detection using aircraft MSS data p 36 A87-42256

WATER QUALITY

- Spatial characterization of acid rain stress in Canadian Shield lakes [NASA-CR-180983] p 36 N87-24031
Spatial characterization of acid rain stress in Canadian Shield lakes [NASA-CR-180982] p 36 N87-24032

WATER VAPOR

- Balloon-borne infrared multichannel radiometer for remote sensing of high resolution low-level water vapor fields p 43 A87-32477

WATER WAVES

- Measurement of the spatial spectrum of ocean waves using a two-frequency scatterometer p 23 A87-36107
Measuring ocean waves from space; Proceedings of the Symposium, Johns Hopkins University, Laurel, MD, Apr. 15-17, 1986 p 24 A87-38826
The present status of operational wave forecasting --- for ocean surface p 24 A87-38831
The operational performance of the fleet numerical oceanography center global spectral ocean-wave model p 24 A87-38832
Recent results with a third-generation ocean-wave model p 24 A87-38833
Some approaches for comparing remote and in-situ estimates of directional wave spectra p 24 A87-38835
The microwave measurement of ocean-wave directional spectra p 24 A87-38836
The physical basis for estimating wave-energy spectra with the radar ocean-wave spectrometer p 25 A87-38839
Wave-measurement capabilities of the surface contour radar and the airborne oceanographic lidar p 25 A87-38840
A practical methodology for estimating wave spectra from the SIR-B p 25 A87-38841
Spectrasat - A hybrid ROWS/SAR approach to monitor ocean waves from space p 25 A87-38845
The Radar Ocean-Wave Spectrometer p 25 A87-38846
A Spectrasat system design based on the Geosat experiment p 26 A87-38848
Airborne microwave Doppler measurements of ocean wave directional spectra p 26 A87-39180
Multilook images of ocean waves by synthetic aperture radars p 28 A87-41068
Report of the workshop on Assimilation of Satellite Wind and Wave Data in Numerical Weather and Wave Prediction Models [WCP-122] p 49 N87-21521
The SIR-B mission: Towards an understanding of internal waves in the ocean [ARE-TR-86122] p 32 N87-23102
Ocean wind and wave model comparisons with GEOSAT (GEOSAT Satellite) satellite data [AD-A178302] p 33 N87-24061

WATERSHEDS

- A soil map through Landsat satellite imagery in a part of the Auranga catchment in the Ranchi and Palamou districts of Bihar, India p 9 A87-41428

WAVE PROPAGATION

- Long waves in the equatorial Atlantic Ocean during 1983 p 23 A87-37564
The propagation of short surface waves on longer gravity waves p 28 A87-40835

WAVEFORMS

- The effect of a non-Gaussian point target response function on radar altimeter returns from the sea surface p 26 A87-39179

WEATHER

- The impact of climate change from increased atmospheric carbon dioxide on American agriculture [DOE/NBB-0077] p 11 N87-23032

WETLANDS

- Remote sensing of coastal wetlands p 9 A87-40944
Inland wetland change detection using aircraft MSS data p 36 A87-42256
Application of Modular Optoelectronic Multispectral Scanner (MOMS) data to hydrology and vegetation studies. Test site: Pantanal Region (Brazil/Paraguay) p 52 N87-24748

WILDLIFE

- Habitat mapping by Landsat for aerial census of kangaroos p 2 A87-32094

WIND (METEOROLOGY)

- Ocean wind and wave model comparisons with GEOSAT (GEOSAT Satellite) satellite data [AD-A178302] p 33 N87-24061

WIND EFFECTS

- The dependence of sea-surface microwave emission on wind speed, frequency, incidence angle, and polarization over the frequency range from 1 to 40 GHz p 22 A87-35515

WIND MEASUREMENT

- Simulation of wind gradient errors in NROSS (Navy Remote Ocean Sensing System) radar scatterometer data in a simplified geometry [AD-A175754] p 49 N87-20642
Report of the workshop on Assimilation of Satellite Wind and Wave Data in Numerical Weather and Wave Prediction Models [WCP-122] p 49 N87-21521

WIND SHEAR

- Observations of intermittent cumulus convection in the boundary layer p 20 A87-32976

WIND VELOCITY

- The 1982-1983 El Nino Atlas: Nimbus-7 microwave radiometer data [NASA-CR-180914] p 31 N87-22386

WINDOWS (INTERVALS)

- The AVHRR/HIRS operational method for satellite based sea surface temperature determination [NOAA-TR-NESDIS-28] p 31 N87-22388

WINTER

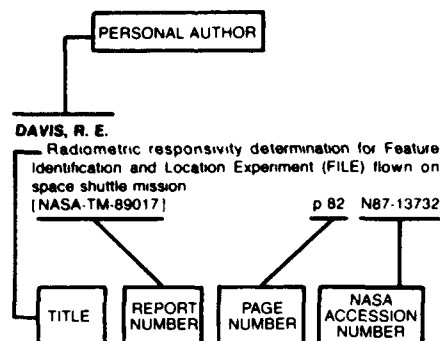
- Nimbus 7 SMMR investigation of snowpack properties in the northern Great Plains for the winter of 1978-1979 p 34 A87-31409
Possibilities of using artificial Earth satellite data for computing heat exchange between the ocean and atmosphere in Newfoundland energy-active zone during winter p 31 N87-21980

Z

ZENITH

- Surface bidirectional reflectance properties of two southwestern Arizona deserts for wavelengths between 0.4 and 2.2 micrometers [NASA-TP-2643] p 49 N87-22281

Typical Personal Author Index Listing



Listings in this index are arranged alphabetically by personal author. The title of the document provides the user with a brief description of the subject matter. The report number helps to indicate the type of document listed (e.g., NASA report, translation, NASA contractor report). The page and accession numbers are located beneath and to the right of the title. Under any one author's name the accession numbers are arranged in sequence with the AIAA accession numbers appearing first.

A

- AARTMAN, L. J.**
A modular and versatile acquisition, recording and preprocessing system for airborne remote sensing
p 52 N87-24751
- ABSHIRE, JAMES B.**
Two-color short-pulse laser altimeter measurements of ocean surface backscatter
p 27 A87-39462
- ACHUTUNI, R.**
A review of national and international activities on modeling the effects of increased CO₂ concentrations on the simulation of regional crop production: A report on linkage between climate and crop models
[DE87-005994]
p 10 N87-22336
- ACHUTUNI, RAO**
The impact of climate change from increased atmospheric carbon dioxide on American agriculture
[DOE/NBB-0077]
p 11 N87-23032
- ACKERMANN, FRIEDRICH**
Improvement of image quality by forward motion compensation, a preliminary report
p 42 N87-24741
The use of camera orientation data in photogrammetry: A review
p 52 N87-24749
- ADAMS, STEVEN**
An assessment of Landsat MSS and TM data for urban and near-urban land-cover digital classification
p 13 A87-37280
- ADIGA, S.**
Indian remote sensing programme
p 56 A87-32955
- AGREEN, RUSSELL**
The Geosat altimeter mission - A milestone in satellite oceanography
p 27 A87-40281
- AHMAD, SURAIYA P.**
Computation of diffuse sky irradiance from multidirectional radiance measurements
p 6 A87-37279
- AL-HINAI, KHATTAB G.**
Landsat image enhancement study of possible submerged sand-dunes in the Arabian Gulf
p 22 A87-35315
- ALBERTZ, JOERG**
Digital data acquisition for close-range photogrammetry
p 54 N87-24785

ALI, ABDALLA ELSADIG

- Optical and digital SAR processing techniques: A statistical comparison of accuracy using SEASAT imagery
p 42 N87-24753
- ALLAN, T. D.**
Ocean-ice panel report
p 30 N87-20635
- ALLEN, L. H., JR.**
Comparison of HCMM and GOES satellite temperatures and evaluation of surface statistics
p 39 A87-38098
- ALLUM, J. A. E.**
Remote sensing of vegetation change near Inco's Sudbury mining complexes
p 8 A87-39185
- AMAYENC, P.**
Energy Balance of the Tropical Systems (BEST): A space experiment proposition
p 36 N87-22373
- AMBROZIAK, RUSSELL ANDREW**
Real-time crop assessment using color theory and satellite data
p 10 N87-20619
- ANDERSON, VIRGIL**
Continental land cover assessment using Landsat MSS data
p 3 A87-32095
- ANDHARIA, H. I.**
Determination of the velocity of ocean gyres through Synthetic Aperture Radar
p 22 A87-35314
- ANNONI, ALESSANDRO**
Comparative evaluation and guide for the integrated utilization of LANDSAT (MSS and TM) and SPOT (HRV) satellites remotely sensed data
[ETN-87-99356]
p 41 N87-22278
- APARINOVA, N. A.**
Statistical evaluation of forest characteristics from aerial and space photographs
p 5 A87-36109
- ARKOS, FERENCZ**
Remote sensing methods of yield forecasting
p 2 A87-32009
- ARMAND, M.**
Towards an automatic identification of urban textures
p 14 N87-24747
- ARMAND, MYRIAM**
Reconnaissance of vegetal formations in a Guinean forest sector by means of Landsat images
p 6 A87-36946
- ARSENAULT, L. D.**
Microwave sea-ice signatures near the onset of melt
p 22 A87-35517
- ASANUMA, ICHIO**
The dependence of sea-surface microwave emission on wind speed, frequency, incidence angle, and polarization over the frequency range from 1 to 40 GHz
p 22 A87-35515
- ASHKENAZI, VIDAL**
GINFEST - Geodetic intercomparison network for evaluating space techniques
p 15 A87-36164
- ATKINSON, L. P.**
Continental shelf processes affecting the oceanography of the South Atlantic Bight
[DE87-005303]
p 30 N87-20716
- AUSTIN, G. L.**
On the relative accuracy of satellite and raingage rainfall measurements over middle latitudes during daylight hours
p 34 A87-33295
- AUSTIN, JOHN**
Analysis of moderate and intense rainfall rates continuously recorded over half a century and influence on microwave communications planning and rain-rate data acquisition
p 46 A87-36933
- AUVINE, BRIAN**
Quick look Atlantic Ocean rain maps for gale
[NASA-CR-180511]
p 30 N87-21533
- AZUMA, YOSHIO**
Airborne observation experiments for MOS-1 verification program (MVP)
p 44 A87-32500

B

- BADHWAR, G. D.**
Landsat classification of Argentina summer crops
p 3 A87-32098
- BADHWAR, GAUTAM D.**
Signature-extendable technology - Global space-based crop recognition
p 1 A87-31414

BAGG, M. T.

- The SIR-B mission: Towards an understanding of internal waves in the ocean
[ARE-TR-86122]
p 32 N87-23102
- BAILEY, CHARLES L.**
Detection of Rift Valley fever viral activity in Kenya by satellite remote sensing imagery
p 7 A87-37827
- BAKER, WAYMAN E.**
Impact of satellite-based data on FGGE general circulation statistics
p 44 A87-32985
- BARAT, J.**
Energy Balance of the Tropical Systems (BEST): A space experiment proposition
p 36 N87-22373
- BARDINET, C.**
Image preprocessing for line detection based on local structure analysis
p 39 A87-37801
Multisatellite data processing
p 39 A87-37803
- BARKER, J. L.**
Thematic Mapper bandpass solar exoatmospheric irradiances
p 40 A87-39192
- BASKARAN, M.**
Geochronological studies of strandlines of Saurashtra, India, detected by remote sensing techniques
p 15 A87-35308
- BATES, JOHN JOSEPH**
A technique to estimate the ocean surface energy flux using VAS multispectral data
p 30 N87-20710
- BATTRICK, B.**
Proceedings of the European Symposium on Polar platform Opportunities and Instrumentation for Remote-Sensing (ESPOIR)
[ESA-SP-266]
p 48 N87-20621
Proceedings of the International Symposium on Progress in Imaging Sensors
[ESA-SP-252]
p 50 N87-24738
- BAUERSIMA, I.**
Using the Global Positioning System (GPS) for high precision geodetic surveys - Highlights and problem areas
p 16 A87-41383
- BAUMANN, ROBERT H.**
Utilizing remote sensing of thematic mapper data to improve our understanding of estuarine processes and their influence on the productivity of estuarine-dependent fisheries
[NASA-CR-180984]
p 33 N87-24012
- BAUMER, GEORGE M.**
High resolution remote sensing of spatially and spectrally complex coal surface mines of central Pennsylvania - A comparison between simulated SPOT MSS and Landsat-5 thematic mapper
p 18 A87-39468
- BAUMGARDNER, M. F.**
Remote sensing research in global agricultural productivity
p 2 A87-32008
- BAUMGARDNER, R. W.**
LANDSAT-based lineament analysis, East Texas Basin, and structural history of the Sabine Uplift area, East Texas and North Louisiana
[PB87-176327]
p 19 N87-24043
- BEAL, ROBERT C.**
Measuring ocean waves from space; Proceedings of the Symposium, Johns Hopkins University, Laurel, MD, Apr. 15-17, 1986
p 24 A87-38826
Spectrasat - A hybrid ROWS/SAR approach to monitor ocean waves from space
p 25 A87-38845
- BECK, SHERWIN M.**
Operational overview of NASA GTE/CITE 1 airborne instrument intercomparisons - Carbon monoxide, nitric oxide, and hydroxyl instrumentation
p 45 A87-33426
- BECKER, ROLF**
Very high resolution aerial films
p 54 N87-24776
- BECKOW, STEPHEN**
Mapping from space
p 38 A87-36361
- BEGIN, DANIEL**
Radiometric correction of SAR images - A new correction algorithm
p 40 A87-39184
- BEGIN, G.**
SPOT image quality
p 42 N87-24804
- BEHNKE, JEANNE M.**
Quick-look guide to the crustal dynamics project's data information system
[NASA-TM-87818]
p 16 N87-23018

BELIAEV, M. IU.

Optimization of a program of experiments in connection with the operational planning of studies carried out with a spacecraft p 56 A87-34208

BELLON, A.

On the relative accuracy of satellite and raingage rainfall measurements over middle latitudes during daylight hours p 34 A87-33295

BELWARD, A. S.

A comparison of supervised maximum likelihood and decision tree classification for crop cover estimation from multitemporal Landsat MSS data p 5 A87-35312

BENDURA, RICHARD J.

Operational overview of NASA GTE/CITE 1 airborne instrument intercomparisons - Carbon monoxide, nitric oxide, and hydroxyl instrumentation p 45 A87-33426

BENTLEY, CHARLES R.

West Antarctic ice streams draining into the Ross ice Shelf Configuration and mass balance p 19 A87-31592

BERNARD, R.

Evaluation of a surface/vegetation parameterization using satellite measurements of surface temperature p 3 A87-33298

Nadir looking airborne radar and possible applications to forestry p 7 A87-38095

Energy Balance of the Tropical Systems (BEST): A space experiment proposition p 36 A87-22373

BEUTLER, G.

Using the Global Positioning System (GPS) for high precision geodetic surveys - Highlights and problem areas p 16 A87-41383

BHARTIA, P. K.

Reflectivity of earth's surface and clouds in ultraviolet from satellite observations p 47 A87-40768

BINNIE, DOUGLAS R.

The Denali image map p 38 A87-37288

BISWAS, R. R.

A soil map through Landsat satellite imagery in a part of the Auranga catchment in the Ranchi and Palamou districts of Bihar, India p 9 A87-41428

BLAZQUEZ, C. H.

Ground and aerial use of an infrared video camera with a mid-infrared filter (1.45 to 2.0 microns) p 48 A87-41588

BLECHINGER, F.

Advanced imaging spectrometer for ocean color/fluorescence measurements and further applications p 33 A87-24766

BLIZARD, MARVIN A.

Ocean optics VIII; Proceedings of the Meeting, Orlando, FL, Mar. 31-Apr. 2, 1986 [SPIE-637] p 28 A87-42637

BLUSSON, ANNICK

Spacelab data - A new contribution for structural interpretations of remotely sensed data in geology p 18 A87-39790

BOBERG, ANDERS E.

Image quality problems in practical aerial photography p 43 A87-24814

BODECHTEL, J.

Land panel report p 49 A87-20634

The Modular Optoelectronic Multispectral Scanner (MOMS) program of the Bundesministerium fuer Forschung und Technologie (BMFT). Milestones in the development of an operational Earth Observation system p 55 A87-24815

BOERNER, WOLFGANG-M.

Interpretation of the polarimetric co-polarization phase term in radar images obtained with the JPL airborne L-band SAR system p 36 A87-31412

BOISSIN, B.

SPOT image quality p 42 A87-24804

BOLSHAKOV, A. N.

Cloud-cover and precipitation patterns over the Republic of Guinea according to ground-based and satellite observations p 35 A87-36102

BONN, FERDINAND

Radiometric correction of SAR images - A new correction algorithm p 40 A87-39184

BOTKIN, D. B.

New dimension analyses with error analysis for quaking aspen and black spruce [NASA-TM-89219] p 11 A87-24735

BOTKIN, DANIEL B.

Earth science research [NASA-CR-180512] p 11 A87-24733

Ten year change in forest succession and composition measured by remote sensing [NASA-CR-180948] p 11 A87-24736

BOUR, WILLIAM

Coral reef remote sensing applications p 20 A87-32951

BOURNE, CARLTON M.

Laser reflectance as a function of rough water glitter profile [AD-A178774] p 32 A87-23016

BOWELL, J. A.

Enhanced LANDSAT images of Antarctica and planetary exploration p 50 A87-23558

BOZO, P.

The application of remote sensing in agricultural meteorology at the Meteorological Service of the HPR p 2 A87-32010

BRACHET, G.

Remote sensing applications: Commercial issues and opportunities for space station p 57 A87-20626

BRADSHAW, J. D.

Free tropospheric and boundary layer measurements of NO over the central and eastern North Pacific Ocean p 21 A87-33432

BRAUN, HANS MARTIN

The first ESA remote sensing satellite (status and outlook) p 57 A87-24777

BREST, CHRISTOPHER L.

Deriving surface albedo measurements from narrow band satellite data p 13 A87-39182

BROCHE, P.

VHF radar for ocean surface current and sea state remote sensing p 19 A87-31631

BROCHU, RICHARD

Radiometric comparison of the Landsat-5 TM and MSS sensors p 47 A87-41432

BROCKHAUS, JOHN A.

Comparison of Landsat MSS and TM data for urban land-use classification p 13 A87-35523

BROOME, R. D.

Ocean wind and wave model comparisons with GEOSAT (GEOSAT Satellite) satellite data [AD-A178302] p 33 A87-24061

BROSSIER, R.

Applications of laser airborne telemetry at Institut Geographique National (IGN), France p 53 A87-24761

BROWDER, JOAN A.

Utilizing remote sensing of thematic mapper data to improve our understanding of estuarine processes and their influence on the productivity of estuarine-dependent fisheries [NASA-CR-180984] p 33 A87-24012

BROWELL, EDWARD

Trace gas exchanges and transports over the Amazonian rain forest p 12 A87-32196

BROWN, WILLIE A.

DUCK '85 nearshore waves and currents experiment data summary report [AD-A177419] p 31 A87-22382

BRUEMMER, BURGHARD

Observations of intermittent cumulus convection in the boundary layer p 20 A87-32976

BRYANT, NEVIN

An assessment of Landsat MSS and TM data for urban and near-urban land-cover digital classification p 13 A87-37280

BUDKO, V. M.

The geostructural characteristics of the rift zone on the Lambert glacier (Antarctica) according to space images p 18 A87-36105

BUKHMAN, E. V.

Rapid analysis of satellite radar images of sea ice p 22 A87-35873

BULATOV, M. G.

Measurement of the spatial spectrum of ocean waves using a two-frequency scatterometer p 23 A87-36107

BUNNIK, N. J. J.

Foundations and applications of multispectral scanning in agriculture [NLR-MP-85015-U] p 10 A87-21408

BUNTING, JAMES T.

Atmospheric remote sensing in arctic regions [AD-A179550] p 50 A87-23012

BURGUENO, AUGUST

Analysis of moderate and intense rainfall rates continuously recorded over half a century and influence on microwave communications planning and rain-rate data acquisition p 46 A87-36933

BURLESHIN, M. I.

The geometry of the intersections of tectonic structures detected on satellite images p 17 A87-36104

BURNS, B. A.

Remote sensing of the Fram Strait marginal ice zone p 27 A87-40433

BURNS, D. A.

Ocean wind and wave model comparisons with GEOSAT (GEOSAT Satellite) satellite data [AD-A178302] p 33 A87-24061

BUSH, PETER R.

Landsat image enhancement study of possible submerged sand-dunes in the Arabian Gulf p 22 A87-35315

BUSS, W. D.

NASA/MSFC large stretch press study [NASA-CR-180376] p 41 A87-20554

C**CAI, JUNLIANG**

On the matching of resolution in aerial photographic systems p 54 A87-24773

CAMPBELL, CHARLES

Polarized views of the earth from orbital altitude p 48 A87-42639

CAMPBELL, N. A.

Some observations on crop profile modelling p 5 A87-35310

CAMPBELL, W. J.

Ice-edge eddies in the Fram Strait marginal ice zone p 27 A87-40432

Remote sensing of the Fram Strait marginal ice zone p 27 A87-40433

CAMPBELL, WILLIAM J.

Arctic Sea ice, 1973-1976. Satellite passive-microwave observations [NASA-SP-489] p 33 A87-24870

CARDER, KENDALL L.

The interaction of light with phytoplankton in the marine environment p 29 A87-42640

CARDONE, VINCENT J.

The present status of operational wave forecasting p 24 A87-38831

CARLSON, T.

Evaluation of a surface/vegetation parameterization using satellite measurements of surface temperature p 3 A87-33298

CARROLL, M. A.

Measurements of nitric oxide in the boundary layer and free troposphere over the Pacific Ocean p 21 A87-33431

CARSEY, F. D.

Remote sensing as a research tool p 28 A87-40648

CASE, DAVID

Continental land cover assessment using Landsat MSS data p 3 A87-32095

CASTELLANI, ANTONIO

Balloon-borne infrared multichannel radiometer for remote sensing of high resolution low-level water vapor fields p 43 A87-32477

CAVALIERI, DONALD J.

Arctic Sea ice, 1973-1976. Satellite passive-microwave observations [NASA-SP-489] p 33 A87-24870

CHALLENGER, P. G.

The effect of a non-Gaussian point target response function on radar altimeter returns from the sea surface p 26 A87-39179

CHANG, A. T. C.

Quantifying spatial and temporal variabilities of microwave brightness temperature over the U.S. Southern Great Plains p 5 A87-35309

CHANG, JY-TAI

Concerning the relationship between evapotranspiration and soil moisture p 8 A87-40244

CHAO, TIEN-HSIN

Optical image subtraction techniques, 1975-1985 p 40 A87-42659

CHAPLET, MICHEL

Fault patterns by space remote sensing and the rotation of western Oregon during Cenozoic times p 18 A87-36525

CHARBONNEAU, LISE

Radiometric comparison of the Landsat-5 TM and MSS sensors p 47 A87-41432

CHEN, E.

Comparison of HCMM and GOES satellite temperatures and evaluation of surface statistics p 39 A87-38098

CHEN, HUIPING

On the matching of resolution in aerial photographic systems p 54 A87-24773

CHEN, WEIYING

High resolution sea surface temperature field derived p 33 A87-24731

CHENEY, ROBERT

The Geosat altimeter mission - A milestone in satellite oceanography p 27 A87-40281

CHESHIRE, HEATHER M.

Comparison of Landsat MSS and TM data for urban land-use classification p 13 A87-35523

- CHHIKARA, R. S.**
Error analysis of leaf area estimates made from allometric regression models
[NASA-TM-89220] p 11 N87-24010
- CHIMOT, J. M.**
Aircraft radiopositioning for airborne photography during hydrographic coastal surveys p 23 A87-36945
- CHOATE, M. W.**
NASA/MSFC large stretch press study
[NASA-CR-180376] p 41 N87-20554
- CHOROWICZ, JEAN**
Fault patterns by space remote sensing and the rotation of western Oregon during Cenozoic times p 18 A87-36525
- CHOUDHURY, A. M.**
Monsoon flood boundary delineation and damage assessment using space borne imaging radar and Landsat data p 35 A87-39467
- CHOUDHURY, B. J.**
Quantifying spatial and temporal variabilities of microwave brightness temperature over the U.S. Southern Great Plains p 5 A87-35309
Monitoring vegetation using Nimbus-7 scanning multichannel microwave radiometer's data p 8 A87-39194
- CHRISTENSEN, ERIC J.**
Inland wetland change detection using aircraft MSS data p 36 A87-42256
- CIHLAR, J.**
Procedures for the description of agricultural crops and soils in optical and microwave remote sensing studies p 8 A87-39187
- CLARK, DENNIS K.**
Coastal zone color scanner imagery of phytoplankton pigment distribution in Icelandic waters p 29 A87-42645
- CLARK, H. LAWRENCE**
The interaction of light with phytoplankton in the marine environment p 29 A87-42640
- CLARK, THOMAS A.**
Creation of a global geodetic network using Mark III VLBI p 15 A87-36166
- CLEVERS, J. G. P. W.**
Determination of spectral reflectance of crops during growth from calibrated multispectral small format aerial photography p 12 N87-24801
- CLEVERS, JAN G. P. W.**
An application of low altitude multispectral photography to agricultural field trials p 6 A87-37054
- COLLINS, DONALD J.**
The interaction of light with phytoplankton in the marine environment p 29 A87-42640
A model for the use of satellite remote sensing for the measurement of primary production in the ocean p 29 A87-42644
- COLVOCORESSES, ALDEN P.**
The Denali image map p 38 A87-37288
- COMISO, J. C.**
Recurring polynyas over the Cosmonaut Sea and the Maud Rise p 23 A87-37563
- COMISO, JOSEFINO C.**
Arctic Sea ice, 1973-1976: Satellite passive-microwave observations
[NASA-SP-489] p 33 N87-24870
- CONDON, ESTELLE P.**
Operational overview of NASA GTE/CITE 1 airborne instrument intercomparisons - Carbon monoxide, nitric oxide, and hydroxyl instrumentation p 45 A87-33426
Carbon monoxide measurements over the eastern Pacific during GTE/CITE 1 p 21 A87-33435
- CORNILLON, PETER**
Satellite measurements of sea surface cooling during hurricane Gloria p 24 A87-37886
- COULSON, KINSELL L.**
Polarized views of the earth from orbital altitude p 48 A87-42639
- CRACKNELL, A. P.**
A two-look technique for studying atmospheric effects in optical scanner data for the ocean p 26 A87-39178
- CRAUBNER, SIEGFRIED**
Infrared Earth horizon sensor concepts in various spectral bands p 52 N87-24752
- CRIPPEN, ROBERT E.**
The regression intersection method of adjusting image data for band ratioing p 45 A87-35306
- CROCHET, M.**
VHF radar for ocean surface current and sea state remote sensing p 19 A87-31631
- CROTEAU, J. C.**
Spectrophotometric measurements on color aerial photographs p 55 N87-24798
- CUBASCH, ULRICH**
The impact of initial conditions and SST Anomalies on extended range predictions for the El Nino period p 32 N87-23046
- CURFMAN, HOWARD J., JR.**
Operational overview of NASA GTE/CITE 1 airborne instrument intercomparisons - Carbon monoxide, nitric oxide, and hydroxyl instrumentation p 45 A87-33426
- CURLANDER, JOHN C.**
Rectification of terrain induced distortions in radar imagery p 48 A87-42254
Radiometric calibration of the Shuttle Imaging Radar (SIR-C) system p 53 N87-24756
- CURRAN, P. J.**
GLAI estimation using measurements of red, near infrared, and middle infrared radiance p 4 A87-35119
A polar platform for the remote sensing needs of ecology and agriculture - A view from the UK p 9 A87-41430
- CZAPLEWSKI, RAYMOND L.**
Comparison between digital and manual interpretation of high altitude aerial photographs p 48 A87-42257
- D**
- DALU, G.**
Remotely sensed sea surface temperature for the Alpine Experiment (ALPEX) p 30 N87-21497
- DANDJINO, TOUNDE**
First results of latent cover mapping with SPOT images The Kangaba region (South-Mali) p 18 A87-36925
- DANIELSEN, EDWIN F.**
Carbon monoxide measurements over the eastern Pacific during GTE/CITE 1 p 21 A87-33435
- DAUGHERTY, C. S. T.**
Remote sensing research in global agricultural productivity p 2 A87-32008
Variations in the polarized leaf reflectance of Sorghum bicolor p 7 A87-38097
- DAVIDSON, J. M.**
GPS-based geodesy in California, Mexico and the Caribbean p 16 A87-41380
- DAVIDSON, K. L.**
Optical properties of the marine atmospheric boundary layer - Aerosol profiles p 28 A87-42638
- DAVIES, F. GLYN**
Detection of Rift Valley fever viral activity in Kenya by satellite remote sensing imagery p 7 A87-37827
- DAVIS, D. D.**
Free tropospheric and boundary layer measurements of NO over the central and eastern North Pacific Ocean p 21 A87-33432
- DAVIS, L. I., JR.**
OH measurement near the intertropical convergence zone in the Pacific p 21 A87-33430
- DAY, RICHARD**
Tectonic evaluation of the Nubian Shield of northeastern Sudan using Thematic Mapper imagery
[NASA-CR-180575] p 19 N87-22319
- DE BOER, E. S.**
Some observations on crop profile modelling p 5 A87-35310
- DE HOYOS, A.**
A comparison of supervised maximum likelihood and decision tree classification for crop cover estimation from multitemporal Landsat MSS data p 5 A87-35312
- DE KOOMEN, J. H.**
The Netherlands-Indonesian remote-sensing satellite TERS p 43 A87-32210
- DE MAISTRE, J. C.**
VHF radar for ocean surface current and sea state remote sensing p 19 A87-31631
- DECKER, W. L.**
A review of national and international activities on modeling the effects of increased CO2 concentrations on the simulation of regional crop production: A report on linkage between climate and crop models
[DE87-005994] p 10 N87-22336
- DECKER, WAYNE L.**
The impact of climate change from increased atmospheric carbon dioxide on American agriculture
[DOE/NBB-0077] p 11 N87-23032
- DEDIEU, G.**
Satellite estimation of a solar irradiance at the surface of the earth and of surface albedo using a physical model applied to Meteosat data p 47 A87-40246
- DEEKSHATULU, B. L.**
Indian remote sensing programme p 56 A87-32955
- DEERING, DONALD W.**
Computation of diffuse sky irradiance from multidirectional radiance measurements p 6 A87-37279
- DELLA VENTURA, ANNA**
Development of a satellite remote sensing technique for the study of alpine glaciers p 34 A87-35311
- DESBOIS, MICHEL**
Measurement and detection of precipitation Satellite methods in the visible and the infrared p 36 A87-22364
- DESCHAMPS, P. Y.**
Satellite estimation of a solar irradiance at the surface of the earth and of surface albedo using a physical model applied to Meteosat data p 47 A87-40246
- DEVENON, J. L.**
VHF radar for ocean surface current and sea state remote sensing p 19 A87-31631
- DI RUSCIO, MAURIZIO**
Balloon-borne infrared multichannel radiometer for remote sensing of high resolution low-level water vapor fields p 43 A87-32477
- DIETRICH, R.**
Investigation of tectonic deformations using global satellite laser ranging data p 14 A87-33375
- DIETZ, KLAUR R.**
Large Format Camera photographs of the Black Hills, USA, and their suitability for topographic and thematic mapping p 55 N87-24792
- DIXON, T. H.**
GPS-based geodesy in California, Mexico and the Caribbean p 16 A87-41380
- DOBSON, M. C.**
Procedures for the description of agricultural crops and soils in optical and microwave remote sensing studies p 8 A87-39187
- DOBSON, MYRON C.**
Relating polarization phase difference of SAR signals to scene properties p 1 A87-31413
- DOEOES, B. R.**
The observational objectives and the implementation of the Global Weather Experiment p 49 N87-21474
- DOLLHOFF, KEVIN J.**
An evaluation of satellite-based insolation estimates for Ohio p 34 A87-33297
- DONEAUD, ANDRE A.**
The area-time-integral technique to estimate convective rain volumes over areas applied to satellite data - A preliminary investigation p 35 A87-40249
- DOROFEEV, V. L.**
Use of satellite altimetry for ocean monitoring p 23 A87-36101
- DOUGLAS, BRUCE**
The Geosat altimeter mission - A milestone in satellite oceanography p 27 A87-40281
- DOZIER, JEFF**
Recent research in snow hydrology p 35 A87-40309
- DREISINGER, B. R.**
Remote sensing of vegetation change near Inco's Sudbury mining complexes p 8 A87-39185
- DRESCHER, A.**
Stereoscopic line scan imaging and satellite control
[DGLR PAPER 86-106] p 38 A87-36757
- DUDA, C.**
Exposure test with high resolution films from high altitude p 54 N87-24775
- DUGGIN, MICHAEL J.**
Impact of radiance variations on satellite sensor calibration p 47 A87-39457
- DYE, DENNIS**
Comparison of North and South American biomes from AVHRR observations p 9 A87-40362
- DZIEWONSKI, ADAM M.**
Global images of the earth's interior p 15 A87-37918
- E**
- EBERHARDT, JOHN E.**
Mid-infrared remote sensing systems and their application to lithologic mapping p 17 A87-35522
- ECK, T. F.**
Reflectivity of earth's surface and clouds in ultraviolet from satellite observations p 47 A87-40768
- EDWARDS, A. C.**
The SIR-B mission: Towards an understanding of internal waves in the ocean
[ARE-TR-86122] p 32 N87-23102
- EDWARDS, K.**
Enhanced LANDSAT images of Antarctica and planetary exploration p 50 N87-23558
- EHLERS, MANFRED**
Merging multiresolution SPOT HRV and Landsat TM data p 38 A87-37287
- EL-SAYED, SAYED Z.**
Remote sensing of chlorophyll concentrations in the northern Gulf of Mexico p 29 A87-42643
- ELACHI, CHARLES**
Spaceborne imaging radar research in the 1990s - An overview p 46 A87-38837
Earth surface sensing in the '90's p 51 N87-24739
- ELIASON, E. M.**
Enhanced LANDSAT images of Antarctica and planetary exploration p 50 N87-23558

ELMAN, R. I.

- ELMAN, R. I.**
Statistical evaluation of forest characteristics from aerial and space photographs p 5 A87-36109
- EMERY, W. J.**
Comparison of satellite derived sea surface temperatures with in situ skin measurements p 23 A87-37565
- ENGELIS, THEODOSSIOS**
Radial orbit error reduction and sea surface topography determination using satellite altimetry [NASA-CR-180570] p 33 N87-24816
- EOM, HYO J.**
Interpretation of the polarimetric co-polarization phase term in radar images obtained with the JPL airborne L band SAR system p 36 A87-31412
- ERMOLAEV, A. G.**
Physical principles of image convergence in remote sensing p 40 A87-41925
- ESCOBAR, D. E.**
Ground and aerial use of an infrared video camera with a mid-infrared filter (1.45 to 2.0 microns) p 48 A87-41588
- ESTES, JOHN E.**
Remote Sensing Information Sciences Research Group Santa Barbara Information Sciences Research Group, year 4 [NASA-CR-181073] p 43 N87-24817
- ETKIN, V. S.**
Measurement of the spatial spectrum of ocean waves using a two-frequency scatterometer p 23 A87-36107
- EVERITT, J. H.**
Ground and aerial use of an infrared video camera with a mid-infrared filter (1.45 to 2.0 microns) p 48 A87-41588
- EWING, J. A.**
Simulations of the GOES visible sensor to changing surface and atmospheric conditions p 47 A87-40756
- EYEMARD, L.**
Energy Balance of the Tropical Systems (BEST) A space experiment proposition p 36 N87-22373

F

- FAGBAMI, AYODELE**
Reflectance characteristics and its application in the classification of Nigerian Savanna soils p 3 A87-32954
- FAGERLUND, ERIK**
Influence of different nitrogen and irrigation treatments on the spectral reflectance of barley p 2 A87-32090
- FAIRALL, C. W.**
Optical properties of the marine atmospheric boundary layer - Aerosol profiles p 28 A87-42638
- FEDCHENKO, PETR PETROVICH**
Aerial and space investigations of soils and vegetation p 6 A87-36579
- FEDOTOV, A. B.**
Use of satellite altimetry for ocean monitoring p 23 A87-36101
- FEIVISON, A. H.**
Error analysis of leaf area estimates made from allometric regression models [NASA-TM-89220] p 11 N87-24010
New dimension analyses with error analysis for quaking aspen and black spruce [NASA-TM-89219] p 11 N87-24735
- FEIZULLAEV, A. A.**
The possibility of using satellite measurements of methane in the atmosphere to study the global-distribution characteristics of its sources p 13 A87-36125
- FELDE, GERALD W.**
Atmospheric remote sensing in arctic regions [AD-A179550] p 50 N87-23012
- FELLOUS, JEAN-LOUIS**
The French Space Oceanography Program p 20 A87-32503
- FERENCZ ARKOS, I.**
Surface models including direct cross-radiation - A simple model of furrowed surfaces p 40 A87-39189
- FERENCZ, CS.**
Remote sensing methods of yield forecasting p 2 A87-32009
Surface models including direct cross-radiation - A simple model of furrowed surfaces p 40 A87-39189
- FERGUSON, H. M.**
Enhanced LANDSAT images of Antarctica and planetary exploration p 50 N87-23558
- FIELD, R. T.**
Measurement of the surface emissivity of turbid waters p 19 A87-32097
- FISHMAN, JACK**
OH measurement near the intertropical convergence zone in the Pacific p 21 A87-33430

- FLAMANT, P.**
Energy Balance of the Tropical Systems (BEST) A space experiment proposition p 36 N87-22373
- FOO, BING-YUEN**
Interpretation of the polarimetric co-polarization phase term in radar images obtained with the JPL airborne L band SAR system p 36 A87-31412
- FORGET, P.**
VHF radar for ocean surface current and sea state remote sensing p 19 A87-31631
- FORSBERG, RENE**
A new covariance model for inertial gravimetry and gradiometry p 14 A87-31591
- FRAIN, WILLIAM E.**
A Spectrasat system design based on the Geosat experiment p 26 A87-38848
- FRANCIS, PETER W.**
Synergistic use of MOMS-01 and Landsat TM data p 46 A87-39190
- FRASER, S. J.**
A software defoliant for geological analysis of band ratios p 18 A87-39193
- FREYSSINET, PHILIPPE**
First results of lateritic cover mapping with SPOT images The Kangaba region (South-Mali) p 18 A87-36925
- FREZAL, M. E.**
Nadir looking airborne radar and possible applications to forestry p 7 A87-38095
- FRIESS, PETER**
The effects of camera position and attitude data in aerial triangulation, a simulation study p 52 N87-24750
- FUJITA, MASAHARU**
Observation of precipitation from space by the weather radar p 44 A87-32507
- FUKUE, KIYONARI**
Global vegetation monitoring using NOAA vegetation index data p 3 A87-32495
- FUSCO, L.**
AVHRR data services in Europe - The Earthnet approach p 39 A87-37922

G

- GADZHIR-ZADE, F. M.**
The possibility of using satellite measurements of methane in the atmosphere to study the global-distribution characteristics of its sources p 13 A87-36125
- GAFOOR, A.**
Monsoon flood boundary delineation and damage assessment using space borne imaging radar and Landsat data p 35 A87-39467
- GALLAGHER, JOHN G.**
The relation of millimeter-wavelength backscatter to surface snow properties p 34 A87-35518
- GANTT, R. G.**
Measurement of the surface emissivity of turbid waters p 19 A87-32097
- GARGANTINI, C. E.**
Landsat classification of Argentina summer crops p 3 A87-32098
- GARSTANG, MICHAEL**
Trace gas exchanges and transports over the Amazonian rain forest p 12 A87-32196
- GASCARD, J. C.**
Mesoscale oceanographic processes beneath the ice of Fram Strait p 28 A87-40434
- GAUTHIER, R. P.**
The Multidetector Electro-optical Imaging Sensor (MEIS) 2 pushbroom imager: Four years of operation p 53 N87-24767
- GENDT, G.**
Investigation of tectonic deformations using global satellite laser ranging data p 14 A87-33375
- GERSTL, S. A. W.**
An atmospheric correction algorithm for remote identification of non-Lambertian surfaces and its range of validity [DE87-006059] p 41 N87-24011
Modelling of atmospheric effects on the angular distribution of a backscattering peak [DE87-006060] p 41 N87-24014
- GIBSON, J. R.**
The use of auxiliary data in photogrammetric adjustments p 42 N87-24808
- GIERLOFF-EMDEN, H.-G.**
Large format camera image analysis for mapping of land use patterns in the region Noale - Musone, Po-River-Plain, North Italy p 55 N87-24789
- GLOERSEN, PER**
Arctic Sea ice, 1973-1976 Satellite passive-microwave observations [NASA-SP-489] p 33 N87-24870
- GOEL, NARENDRA S.**
Estimation of canopy parameters of row planted vegetation canopies using reflectance data for only four view directions p 2 A87-32093
Inversion of canopy reflectance models for estimation of vegetation parameters [NASA-CR-181059] p 12 N87-24737
- GOETZ, SCOTT J.**
Ten year change in forest succession and composition measured by remote sensing [NASA-CR-180948] p 11 N87-24736
- GOLDBERG, MICHAEL J.**
Problems in merging Earth sensing satellite data sets [NASA-TM-87820] p 50 N87-22457
- GOLUS, R. E.**
Quantifying spatial and temporal variabilities of microwave brightness temperature over the U.S. Southern Great Plains p 5 A87-35309
Monitoring vegetation using Nimbus 7 scanning multichannel microwave radiometer data p 8 A87-39194
- GOMBERG, LOUIS**
United States remote sensing satellites (RSSs) past, present, and future p 56 A87-32502
- GONZALEZ, FRANK I.**
The age and source of ocean swell observed in Hurricane Josephine p 25 A87-38843
- GORDON, A. L.**
Recurring polynyas over the Cosmonaut Sea and the Maud Rise p 23 A87-37563
- GOSSELINK, JAMES G.**
Utilizing remote sensing of thematic mapper data to improve our understanding of estuarine processes and their influence on the productivity of estuarine dependent fisheries [NASA-CR-180984] p 33 N87-24012
- GOWARD, S. N.**
Quantifying spatial and temporal variabilities of microwave brightness temperature over the U.S. Southern Great Plains p 5 A87-35309
- GOWARD, SAMUEL N.**
Deriving surface albedo measurements from narrow band satellite data p 13 A87-39182
Comparison of North and South American biomes from AVHRR observations p 9 A87-40303
- GRANT, LOIS**
Variations in the polarized leaf reflectance of Sorghum bicolor p 7 A87-38097
- GRASSL, H.**
Comparison of satellite-derived sea surface temperatures with in situ skin measurements p 23 A87-37565
- GRATZKI, A.**
An atmospheric correction algorithm for remote identification of non-Lambertian surfaces and its range of validity [DE87-006059] p 41 N87-24011
- GRAY, A. LAURENCE**
Seasonal and regional variations of active/passive microwave signatures of sea ice p 22 A87-35516
Microwave sea ice signatures near the onset of melt p 22 A87-35517
- GRECO, B.**
The effect of a non-Gaussian point target response function on radar altimeter returns from the sea surface p 26 A87-39179
- GRECO, STEVE**
Trace gas exchanges and transports over the Amazonian rain forest p 12 A87-32196
- GREEN, A. A.**
A software defoliant for geological analysis of band ratios p 18 A87-39193
- GREEN, ANDREW A.**
Mid-infrared remote sensing systems and their application to lithologic mapping p 17 A87-35522
- GREGORY, G. L.**
Measurements of nitric oxide in the boundary layer and free troposphere over the Pacific Ocean p 21 A87-33431
- GREGORY, GERALD L.**
Operational overview of NASA GTE/CITE 1 airborne instrument intercomparisons - Carbon monoxide, nitric oxide, and hydroxyl instrumentation p 45 A87-33426
- GRIER, TOBY**
Estimation of canopy parameters of row planted vegetation canopies using reflectance data for only four view directions p 2 A87-32093
- GRIFFITH, DOUGLAS M.**
A comparison of optical bar, high-altitude, and black-and-white photography in land classification p 4 A87-35122
- GROSS, M. F.**
Remote sensing of coastal wetlands p 9 A87-40944

- GROVES, J. E.**
Statistical description of the summertime ice edge in the Chukchi Sea, task 2
[DE87-001056] p 31 N87-22387
- GUENTHER, GARY C.**
Wind and nadir angle effects on airborne lidar water 'surface' returns p 29 A87-42641
- GULIEV, I. S.**
The possibility of using satellite measurements of methane in the atmosphere to study the global-distribution characteristics of its sources p 13 A87-36125
- GUO, CHUAN**
OH measurement near the intertropical convergence zone in the Pacific p 21 A87-33430
- GURTNER, W.**
Using the Global Positioning System (GPS) for high precision geodetic surveys - Highlights and problem areas p 16 A87-41383
- GUYON, D.**
Nadir looking airborne radar and possible applications to forestry p 7 A87-38095
- GWYN, Q. H. J.**
Radiometric correction of SAR images - A new correction algorithm p 40 A87-39184

H

- HAACK, BARRY**
An assessment of Landsat MSS and TM data for urban and near-urban land-cover digital classification p 13 A87-37280
- HAKKINEN, SIRPA**
Feedback between ice flow, barotropic flow, and baroclinic flow in the presence of bottom topography p 27 A87-40289
- HALL-KONYVES, KARIN**
The topographic effect on Landsat data in gently undulating terrain in southern Sweden p 4 A87-35307
- HALL, FORREST G.**
Signature-extendable technology - Global space-based crop recognition p 1 A87-31414
Ten year change in forest succession and composition measured by remote sensing [NASA-CR-180948] p 11 N87-24736
- HALLIKAINEN, MARTTI T.**
Applications of satellite microwave radiometry in Finland p 44 A87-32952
- HAMAR, D.**
Remote sensing methods of yield forecasting p 2 A87-32009
Surface models including direct cross-radiation - A simple model of furrowed surfaces p 40 A87-39189
- HANCOCK, DAVID W., III**
Wave-measurement capabilities of the surface contour radar and the airborne oceanographic lidar p 25 A87-38840
- HANDY, J. R.**
Spectrophotometric measurements on color aerial photographs p 55 N87-24798
- HARADA, YOSHIHIRO**
Earth resources satellite-1 (ERS-1) p 44 A87-32501
- HARDER, PAUL H., II**
Nimbus 7 SMMR investigation of snowpack properties in the northern Great Plains for the winter of 1978-1979 p 34 A87-31409
- HARDISKY, M. A.**
Remote sensing of coastal wetlands p 9 A87-40944
- HARDY, KENNETH R.**
Atmospheric remote sensing in arctic regions [AD-A179550] p 50 N87-23012
- HARLOW, CHARLES A.**
The integration of spectral and spatial analysis for land use classification [AD-A178703] p 14 N87-23015
- HARNISH, DAVID**
Tectonic evaluation of the Nubian Shield of northeastern Sudan using Thematic Mapper imagery [NASA-CR-180575] p 19 N87-22319
- HARRIS, JEFF**
Shuttle Imaging Radar (SIR-B) investigations of the Canadian shield - Initial Report p 17 A87-31410
- HARRISS, ROBERT**
Trace gas exchanges and transports over the Amazonian rain forest p 12 A87-32196
- HARTL, PH.**
Smart sensors: An overview and selected examples p 51 N87-24740
Application of Global Positioning System (GPS) receivers for Earth observation p 53 N87-24763
- HAUB, JOHN G.**
Mid-infrared remote sensing systems and their application to lithologic mapping p 17 A87-35522

- HAUCK, MARTIN**
Application of Modular Optoelectronic Multispectral Scanner (MOMS) data to hydrology and vegetation studies. Test site: Pantanal Region (Brazil/Paraguay) p 52 N87-24748
- HE, DONG-CHEN**
Automatic classification of Pointe d'Arcay landscapes using Thematic Mapper data with the aid of a textural analysis p 37 A87-35305
Introduction of initial centers for the algorithm of clustering around mobile centers p 37 A87-35313
- HELD, DANIEL**
Relating polarization phase difference of SAR signals to scene properties p 1 A87-31413
- HENDERSON, FLOYD M.**
Polarization, land use type and intraurban location as variables in SAR mapping accuracy p 12 A87-32953
Urban land use separability as a function of radar polarization p 14 A87-39188
- HERNANDEZ, M.**
Towards an automatic identification of urban textures p 14 N87-24747
- HIBLER, W. D., III**
An evaluation of the polar ice prediction system [AD-A178522] p 41 N87-23014
- HICK, P. T.**
Some observations on crop profile modelling p 5 A87-35310
- HILL, GERALD F.**
Operational overview of NASA GTE/CITE 1 airborne instrument intercomparisons - Carbon monoxide, nitric oxide, and hydroxyl instrumentation p 45 A87-33426
Carbon monoxide measurements over the eastern Pacific during GTE/CITE 1 p 21 A87-33435
- HILL, GREG J. E.**
Habitat mapping by Landsat for aerial census of kangaroos p 2 A87-32094
- HILLER, KONRAD**
Application of Modular Optoelectronic Multispectral Scanner (MOMS) data to hydrology and vegetation studies. Test site: Pantanal Region (Brazil/Paraguay) p 52 N87-24748
- HINES, DONALD E.**
Wave-measurement capabilities of the surface contour radar and the airborne oceanographic lidar p 25 A87-38840
- HO, DIEM**
A soil thermal model for remote sensing p 5 A87-35521
- HOCK, JOAN C.**
Preliminary report on the development of marine geographic information systems p 23 A87-37056
- HOELL, JAMES M., JR.**
Operational overview of NASA GTE/CITE 1 airborne instrument intercomparisons - Carbon monoxide, nitric oxide, and hydroxyl instrumentation p 45 A87-33426
- HOFMANN, OTTO**
The stereo pushbroom scanner system Digital Photogrammetry System (DPS) and its accuracy p 53 N87-24768
- HOLBEN, BRENT**
Satellite detection of tropical burning in Brazil p 8 A87-39191
- HOLLIER, P.**
Definition of a thermal infrared pushbroom imager for Earth observation p 53 N87-24765
- HOLT, BENJAMIN M.**
The age and source of ocean swell observed in Hurricane Josephine p 25 A87-38843
- HOOGBOOM, P.**
Procedures for the description of agricultural crops and soils in optical and microwave remote sensing studies p 8 A87-39187
- HORNING, NED**
Continental land cover assessment using Landsat MSS data p 3 A87-32095
- HORTON, C. A.**
Determination of spectral reflectance of crops during growth from calibrated multispectral small format aerial photography p 12 N87-24801
- HORTON, CHARLES**
An application of low altitude multispectral photography to agricultural field trials p 6 A87-37054
- HOSOMURA, TSUKASA**
Global vegetation monitoring using NOAA vegetation index data p 3 A87-32495
- HOUGHTON, R. A.**
Deforestation in the tropics - New measurements in the Amazon Basin using Landsat and NOAA advanced very high resolution radiometer imagery p 4 A87-33441
- HUBERTZ, JON M.**
DUCK '85 nearshore waves and currents experiment data summary report [AD-A177419] p 31 N87-22382

- HUNKINS, K. L.**
Mesoscale oceanographic processes beneath the ice of Fram Strait p 28 A87-40434
- HUSSEY, M. A.**
Ground and aerial use of an infrared video camera with a mid-infrared filter (1.45 to 2.0 microns) p 48 A87-41588
- HWANG, P. H.**
Reflectivity of earth's surface and clouds in ultraviolet from satellite observations p 47 A87-40768
- IMHOFF, MARC L.**
Monsoon flood boundary delineation and damage assessment using space borne imaging radar and Landsat data p 35 A87-39467
- ISAEV, A. A.**
Remote-sensing method for determining monthly precipitation sums using Meteor-satellite data on the Atlantic Ocean p 21 A87-34447
- ISHIZAWA, YOSHIHIRO**
Marine Observation Satellite-1 (MOS-1) p 20 A87-32499
Earth resources satellite-1 (ERS-1) p 44 A87-32501
- IVANCHIK, M. V.**
Cloud-cover and precipitation patterns over the Republic of Guinea according to ground-based and satellite observations p 35 A87-36102
- JACKSON, FREDERICK C.**
The physical basis for estimating wave-energy spectra with the radar ocean-wave spectrometer p 25 A87-38839
The Radar Ocean-Wave Spectrometer p 25 A87-38846
- JACKSON, M. L. W.**
LANDSAT-based lineament analysis. East Texas Basin, and structural history of the Sabine Uplift area. East Texas and North Louisiana [PB87-176327] p 19 N87-24043
- JACKSON, T. J.**
Temporal observations of surface soil moisture using a passive microwave sensor p 7 A87-38094
- JACKSON, THOMAS J.**
Salinity effects on the microwave emission of soils p 5 A87-35520
- JAEGER, ERNST**
The VICOM system for digital image processing at the Institute of Cartography of Technical University, Hanover (West Germany) p 16 N87-22290
- JAMES, JOHN V.**
OH measurement near the intertropical convergence zone in the Pacific p 21 A87-33430
- JANSE, A. R. P.**
Procedures for the description of agricultural crops and soils in optical and microwave remote sensing studies p 8 A87-39187
- JAY, G. C.**
NASA/MSFC large stretch press study [NASA-CR-180376] p 41 N87-20554
- JEANNIN, P. F.**
Mesoscale oceanographic processes beneath the ice of Fram Strait p 28 A87-40434
- JEGOU, J. P.**
Energy Balance of the Tropical Systems (BEST): A space experiment proposition p 36 N87-22373
- JELINEK, D. A.**
Measured radar return at the near vertical from forested terrains [DE87-009384] p 11 N87-24593
- JENSEN, JOHN R.**
Inland wetland change detection using aircraft MSS data p 36 A87-42256
- JIA, WEN-KUI**
Exploration of geomagnetic field anomaly with balloon for geophysical research p 17 A87-32478
- JOHANNESSEN, J. A.**
Ice-edge eddies in the Fram Strait marginal ice zone p 27 A87-40432
- JOHANNESSEN, O. M.**
Ice-edge eddies in the Fram Strait marginal ice zone p 27 A87-40432
Remote sensing of the Fram Strait marginal ice zone p 27 A87-40433
- JOHNSON, GARY E.**
The use of AVHRR data in operational agricultural assessment in Africa p 9 A87-40304
- JOHNSON, J. W.**
Airborne microwave Doppler measurements of ocean wave directional spectra p 26 A87-39180

JOHNSON, L. RONALD

The area-time-integral technique to estimate convective rain volumes over areas applied to satellite data - A preliminary investigation p 35 A87-40249

JOLMA, PETRI A.

Applications of satellite microwave radiometry in Finland p 44 A87-32952

JONES, ARWYN RHYS

Landform investigation utilizing digitally processed satellite Thematic Mapper imagery p 38 A87-36546

JONES, VERNON K.

The impact of climate change from increased atmospheric carbon dioxide on American agriculture [DOE/NBB-0077] p 11 A87-23032

JOSBERGER, E. G.

Remote sensing of the Fram Strait marginal ice zone p 27 A87-40433

JUPP, DAVID L. B.

Coral reef remote sensing applications p 20 A87-32951

K

KALB, VIRGINIA

Comparison of North and South American biomes from AVHRR observations p 9 A87-40303

KALNAY, EUGENIA

Impact of satellite-based data on FGGE general circulation statistics p 44 A87-32985

KAMEDA, KAZUAKI

Landcover change in Hiroshima during 1979/1984 detected by Landsat MSS and TM data p 12 A87-32494

KAUFMAN, YORAM J.

Satellite sensing of aerosol absorption p 47 A87-40770

KAWATA, YOSHIYUKI

Spectral classification of Landsat-5 Thematic Mapper data p 37 A87-32488
Correction for atmospheric and topographic effects on the Landsat MSS data p 37 A87-32489

KAZMIN, A. S.

Surface manifestations of hydrophysical processes in the Strait of Gibraltar according to 'Salyut-6' photographs p 35 A87-36103

KELLER, SAM

Space remote sensors p 47 A87-40379

KELLER, W. C.

Airborne microwave Doppler measurements of ocean wave directional spectra p 26 A87-39180

KELLY, GAIL D.

Habitat mapping by Landsat for aerial census of kangaroos p 2 A87-32094

KERBER, ARLENE

Comparison of North and South American biomes from AVHRR observations p 9 A87-40303

KERR, Y. H.

Satellite estimation of a solar irradiance at the surface of the earth and of surface albedo using a physical model applied to Meteosat data p 47 A87-40246

KESHENG, S.

Free tropospheric and boundary layer measurements of NO over the central and eastern North Pacific Ocean p 21 A87-33432

KETSKEMETY, L.

The application of remote sensing in agricultural meteorology at the Meteorological Service of the HPR p 2 A87-32010

KHORRAM, SIAMAK

Comparison of Landsat MSS and TM data for urban land-use classification p 13 A87-35523

KHOSRAVIANI, G.

A two-look technique for studying atmospheric effects in optical scanner data for the ocean p 26 A87-39178

KIEFER, DALE A.

A model for the use of satellite remote sensing for the measurement of primary production in the ocean p 29 A87-42644

KILGUS, CHARLES C.

A Spectrasat system design based on the Geosat experiment p 26 A87-38848

KIM, HONGSUK H.

Sunlight induced 685 nm fluorescence imagery p 30 A87-42646

KINDRED, D. R.

A curious sea-surface-temperature phenomenon observed by Meteosat p 19 A87-31572

KING, DOMINIC

Sensors for imaging p 45 A87-36360

KIRCHHOF, W.

Comparative analysis of Thematic Mapper and SPOT image data for land use investigation p 51 A87-24746

KIREEV, S. V.

Physical principles of image convergence in remote sensing p 40 A87-41925

KISELEV, V. V.

Problems in the automation of map-compilation processes on the basis of remote-sensing data p 38 A87-35925

KITCHEN, JAMES C.

Optical dynamics experiment (ODEX) data report R/V acania expedition 10 October-17 November 1982 Volume 2 Particle size distributions. Volume 6 Scalar spectral-radiometer data [AD-A178535] p 32 A87-23104

KLEMAN, JOHAN

Influence of different nitrogen and irrigation treatments on the spectral reflectance of barley p 2 A87-32090

KLEMAS, V.

Measurement of the surface emissivity of turbid waters p 19 A87-32097
Remote sensing of coastal wetlands p 9 A87-40944

KLINK, JOHN C.

An evaluation of satellite-based insolation estimates for Ohio p 34 A87-33297

KOHNO, ITOSHI

Simulation software of synthetic aperture radar p 37 A87-32506

KOJIMA, MASAHIRO

Airborne observation experiments for MOS-1 verification program (MVP) p 44 A87-32500

KOMAI, JIRO

Simulation software of synthetic aperture radar p 37 A87-32506

KOMEN, GERBRAND J.

Recent results with a third-generation ocean-wave model p 24 A87-38833

KONDRATEV, KIRILL IAKOVLEVICH

Aerial and space investigations of soils and vegetation p 6 A87-36579

KONENCY, G.

Introduction of geometric information to radar image data p 42 A87-24754

KONG, J. A.

Radar scene generation for tactical decision aids [NASA-CR-180234] p 40 A87-20449

KONG, JIN A.

Active and passive remote sensing of ice [AD-A179461] p 32 A87-24009

KOVALICK, W.

Deforestation in the tropics - New measurements in the Amazon Basin using Landsat and NOAA advanced very high resolution radiometer imagery p 4 A87-33441

KOZODEROV, VLADIMIR VASILEVICH

Aerial and space investigations of soils and vegetation p 6 A87-36579

KRASIUK, V. S.

Rapid analysis of satellite radar images of sea ice p 22 A87-35873

KRUCK, E.

Aerial triangulation of CCD line-scanner images p 54 A87-24769

KUCHLER, DEBORAH A.

Coral reef remote sensing applications p 20 A87-32951

KUNKEL, B.

Advanced imaging spectrometer for ocean color/fluorescence measurements and further applications p 33 A87-24766

KUPFER, G.

Geometrical system calibration, especially for metric aerial cameras p 51 A87-24745

KUSAKA, TAKASHI

Spectral classification of Landsat-5 Thematic Mapper data p 37 A87-32488

KUX, HERMANN J. H.

Application of Modular Optoelectronic Multispectral Scanner (MOMS) data to hydrology and vegetation studies. Test site: Pantanal Region (Brazil/Paraguay) p 52 A87-24748

KUZENKOV, L. A.

Statistical evaluation of forest characteristics from aerial and space photographs p 5 A87-36109

KWOK, RONALD

Rectification of terrain induced distortions in radar imagery p 48 A87-42254

L

LABOVITZ, M. L.

Stochastic nature of Landsat MSS data p 46 A87-38093

LABOVITZ, MARK L.

Derivation of a fast algorithm to account for distortions due to terrain in earth-viewing satellite sensor images p 38 A87-35524

LANDREVILLE, M. L.

Proposed changes to the Canadian camera calibration report p 53 A87-24757

LANZL, F.

Land panel report p 49 A87-20634
Earth observation experiments on the German Spacelab mission D2 p 55 A87-24811
The Monocular Electro-Optical Stereo Scanner (MEOSS) satellite experiment p 55 A87-24812

LAYBE, PATRICK

The area-time-integral technique to estimate convective rain volumes over areas applied to satellite data - A preliminary investigation p 35 A87-40249

LE GOUIC, M.

Aircraft radiopositioning for airborne photography during hydrographic coastal surveys p 23 A87-36945

LECROY, STUART R.

Surface bidirectional reflectance properties of two southwestern Arizona deserts for wavelengths between 0.4 and 2.2 micrometers [NASA-TP-2643] p 49 A87-22281

LEGECKIS, RICHARD

Long waves in the equatorial Atlantic Ocean during 1983 p 23 A87-37564

LEICHT, DIETER

Strategies and technologies for monitoring the environment p 14 A87-39593

LEROY, M.

SPOT image quality p 42 A87-24804

LESZTAK, S.

The application of remote sensing in agricultural meteorology at the Meteorological Service of the HPR p 2 A87-32010

LICHTENBERGER, J.

Remote sensing methods of yield forecasting p 2 A87-32009

Surface models including direct cross-radiation - A simple model of furrowed surfaces p 40 A87-39189

LINDER, HENRY G.

Quick-look guide to the crustal dynamics project's data information system [NASA-TM-87818] p 16 A87-23018

LINTHICUM, KENNETH J.

Detection of Rift Valley fever viral activity in Kenya by satellite remote sensing imagery p 7 A87-37827

LIU, HUA-KUANG

Optical image subtraction techniques, 1975-1985 p 40 A87-42659

LIU, W. TIMOTHY

The 1982-1983 El Nino Atlas: Nimbus-7 microwave radiometer data [NASA-CR-180914] p 31 A87-22386

LIU, WEN-YAO

Measurement of the surface emissivity of turbid waters p 19 A87-32097

LIVINGSTONE, CHARLES E.

Seasonal and regional variations of active/passive microwave signatures of sea ice p 22 A87-35516
Microwave sea-ice signatures near the onset of melt p 22 A87-35517

LO, CHOR PONG

Applied remote sensing p 45 A87-33122

LOEDEMANN, J. H.

Determination of spectral reflectance of crops during growth from calibrated multispectral small format aerial photography p 12 A87-24801

LOHMANN, G.

MIDAS - A new image-processing system for remote sensing p 37 A87-35183

LOHMANN, P.

Aerial triangulation of CCD line-scanner images p 54 A87-24769

LONG, CHARLES E.

DUCK '85 nearshore waves and currents experiment data summary report [AD-A177419] p 31 A87-22382

LONGUET-HIGGINS, M. S.

The propagation of short surface waves on longer gravity waves p 28 A87-40835

LORCH, W.

The RMK aerial camera system: Performance potential of aerial photography with forward motion compensation p 54 A87-24781

LOTZ-IWEN, H.-J.

MIDAS - A new image-processing system for remote sensing p 37 A87-35183

LOWMAN, PAUL D., JR.

Shuttle Imaging Radar (SIR-B) investigations of the Canadian shield - Initial Report p 17 A87-31410

LUCAS, JAMES R.

Aerotriangulation without ground control p 46 A87-37289

LUCCHITTA, B. K.

Enhanced LANDSAT images of Antarctica and planetary exploration p 50 A87-23558

LUEST, REIMAR

Ananiaspace top performance benefits ESA p 57 A87-24493

- LUTZ, R.**
Advanced imaging spectrometer for ocean color/fluorescence measurements and further applications p 33 N87-24766
- LYON, JOHN GRIMSON**
Use of maps, aerial photographs, and other remote sensor data for practical evaluations of hazardous waste sites p 14 A87-42255
- LYON, RONALD J. P.**
Mid-infrared remote sensing systems and their application to lithologic mapping p 17 A87-35522
- M**
- MA, CHOPO**
Creation of a global geodetic network using Mark III VLBI p 15 A87-36166
- MACARTHUR, JOHN L.**
Spectrasat instrument design using maximum heritage p 26 A87-38847
- MACKAY, HALKARD E., JR.**
Inland wetland change detection using aircraft MSS data p 36 A87-42256
- MAEDA, KOREHIRO**
Airborne observation experiments for MOS-1 verification program (MVP) p 44 A87-32500
- MALIN, JANICE A.**
Models for radar scatterer density in terrain images p 45 A87-35344
- MANLEY, T. O.**
Mesoscale oceanographic processes beneath the ice of Fram Strait p 28 A87-40434
- MARKHAM, B. L.**
Thematic Mapper bandpass solar exoatmospheric irradiances p 40 A87-39192
- MARKWITZ, W.**
MIDAS - A new image-processing system for remote sensing p 37 A87-35183
- MARTIN, A.**
CHART - A computer plotting package for the display of position-dependent marine data [PB87-148607] p 31 N87-22297
- MARTIN, DAVID W.**
Quick look Atlantic Ocean rain maps for gale [NASA-CR-180511] p 30 N87-21533
- MARULLO, S.**
Remotely sensed sea surface temperature for the Alpine Experiment (ALPEX) p 30 N87-21497
- MARVIN, JOHN W.**
Derivation of a fast algorithm to account for distortions due to terrain in earth-viewing satellite sensor images p 38 A87-35524
- MASUDA, TAKESHI**
Marine Observation Satellite-1 (MOS-1) p 20 A87-32499
- MASUKO, HARUNOBU**
Observation of precipitation from space by the weather radar p 44 A87-32507
- MASUOKA, E. J.**
Stochastic nature of Landsat MSS data p 46 A87-38093
- MASUOKA, PENNY M.**
Shuttle Imaging Radar (SIR-B) investigations of the Canadian shield - Initial Report p 17 A87-31410
- MATSON, MICHAEL**
Satellite detection of tropical burning in Brazil p 8 A87-39191
- MATTHEWS, ELAINE**
Regional and seasonal variations of surface reflectance from satellite observations at 0.6 micron p 27 A87-40250
- MAUSER, W.**
Comparative analysis of Thematic Mapper and SPOT image data for land use investigation p 51 N87-24746
- MAY, L. NELSON, JR.**
Utilizing remote sensing of thematic mapper data to improve our understanding of estuarine processes and their influence on the productivity of estuarine-dependent fisheries [NASA-CR-180984] p 33 N87-24012
- MAYER, G.**
Stereoscopic line scan imaging and satellite control [DGLR PAPER 86-106] p 38 A87-36757
- MAYNARD, NANCY G.**
Coastal zone color scanner imagery of phytoplankton pigment distribution in Icelandic waters p 29 A87-42645
- MCCOLL, W. D.**
The Multidetector Electro-optical Imaging Sensor (MEIS) 2 pushbroom imager. Four years of operation p 53 N87-24767
- MCCRACKEN, KENNETH G.**
Australian utilization and research into remote sensing p 20 A87-32490

- MCDONALD, KYLE C.**
Relating polarization phase difference of SAR signals to scene properties p 1 A87-31413
- MCDUGAL, DAVID S.**
Operational overview of NASA GTE/CITE 1 airborne instrument intercomparisons - Carbon monoxide, nitric oxide, and hydroxyl instrumentation p 45 A87-33426
- MCDUGAL, PATRICK**
Intelsat's small earth stations - Impact on the developing world p 56 A87-34799
- MCELROY, JAMES L.**
Lidar observation of elevated pollution layers over Los Angeles p 13 A87-33292
- MCFARLAND, MARSHALL J.**
Nimbus 7 SMMR investigation of snowpack properties in the northern Great Plains for the winter of 1978-1979 p 34 A87-31409
- MCGARRY, JAN F.**
Two-color short-pulse laser altimeter measurements of ocean surface backscatter p 27 A87-39462
- MCMAHON MOORE, JOHN**
Landsat image enhancement study of possible submerged sand-dunes in the Arabian Gulf p 22 A87-35315
- MEGIE, G.**
Energy Balance of the Tropical Systems (BEST). A space experiment proposition p 36 N87-22373
- MEHLBREUER, ALFRED**
Digital data acquisition for close-range photogrammetry p 54 N87-24785
- MEISSNER, D.**
The Modular Optoelectronic Multispectral Scanner (MOMS) program of the Bundesministerium fuer Forschung und Technologie (BMFT). Milestones in the development of an operational Earth Observation system p 55 N87-24815
- MELBOURNE, W. G.**
GPS-based geodesy in California, Mexico and the Caribbean p 16 A87-41380
- MENSHIKH, A. E.**
Problems in the automation of map-compilation processes on the basis of remote-sensing data p 38 A87-35925
- MENZIES, DAVID W.**
Optical dynamics experiment (ODEX) data report R/V acania expedition 10 October-17 November 1982. Volume 2: Particle size distributions. Volume 6: Scalar spectral-radiometer data [AD-A178535] p 32 N87-23104
- MERRITT, NORMAN E.**
Comparison between digital and manual interpretation of high altitude aerial photographs p 48 A87-42257
- MESIAS, JORGE M.**
The interaction of light with phytoplankton in the marine environment p 29 A87-42640
- MEYER, DAVID S.**
French spot and the U.S. Landsat jockey for position in the race for a multimillion-dollar remote sensing market p 56 A87-34600
- MIDDLETON, ELIZABETH M.**
Computation of diffuse sky irradiance from multidirectional radiance measurements p 6 A87-37279
- MILBERT, DENNIS**
The Geosat altimeter mission - A milestone in satellite oceanography p 27 A87-40281
- MILLER, BERNARD L.**
Convective heating and precipitation estimates for the tropical South Pacific during FGGE, 10-18 January 1979 p 21 A87-32982
- MILLER, JAMES R., JR.**
The area-time-integral technique to estimate convective rain volumes over areas applied to satellite data - A preliminary investigation p 35 A87-40249
- MILLER, LAURY**
The Geosat altimeter mission - A milestone in satellite oceanography p 27 A87-40281
- MIYASHITA, KIYOE**
Fundamental study on systematization of selecting new development area with Landsat data and topographic informations p 12 A87-32496
- MOCCIA, A.**
The Tethered Satellite System as a new remote sensing platform p 46 A87-39183
- MOGILSKI, KELLY A.**
Urban land use separability as a function of radar polarization p 14 A87-39188
- MONALDO, FRANK M.**
A practical methodology for estimating wave spectra from the SIR-B p 25 A87-38841
- MONGET, J. M.**
The Geomulti database management system p 39 A87-37802
- MOREL, A.**
Multisatellite data processing p 39 A87-37803
- MOREL, A.**
Ocean-ice panel report p 30 N87-24635

- MORRIS, PETER T.**
OH measurement near the intertropical convergence zone in the Pacific p 21 A87-33430
- MUELLER, JAMES L.**
Simulation of wind gradient errors in NROSS (Navy Remote Ocean Sensing System) radar scatterometer data in a simplified geometry [AD-A175754] p 49 N87-20642
- MUIRHEAD, K.**
AVHRR data services in Europe. The Earthnet approach p 39 A87-37922
- MULDER, NANNO J.**
What, where, when... why? Extracting information from remote sensing data p 46 A87-37055
- MULHERAN, P. J.**
Studies of the east Australian current off northern New South Wales [AD-A178461] p 32 N87-23103
- MUNEYAMA, KEI**
The dependence of sea-surface microwave emission on wind speed, frequency, incidence angle, and polarization over the frequency range from 1 to 40 GHz p 22 A87-35515
- MURAI, SHUNJI**
Earth Resources Satellite (ERS-1) project in Japan p 57 N87-24797
- MURATA, MASAOKI**
Earth rotation, station coordinates and orbit determination from satellite laser ranging p 43 A87-32349
- MURPHY, JENNIFER M.**
Radiometric comparison of the Landsat-5 TM and MSS sensors p 47 A87-41432

N

- NAGESWARA RAO, P. P.**
Rice crop identification and area estimation using remotely-sensed data from Indian cropping patterns p 9 A87-41434
- NAGY, E.**
Spectrophotometric measurements on color aerial photographs p 55 N87-24798
- NAHVI, M. J.**
Smart sensors. An overview and selected examples p 51 N87-24740
- NAITO, GENICHI**
The dependence of sea-surface microwave emission on wind speed, frequency, incidence angle, and polarization over the frequency range from 1 to 40 GHz p 22 A87-35515
- NAKAMURA, KENJI**
Observation of precipitation from space by the weather radar p 44 A87-32507
- NAKAYAMA, YASUNORI**
Relation between precipitation and brightness of earth surface in the NOAA/GVIP data p 3 A87-32498
- NASONOVA, O. N.**
Remote-sensing method for determining monthly precipitation sums using Meteor-satellite data on the Atlantic Ocean p 21 A87-34447
- NAZIROV, M.**
Rapid analysis of satellite radar images of sea ice p 22 A87-35873
- NEALSON, W. P.**
NASA/MSFC large stretch press study [NASA-CR-180376] p 41 N87-20554
- NELSON, R. F.**
Deforestation in the tropics - New measurements in the Amazon Basin using Landsat and NOAA advanced very high resolution radiometer imagery p 4 A87-33441
- NELSON, ROSS**
Continental land cover assessment using Landsat MSS data p 3 A87-32095
- NEVILLE, R. A.**
The Multidetector Electro-optical Imaging Sensor (MEIS) 2 pushbroom imager. Four years of operation p 53 N87-24767
- NEWCOMB, W. W.**
Monitoring vegetation using Nimbus-7 scanning multichannel microwave radiometer's data p 8 A87-39194
- NIKITIN, P. A.**
Rapid analysis of satellite radar images of sea ice p 22 A87-35873
- NIXON, P. R.**
Ground and aerial use of an infrared video camera with a mid-infrared filter (1.45 to 2.0 microns) p 48 A87-41588
- NOLL, CAREY E.**
Quick-look guide to the crustal dynamics project's data information system [NASA-TM-87818] p 16 N87-23018

NOVIKOV, IULIAN

Environmental protection from space
p 13 A87-36363

O

O'NEILL, P.

Temporal observations of surface soil moisture using
a passive microwave sensor p 7 A87-38094

OCHIAI, HIROAKI

Monitoring of snow and ice in Hokkaido Island using
multitemporal NOAA-AVHRR data p 20 A87-32497

OETTL, HERWIG

Scientific goals and technical limitations of the
shuttleborne synthetic aperture experiment X-SAR
p 44 A87-32505

OGURA, IWAO

Estimation of roughness of the earth's surface using
Landsat MSS data on the assumption of reciprocity on
light scattering p 12 A87-32493

OKAMOTO, KENICHI

Observation of precipitation from space by the weather
radar p 44 A87-32507

OKAYAMA, HIROSHI

Estimation of roughness of the earth's surface using
Landsat MSS data on the assumption of reciprocity on
light scattering p 12 A87-32493

OLSON, CHARLES E., JR.

Evaluation of the airborne imaging spectrometer for
remote sensing of forest stand conditions
[NASA-CR-180918] p 10 N87-22296

ONEILL, PEGGY E.

Salinity effects on the microwave emission of soils
p 5 A87-35520

ONO, MAKOTO

Simulation software of synthetic aperture radar
p 37 A87-32506

ONSTOTT, R. G.

Microwave sea-ice signatures near the onset of melt
p 22 A87-35517

ORMSBY, J. P.

Quantifying spatial and temporal variabilities of
microwave brightness temperature over the U.S. Southern
Great Plains p 5 A87-35309

OSHIMA, TAICHI

Fundamental study on systematization of selecting new
development area with Landsat data and topographic
informations p 12 A87-32496

OTTERMAN, J.

Inferring spectral reflectances of plant elements by
simple inversion of bidirectional reflectance
measurements p 7 A87-37281

OUCHI, KAZUO

Multilook images of ocean waves by synthetic aperture
radars p 28 A87-41068

OWE, M.

Quantifying spatial and temporal variabilities of
microwave brightness temperature over the U.S. Southern
Great Plains p 5 A87-35309

P

PAK, HASONG

Optical dynamics experiment (ODEX) data report R/V
Acacia expedition 10 October-17 November 1982. Volume
2: Particle size distributions. Volume 6: Scalar
spectral-radiometer data
[AD-A178535] p 32 N87-23104

PANG, SHIRLEY S.

Rectification of terrain induced distortions in radar
imagery p 48 A87-42254

PARKINSON, CLAIRE L.

Arctic Sea ice, 1973-1976: Satellite passive-microwave
observations
[NASA-SP-489] p 33 A87-24870

PARKS, NANCY F.

High resolution remote sensing of spatially and spectrally
complex coal surface mines of central Pennsylvania - A
comparison between simulated SPOT MSS and Landsat-5
thematic mapper p 18 A87-39468

PELON, J.

Energy Balance of the Tropical Systems (BEST): A space
experiment proposition p 36 N87-22373

PERRY, J. R.

The SIR-B mission: Towards an understanding of internal
waves in the ocean
[ARE-TR-86122] p 32 N87-23102

PERRY, MARY JANE

The interaction of light with phytoplankton in the marine
environment p 29 A87-42640

PETERSEN, GARY W.

High resolution remote sensing of spatially and spectrally
complex coal surface mines of central Pennsylvania - A
comparison between simulated SPOT MSS and Landsat-5
thematic mapper p 18 A87-39468

PEIFFER, B.

The Earth observation activities of the European Space
Agency and the use of the polar platform of the
International Space Station p 49 N87-20622

PHILIPSON, WARREN R.

Identifying vegetable crops with Landsat Thematic
Mapper data p 4 A87-35120

PHILPOT, WILLIAM D.

Identifying vegetable crops with Landsat Thematic
Mapper data p 4 A87-35120

PHINNEY, DAVID A.

The relationship between phytoplankton concentration
and light attenuation in ocean waters p 29 A87-42642

PICKETT, R. L.

Ocean wind and wave model comparisons with GEOSAT
(GEOSAT Satellite) satellite data
[AD-A178302] p 33 N87-24061

PIERSON, WILLARD J., JR.

Some approaches for comparing remote and in-situ
estimates of directional wave spectra p 24 A87-38835

PILLAI, SREE

Continental land cover assessment using Landsat MSS
data p 3 A87-32095

PINKER, R. T.

Simulations of the GOES visible sensor to changing
surface and atmospheric conditions p 47 A87-40756

PION, JEAN-CLAUDE

First results of lateritic cover mapping with SPOT images
The Kangaba region (South-Mali) p 18 A87-36925

PLACE, J. L.

Radar as a complement to topographic maps for
delineating marine terraces
[PB87-154597] p 41 N87-24013

PLANT, W. J.

Airborne microwave Doppler measurements of ocean
wave directional spectra p 26 A87-39180

PLANT, WILLIAM J.

The microwave measurement of ocean-wave directional
spectra p 24 A87-38836

PLUMMER, J. E. W.

Proposed changes to the Canadian camera calibration
report p 53 N87-24757

PLUMMER, S. E.

A polar platform for the remote sensing needs of ecology
and agriculture - A view from the U.K. p 9 A87-41430

POLCARO, VITO FRANCESCO

Balloon-borne infrared multichannel radiometer for
remote sensing of high resolution low-level water vapor
fields p 43 A87-32477

POUWELS, H.

A modular and versatile acquisition, recording and
preprocessing system for airborne remote sensing
p 52 N87-24751

POWERS, B. J.

Modelling of atmospheric effects on the angular
distribution of a backscattering peak
[DE87-006060] p 41 N87-24014

PRICE, JAMES F.

Satellite measurements of sea surface cooling during
hurricane Gloria p 24 A87-37886

PRICE, JOHN C.

Calibration of satellite radiometers and the comparison
of vegetation indices
Combining panchromatic and multispectral imagery from
dual resolution satellite instruments p 38 A87-37276

PRYOR, ARTHUR W.

Mid-infrared remote sensing systems and their
application to lithologic mapping p 17 A87-35522

PUIGSERVER, MANUEL

Analysis of moderate and intense rainfall rates
continuously recorded over half a century and influence
on microwave communications planning and rain-rate data
acquisition p 46 A87-36933

PULS, J.

Stereoscopic line scan imaging and satellite control
[DGLR PAPER 86-106] p 38 A87-36757

PURGOLD, G. CARLTON

Surface bidirectional reflectance properties of two
southwestern Arizona deserts for wavelengths between
0.4 and 2.2 micrometers
[NASA-TP-2643] p 49 N87-22281

PUTSAY, M.

The application of remote sensing in agricultural
meteorology at the Meteorological Service of the HPR
p 2 A87-32010

PYTEV, I. P.

Physical principles of image convergence in remote
sensing p 40 A87-41925

R

RABAGLIATI, RICCARDO

Development of a satellite remote sensing technique
for the study of alpine glaciers p 34 A87-35311

RAEV, M. D.

Measurement of the spatial spectrum of ocean waves
using a two-frequency scatterometer p 23 A87-36107

RAJANGAM, R. K.

Data Compression System for video images
p 46 A87-37421

RAJYALAKSHMI, P. S.

Data Compression System for video images
p 46 A87-37421

RAMPINI, ANNA

Development of a satellite remote sensing technique
for the study of alpine glaciers p 34 A87-35311

RAMSEY, ELIJAH W.

Inland wetland change detection using aircraft MSS
data p 36 A87-42256

RANSON, K. J.

Inferring spectral reflectances of plant elements by
simple inversion of bidirectional reflectance
measurements p 7 A87-37281

RAO, DESIRAJU B.

Tidal estimation in the Atlantic and Indian Oceans. 3
deg x 3 deg solution
[NASA-TM-87812] p 30 N87-21534

RAO, V. R.

Rice crop identification and area estimation using
remotely-sensed data from Indian cropping patterns
p 9 A87-41434

RAST, M.

Definition of a thermal infrared pushbroom imager for
Earth observation p 53 N87-24765

REDONDO, F. V.

Landsat classification of Argentina summer crops
p 3 A87-32098

REEVES, A. B.

Airborne microwave Doppler measurements of ocean
wave directional spectra p 26 A87-39180

REVERDIN, GILLES

Long waves in the equatorial Atlantic Ocean during
1983 p 23 A87-37564

REYNOLDS, M. L.

Definition of a thermal infrared pushbroom imager for
Earth observation p 53 N87-24765

RICHTER, RUDOLF

Infrared Earth horizon sensor concepts in various
spectral bands p 52 N87-24752

RIDLEY, B. A.

Measurements of nitric oxide in the boundary layer and
free troposphere over the Pacific Ocean
p 21 A87-33431

RIOM, J.

Nadir looking airborne radar and possible applications
to forestry p 7 A87-38095

RIVERS, PANOLA

DUCK '85 nearshore waves and currents experiment
data summary report
[AD-A177419] p 31 N87-22382

ROBERTS, G. A.

An expert system for labeling segments in forward
looking infrared (FLIR) imagery p 40 A87-42628

RODGERS, M. O.

Free tropospheric and boundary layer measurements
of NO over the central and eastern North Pacific Ocean
p 21 A87-33432

ROHRBACH, ARTHUR

Wild AvioPhot (TM) RC20 aerial camera system. The
other approach to image motion compensation in aerial
photography p 54 N87-24782

ROLFE, E. J.

Proceedings of the European Symposium on Polar
platform Opportunities and Instrumentation for
Remote-Sensing (ESPOIR)
[ESA-SP-266] p 48 N87-20621

Proceedings of the International Symposium on Progress
in Imaging Sensors
[ESA-SP-252] p 50 N87-24738

ROQUIN, CLAUDE

First results of lateritic cover mapping with SPOT images
The Kangaba region (South-Mali) p 18 A87-36925

ROSEN, RICHARD D.

Impact of satellite-based data on FGGE general
circulation statistics p 44 A87-32985

ROSENBRUCH, K.-J.

Optical Transfer Function (OTF)-based quality criteria
for aerial cameras and imaging systems p 51 N87-24742

ROSENTHAL, ALAN

Utilizing remote sensing of thematic mapper data to
improve our understanding of estuarine processes and
their influence on the productivity of estuarine-dependent
fisheries
[NASA-CR-180984] p 33 N87-24012

- ROSSOW, WILLIAM B.**
Regional and seasonal variations of surface reflectance from satellite observations at 0.6 micron
p 27 A87-40250
- ROTHACHER, M.**
Using the Global Positioning System (GPS) for high precision geodetic surveys - Highlights and problem areas
p 16 A87-41383
- ROTHERY, DAVID A.**
Synergistic use of MOMS-01 and Landsat TM data
p 46 A87-39190
- ROURE, FRANCOIS**
Fault patterns by space remote sensing and the rotation of western Oregon during Cenozoic times
p 18 A87-36525
- ROWNTREE, ROWAN A.**
Testing the consistency for mapping urban vegetation with high-altitude aerial photographs and Landsat MSS data
p 13 A87-37277
- ROY, PARTH SARATHI**
Montane vegetation stratification through digital processing of Landsat MSS data
p 9 A87-40302
- ROYER, ALAIN**
Radiometric comparison of the Landsat-5 TM and MSS sensors
p 47 A87-41432
- RULEV, D. N.**
Optimization of a program of experiments in connection with the operational planning of studies carried out with a spacecraft
p 56 A87-34208
- RYAN, JAMES W.**
Creation of a global geodetic network using Mark III VLBI
p 15 A87-36166
- RZHEPLINSKIY, D. G.**
Possibilities of using artificial Earth satellite data for computing heat exchange between the ocean and atmosphere in Newfoundland energy-active zone during winter
p 31 N87-21980

S

- SACHSE, GLEN W.**
Operational overview of NASA GTE/CITE 1 airborne instrument intercomparisons - Carbon monoxide, nitric oxide, and hydroxyl instrumentation
p 45 A87-33426
Carbon monoxide measurements over the eastern Pacific during GTE/CITE 1
p 21 A87-33435
- SACHSE, GLENN**
Trace gas exchanges and transports over the Amazonian rain forest
p 12 A87-32196
- SADER, STEVEN A.**
Multipolarization SAR data for surface feature delineation and forest vegetation characterization
p 1 A87-31411
Forest biomass, canopy structure, and species composition relationships with multipolarization L-band synthetic aperture radar data
p 4 A87-35121
Airborne remote sensing of forest biomes
p 9 A87-40301
- SADOWSKI, FRANK G.**
Testing the consistency for mapping urban vegetation with high-altitude aerial photographs and Landsat MSS data
p 13 A87-37277
- SAHAI, BALDEV**
Geochronological studies of strandlines of Saurashtra, India, detected by remote sensing techniques
p 15 A87-35308
- SAITO, NORIO**
Earth resources satellite-1 (ERS-1)
p 44 A87-32501
- SAKAMOTO, CLARENCE M.**
The use of AVHRR data in operational agricultural assessment in Africa
p 9 A87-40304
- SAKATA, TOSHIBUMI**
Global vegetation monitoring using NOAA vegetation index data
p 3 A87-32495
- SALSTEIN, DAVID A.**
Impact of satellite-based data on FGGE general circulation statistics
p 44 A87-32985
- SANCHEZ, BRAULIO V.**
Tidal estimation in the Atlantic and Indian Oceans, 3 deg x 3 deg solution
[NASA-TM-87812]
p 30 N87-21534
- SANDHAM, L. A.**
Landsat as an aid in evaluating the adequacy of a grain silo network
p 7 A87-37282
- SANDHOLM, S. T.**
Free tropospheric and boundary layer measurements of NO over the central and eastern North Pacific Ocean
p 21 A87-33432
- SANDWELL, DAVID T.**
Biharmonic spline interpolation of GEOS-3 and Seasat altimeter data
p 20 A87-32770

- SASAKI, YASUNORI**
The dependence of sea-surface microwave emission on wind speed, frequency, incidence angle, and polarization over the frequency range from 1 to 40 GHz
p 22 A87-35515
- SCALA, JOHN**
Trace gas exchanges and transports over the Amazonian rain forest
p 12 A87-32196
- SCHILDKNECHT, T.**
Using the Global Positioning System (GPS) for high precision geodetic surveys - Highlights and problem areas
p 16 A87-41383
- SCHLIENGER, ROLAND**
Wild Avophot (TM) RC20 aerial camera system. The other approach to image motion compensation in aerial photography
p 54 N87-24782
- SCHLUEDE, F.**
European utilization aspects studies
p 49 N87-20624
- SCHLUESSEL, P.**
Comparison of satellite-derived sea surface temperatures with in situ skin measurements
p 23 A87-37565
- SCHMUGGE, T.**
Procedures for the description of agricultural crops and soils in optical and microwave remote sensing studies
p 8 A87-39187
- SCHMUGGE, THOMAS**
Remote sensing applications in hydrology
p 35 A87-40308
- SCHNEIDER, MANFRED**
Report on the Special Program 78 satellite geodesy of the Technical University of Munich [ASTRON-GEODAET-ARB-48]
p 16 N87-20618
- SCHNEIDER, W.**
Photographic quality of color IR aerial photos as a function of atmospheric parameters
p 42 N87-24799
- SCHOELLER, W.**
Application of Global Positioning System (GPS) receivers for Earth observation
p 53 N87-24763
- SCHREUDER, HANS T.**
A comparison of optical bar, high-altitude, and black-and-white photography in land classification
p 4 A87-35122
- SCHROEDER, M.**
Exposure test with high resolution films from high altitude
p 54 N87-24775
- SCHUHR, W.**
Introduction of geometric information to radar image data
p 42 N87-24754
- SCHUTZ, B. E.**
Altimeter measurements for the determination of the Earth's gravity field [NASA-CR-180520]
p 17 N87-23033
- SCOTT, CHARLES T.**
A comparison of optical bar, high-altitude, and black-and-white photography in land classification
p 4 A87-35122
- SCOTT, J. C.**
The SIR-B mission: Towards an understanding of internal waves in the ocean [ARE-TR-86122]
p 32 N87-23102
- SCOTT, JOHN F.**
Wave-measurement capabilities of the surface contour radar and the airborne oceanographic lidar
p 25 A87-38840
- SEIGE, P.**
Modern CCD sensors and their applications in Earth observation and planetary missions
p 55 N87-24813
The Modular Optoelectronic Multispectral Scanner (MOMS) program of the Bundesministerium fuer Forschung und Technologie (BMFT). Milestones in the development of an operational Earth Observation system
p 55 N87-24815
- SELLERS, P. J.**
Canopy reflectance, photosynthesis, and transpiration. II - The role of biophysics in the linearity of their interdependence
p 6 A87-37278
- SENIOR, THOMAS B. A.**
Relating polarization phase difference of SAR signals to scene properties
p 1 A87-31413
- SERANDREI BARBERO, ROSSANA**
Development of a satellite remote sensing technique for the study of alpine glaciers
p 34 A87-35311
- SEVOSTIANOV, A. I.**
Cloud-cover and precipitation patterns over the Republic of Guinea according to ground-based and satellite observations
p 35 A87-36102
- SHABTAIE, SION**
West Antarctic ice streams draining into the Ross Ice Shelf Configuration and mass balance
p 19 A87-31592
- SHALAEV, V. S.**
The geostructural characteristics of the rift zone on the Lambert glacier (Antarctica) according to space images
p 18 A87-36105

- SHARITZ, REBECCA R.**
Inland wetland change detection using aircraft MSS data
p 36 A87-42256
- SHIMODA, HARUHISA**
Global vegetation monitoring using NOAA vegetation index data
p 3 A87-32495
- SHIN, H.-Y.**
Comparison of satellite-derived sea surface temperatures with in situ skin measurements
p 23 A87-37565
- SHUCHMAN, R. A.**
Ice-edge eddies in the Fram Strait marginal ice zone
p 27 A87-40432
Remote sensing of the Fram Strait marginal ice zone
p 27 A87-40433
- SHUM, C. K.**
Altimeter measurements for the determination of the Earth's gravity field [NASA-CR-180520]
p 17 N87-23033
- SHVYRKOV, N. N.**
Possibilities of using artificial Earth satellite data for computing heat exchange between the ocean and atmosphere in Newfoundland energy-active zone during winter
p 31 N87-21980
- SIMPSON, JOANNE**
Trace gas exchanges and transports over the Amazonian rain forest
p 12 A87-32196
- SINGH, KESHAVA P.**
Seasonal and regional variations of active/passive microwave signatures of sea ice
p 22 A87-35516
Microwave sea-ice signatures near the onset of melt
p 22 A87-35517
- SINGHROY, VERNON H.**
Shuttle Imaging Radar (SIR-B) investigations of the Canadian shield - Initial Report
p 17 A87-31410
- SKVORTSOV, E. I.**
Measurement of the spatial spectrum of ocean waves using a two-frequency scatterometer
p 23 A87-36107
- SLANEY, VERNON ROY**
Shuttle Imaging Radar (SIR-B) investigations of the Canadian shield - Initial Report
p 17 A87-31410
- SLOGGETT, DAVID**
Remote sensing - Handling the data
p 38 A87-36359
- SMITH, FRED W.**
Models for radar scatterer density in terrain images
p 45 A87-35344
- SMITH, PAUL H.**
Problems in merging Earth sensing satellite data sets [NASA-TM-87820]
p 50 N87-22457
- SMITH, TERENCE**
Remote Sensing Information Sciences Research Group: Santa Barbara Information Sciences Research Group, year 4
[NASA-CR-181073]
p 43 N87-24817
- SNOOK, PAUL W.**
Comparison between digital and manual interpretation of high altitude aerial photographs
p 48 A87-42257
- SOLOMATIN, M. E.**
Problems in the automation of map-compilation processes on the basis of remote-sensing data
p 38 A87-35925
- SOMAYAJULU, B. L. K.**
Geochronological studies of strandlines of Saurashtra, India, detected by remote sensing techniques
p 15 A87-35308
- SOOD, R. K.**
Geochronological studies of strandlines of Saurashtra, India, detected by remote sensing techniques
p 15 A87-35308
- SOOHOO, JANICE BEELER**
A model for the use of satellite remote sensing for the measurement of primary production in the ocean
p 29 A87-42644
- SROKOSZ, M. A.**
The effect of a non-Gaussian point target response function on radar altimeter returns from the sea surface
p 26 A87-39179
- STACEY, J. A.**
The SIR-B mission: Towards an understanding of internal waves in the ocean [ARE-TR-86122]
p 32 N87-23102
- STALLINGS, CASSON**
A model for the use of satellite remote sensing for the measurement of primary production in the ocean
p 29 A87-42644
- STAR, JEFFREY L.**
Remote Sensing Information Sciences Research Group: Santa Barbara Information Sciences Research Group, year 4
[NASA-CR-181073]
p 43 N87-24817
- STEENROD, STEPHEN D.**
Tidal estimation in the Atlantic and Indian Oceans, 3 deg x 3 deg solution
[NASA-TM-87812]
p 30 N87-21534

STEINVALL, OVE

Potential of laser remote sensing of oil below water surface
[FOA-C-30435-3.1] p 30 N87-20659

STIBIG, H. J.

Comparative analysis of Thematic Mapper and SPOT image data for land use investigation p 51 N87-24746

STONE, T. A.

Deforestation in the tropics - New measurements in the Amazon Basin using Landsat and NOAA advanced very high resolution radiometer imagery p 4 A87-33441

STORY, M. H.

Monsoon flood boundary delineation and damage assessment using space borne imaging radar and Landsat data p 35 A87-39467

STOW, D. A.

Remotely-sensed tracers for hydrodynamic surface flow estimation p 26 A87-39176

STOWE, L. L.

Reflectivity of earth's surface and clouds in ultraviolet from satellite observations p 47 A87-40768

STRAHLER, ALAN H.

The factor of scale in remote sensing p 39 A87-38096

STRAMMA, LOTHAR

Satellite measurements of sea surface cooling during hurricane Gloria p 24 A87-37886

STREBEL, D. E.

Inferring spectral reflectances of plant elements by simple inversion of bidirectional reflectance measurements p 7 A87-37281

STREBEL, DONALD E.

Ten year change in forest succession and composition measured by remote sensing
[NASA-CR-180948] p 11 N87-24736

STRINGER, W. J.

Statistical description of the summertime ice edge in the Chukchi Sea, task 2
[DE87-001056] p 31 N87-22387

STURDEVANT, JAMES A.

Testing the consistency for mapping urban vegetation with high-altitude aerial photographs and Landsat MSS data p 13 A87-37277

SUGA, YUZO

Landcover change in Hiroshima during 1979/1984 detected by Landsat MSS and TM data p 12 A87-32494

SUGIMOTO, NOBUO

Atmospheric environment monitoring system based on an earth-to-satellite Hadamard transform laser long-path absorption spectrometer - A proposal p 45 A87-35502

SUGIMURA, TOSHIRO

A study of elevation measurement using LFC photograph p 43 A87-32491
Landcover change in Hiroshima during 1979/1984 detected by Landsat MSS and TM data p 12 A87-32494

SUZUKI, TSUTOMU

The dependence of sea-surface microwave emission on wind speed, frequency, incidence angle, and polarization over the frequency range from 1 to 40 GHz p 22 A87-35515

SVENDSEN, E.

Ice-edge eddies in the Fram Strait marginal ice zone p 27 A87-40432

SWIFT, ROBERT N.

Wave-measurement capabilities of the surface contour radar and the airborne oceanographic lidar p 25 A87-38840

SZANGOLIES, KLAUS

The production of photographs of the Earth's surface taken from satellites and their application in map production and map revision p 55 N87-24788

T

TACONET, O.

Evaluation of a surface/vegetation parameterization using satellite measurements of surface temperature p 3 A87-33298

TAKAHASHI, KOICHIRO

World-wide weather p 56 A87-33125

TAKAMURA, SHUNJI

Earth resources satellite-1 (ERS-1) p 44 A87-32501

TAKASHIMA, T.

Sea surface temperature measurement from space allowing for the effect of the stratospheric aerosols p 22 A87-35148

TAKAYAMA, Y.

Sea surface temperature measurement from space allowing for the effect of the stratospheric aerosols p 22 A87-35148

TAKEDA, KANAME

Monitoring of snow and ice in Hokkaido Island using multitemporal NOAA-AVHRR data p 20 A87-32497

TAKEUCHI, SHOJI

Monitoring of snow and ice in Hokkaido Island using multitemporal NOAA-AVHRR data p 20 A87-32497

TANAKA, HIROKAZU

Simulation software of synthetic aperture radar p 37 A87-32506

TANAKA, SOTARO

A study of elevation measurement using LFC photograph p 43 A87-32491
Landcover change in Hiroshima during 1979/1984 detected by Landsat MSS and TM data p 12 A87-32494

Relation between precipitation and brightness of earth surface in the NOAA/GVIP data p 3 A87-32498

TANIS, FRED J.

Spatial characterization of acid rain stress in Canadian Shield lakes
[NASA-CR-180983] p 36 N87-24031

Spatial characterization of acid rain stress in Canadian Shield lakes
[NASA-CR-180982] p 36 N87-24032

TAO, WEI-KUO

Trace gas exchanges and transports over the Amazonian rain forest p 12 A87-32196

TAPLEY, B. D.

Altimeter measurements for the determination of the Earth's gravity field
[NASA-CR-180520] p 17 N87-23033

TARCSAI, GY.

Remote sensing methods of yield forecasting p 2 A87-32009
Surface models including direct cross-radiation - A simple model of furrowed surfaces p 40 A87-39189

TARDY, YVES

First results of latent cover mapping with SPOT images The Kangaiba region (South-Mali) p 18 A87-36925

TEILLET, PHILIPPE M.

Radiometric comparison of the Landsat-5 TM and MSS sensors p 47 A87-41432

TESTUD, J.

Energy Balance of the Tropical Systems (BEST): A space experiment proposition p 36 N87-22373

THOMAS, J. O.

The SIR-B mission: Towards an understanding of internal waves in the ocean
[ARE-TR-86122] p 32 N87-23102

THORNTON, C. L.

GPS-based geodesy in California, Mexico and the Caribbean p 16 A87-41380

TILL, S. M.

The Multidetector Electro-optical Imaging Sensor (MEIS) 2 pushbroom imager: Four years of operation p 53 N87-24767

TILLEY, DAVID G.

The age and source of ocean swell observed in Hurricane Josephine p 25 A87-38843

TIMCHENKO, I. E.

Use of satellite altimetry for ocean monitoring p 23 A87-36101

TIMOFEEV, N. A.

Cloud-cover and precipitation patterns over the Republic of Guinea according to ground-based and satellite observations p 35 A87-36102

TOPCHIEV, A. G.

Satellite techniques for studying ice crusts and underground waters in the eastern Pamir p 35 A87-36106

TORRES, ARNOLD

Trace gas exchanges and transports over the Amazonian rain forest p 12 A87-32196

TORRES, ARNOLD L.

Operational overview of NASA GTE/CITE 1 airborne instrument intercomparisons - Carbon monoxide, nitric oxide, and hydroxyl instrumentation p 45 A87-33426

TOSAYA, CAROL

Tectonic evaluation of the Nubian Shield of northeastern Sudan using Thematic Mapper imagery
[NASA-CR-180575] p 19 N87-22319

TREES, CHARLES C.

Remote sensing of chlorophyll concentrations in the northern Gulf of Mexico p 29 A87-42643

TRINDER, J. C.

Measurements on digitized hardcopy images p 39 A87-37290

TSIUPAK, I. M.

The determination of earth-rotation parameters from satellite laser ranging p 15 A87-34186

TSONIS, A. A.

Determining rainfall intensity and type from GOES imagery in the midlatitudes p 34 A87-32092

TUCKER, C. J.

Monitoring vegetation using Nimbus-7 scanning multichannel microwave radiometer s data p 8 A87-39194

TUCKER, COMPTON J.

Detection of Rift Valley fever viral activity in Kenya by satellite remote sensing imagery p 7 A87-37827

TUCKER, W. B. III

An evaluation of the polar ice prediction system
[AD-A178522] p 41 N87-23014

U

UENO, SUEO

Spectral classification of Landsat-5 Thematic Mapper data p 37 A87-32488
Correction for atmospheric and topographic effects on the Landsat MSS data p 37 A87-32489

ULABY, FAWWAZ T.

Relating polarization phase difference of SAR signals to scene properties p 1 A87-31413

ULIANA, E. A.

Airborne microwave Doppler measurements of ocean wave directional spectra p 26 A87-39180

ULIVIERI, CARLO

Balloon-borne infrared multichannel radiometer for remote sensing of high resolution low-level water vapor fields p 43 A87-32477

UMEZONO, SHUHEI

Landcover change in Hiroshima during 1979/1984 detected by Landsat MSS and TM data p 12 A87-32494

V

VADASZ, V.

The application of remote sensing in agricultural meteorology at the Meteorological Service of the HPR p 2 A87-32010

VAN DER PIEPEN, HEINZ

Sunlight induced 685 nm fluorescence imagery p 30 A87-42646

VAN DIJK, ALBERT

The use of AVHRR data in operational agricultural assessment in Africa p 9 A87-40304

VAN R. CLAASEN, DANIEL B.

Coral reef remote sensing applications p 20 A87-32951

VAN RENSBURG, P. A. J.

Landsat as an aid in evaluating the adequacy of a grain silo network p 7 A87-37282

VANDERBILT, V. C.

Variations in the polarized leaf reflectance of Sorghum bicolor p 7 A87-38097

VANDIJK, ALBERT

A crop condition and crop yield estimation method based on NOAA-AVHRR satellite data p 10 N87-22280

VANHEE, DENNIS H.

Preliminary results obtained by DMAAC from the processing of a limited set of GEOSAT satellite radar altimeter data
[AD-A179081] p 50 N87-24734

VASIL'EV, L. N.

Phase portraits of vegetation development trajectories in a multidimensional spectral attribute space p 10 A87-41771

VELTEN, ERICH H.

The first ESA remote sensing satellite (status and outlook) p 57 N87-24777

VERMILLION, C.

Monsoon flood boundary delineation and damage assessment using space borne imaging radar and Landsat data p 35 A87-39467

VETRELLA, S.

The Tethered Satellite System as a new remote sensing platform p 46 A87-39183

VIDAL-MADJAR, D.

Evaluation of a surface/vegetation parameterization using satellite measurements of surface temperature p 3 A87-33298

Nadir looking airborne radar and possible applications to forestry p 7 A87-38095

Energy Balance of the Tropical Systems (BEST): A space experiment proposition p 36 N87-22373

VILAR, ENRIC

Analysis of moderate and intense rainfall rates continuously recorded over half a century and influence on microwave communications planning and rain-rate data acquisition p 46 A87-36933

VILLANUEVA, J. Z.

Mesoscale oceanographic processes beneath the ice of Fram Strait p 28 A87-40434

VINCENT, DAYTON G.

Convective heating and precipitation estimates for the tropical South Pacific during FGGE, 10-18 January 1979
p 21 A87-32982

VIOLA, A.

Remotely sensed sea surface temperature for the Alpine Experiment (ALPEX)
p 30 N87-21497

VONDER HAAR, THOMAS H.

The area-time-integral technique to estimate convective rain volumes over areas applied to satellite data - A preliminary investigation
p 35 A87-40249

VOROZHEIKIN, A. P.

Problems in the automation of map-compilation processes on the basis of remote-sensing data
p 38 A87-35925

VYAS, N. K.

Determination of the velocity of ocean gyres through Synthetic Aperture Radar
p 22 A87-35314

W

WAHR, JOHN M.

Polar motion-induced gravity
p 15 A87-36176

WAKIMOTO, ROGER M.

Lidar observation of elevated pollution layers over Los Angeles
p 13 A87-33292

WALSH, EDWARD J.

Wave-measurement capabilities of the surface contour radar and the airborne oceanographic lidar
p 25 A87-38840

WALTON, CHARLES

The AVHRR/HIRS operational method for satellite based sea surface temperature determination
[NOAA-TR-NESDIS-28]
p 31 N87-22388

WANG, CHARLES C.

OH measurement near the intertropical convergence zone in the Pacific
p 21 A87-33430

WANG, J. R.

Quantifying spatial and temporal variabilities of microwave brightness temperature over the U.S. Southern Great Plains
p 5 A87-35309

WANG, LI

Automatic classification of Pointe d'Arcay landscapes using Thematic Mapper data with the aid of a textural analysis
p 37 A87-35305
Introduction of initial centers for the algorithm of clustering around mobile centers
p 37 A87-35313

WANG, PIN-QING

Predicting the location of kimberlite from a probability analysis of linear structure on remote sensing data
p 18 A87-39186

WANG, RENXIANG

Estimating photogrammetric precision and cartographic potential of space imagery
p 42 N87-24791

WELCH, R.

Merging multiresolution SPOT HRV and Landsat TM data
p 38 A87-37287

WENDEL, MELCHIOR

Observations of intermittent cumulus convection in the boundary layer
p 20 A87-32976

WESTWELL-ROPER, ANDREW

Mapping from space
p 38 A87-36361

WETZEL, PETER J.

Concerning the relationship between evapotranspiration and soil moisture
p 8 A87-40244
Soil moisture estimation using GOES-VISSR infrared data - A case study with a simple statistical method
p 8 A87-40248

WHITEHEAD, VICTOR S.

Polarized views of the earth from orbital altitude
p 48 A87-42639

WHITLOCK, CHARLES H.

Surface bidirectional reflectance properties of two southwestern Arizona deserts for wavelengths between 0.4 and 2.2 micrometers
[NASA-TP-2643]
p 49 N87-22281

WILKE, GREGORY D.

Nimbus 7 SMMR investigation of snowpack properties in the northern Great Plains for the winter of 1978-1979
p 34 A87-31409

WILLIAMS, JONATHAN

Remote sensing - Handling the data
p 38 A87-36359

WILLIAMS, LARRY D.

The relation of millimeter-wavelength backscatter to surface snow properties
p 34 A87-35518

WILLIAMS, VICKI L.

Identifying vegetable crops with Landsat Thematic Mapper data
p 4 A87-35120

WILLIAMSON, H. D.

GLAI estimation using measurements of red, near infrared, and middle infrared radiance
p 4 A87-35119

WILSON, J. J. W.

The effect of receiver amplifier non-linearity on ERS-1 synthetic aperture radar imagery
p 52 N87-24755

WINKENBACH, H.

Advanced imaging spectrometer for ocean color/fluorescence measurements and further applications
p 33 N87-24766

The Modular Optoelectronic Multispectral Scanner (MOMS) program of the Bundesministerium fuer Forschung und Technologie (BMFT). Milestones in the development of an operational Earth Observation system
p 55 N87-24815

WINTER, R.

MIDAS - A new image-processing system for remote sensing
p 37 A87-35183

WINTERBERGER, KENNETH C.

Comparison between digital and manual interpretation of high altitude aerial photographs
p 48 A87-42257

WOLFE, ROBERT E.

Derivation of a fast algorithm to account for distortions due to terrain in earth-viewing satellite sensor images
p 38 A87-35524

WOODCOCK, CURTIS E.

The factor of scale in remote sensing
p 39 A87-38096

WOODHOUSE, JOHN H.

Global images of the earth's interior
p 15 A87-37918

WOODS, K. D.

New dimension analyses with error analysis for quaking aspen and black spruce
[NASA-TM-89219]
p 11 N87-24735

WOODS, KERRY K.

Ten year change in forest succession and composition measured by remote sensing
[NASA-CR-180948]
p 11 N87-24736

WOODWARD, ROBERT H.

Soil moisture estimation using GOES-VISSR infrared data - A case study with a simple statistical method
p 8 A87-40248

WOODWELL, G. M.

Deforestation in the tropics - New measurements in the Amazon Basin using Landsat and NOAA advanced very high resolution radiometer imagery
p 4 A87-33441

WU, J.

Investigation of simulated Monocular Electro-Optical Stereo Scanner (MEOSS)-imagery for sensor navigation and terrain derivation
p 54 N87-24771

WU, SHIH-TSENG

Multipolarization SAR data for surface feature delineation and forest vegetation characterization
p 1 A87-31411

Y

YANG, SHI-REN

The application of remote sensing techniques in China
p 57 A87-41435

YANG, WEI-LIANG

A model for the use of satellite remote sensing for the measurement of primary production in the ocean
p 29 A87-42644

YENTSCH, CHARLES S.

The relationship between phytoplankton concentration and light attenuation in ocean waters
p 29 A87-42642

YOSHIKADO, SHIN

Observation of precipitation from space by the weather radar
p 44 A87-32507

YOSHIMURA, MITSUNORI

A study of elevation measurement using LFC photograph
p 43 A87-32491

YOSHITOMI, SUSUMU

Marine Observation Satellite-1 (MOS-1)
p 20 A87-32499

YU, ZHENG

Image preprocessing for line detection based on local structure analysis
p 39 A87-37801

YUWEI, WANG

Applied formulae for calibration of aerial photogrammetric cameras
p 51 N87-24744

Z

ZAMBRESKY, LIANA F.

The operational performance of the fleet numerical oceanography center global spectral ocean-wave model
p 24 A87-38832

ZHANG, LIXIA

High resolution sea surface temperature field derived
p 33 N87-24731

ZHOU, SISONG

High resolution sea surface temperature field derived
p 33 N87-24731

ZIEMANN, H.

Proposed changes to the Canadian camera calibration report
p 53 N87-24757

Spectrophotometric measurements on color aerial photographs
p 55 N87-24798

ZIEMANN, HARTMUT

Thoughts on a standard algorithm for camera calibration
p 51 N87-24743
The role of government specifications in aerial photography
p 57 N87-24780

ZILGER, J.

The Modular Optoelectronic Multispectral Scanner (MOMS) program of the Bundesministerium fuer Forschung und Technologie (BMFT). Milestones in the development of an operational Earth Observation system
p 55 N87-24815

ZINI, ENRICO

Comparative evaluation and guide for the integrated utilization of LANDSAT (MSS and TM) and SPOT (HRV) satellites to remotely sensed data
[ETN-87-96-10]
p 41 N87-22278

ZWALLY, H. J.

Remote sensing as a research tool
p 28 A87-40648

ZWALLY, H. JAY

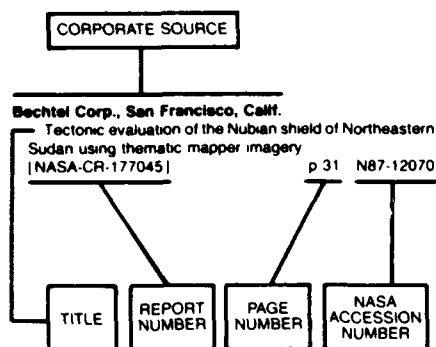
Arctic Sea ice, 1973-1976. Satellite passive-microwave observations
[NASA-SP-489]
p 33 N87-24870

CORPORATE SOURCE INDEX

EARTH RESOURCES / A Continuing Bibliography (Issue 55)

NOVEMBER 1987

Typical Corporate Source Index Listing



Listings in this index are arranged alphabetically by corporate source. The title of the document is used to provide a brief description of the subject matter. The page number and the accession number are included in each entry to assist the user in locating the abstract in the abstract section. If applicable, a report number is also included as an aid in identifying the document.

A

- Admiralty Research Establishment, Portland (England).**
The SIR-B mission: Towards an understanding of internal waves in the ocean
[ARE-TR-86122] p 32 N87-23102
- Air Force Geophysics Lab., Hanscom AFB, Mass.**
Atmospheric remote sensing in arctic regions
[AD-A179550] p 50 N87-23012
- Air/Ocean Remote Sensing Co., San Diego, Calif.**
Simulation of wind gradient errors in NROSS (Navy Remote Ocean Sensing System) radar scatterometer data in a simplified geometry
[AD-A175754] p 46 N87-20642
- Alaska Univ., Fairbanks.**
Statistical description of the summertime ice edge in the Chukchi Sea, task 2
[DE87-001056] p 31 N87-22387
- Army Cold Regions Research and Engineering Lab., Hanover, N. H.**
An evaluation of the polar ice prediction system
[AD-A178522] p 41 N87-23014
- Army Medical Research Inst. of Infectious Diseases, Fort Detrick, Md.**
Detection of Rift Valley fever viral activity in Kenya by satellite remote sensing imagery p 7 A87-37827
- Aster Consulting Associates, Inc., La Jolla, Calif.**
Inversion of canopy reflectance models for estimation of vegetation parameters
[NASA-CR-181059] p 12 N87-24737
- Atmospheric and Environmental Research, Inc., Cambridge, Mass.**
Impact of satellite-based data on FGGE general circulation statistics p 44 A87-32985

B

- Bangladesh Space Research and Remote Sensing Organization, Dhaka.**
Monsoon flood boundary delineation and damage assessment using space borne imaging radar and Landsat data p 35 A87-39467
- Bayerische Akademie der Wissenschaften, Munich (West Germany).**
Report on the Special Program 78 satellite geodesy of the Technical University of Munich
[ASTRON-GEODAE-ARB-48] p 16 N87-20618
- Bechtel National, Inc., San Francisco, Calif.**
Tectonic evaluation of the Nubian Shield of northeastern Sudan using Thematic Mapper imagery
[NASA-CR-180575] p 19 N87-22319
- Bercha (F. G.) and Associates Ltd., Calgary (Alberta).**
Shuttle Imaging Radar (SIR-B) investigations of the Canadian shield - Initial Report p 17 A87-31410
- Bigelow Lab. for Ocean Sciences, West Boothbay Harbor, Maine.**
The relationship between phytoplankton concentration and light attenuation in ocean waters p 29 A87-42642
- Bionetics Corp., Hampton, Va.**
Operational overview of NASA GTE/CITE 1 airborne instrument intercomparisons - Carbon monoxide, nitric oxide, and hydroxyl instrumentation p 45 A87-33426
- Boeing Aerospace Co., Seattle, Wash.**
NASA/MSFC large stretch press study
[NASA-CR-180376] p 41 N87-20554
- Bonn Univ. (West Germany).**
Geometrical system calibration, especially for metric aerial cameras p 51 N87-24745
- Boston Univ., Mass.**
The factor of scale in remote sensing p 39 A87-38096

C

- California Univ., Davis.**
Polarized views of the earth from orbital altitude p 48 A87-42639
- California Univ., La Jolla.**
Remote sensing of chlorophyll concentrations in the northern Gulf of Mexico p 29 A87-42643
Coastal zone color scanner imagery of phytoplankton pigment distribution - Icelandic waters p 29 A87-42645
- California Univ., Santa Barbara.**
The regression intersection method of adjusting image data for band ratioing p 45 A87-35306
Recent research in snow hydrology p 35 A87-40309
- Earth science research
[NASA-CR-180512] p 11 N87-24733
New dimension analyses for analysis for quaking aspen and black spruce
[NASA-TM-89219] p 11 N87-24735
- Remote Sensing Information as Research Group:
Santa Barbara Information Science Research Group, year 4
[NASA-CR-181073] p 43 N87-24817
- Canada Centre for Remote Sensing, Ottawa (Ontario).**
Procedures for the description of agricultural crops and soils in optical and microwave remote sensing studies p 8 A87-39187
- The Multidetector Electro-optical Imaging Sensor (MEIS)
2 pushbroom imager: Four years of operation p 53 N87-24767
- The use of auxiliary data in photogrammetric adjustments p 42 N87-24808
- Centre de Recherches en Physique de l'Environnement Terrestre et Planetaire, Orleans (France).**
Measurement and detection of precipitation. Satellite methods in the visible and the infrared p 36 N87-22364
- Energy Balance of the Tropical Systems (BEST): A space experiment proposition p 36 N87-22373

- Centre de Recherches en Physique de l'Environnement, Issy-les-Moulineaux (France).**
Evaluation of a surface/vegetation parameterization using satellite measurements of surface temperature p 3 A87-33298
- Centre National d'Etudes Spatiales, Toulouse (France).**
Remote sensing applications: Commercial issues and opportunities for space station p 57 N87-20626
SPOT image quality p 42 N87-24804
- Coastal Engineering Research Center, Vicksburg, Miss.**
DUCK '85 nearshore waves and currents experiment data summary report
[AD-A177419] p 31 N87-22382
- Colorado State Univ., Fort Collins.**
The area-time-integral technique to estimate convective rain volumes over areas applied to satellite data - A preliminary investigation p 35 A87-40249
- Colorado Univ., Boulder.**
Measurements of nitric oxide in the boundary layer and free troposphere over the Pacific Ocean p 21 A87-33431
- Polar motion-induced gravity p 15 A87-36176
- Comision Nacional de Investigaciones Espaciales, Buenos Aires (Argentina).**
Landsat classification of Argentina summer crops p 3 A87-32098

D

- Defense Mapping Agency Aerospace Center, St. Louis, Mo.**
Preliminary results obtained by DMAAC from the processing of a limited set of GEOSAT satellite radar altimeter data
[AD-A179081] p 50 N87-24734
- Delaware Univ., Newark.**
Remote sensing of coastal wetlands p 9 A87-40944
- Real-time crop assessment using color theory and satellite data p 10 N87-20619
- Department of Agriculture, Beltsville, Md.**
Salinity effects on the microwave emission of soils p 5 A87-35520
- Temporal observations of surface soil moisture using a passive microwave sensor p 7 A87-38094
- Deutsche Forschungs- und Versuchsanstalt fuer Luft- und Raumfahrt, Cologne (West Germany).**
Application of Modular Optoelectronic Multispectral Scanner (MOMS) data to hydrology and vegetation studies. Test site: Pantanal Region (Brazil/Paraguay) p 52 N87-24748
- Deutsche Forschungs- und Versuchsanstalt fuer Luft- und Raumfahrt, Oberpfaffenhofen (West Germany).**
European utilization aspects studies p 49 N87-20624
- Land panel report p 49 N87-20634
- Comparative analysis of Thematic Mapper and SPOT image data for land use investigation p 51 N87-24746
- Investigation of simulated Monocular Electro-Optical Stereo Scanner (MEOSS)-imagery for sensor navigation and terrain derivation p 54 N87-24771
- Exposure test with high resolution films from high altitude p 54 N87-24775
- Earth observation experiments on the German Spacelab mission D2 p 55 N87-24811
- The Monocular Electro-Optical Stereo Scanner (MEOSS) satellite experiment p 55 N87-24812
- Modern CCD sensors and their applications in Earth observation and planetary missions p 55 N87-24813
- Deutsche Forschungs- und Versuchsanstalt fuer Luft- und Raumfahrt, Wessling (West Germany).**
Sunlight induced 685 nm fluorescence imagery p 30 A87-42646
- Infrared Earth horizon sensor concepts in various spectral bands p 52 N87-24752
- Dornier-Werke G.m.b.H., Friedrichshafen (West Germany).**
The first ESA remote sensing satellite (status and outlook) p 57 N87-24777

E

EG and G Washington Analytical Services Center, Inc., Pocomoke City, Md.

Wave-measurement capabilities of the surface contour radar and the airborne oceanographic lidar p 25 A87-38840

European Centre for Medium-Range Weather Forecasts, Reading (England).

The impact of initial conditions and SST Anomalies on extended range predictions for the El Nino period p 32 N87-23046

European Space Agency, Paris (France).

Proceedings of the European Symposium on Polar platform Opportunities and Instrumentation for Remote-Sensing (ESPOIR) [ESA-SP-266] p 48 N87-20621

Proceedings of the International Symposium on Progress in Imaging Sensors [ESA-SP-252] p 50 N87-24738

European Space Agency, European Space Research and Technology Center, ESTEC, Noordwijk (Netherlands).

The Earth observation activities of the European Space Agency and the use of the polar platform of the International Space Station p 49 N87-20622
Definition of a thermal infrared pushbroom imager for Earth observation p 53 N87-24765

F

Firma Maps G.m.b.H., Munich (West Germany).

Very high resolution aerial films p 54 N87-24776

Florida Univ., Gainesville.

Comparison of HCMM and GOES satellite temperatures and evaluation of surface statistics p 39 A87-38098

Ford Motor Co., Dearborn, Mich.

OH measurement near the intertropical convergence zone in the Pacific p 21 A87-33430

Freiburg Univ. (West Germany).

Comparative analysis of Thematic Mapper and SPOT image data for land use investigation p 51 N87-24746

G

General Software Corp., Landover, Md.

Soil moisture estimation using GOES-VISSR infrared data - A case study with a simple statistical method p 8 A87-40248

Geological Survey, Flagstaff, Ariz.

Enhanced LANDSAT images of Antarctica and planetary exploration p 50 N87-23558

Geological Survey, Reston, Va.

Radar as a complement to topographic maps for delineating marine terraces [PB87-154597] p 41 N87-24013

Geological Survey of Canada, Ottawa (Ontario).

Shuttle Imaging Radar (SIR-B) investigations of the Canadian shield - Initial Report p 17 A87-31410

George Mason Univ., Fairfax, Va.

An assessment of Landsat MSS and TM data for urban and near-urban land-cover digital classification p 13 A87-37280

Georgia Inst. of Tech., Atlanta.

Free tropospheric and boundary layer measurements of NO over the central and eastern North Pacific Ocean p 21 A87-33432

H

Houston Univ., Clear Lake, Tex.

Error analysis of leaf area estimates made from allometric regression models [NASA-TM-89220] p 11 N87-24010

Hunter Coll., New York.

The factor of scale in remote sensing p 39 A87-38096

I

IBM France S. A., Paris.

Towards an automatic identification of urban textures p 14 N87-24747

Institut fuer Angewandte Geodasie, Frankfurt am Main (West Germany).

Reports on cartography and geodesy, series 1, number 96 [ISSN-0469-4236] p 16 N87-22282

Reports on cartography and geodesy, series 1, number 97 [ISSN-0469-4236] p 16 N87-22286

The VICOM system for digital image processing at the Institute of Cartography of Technical University, Hanover (West Germany) p 16 N87-22290

Institut Geographique National, Paris (France).

Applications of laser airborne telemetry at Institut Geographique National (IGN), France p 53 N87-24761

Instituto de Pesquisas Espaciais, Sao Jose dos Campos (Brazil).

Application of Modular Optoelectronic Multispectral Scanner (MOMS) data to hydrology and vegetation studies Test site: Pantanal Region (Brazil/Paraguay) p 52 N87-24748

International Council of Scientific Unions, Rome (Italy).

Report of the workshop on Assimilation of Satellite Wind and Wave Data in Numerical Weather and Wave Prediction Models [WCP-122] p 49 N87-21521

International Meteorological Inst., Stockholm (Sweden).

The observational objectives and the implementation of the Global Weather Experiment p 49 N87-21474

Istituto di Fisica dell'Atmosfera, Rome (Italy).

Remotely sensed sea surface temperature for the Alpine Experiment (ALPEX) p 30 N87-21497

J

Jet Propulsion Lab., California Inst. of Tech., Pasadena.

Relating polarization phase difference of SAR signals to scene properties p 1 A87-31413

An assessment of Landsat MSS and TM data for urban and near-urban land-cover digital classification p 13 A87-37280

Spaceborne imaging radar research in the 1990s - An overview p 46 A87-38837

The age and source of ocean swell observed in Hurricane Josephine p 25 A87-38843

Remote sensing as a research tool p 28 A87-40648

GPS-based geodesy in California, Mexico and the Caribbean p 16 A87-41380

Rectification of terrain induced distortions in radar imagery p 48 A87-42254

The interaction of light with phytoplankton in the marine environment p 29 A87-42640

A model for the use of satellite remote sensing for the measurement of primary production in the ocean p 29 A87-42644

Coastal zone color scanner imagery of phytoplankton pigment distribution in Icelandic waters p 29 A87-42645

Optical image subtraction techniques, 1975-1985 p 40 A87-42659

The 1982-1983 El Nino Atlas: Nimbus-7 microwave radiometer data [NASA-CR-180914] p 31 N87-22386

Earth surface sensing in the '90's p 51 N87-24739

Radiometric calibration of the Shuttle Imaging Radar (SIR-C) system p 53 N87-24756

Johns Hopkins Univ., Laurel, Md.

Measuring ocean waves from space, Proceedings of the Symposium, Johns Hopkins University, Laurel, MD, Apr. 15-17, 1986 p 24 A87-38826

The age and source of ocean swell observed in Hurricane Josephine p 25 A87-38843

Spectrasat - A hybrid ROWS/SAR approach to monitor ocean waves from space p 25 A87-38845

Joint Publications Research Service, Arlington, Va.

Possibilities of using artificial Earth satellite data for computing heat exchange between the ocean and atmosphere in Newfoundland energy-active zone during winter p 31 N87-21980

Arianespace top performance benefits ESA p 57 N87-24493

High resolution sea surface temperature field derived p 33 N87-24731

K

Khartoum Univ. (Sudan).

Optical and digital SAR processing techniques: A statistical comparison of accuracy using SEASAT imagery p 42 N87-24753

L

Lamont-Doherty Geological Inst., Palisades, N.Y.

Recurring polynyas over the Cosmonaut Sea and the Maud Rise p 23 A87-37563

Lockheed Engineering and Management Services Co., Inc., Houston, Tex.

Polarized views of the earth from orbital altitude p 48 A87-42639

Los Alamos National Lab., N. Mex.

An atmospheric correction algorithm for remote identification of non-Lambertian surfaces and its range of validity [DE87-006059] p 41 N87-24011

Modeling of atmospheric effects on the angular distribution of a backscattering peak [DE87-006060] p 41 N87-24014

Louisiana State Univ., Baton Rouge.

The integration of spectral and spatial analysis for land use classification [AD-A178703] p 14 N87-23015

Utilizing remote sensing of thematic mapper data to improve our understanding of estuarine processes and their influence on the productivity of estuarine-dependent fisheries [NASA-CR-180984] p 33 N87-24012

Ludwig-Maximilians-Universitaet, Munich (West Germany).

Large Format Camera photographs of the Black Hills, USA, and their suitability for topographic and thematic mapping p 55 N87-24792

M

Marconi Co. Ltd., Great Baddow (England).

The effect of receiver amplifier non-linearity on ERS-1 synthetic aperture radar imagery p 52 N87-24755

Marine Biological Lab., Woods Hole, Mass.

Deforestation in the tropics - New measurements in the Amazon Basin using Landsat and NOAA advanced very high resolution radiometer imagery p 4 A87-33441

Maryland Univ., College Park.

Quantifying spatial and temporal variabilities of microwave brightness temperature over the U.S. Southern Great Plains p 5 A87-35309

Canopy reflectance, photosynthesis, and transpiration. II - The role of biophysics in the linearity of their interdependence p 6 A87-37278

Deriving surface albedo measurements from narrow band satellite data p 13 A87-39182

Comparison of North and South American biomes from AVHRR observations p 9 A87-40303

Massachusetts Inst. of Tech., Cambridge.

Radar scene generation for tactical decision aids [NASA-CR-180234] p 40 N87-20449

Active and passive remote sensing of ice [AD-A179461] p 32 N87-24009

Messerschmitt-Boelkow-Blohm G.m.b.H., Munich (West Germany).

The stereo pushbroom scanner system Digital Photogrammetry System (DPS) and its accuracy p 53 N87-24768

Messerschmitt-Boelkow-Blohm G.m.b.H., Ottobrunn (West Germany).

Advanced imaging spectrometer for ocean color/fluorescence measurements and further applications p 33 N87-24766

Meteorological Office, Bracknell (England).

Ocean-ice panel report p 30 N87-20635

Michigan Univ., Ann Arbor.

Relating polarization phase difference of SAR signals to scene properties p 1 A87-31413

Procedures for the description of agricultural crops and soils in optical and microwave remote sensing studies p 8 A87-39187

Evaluation of the airborne imaging spectrometer for remote sensing of forest stand conditions [NASA-CR-180918] p 10 N87-22296

Missouri Univ., Columbia.

A crop condition and crop yield estimation method based on NOAA/AVHRR satellite data p 10 N87-22280

A review of national and international activities on modeling the effects of increased CO2 concentrations on the simulation of regional crop production: A report on linkage between climate and crop models [DE87-005994] p 10 N87-22336

The impact of climate change from increased atmospheric carbon dioxide on American agriculture [DOE/NBB-0077] p 11 N87-23032

N

National Aeronautics and Space Administration, Washington, D.C.

Carbon monoxide measurements over the eastern Pacific during GTE/CITE 1 p 21 A87-33435

Space remote sensors p 47 A87-40379

National Aeronautics and Space Administration, Ames Research Center, Moffett Field, Calif.

Operational overview of NASA GTE/CITE 1 airborne instrument intercomparisons - Carbon monoxide, nitric oxide, and hydroxyl instrumentation p 45 A87-33426
Variations in the polarized leaf reflectance of Sorghum bicolor p 7 A87-38097

National Aeronautics and Space Administration, Goddard Inst. for Space Studies, New York, N.Y.

Deriving surface albedo measurements from narrow band satellite data p 13 A87-39182
Regional and seasonal variations of surface reflectance from satellite observations at 0.6 micron p 27 A87-40250

National Aeronautics and Space Administration, Goddard Space Flight Center, Greenbelt, Md.

Shuttle Imaging Radar (SIR-B) investigations of the Canadian shield - Initial Report p 17 A87-31410
Signature-extendable technology - Global space-based crop recognition p 1 A87-31414
Continental land cover assessment using Landsat MSS data p 3 A87-32095
Trace gas exchanges and transports over the Amazonian rain forest p 12 A87-32196
Impact of satellite-based data on FGGE general circulation statistics p 44 A87-32985
Deforestation in the tropics - New measurements in the Amazon Basin using Landsat and NOAA advanced very high resolution radiometer imagery p 4 A87-33441
Quantifying spatial and temporal variabilities of microwave brightness temperature over the U.S. Southern Great Plains p 5 A87-35309
Salinity effects on the microwave emission of soils p 5 A87-35520

Creation of a global geodetic network using Mark III VLBI p 15 A87-36166
Computation of diffuse sky irradiance from multidirectional radiance measurements p 6 A87-37279

Inferring spectral reflectances of plant elements by simple inversion of bidirectional reflectance measurements p 7 A87-37281
Recurring polynyas over the Cosmonaut Sea and the Maud Rise p 23 A87-37563

Detection of Rift Valley fever viral activity in Kenya by satellite remote sensing imagery p 7 A87-37827
Stochastic nature of Landsat MSS data p 46 A87-38093

Temporal observations of surface soil moisture using a passive microwave sensor p 7 A87-38094
The physical basis for estimating wave-energy spectra with the radar ocean-wave spectrometer p 25 A87-38839

Wave-measurement capabilities of the surface contour radar and the airborne oceanographic lidar p 25 A87-38840
The Radar Ocean-Wave Spectrometer p 25 A87-38846

Procedures for the description of agricultural crops and soils in optical and microwave remote sensing studies p 8 A87-39187
Satellite detection of tropical burning in Brazil p 8 A87-39191

Thematic Mapper bandpass solar exoatmospheric irradiances p 40 A87-39192
Monitoring vegetation using Nimbus-7 scanning multichannel microwave radiometer's data p 8 A87-39194

Two-color short-pulse laser altimeter measurements of ocean surface backscatter p 27 A87-39462
Monsoon flood boundary delineation and damage assessment using space borne imaging radar and Landsat data p 35 A87-39467

Concerning the relationship between evapotranspiration and soil moisture p 8 A87-40244
Soil moisture estimation using GOES-VISSR infrared data - A case study with a simple statistical method p 8 A87-40248

Feedback between ice flow, barotropic flow, and baroclinic flow in the presence of bottom topography p 27 A87-40289
Comparison of North and South American biomes from AVHRR observations p 9 A87-40303

Remote sensing as a research tool p 28 A87-40648
Reflectivity of earth's surface and clouds in ultraviolet from satellite observations p 47 A87-40768

Satellite sensing of aerosol absorption p 47 A87-40770
Sunlight induced 685 nm fluorescence imagery p 30 A87-42646

Tidal estimation in the Atlantic and Indian Oceans, 3 deg x 3 deg solution [NASA-TM-87812] p 30 A87-21534
Problems in merging Earth sensing satellite data sets [NASA-TM-87820] p 50 A87-22457

Quick-look guide to the crustal dynamics project's data information system [NASA-TM-87818] p 16 A87-23018

Spatial characterization of acid rain stress in Canadian Shield lakes [NASA-CR-180983] p 36 A87-24031

Spatial characterization of acid rain stress in Canadian Shield lakes [NASA-CR-180982] p 36 A87-24032
Ten year change in forest succession and composition measured by remote sensing [NASA-CR-180948] p 11 A87-24736

Arctic Sea ice, 1973-1976 Satellite passive-microwave observations [NASA-SP-489] p 33 A87-24870

National Aeronautics and Space Administration, Lyndon B. Johnson Space Center, Houston, Tex.

Signature-extendable technology - Global space-based crop recognition p 1 A87-31414
Landsat classification of Argentina summer crops p 3 A87-32098

Polarized views of the earth from orbital altitude p 48 A87-42639
Error analysis of leaf area estimates made from allometric regression models [NASA-TM-89220] p 11 A87-24010

New dimension analyses with error analysis for quaking aspen and black spruce [NASA-TM-89219] p 11 A87-24735

National Aeronautics and Space Administration, Langley Research Center, Hampton, Va.

Trace gas exchanges and transports over the Amazonian rain forest p 12 A87-32196
Operational overview of NASA GTE/CITE 1 airborne instrument intercomparisons - Carbon monoxide, nitric oxide, and hydroxyl instrumentation p 45 A87-33426

OH measurement near the intertropical convergence zone in the Pacific p 21 A87-33430
Measurements of nitric oxide in the boundary layer and free troposphere over the Pacific Ocean p 21 A87-33431

Carbon monoxide measurements over the eastern Pacific during GTE/CITE 1 p 21 A87-33431
Airborne microwave Doppler measurements of ocean wave directional spectra p 26 A87-39180

Surface bidirectional reflectance properties of two southwestern Arizona deserts for wavelengths between 0.4 and 2.2 micrometers [NASA-TP-2643] p 49 A87-22281

National Aeronautics and Space Administration, National Space Technology Labs., Bay Saint Louis, Miss.

Multipolarization SAR data for surface feature delineation and forest vegetation characterization p 1 A87-31411
Forest biomass, canopy structure, and species composition relationships with multipolarization L-band synthetic aperture radar data p 4 A87-35121

Airborne remote sensing of forest biomes p 9 A87-40301

National Aeronautics and Space Administration, Wallops Flight Center, Wallops Island, Va.

Trace gas exchanges and transports over the Amazonian rain forest p 12 A87-32196
Operational overview of NASA GTE/CITE 1 airborne instrument intercomparisons - Carbon monoxide, nitric oxide, and hydroxyl instrumentation p 45 A87-33426

Wave-measurement capabilities of the surface contour radar and the airborne oceanographic lidar p 25 A87-38840

National Aerospace Lab., Amsterdam (Netherlands), Foundations and applications of multispectral scanning in agriculture [NLR-MP-85015-U] p 10 A87-21408

A modular and versatile acquisition, recording and preprocessing system for airborne remote sensing p 52 A87-24751

National Center for Atmospheric Research, Boulder, Colo.

Measurements of nitric oxide in the boundary layer and free troposphere over the Pacific Ocean p 21 A87-33431

National Marine Fisheries Service, Miami, Fla.

Utilizing remote sensing of thematic mapper data to improve our understanding of estuarine processes and their influence on the productivity of estuarine-dependent fisheries [NASA-CR-180984] p 33 A87-24012

National Oceanic and Atmospheric Administration, Seattle, Wash.

The age and source of ocean swell observed in Hurricane Josephine p 25 A87-38843

National Oceanic and Atmospheric Administration, Washington, D. C.

Satellite detection of tropical burning in Brazil p 8 A87-39191

Reflectivity of earth's surface and clouds in ultraviolet from satellite observations p 47 A87-40768

Coastal zone color scanner imagery of phytoplankton pigment distribution in Icelandic waters p 29 A87-42645

The AVHRR/HIRS operational method for satellite based sea surface temperature determination [NOAA-TR-NESDIS-28] p 31 A87-22388

National Research Council of Canada, Ottawa (Ontario).

Thoughts on a standard algorithm for camera calibration p 51 A87-24743
Proposed changes to the Canadian camera calibration report p 53 A87-24757

The role of government specifications in aerial photography p 57 A87-24780
Spectrophotometric measurements on color aerial photographs p 55 A87-24798

National Science Foundation, Washington, D.C.

The interaction of light with phytoplankton in the marine environment p 29 A87-42640

Naval Ocean Research and Development Activity, Bay St. Louis, Miss.

Ocean wind and wave model comparisons with GEOSAT (GEOSAT Satellite) satellite data [AD-A178302] p 33 A87-24061

Naval Postgraduate School, Monterey, Calif.

Laser reflectance as a function of rough water glitter profile [AD-A178774] p 32 A87-23016

Naval Research Lab., Washington, D.C.

Airborne microwave Doppler measurements of ocean wave directional spectra p 26 A87-39180

Netherlands Organization for Applied Scientific Research TNO, Delft.

Procedures for the description of agricultural crops and soils in optical and microwave remote sensing studies p 8 A87-39187

New York State Univ., Binghamton.

Estimation of canopy parameters of row planted vegetation canopies using reflectance data for only four view directions p 2 A87-32093

O**Ohio State Univ., Columbus.**

Radial orbit error reduction and sea surface topography determination using satellite altimetry [NASA-CR-180570] p 33 A87-24816

Old Dominion Univ., Norfolk, Va.

Continental shelf processes affecting the oceanography of the South Atlantic Bight [DE87-005303] p 30 A87-20716

Ontario Centre for Remote Sensing, Toronto.

Shuttle Imaging Radar (SIR-B) investigations of the Canadian shield - Initial Report p 17 A87-31410

Open Univ., Milton (England).

Synergistic use of MOMS-01 and Landsat TM data p 46 A87-39190

Oregon State Univ., Corvallis.

Optical dynamics experiment (ODEX) data report R/V acania expedition 10 October-17 November 1982 Volume 2 Particle size distributions Volume 6 Scalar spectral-radiometer data [AD-A178535] p 32 A87-23104

P**Physikalisch-Technische Bundesanstalt, Brunswick (West Germany).**

Optical Transfer Function (OTF)-based quality criteria for aerial cameras and imaging systems p 51 A87-24742

Purdue Univ., West Lafayette, Ind.

Continental land cover assessment using Landsat MSS data p 3 A87-32095
Convective heating and precipitation estimates for the tropical South Pacific during FGGE, 10-18 January 1979 p 21 A87-32982

Variations in the polarized leaf reflectance of Sorghum bicolor p 7 A87-38097

R**Regione del Veneto, Mestre-Venezia (Italy).**

Comparative evaluation and guide for the integrated utilization of LANDSAT (MSS and TM) and SPOT (HRV) satellites remotely sensed data [ETN-87-99356] p 41 A87-22278

Research Inst. of National Defence, Linköping (Sweden).

Potential of laser remote sensing of oil below water surface [FOA-C-30435-3.1] p 30 A87-20659

Z

- RMS Technologies, Inc., Landover, Md.**
Monitoring vegetation using Nimbus-7 scanning multichannel microwave radiometer's data p 8 A87-39194
- Royal Australian Navy Research Lab., Edgecliff.**
Studies of the east Australian current off northern New South Wales [AD-A178461] p 32 N87-23103
- Royal Inst. of Tech., Stockholm (Sweden).**
Image quality problems in practical aerial photography p 43 N87-24814

S

- San Diego State Univ., Calif.**
Remotely-sensed tracers for hydrodynamic surface flow estimation p 26 A87-39176
- Sandia National Labs., Albuquerque, N. Mex.**
Measured radar return at the near vertical from forested terrains [DE87-009384] p 11 N87-24593
- SAR, Inc., Lanham, Md.**
Deforestation in the tropics - New measurements in the Amazon Basin using Landsat and NOAA advanced very high resolution radiometer imagery p 4 A87-33441
- SASC Technologies, Inc., Hyattsville, Md.**
Concerning the relationship between evapotranspiration and soil moisture p 8 A87-40244
- SASC Technologies, Inc., Lanham, Md.**
Stochastic nature of Landsat MSS data p 46 A87-38093
- Science Applications International Corp., Washington, D.C.**
Monitoring vegetation using Nimbus-7 scanning multichannel microwave radiometer's data p 8 A87-39194
- Science Applications Research, Lanham, Md.**
Shuttle Imaging Radar (SIR-B) investigations of the Canadian shield - Initial Report p 17 A87-31410
Quantifying spatial and temporal variabilities of microwave brightness temperature over the U.S. Southern Great Plains p 5 A87-35309
Computation of diffuse sky irradiance from multidirectional radiance measurements p 6 A87-37279
Inferring spectral reflectances of plant elements by simple inversion of bidirectional reflectance measurements p 7 A87-37281
Monsoon flood boundary delineation and damage assessment using space borne imaging radar and Landsat data p 35 A87-39467
Reflectivity of earth's surface and clouds in ultraviolet from satellite observations p 47 A87-40768
- Scranton Univ., Pa.**
Remote sensing of coastal wetlands p 9 A87-40944
- South Dakota School of Mines and Technology, Rapid City.**
The area-time-integral technique to estimate convective rain volumes over areas applied to satellite data - A preliminary investigation p 35 A87-40249
- Stuttgart Univ. (West Germany).**
Smart sensors: An overview and selected examples p 51 N87-24740
Improvement of image quality by forward motion compensation, a preliminary report p 42 N87-24741
The use of camera orientation data in photogrammetry: A review p 52 N87-24749
The effects of camera position and attitude data in aerial triangulation, a simulation study p 52 N87-24750
Application of Global Positioning System (GPS) receivers for Earth observation p 53 N87-24763

T

- Technische Univ., Berlin (West Germany).**
Digital data acquisition for close-range photogrammetry p 54 N87-24785
- Technische Univ., Dresden (East Germany).**
The production of photographs of the Earth's surface taken from satellites and their application in map production and map revision p 55 N87-24788
- Technische Univ., Hanover (West Germany).**
Introduction of geometric information to radar image data p 42 N87-24754
Aerial triangulation of CCD line-scanner images p 54 N87-24769
- Technische Univ., Munich (West Germany).**
Large format camera image analysis for mapping of land use patterns in the region Noale - Musone, Po-River-Plain, North Italy p 55 N87-24789

- The Modular Optoelectronic Multispectral Scanner (MOMS) program of the Bundesministerium fuer Forschung und Technologie (BMFT). Milestones in the development of an operational Earth Observation system p 55 N87-24815
- Technische Univ., Vienna (Austria).**
Photographic quality of color IR aerial photos as a function of atmospheric parameters p 42 N87-24799
- Tel-Aviv Univ. (Israel).**
Inferring spectral reflectances of plant elements by simple inversion of bidirectional reflectance measurements p 7 A87-37281
- Texas A&M Univ., College Station.**
Remote sensing of chlorophyll concentrations in the northern Gulf of Mexico p 29 A87-42643
- Texas Univ., Austin.**
Biharmonic spline interpolation of GEOS-3 and Seasat altimeter data p 20 A87-32770
Altimeter measurements for the determination of the Earth's gravity field [NASA-CR-180520] p 17 N87-23033
LANDSAT-based lineament analysis, East Texas Basin, and structural history of the Sabine Uplift area, East Texas and North Louisiana [PB87-176327] p 19 N87-24043
- Tokyo Univ. (Japan).**
Earth Resources Satellite (ERS-1) project in Japan p 57 N87-24797

U

- University of South Florida, St. Petersburg.**
The interaction of light with phytoplankton in the marine environment p 29 A87-42640
- University of Southern California, Los Angeles.**
A model for the use of satellite remote sensing for the measurement of primary production in the ocean p 29 A87-42644

V

- Virginia Univ., Charlottesville.**
Trace gas exchanges and transports over the Amazonian rain forest p 12 A87-32196

W

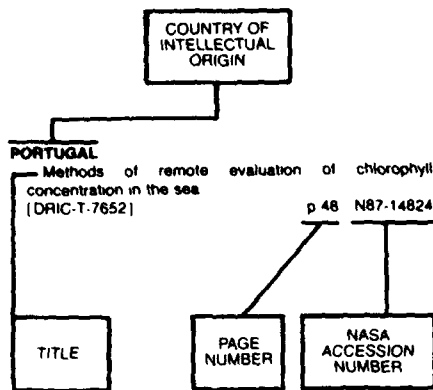
- Wageningen Agricultural Univ. (Netherlands).**
Procedures for the description of agricultural crops and soils in optical and microwave remote sensing studies p 8 A87-39187
Determination of spectral reflectance of crops during growth from calibrated multispectral small format aerial photography p 12 N87-24801
- Washington Univ., Seattle.**
The interaction of light with phytoplankton in the marine environment p 29 A87-42640
- Wayne State Univ., Detroit, Mich.**
OH measurement near the intertropical convergence zone in the Pacific p 21 A87-33430
- Wild Heerbrugg Ltd. (Switzerland).**
Wild Aviophot (TM) RC20 aerial camera system. The other approach to image motion compensation in aerial photography p 54 N87-24782
- Wisconsin Univ., Madison.**
A technique to estimate the ocean surface energy flux using VAS multispectral data p 30 N87-20710
Quick look Atlantic Ocean rain maps for gale [NASA-CR-180511] p 30 N87-21533
- Woods Hole Oceanographic Institution, Mass.**
Deforestation in the tropics - New measurements in the Amazon Basin using Landsat and NOAA advanced very high resolution radiometer imagery p 4 A87-33441
CHART: A computer plotting package for the display of position-dependent marine data [PB87-148607] p 31 N87-22297
- World Climate Programme, Geneva (Switzerland).**
Report of the workshop on Assimilation of Satellite Wind and Wave Data in Numerical Weather and Wave Prediction Models [WCP-122] p 49 N87-21521
- X**
- Xian Research Inst. of Surveying and Mapping (China).**
Applied formulae for calibration of aerial photogrammetric cameras p 51 N87-24744
On the matching of resolution in aerial photographic systems p 54 N87-24773
Estimating photogrammetric precision and cartographic potential of space imagery p 42 N87-24791

FOREIGN TECHNOLOGY INDEX

EARTH RESOURCES / A Continuing Bibliography (Issue 55)

NOVEMBER 1987

Typical Foreign Technology Index Listing



Listings in this index are arranged alphabetically by country of intellectual origin. The title of the document is used to provide a brief description of the subject matter. The page number and the accession number are included in each entry to assist the user in locating the citation in the abstract section.

A

AUSTRALIA

- Habitat mapping by Landsat for aerial census of kangaroos p 2 A87-32094
- Australian utilization and research into remote sensing p 20 A87-32490
- Coral reef remote sensing applications p 20 A87-32951
- Some observations on crop profile modelling p 5 A87-35310
- Mid-infrared remote sensing systems and their application to lithologic mapping p 17 A87-35522
- Measurements on digitized hardcopy images p 39 A87-37290
- A software defoliant for geological analysis of band ratios p 18 A87-39193
- Studies of the east Australian current off northern New South Wales [AD-A178461] p 32 N87-23103

AUSTRIA

- Photographic quality of color IR aerial photos as a function of atmospheric parameters p 42 N87-24799

C

CANADA

- On the relative accuracy of satellite and raingage rainfall measurements over middle latitudes during daylight hours p 34 A87-33295
- Seasonal and regional variations of active/passive microwave signatures of sea ice p 22 A87-35516
- Microwave sea-ice signatures near the onset of melt p 22 A87-35517
- Mapping from space p 38 A87-36361
- Radiometric correction of SAR images - A new correction algorithm p 40 A87-39184
- Remote sensing of vegetation change near Inco's Sudbury mining complexes p 8 A87-39185

Procedures for the description of agricultural crops and soils in optical and microwave remote sensing studies p 8 A87-39187

Radiometric comparison of the Landsat-5 TM and MSS sensors p 47 A87-41432

Thoughts on a standard algorithm for camera calibration p 51 N87-24743

Proposed changes to the Canadian camera calibration report p 53 N87-24757

The Multidetector Electro-optical Imaging Sensor (MEIS) 2 pushbroom imager: Four years of operation p 53 N87-24767

The role of government specifications in aerial photography p 57 N87-24780

Spectrophotometric measurements on color aerial photographs p 55 N87-24798

The use of auxiliary data in photogrammetric adjustments p 42 N87-24808

CHINA, PEOPLE'S REPUBLIC OF

Exploration of geomagnetic field anomaly with balloon for geophysical research p 17 A87-32478

Predicting the location of kimberlite from a probability analysis of linear structure on remote sensing data p 18 A87-39186

The application of remote sensing techniques in China p 57 A87-41435

High resolution sea surface temperature field derived p 33 N87-24731

Applied formulae for calibration of aerial photogrammetric cameras p 51 N87-24744

On the matching of resolution in aerial photographic systems p 54 N87-24773

Estimating photogrammetric precision and cartographic potential of space imagery p 42 N87-24791

D

DENMARK

A new covariance model for inertial gravimetry and gradiometry p 14 A87-31591

F

FINLAND

Applications of satellite microwave radiometry in Finland p 44 A87-32952

FRANCE

VHF radar for ocean surface current and sea state remote sensing p 19 A87-31631

Evaluation of a surface/vegetation parameterization using satellite measurements of surface temperature p 3 A87-33296

Automatic classification of Pointe d'Arcay landscapes using Thematic Mapper data with the aid of a textural analysis p 37 A87-35305

Introduction of initial centers for the algorithm of clustering around mobile centers p 37 A87-35313

A soil thermal model for remote sensing p 5 A87-35521

Sensors for imaging p 45 A87-36360

Fault patterns by space remote sensing and the rotation of western Oregon during Cenozoic times p 18 A87-36525

First results of lateritic cover mapping with SPOT images The Kangaba region (South-Mali) p 18 A87-36925

Aircraft radiopositioning for airborne photography during hydrographic coastal surveys p 23 A87-36945

Reconnaissance of vegetal formations in a Guinean forest sector by means of Landsat images p 6 A87-36946

Image preprocessing for line detection based on local structure analysis p 39 A87-37801

The Geomulti database management system p 39 A87-37802

Multisatellite data processing p 39 A87-37803

Nadir looking airborne radar and possible applications to forestry p 7 A87-38095

Spacelab data - A new contribution for structural interpretations of remotely sensed data in geology p 18 A87-39790

Satellite estimation of a solar irradiance at the surface of the earth and of surface albedo using a physical model applied to Meteosat data p 47 A87-40246

Proceedings of the European Symposium on Polar platform Opportunities and Instrumentation for Remote-Sensing (ESPOIR) [ESA-SP-266] p 48 N87-20621

Remote sensing applications: Commercial issues and opportunities for space station p 57 N87-20626

Measurement and detection of precipitation. Satellite methods in the visible and the infrared p 36 N87-22364

Energy Balance of the Tropical Systems (BEST): A space experiment proposition p 36 N87-22373

Proceedings of the International Symposium on Progress in Imaging Sensors [ESA-SP-252] p 50 N87-24738

Towards an automatic identification of urban textures p 14 N87-24747

Applications of laser airborne telemetry at Institut Geographique National (IGN), France p 53 N87-24761

SPOT image quality p 42 N87-24804

G

GERMANY, FEDERAL REPUBLIC OF

Scientific goals and technical limitations of the shuttleborne synthetic aperture experiment X-SAR p 44 A87-32505

Observations of intermittent cumulus convection in the boundary layer p 20 A87-32976

MIDAS - A new image-processing system for remote sensing p 37 A87-35183

Stereoscopic line scan imaging and satellite control [DGLR PAPER 86-106] p 38 A87-36757

Comparison of satellite-derived sea surface temperatures with in situ skin measurements p 23 A87-37565

Strategies and technologies for monitoring the environment p 14 A87-39593

Report on the Special Program 78 satellite geodesy of the Technical University of Munich [ASTRON-GEODAET-ARB-48] p 16 N87-20618

European utilization aspects studies p 49 N87-20624

Land panel report p 49 N87-20634

Reports on cartography and geodesy, series 1, number 96 [ISSN-0469-4236] p 16 N87-22282

Reports on cartography and geodesy, series 1, number 97 [ISSN-0469-4236] p 16 N87-22286

The VICOM system for digital image processing at the Institute of Cartography of Technical University, Hanover (West Germany) p 16 N87-22290

Arianespace top performance benefits ESA p 57 N87-24493

Smart sensors: An overview and selected examples p 51 N87-24740

Improvement of image quality by forward motion compensation, a preliminary report p 42 N87-24741

Optical Transfer Function (OTF)-based quality criteria for aerial cameras and imaging systems p 51 N87-24742

Geometrical system calibration, especially for metric aerial cameras p 51 N87-24745

Comparative analysis of Thematic Mapper and SPOT image data for land use investigation p 51 N87-24746

Application of Modular Optoelectronic Multispectral Scanner (MOMS) data to hydrology and vegetation studies. Test site: Pantanal Region (Brazil/Paraguay) p 52 N87-24748

The use of camera orientation data in photogrammetry: A review p 52 N87-24749

The effects of camera position and attitude data in aerial triangulation, a simulation study p 52 N87-24750

Infrared Earth horizon sensor concepts in various spectral bands p 52 N87-24752

Introduction of geometric information to radar image data p 42 N87-24754

FOREIGN

Application of Global Positioning System (GPS) receivers for Earth observation p 53 N87-24763

Advanced imaging spectrometer for ocean color/fluorescence measurements and further applications p 33 N87-24766

The stereo pushbroom scanner system Digital Photogrammetry System (DPS) and its accuracy p 53 N87-24768

Aerial triangulation of CCD line-scanner images p 54 N87-24769

Investigation of simulated Monocular Electro-Optical Stereo Scanner (MEOSS)-imagery for sensor navigation and terrain derivation p 54 N87-24771

Exposure test with high resolution films from high altitude p 54 N87-24775

Very high resolution aerial films p 54 N87-24776

The first ESA remote sensing satellite (status and outlook) p 57 N87-24777

The RMK aerial camera system: Performance potential of aerial photography with forward motion compensation p 54 N87-24781

Digital data acquisition for close-range photogrammetry p 54 N87-24785

The production of photographs of the Earth's surface taken from satellites and their application in map production and map revision p 55 N87-24788

Large format camera image analysis for mapping of land use patterns in the region Noale - Musone, Po-River-Plain, North Italy p 55 N87-24789

Large Format Camera photographs of the Black Hills, USA, and their suitability for topographic and thematic mapping p 55 N87-24792

Earth observation experiments on the German Spacelab mission D2 p 55 N87-24811

The Monocular Electro-Optical Stereo Scanner (MEOSS) satellite experiment p 55 N87-24812

Modern CCD sensors and their applications in Earth observation and planetary missions p 55 N87-24813

The Modular Optoelectronic Multispectral Scanner (MOMS) program of the Bundesministerium fuer Forschung und Technologie (BMFT). Milestones in the development of an operational Earth Observation system p 55 N87-24815

GERMANY, PEOPLES DEMOCRATIC REPUBLIC OF

Investigation of tectonic deformations using global satellite laser ranging data p 14 N87-33375

H

HUNGARY

Remote sensing methods of yield forecasting p 2 N87-32009

The application of remote sensing in agricultural meteorology at the Meteorological Service of the HPR p 2 N87-32010

Surface models including direct cross-radiation - A simple model of furrowed surfaces p 40 N87-39189

I

INDIA

Indian remote sensing programme p 56 N87-32955

Geochronological studies of strandlines of Saurashtra, India, detected by remote sensing techniques p 15 N87-35308

Determination of the velocity of ocean gyres through Synthetic Aperture Radar p 22 N87-35314

Data Compression System for video images p 46 N87-37421

Montane vegetation stratification through digital processing of Landsat MSS data p 9 N87-40302

A soil map through Landsat satellite imagery in a part of the Auranga catchment in the Ranchi and Palamou districts of Bihar, India p 9 N87-41428

Rice crop identification and area estimation using remotely-sensed data from Indian cropping patterns p 9 N87-41434

INTERNATIONAL ORGANIZATION

A curious sea-surface-temperature phenomenon observed by Meteosat p 19 N87-31572

Workshop on Space Remote Sensing for Agricultural and Thematic Mapping, Budapest, Hungary, Apr. 18, 1986, Proceedings p 1 N87-32007

Intelsat's small earth stations - Impact on the developing world p 56 N87-34799

AVHRR data services in Europe - The Earthnet approach p 39 N87-37922

The operational performance of the fleet numerical oceanography center global spectral ocean-wave model p 24 N87-38832

ITALY

Balloon-borne infrared multichannel radiometer for remote sensing of high resolution low-level water vapor fields p 43 N87-32477

Development of a satellite remote sensing technique for the study of alpine glaciers p 34 N87-35311

The Tethered Satellite System as a new remote sensing platform p 46 N87-39183

Remotely sensed sea surface temperature for the Alpine Experiment (ALPEX) p 30 N87-21497

Comparative evaluation and guide for the integrated utilization of LANDSAT (MSS and TM) and SPOT (HRV) satellites remotely sensed data [ETN-87-99356] p 41 N87-22278

J

JAPAN

Earth rotation, station coordinates and orbit determination from satellite laser ranging p 43 N87-32349

Spectral classification of Landsat-5 Thematic Mapper data p 37 N87-32488

Correction for atmospheric and topographic effects on the Landsat MSS data p 37 N87-32489

A study of elevation measurement using LFC photograph p 43 N87-32491

Estimation of roughness of the earth's surface using Landsat MSS data on the assumption of reciprocity on light scattering p 12 N87-32493

Landcover change in Hiroshima during 1979/1984 detected by Landsat MSS and TM data p 12 N87-32494

Global vegetation monitoring using NOAA vegetation index data p 3 N87-32495

Fundamental study on systematization of selecting new development area with Landsat data and topographic information p 12 N87-32496

Monitoring of snow and ice in Hokkaido Island using multitemporal NOAA-AVHRR data p 20 N87-32497

Relation between precipitation and brightness of earth surface in the NOAA/GVIP data p 3 N87-32498

Marine Observation Satellite-1 (MOS-1) p 20 N87-32499

Airborne observation experiments for MOS-1 verification program (MVP) p 44 N87-32500

Earth resources satellite-1 (ERS-1) p 44 N87-32501

The French Space Oceanography Program p 20 N87-32503

Simulation software of synthetic aperture radar p 37 N87-32506

Observation of precipitation from space by the weather radar p 44 N87-32507

World-wide weather p 56 N87-33125

Sea surface temperature measurement from space allowing for the effect of the stratospheric aerosols p 22 N87-35148

Atmospheric environment monitoring system based on an earth-to-satellite Hadamard transform laser long-path absorption spectrometer - A proposal p 45 N87-35502

The dependence of sea-surface microwave emission on wind speed, frequency, incidence angle, and polarization over the frequency range from 1 to 40 GHz p 22 N87-35515

Earth Resources Satellite (ERS-1) project in Japan p 57 N87-24797

N

NETHERLANDS

The Netherlands-Indonesian remote-sensing satellite TERS p 43 N87-32210

An application of low altitude multispectral photography to agricultural field trials p 6 N87-37054

What, where, when ..., why? Extracting information from remote sensing data p 46 N87-37055

Recent results with a third-generation ocean-wave model p 24 N87-38833

The Earth observation activities of the European Space Agency and the use of the polar platform of the International Space Station p 49 N87-20622

Foundations and applications of multispectral scanning in agriculture [NLR-MP-85015-U] p 10 N87-21408

A modular and versatile acquisition, recording and preprocessing system for airborne remote sensing p 52 N87-24751

Definition of a thermal infrared pushbroom imager for Earth observation p 53 N87-24765

Determination of spectral reflectance of crops during growth from calibrated multispectral small format aerial photography p 12 N87-24801

NIGERIA

Reflectance characteristics and its application in the classification of Nigerian Savanna soils p 3 N87-32954

NORWAY

Ice-edge eddies in the Fram Strait marginal ice zone p 27 N87-40432

S

SOUTH AFRICA, REPUBLIC OF

Landsat as an aid in evaluating the adequacy of a grain silo network p 7 N87-37282

SPAIN

Analysis of moderate and intense rainfall rates continuously recorded over half a century and influence on microwave communications planning and rain-rate data acquisition p 46 N87-36933

SUDAN

Optical and digital SAR processing techniques. A statistical comparison of accuracy using SEASAT imagery p 42 N87-24753

SWEDEN

Influence of different nitrogen and irrigation treatments on the spectral reflectance of barley p 2 N87-32090

The topographic effect on Landsat data in gently undulating terrain in southern Sweden p 4 N87-35307

Potential of laser remote sensing of oil below water surface [FOA-C-30435-3.1] p 30 N87-20659

The observational objectives and the implementation of the Global Weather Experiment p 49 N87-21474

Image quality problems in practical aerial photography p 43 N87-24814

SWITZERLAND

Using the Global Positioning System (GPS) for high precision geodetic surveys - Highlights and problem areas p 16 N87-41383

Report of the workshop on Assimilation of Satellite Wind and Wave Data in Numerical Weather and Wave Prediction Models [WCP-122] p 49 N87-21521

U

U.S.S.R.

The determination of earth-rotation parameters from satellite laser ranging p 15 N87-34186

Optimization of a program of experiments in connection with the operational planning of studies carried out with a spacecraft p 56 N87-34208

Remote-sensing method for determining monthly precipitation sums using Meteor-satellite data on the Atlantic Ocean p 21 N87-34447

Rapid analysis of satellite radar images of sea ice p 22 N87-35873

Problems in the automation of map-compilation processes on the basis of remote-sensing data p 38 N87-35925

Use of satellite altimetry for ocean monitoring p 23 N87-36101

Cloud-cover and precipitation patterns over the Republic of Guinea according to ground-based and satellite observations p 35 N87-36102

Surface manifestations of hydrophysical processes in the Strait of Gibraltar according to 'Salyut-6' photographs p 35 N87-36103

The geometry of the intersections of tectonic structures detected on satellite images p 17 N87-36104

The geotectonic characteristics of the rift zone on the Lambert glacier (Antarctica) according to space images p 18 N87-36105

Satellite techniques for studying ice crusts and underground waters in the eastern Pamir p 35 N87-36106

Measurement of the spatial spectrum of ocean waves using a two-frequency scatterometer p 23 N87-36107

Statistical evaluation of forest characteristics from aerial and space photographs p 5 N87-36109

The possibility of using satellite measurements of methane in the atmosphere to study the global-distribution characteristics of its sources p 13 N87-36125

Environmental protection from space p 13 N87-36363

Aerial and space investigations of soils and vegetation p 6 N87-36579

Phase portraits of vegetation development trajectories in a multidimensional spectral attribute space p 10 N87-41771

Physical principles of image convergence in remote sensing p 40 N87-41925

Possibilities of using artificial Earth satellite data for computing heat exchange between the ocean and atmosphere in Newfoundland energy-active zone during winter p 31 N87-21980

UNITED KINGDOM

GLAI estimation using measurements of red, near infrared, and middle infrared radiance p 4 N87-35119

A comparison of supervised maximum likelihood and decision tree classification for crop cover estimation from multitemporal Landsat MSS data p 5 A87-35312

Landsat image enhancement study of possible submerged sand-dunes in the Arabian Gulf p 22 A87-35315

The relation of millimeter-wavelength backscatter to surface snow properties p 34 A87-35518

GINFEST - Geodetic intercomparison network for evaluating space techniques p 15 A87-36164

Remote sensing - Handling the data p 38 A87-36359

Landform investigation utilizing digitally processed satellite Thematic Mapper imagery p 38 A87-36546

A two-look technique for studying atmospheric effects in optical scanner data for the ocean p 26 A87-39178

The effect of a non-Gaussian point target response function on radar altimeter returns from the sea surface p 26 A87-39179

Synergistic use of MOMS-01 and Landsat TM data p 46 A87-39190

The propagation of short surface waves on longer gravity waves p 28 A87-40835

Multilook images of ocean waves by synthetic aperture radars p 28 A87-41068

A polar platform for the remote sensing needs of ecology and agriculture - A view from the U.K. p 9 A87-41430

Ocean-ice panel report p 30 N87-20635

The impact of initial conditions and SST Anomalies on extended range predictions for the El Nino period p 32 N87-23046

The SIR-B mission: Towards an understanding of internal waves in the ocean p 32 N87-23102

[ARE-TR-86122]

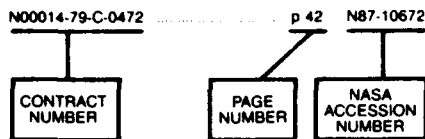
The effect of receiver amplifier non-linearity on ERS-1 synthetic aperture radar imagery p 52 N87-24755

CONTRACT NUMBER INDEX

RTH RESOURCES / A Continuing Bibliography (Issue 55)

NOVEMBER 1987

Typical Contract Number Index Listing



Listings in this index are arranged alpha-numerically by contract number. Under each contract number, the accession numbers denoting documents that have been produced as a result of research done under that contract are arranged in ascending order with the AIAA accession numbers appearing first. The accession number denotes the number by which the citation is identified in the abstract section. Preceding the accession number is the page number on which the citation may be found.

CEC-CLI-083-F p 28 A87-40434
 CNEXO-84/3147 p 28 A87-40434
 CNRS-981-022 p 28 A87-40434
 DAAG29-82-K-0189 p 14 N87-23015
 DE-AC02-83ER-60182 p 18 A87-39468
 DE-AC04-76DP-00789 p 11 N87-24593
 DE-AC05-84OR-21400 p 4 A87-33441
 DE-AC09-76SR-00001 p 36 A87-42256
 DE-AC09-76SR-00819 p 36 A87-42256
 DE-AC21-83MC-20037 p 31 N87-22387
 DE-FG02-86ER-60444 p 10 N87-22336
 DE-FG05-85ER-60348 p 30 N87-20716
 F33615-83-C-1071 p 45 A87-35344
 GRI-5082-211-0708 p 19 N87-24043
 JPL-956578 p 10 N87-22296
 MOD(PE)-NUW-72A/1287 p 32 N87-23102
 MOESC-60129032 p 37 A87-32488
 NAGW-374 p 9 A87-40944
 NAGW-455 p 45 A87-35306
 NAGW-465 p 43 N87-24817
 NAGW-465 p 29 A87-42640
 NAG1-50 p 21 A87-33432
 NAG5-177 p 45 A87-35306
 NAG5-184 p 3 A87-33298
 NAG5-269 p 7 A87-38097
 NAG5-386 p 35 A87-40249
 NAG5-492 p 6 A87-37278
 NAG5-519 p 33 N87-24816
 NAG5-548 p 11 N87-24010
 NAG5-548 p 11 N87-24733
 NAG5-548 p 11 N87-24736
 NAG5-742 p 30 N87-21533
 NAG5-746 p 17 N87-23033
 NAG5-769 p 40 N87-20449
 NAG5-787 p 20 A87-32770
 NAG6-17 p 29 A87-42642
 NASA ORDER L-200080 p 39 A87-38096
 NASA ORDER S-56107-D p 33 N87-24012
 NAS2-8759 p 46 A87-39190
 NAS5-22966 p 29 A87-42643
 NAS5-26453 p 39 A87-38098
 NAS5-26515 p 44 A87-32985
 NAS5-27644 p 15 A87-36176
 NAS5-27745 p 44 A87-32985
 NAS5-28200 p 6 A87-37279
 NAS5-28200 p 7 A87-37281
 NAS5-28757 p 19 N87-22319
 NAS5-28770 p 35 A87-40309
 NAS5-28779 p 36 N87-24031
 NAS5-28779 p 36 N87-24032
 NAS5-29472 p 12 N87-24737

NAS7-918 p 13 A87-37280
 NAS8-35187 p 21 A87-32982
 NAS8-35969 p 41 N87-20554
 NAS9-16528 p 7 A87-37281
 NAS9-16684 p 39 A87-38096
 NATO-27-0523/85 p 24 A87-38833
 NATO-320/82 p 14 A87-31591
 NCC1-95 p 12 A87-32196
 NCC5-20 p 13 A87-39182
 NCC5-26 p 9 A87-40303
 NERC-GR/3/5096 p 4 A87-35119
 NERC-P60/G6/16 p 9 A87-41430
 NOAA-NA-81AAD0095 p 14 A87-42255
 NOAA-NA-84AAH00026 p 47 A87-40756
 NOAA-NA-85AADSG033 p 9 A87-40944
 NOAA-04/M01-B4 p 14 A87-42255
 NSERC-A-5252 p 47 A87-41432
 NSERC-A-8643 p 47 A87-41432
 NSF ATM-84-05748 p 21 A87-32982
 NSF CEE-82-10857 p 19 A87-32097
 NSF DAR-80-17836 p 9 A87-40944
 NSF DPP-81-20332 p 19 A87-31592
 NSF DPP-84-12404 p 19 A87-31592
 NSF DPP-85-02386 p 23 A87-37563
 NSF EAR-81-20944 p 15 A87-37918
 NSF EAR-82-13330 p 15 A87-37918
 NSF EAR-83-17594 p 15 A87-37918
 NSF EAR-84-18332 p 15 A87-37918
 NSF EAR-85-11400 p 15 A87-37918
 NSF SES-81-12797 p 12 A87-32953
 N00014-76-C-0004 p 28 A87-40434
 N00014-81-C-0043 p 29 A87-42642
 N00014-81-C-0062 p 24 A87-37886
 N00014-81-C-0295 p 27 A87-40433
 N00014-83-C-0404 p 27 A87-40433
 N00014-83-K-0020 p 28 A87-40434
 N00014-83-K-0258 p 32 N87-24009
 N00014-84-C-0111 p 29 A87-42640
 N00014-84-C-0132 p 28 A87-40434
 N00014-84-C-0134 p 24 A87-37886
 N00014-84-C-0218 p 32 N87-23104
 N62271-86-M-0235 p 49 N87-20642
 USDA-58-319T-3-0208X p 4 A87-35120
 USDA-58-319T-40238X p 47 A87-39457
 W-7405-ENG-36 p 41 N87-24011
 W-7405-ENG-36 p 41 N87-24014
 W-7405-ENG-48 p 11 N87-23032
 672-40-04-70 p 49 N87-22281

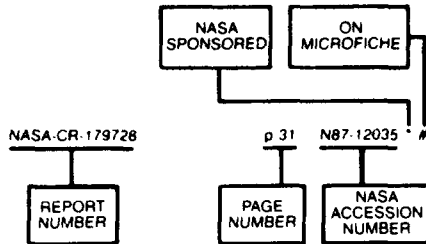
CONTRACT

REPORT NUMBER INDEX

EARTH RESOURCES / A Continuing Bibliography (Issue 55)

NOVEMBER 1987

Typical Report Number Index Listing



Listings in this index are arranged alphabetically by report number. The page number indicates the page on which the citation is located. The accession number denotes the number by which the citation is identified. An asterisk (*) indicates that the item is a NASA report. A pound sign (#) indicates that the item is available on microfiche.

ACCN-74513	p 32	N87-23102	#	ESA-SP-266	p 48	N87-20621	#	NASA-TF-2643	p 49	N87-22281	* #
AD-A17574	p 49	N87-20642	#	ETN-87-98974	p 16	N87-20618	#	NEPRF-CR-86-05	p 49	N87-20642	#
AD-A177419	p 31	N87-22382	#	ETN-87-99183	p 49	N87-21521	#	NLR-MP-85015-U	p 10	N87-21408	#
AD-A178302	p 33	N87-24061	#	ETN-87-99283	p 10	N87-21408	#	NOAA-TR-NESDIS-28	p 31	N87-22388	#
AD-A178461	p 32	N87-23103	#	ETN-87-99328	p 16	N87-22282	#	NORDA-168	p 33	N87-24061	#
AD-A178522	p 41	N87-23014	#	ETN-87-99329	p 16	N87-22286	#	PB87-148607	p 31	N87-22297	#
AD-A178535	p 32	N87-23104	#	ETN-87-99356	p 41	N87-22278	#	PB87-154597	p 41	N87-24013	#
AD-A178703	p 14	N87-23015	#	ETN-87-99434	p 48	N87-20621	#	PB87-176327	p 19	N87-24043	#
AD-A178774	p 32	N87-23016	#	ETN-87-99441	p 30	N87-20659	#	RANRL-TN-6/86	p 32	N87-23103	#
AD-A179081	p 50	N87-24734	#	ETN-87-99809	p 32	N87-23102	#	REF-86-10-VOL-2/6	p 32	N87-23104	#
AD-A179461	p 32	N87-24009	#	ETN-87-99861	p 50	N87-24738	#	REPT-377	p 33	N87-24816	* #
AD-A179550	p 50	N87-23012	#	FOA-C-30435-3.1	p 30	N87-20659	#	REPT-87B0163	p 30	N87-21534	* #
AFGL-TR-87-0128	p 50	N87-23012	#	GRI-87/0077	p 19	N87-24043	#	REPT-87B0275	p 50	N87-22457	* #
AO1-1(ST1)	p 49	N87-20642	#	ISBN-3-7696-9791-X	p 16	N87-20618	#	SAND-86-2618	p 11	N87-24593	#
ARE-TR-86122	p 32	N87-23102	#	ISSN-0340-7691	p 16	N87-20618	#	SAPR-4	p 33	N87-24012	* #
ARO-19327.9-GS	p 14	N87-23015	#	ISSN-0347-3708	p 30	N87-20659	#	SPIE-637	p 28	A87-42637	#
ASTRON-GEODAET-ARB-48	p 16	N87-20618	#	ISSN-0379-6566	p 48	N87-20621	#	USGS/OFR-86/010	p 41	N87-24013	#
BR101469	p 32	N87-23102	#	ISSN-0379-6566	p 50	N87-24738	#	WCP-122	p 49	N87-21521	#
CERC-MP-87-3	p 31	N87-22382	#	ISSN-0469-4236	p 16	N87-22282	#	WHOI-86-43	p 31	N87-22297	#
CONF-870576-1	p 41	N87-24014	#	ISSN-0469-4236	p 16	N87-22286	#	WMO-TD-148	p 49	N87-21521	#
CONF-870576-2	p 41	N87-24011	#	JPL-PUB-87-5	p 31	N87-22386	* #				
DATA-124-VOL-2/6	p 32	N87-23104	#	JPL-9950-1281	p 10	N87-22296	* #				
DE87-001056	p 31	N87-22387	#	L-16159	p 49	N87-22281	* #				
DE87-005303	p 30	N87-20716	#	LA-UR-87-571	p 41	N87-24011	#				
DE87-005994	p 10	N87-22336	#	LA-UR-87-572	p 41	N87-24014	#				
DE87-006059	p 41	N87-24011	#	LC-86-23876	p 33	N87-24870	* #				
DE87-006060	p 41	N87-24014	#	NAS 1.15:87812	p 30	N87-21534	* #				
DE87-009384	p 11	N87-24593	#	NAS 1.15:87818	p 16	N87-23018	* #				
DGLR PAPER 86-106	p 38	A87-36757	#	NAS 1.15:87820	p 50	N87-22457	* #				
DOE/ER-60348/5	p 30	N87-20716	#	NAS 1.15:89219	p 11	N87-24735	* #				
DOE/ER-60444/T1	p 10	N87-22336	#	NAS 1.15:89220	p 11	N87-24010	* #				
DOE/MC-20037/2265	p 31	N87-22387	#	NAS 1.21:489	p 33	N87-24870	* #				
DOE/NBB-0077	p 11	N87-23032	#	NAS 1.26:180234	p 40	N87-20449	* #				
D180-27884-3	p 41	N87-20554	* #	NAS 1.26:180376	p 41	N87-20554	* #				
ERIM-189400-21-L	p 36	N87-24032	* #	NAS 1.26:180511	p 30	N87-21533	* #				
ERIM-198400-19-L	p 36	N87-24031	* #	NAS 1.26:180512	p 11	N87-24733	* #				
ESA-SP-252	p 50	N87-24738	#	NAS 1.26:180520	p 17	N87-23033	* #				
				NAS 1.26:180570	p 33	N87-24816	* #				
				NAS 1.26:180575	p 19	N87-22319	* #				
				NAS 1.26:180914	p 31	N87-22386	* #				
				NAS 1.26:180918	p 10	N87-22296	* #				
				NAS 1.26:180948	p 11	N87-24736	* #				
				NAS 1.26:180982	p 36	N87-24032	* #				
				NAS 1.26:180983	p 36	N87-24031	* #				
				NAS 1.26:180984	p 33	N87-24012	* #				
				NAS 1.26:181059	p 12	N87-24737	* #				
				NAS 1.26:181073	p 43	N87-24817	* #				
				NAS 1.60:2643	p 49	N87-22281	* #				
				NASA-CR-180234	p 40	N87-20449	* #				
				NASA-CR-180376	p 41	N87-20554	* #				
				NASA-CR-180511	p 30	N87-21533	* #				
				NASA-CR-180512	p 11	N87-24733	* #				
				NASA-CR-180520	p 17	N87-23033	* #				
				NASA-CR-180570	p 33	N87-24816	* #				
				NASA-CR-180575	p 19	N87-22319	* #				
				NASA-CR-180914	p 31	N87-22386	* #				
				NASA-CR-180918	p 10	N87-22296	* #				
				NASA-CR-180948	p 11	N87-24736	* #				
				NASA-CR-180982	p 36	N87-24032	* #				
				NASA-CR-180983	p 36	N87-24031	* #				
				NASA-CR-180984	p 33	N87-24012	* #				
				NASA-CR-181059	p 12	N87-24737	* #				
				NASA-CR-181073	p 43	N87-24817	* #				
				NASA-SP-489	p 33	N87-24870	* #				
				NASA-TM-87812	p 30	N87-21534	* #				
				NASA-TM-87818	p 16	N87-23018	* #				
				NASA-TM-87820	p 50	N87-22457	* #				
				NASA-TM-89219	p 11	N87-24735	* #				
				NASA-TM-89220	p 11	N87-24010	* #				

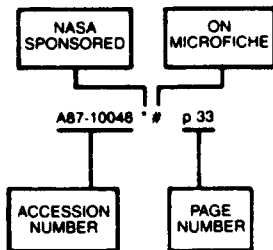
REPORT

ACCESSION NUMBER INDEX

EARTH RESOURCES / A Continuing Bibliography (Issue 55)

NOVEMBER 1987

Typical Accession Number Index Listing



Listings in this index are arranged alpha-numerically by accession number. The page number listed to the right indicates the page on which the citation is located. An asterisk (*) indicates the item is a NASA report. A pound sign (#) indicates that the item is available on microfiche.

A87-31409 #	p 34	A87-33125 #	p 13	A87-39468 #	p 18	N87-22319 * #	p 19
A87-31410 * #	p 17	A87-33292 #	p 13	A87-39593 #	p 14	N87-22336 #	p 10
A87-31411 * #	p 1	A87-33295 #	p 34	A87-39790 #	p 18	N87-22364 #	p 36
A87-31412 #	p 36	A87-33297 #	p 34	A87-40244 * #	p 8	N87-22373 #	p 36
A87-31413 * #	p 1	A87-33298 * #	p 3	A87-40246 #	p 47	N87-22382 #	p 31
A87-31414 * #	p 1	A87-33375 #	p 14	A87-40248 * #	p 8	N87-22386 * #	p 31
A87-31572 #	p 19	A87-33426 * #	p 45	A87-40249 * #	p 35	N87-22387 #	p 31
A87-31591 #	p 14	A87-33430 * #	p 21	A87-40250 * #	p 27	N87-22388 #	p 31
A87-31592 #	p 19	A87-33431 * #	p 21	A87-40281 #	p 27	N87-22457 * #	p 50
A87-31631 #	p 19	A87-33432 * #	p 21	A87-40289 * #	p 27	N87-23012 #	p 50
A87-32007 #	p 1	A87-33435 * #	p 21	A87-40301 * #	p 9	N87-23014 #	p 41
A87-32008 #	p 2	A87-33441 * #	p 4	A87-40302 #	p 9	N87-23015 #	p 14
A87-32009 #	p 2	A87-34186 #	p 15	A87-40303 * #	p 9	N87-23016 #	p 32
A87-32010 #	p 2	A87-34208 #	p 56	A87-40304 #	p 9	N87-23018 * #	p 16
A87-32090 #	p 2	A87-34447 #	p 21	A87-40308 #	p 35	N87-23032 #	p 11
A87-32091 #	p 2	A87-34600 #	p 56	A87-40309 * #	p 35	N87-23033 * #	p 17
A87-32092 #	p 34	A87-34799 #	p 56	A87-40379 * #	p 47	N87-23046 #	p 32
A87-32093 * #	p 2	A87-35119 #	p 4	A87-40432 #	p 27	N87-23102 #	p 32
A87-32094 #	p 2	A87-35120 #	p 4	A87-40433 #	p 27	N87-23103 #	p 32
A87-32095 * #	p 3	A87-35121 #	p 4	A87-40434 #	p 28	N87-23104 #	p 32
A87-32097 #	p 19	A87-35122 #	p 4	A87-40648 * #	p 28	N87-23558 * #	p 50
A87-32098 * #	p 3	A87-35148 #	p 22	A87-40756 #	p 47	N87-24009 #	p 32
A87-32196 * #	p 12	A87-35183 #	p 37	A87-40768 * #	p 47	N87-24010 * #	p 11
A87-32210 #	p 43	A87-35305 #	p 37	A87-40770 * #	p 47	N87-24011 #	p 41
A87-32349 #	p 43	A87-35306 * #	p 45	A87-40835 #	p 28	N87-24012 * #	p 33
A87-32477 #	p 43	A87-35307 #	p 4	A87-40944 * #	p 9	N87-24013 #	p 41
A87-32478 #	p 17	A87-35308 #	p 15	A87-41068 #	p 28	N87-24014 #	p 41
A87-32488 #	p 37	A87-35309 * #	p 5	A87-41380 * #	p 16	N87-24031 * #	p 36
A87-32489 #	p 37	A87-35310 #	p 5	A87-41383 #	p 16	N87-24032 * #	p 36
A87-32490 #	p 20	A87-35311 #	p 34	A87-41428 #	p 9	N87-24043 #	p 19
A87-32491 #	p 43	A87-35312 #	p 5	A87-41430 #	p 9	N87-24061 #	p 33
A87-32493 #	p 12	A87-35313 #	p 37	A87-41432 #	p 47	N87-24493 #	p 57
A87-32494 #	p 12	A87-35314 #	p 22	A87-41434 #	p 9	N87-24593 #	p 11
A87-32495 #	p 3	A87-35315 #	p 22	A87-41435 #	p 57	N87-24731 #	p 33
A87-32496 #	p 12	A87-35344 #	p 45	A87-41588 #	p 48	N87-24733 * #	p 11
A87-32497 #	p 20	A87-35502 #	p 45	A87-41771 #	p 10	N87-24734 #	p 50
A87-32498 #	p 3	A87-35515 #	p 22	A87-41925 #	p 40	N87-24735 * #	p 11
A87-32499 #	p 20	A87-35516 #	p 22	A87-42254 * #	p 48	N87-24736 * #	p 11
A87-32500 #	p 44	A87-35517 #	p 22	A87-42255 #	p 14	N87-24737 * #	p 12
A87-32501 #	p 44	A87-35518 #	p 34	A87-42256 #	p 36	N87-24738 #	p 50
A87-32502 #	p 56	A87-35519 * #	p 5	A87-42257 #	p 48	N87-24739 * #	p 51
A87-32503 #	p 20	A87-35520 * #	p 5	A87-42628 #	p 40	N87-24740 #	p 51
A87-32505 #	p 44	A87-35521 #	p 5	A87-42637 #	p 28	N87-24741 #	p 42
A87-32506 #	p 37	A87-35522 #	p 17	A87-42638 #	p 28	N87-24742 #	p 51
A87-32507 #	p 44	A87-35523 #	p 13	A87-42639 * #	p 48	N87-24743 #	p 51
A87-32770 * #	p 20	A87-35524 #	p 38	A87-42640 * #	p 29	N87-24744 #	p 51
A87-32951 #	p 20	A87-35525 #	p 22	A87-42641 * #	p 29	N87-24745 #	p 51
A87-32952 #	p 44	A87-35526 #	p 22	A87-42642 * #	p 29	N87-24746 #	p 51
A87-32953 #	p 12	A87-35527 #	p 38	A87-42643 * #	p 29	N87-24747 #	p 14
A87-32954 #	p 3	A87-35528 #	p 22	A87-42644 * #	p 29	N87-24748 #	p 52
A87-32955 #	p 56	A87-35529 #	p 38	A87-42645 * #	p 29	N87-24749 #	p 52
A87-32976 #	p 20	A87-35530 #	p 23	A87-42646 * #	p 30	N87-24750 #	p 52
A87-32982 * #	p 21	A87-35531 #	p 35	A87-42659 * #	p 40	N87-24751 #	p 52
A87-32985 * #	p 44	A87-35532 #	p 35			N87-24752 #	p 52
A87-33122 #	p 45	A87-35533 #	p 17			N87-24753 #	p 42
		A87-35534 #	p 18			N87-24754 #	p 42
		A87-35535 #	p 35			N87-24755 #	p 52
		A87-35536 #	p 35			N87-24756 * #	p 53
		A87-35537 #	p 17			N87-24757 #	p 53
		A87-35538 #	p 18			N87-24761 #	p 53
		A87-35539 #	p 35			N87-24763 #	p 53
		A87-35540 #	p 23			N87-24765 #	p 53
		A87-35541 #	p 35			N87-24766 #	p 33
		A87-35542 #	p 35			N87-24767 #	p 53
		A87-35543 #	p 17			N87-24768 #	p 53
		A87-35544 #	p 18			N87-24769 #	p 54
		A87-35545 #	p 35			N87-24771 #	p 54
		A87-35546 #	p 23			N87-24773 #	p 54
		A87-35547 #	p 5			N87-24775 #	p 54
						N87-24776 #	p 54
						N87-24777 #	p 57
						N87-24780 #	p 57
						N87-24781 #	p 54
						N87-24782 #	p 54
						N87-24785 #	p 54
						N87-24788 #	p 55
						N87-24789 #	p 55
						N87-24791 #	p 42
						N87-24792 #	p 55
						N87-24797 #	p 57
						N87-24798 #	p 55
						N87-24799 #	p 42
						N87-24801 #	p 12

N87-24804*ACCESSION NUMBER INDEX*

N87-24804 # p 42
N87-24806 # p 42
N87-24811 # p 55
N87-24812 # p 55
N87-24813 # p 55
N87-24814 # p 43
N87-24815 # p 55
N87-24816 * # p 33
N87-24817 * # p 43
N87-24870 * # p 33

AVAILABILITY OF CITED PUBLICATIONS

IAA ENTRIES (A87-10000 Series)

Publications announced in *IAA* are available from the AIAA Technical Information Service as follows: Paper copies of accessions are available at \$10.00 per document (up to 50 pages), additional pages \$0.25 each. Microfiche⁽¹⁾ of documents announced in *IAA* are available at the rate of \$4.00 per microfiche on demand. Standing order microfiche are available at the rate of \$1.45 per microfiche for *IAA* source documents and \$1.75 per microfiche for AIAA meeting papers.

Minimum air-mail postage to foreign countries is \$2.50. All foreign orders are shipped on payment of pro-forma invoices.

All inquiries and requests should be addressed to: Technical Information Service, American Institute of Aeronautics and Astronautics, 555 West 57th Street, New York, NY 10019. Please refer to the accession number when requesting publications.

STAR ENTRIES (N87-10000 Series)

One or more sources from which a document announced in *STAR* is available to the public is ordinarily given on the last line of the citation. The most commonly indicated sources and their acronyms or abbreviations are listed below. If the publication is available from a source other than those listed, the publisher and his address will be displayed on the availability line or in combination with the corporate source line.

Avail: NTIS. Sold by the National Technical Information Service. Prices for hard copy (HC) and microfiche (MF) are indicated by a price code preceded by the letters HC or MF in the *STAR* citation. Current values for the price codes are given in the tables on NTIS PRICE SCHEDULES.

Documents on microfiche are designated by a pound sign (#) following the accession number. The pound sign is used without regard to the source or quality of the microfiche.

Initially distributed microfiche under the NTIS SRIM (Selected Research in Microfiche) is available at greatly reduced unit prices. For this service and for information concerning subscription to NASA printed reports, consult the NTIS Subscription Section, Springfield, Va. 22161.

NOTE ON ORDERING DOCUMENTS: When ordering NASA publications (those followed by the * symbol), use the N accession number. NASA patent applications (only the specifications are offered) should be ordered by the US-Patent-Appl-SN number. Non-NASA publications (no asterisk) should be ordered by the AD, PB, or other *report* number shown on the last line of the citation, not by the N accession number. It is also advisable to cite the title and other bibliographic identification.

Avail: SOD (or GPO). Sold by the Superintendent of Documents, U.S. Government Printing Office, in hard copy. The current price and order number are given following the availability line. (NTIS will fill microfiche requests, as indicated above, for those documents identified by a # symbol.)

(1) A microfiche is a transparent sheet of film, 105 by 148 mm in size containing as many as 60 to 98 pages of information reduced to micro images (not to exceed 26:1 reduction)

- Avail: BLL (formerly NLL): British Library Lending Division, Boston Spa, Wetherby, Yorkshire, England. Photocopies available from this organization at the price shown. (If none is given, inquiry should be addressed to the BLL.)
- Avail: DOE Depository Libraries. Organizations in U.S. cities and abroad that maintain collections of Department of Energy reports, usually in microfiche form, are listed in *Energy Research Abstracts*. Services available from the DOE and its depositories are described in a booklet, *DOE Technical Information Center - Its Functions and Services* (TID-4660), which may be obtained without charge from the DOE Technical Information Center.
- Avail: ESDU. Pricing information on specific data, computer programs, and details on ESDU topic categories can be obtained from ESDU International Ltd. Requesters in North America should use the Virginia address while all other requesters should use the London address, both of which are on the page titled ADDRESSES OF ORGANIZATIONS.
- Avail: Fachinformationszentrum, Karlsruhe. Sold by the Fachinformationszentrum Energie, Physik, Mathematik GMBH, Eggenstein Leopoldshafen, Federal Republic of Germany, at the price shown in deutschmarks (DM).
- Avail: HMSO. Publications of Her Majesty's Stationery Office are sold in the U.S. by Pendragon House, Inc. (PHI), Redwood City, California. The U.S. price (including a service and mailing charge) is given, or a conversion table may be obtained from PHI.
- Avail: NASA Public Document Rooms. Documents so indicated may be examined at or purchased from the National Aeronautics and Space Administration, Public Documents Room (Room 126), 600 Independence Ave., S.W., Washington, D.C. 20546, or public document rooms located at each of the NASA research centers, the NASA Space Technology Laboratories, and the NASA Pasadena Office at the Jet Propulsion Laboratory.
- Avail: Univ. Microfilms. Documents so indicated are dissertations selected from *Dissertation Abstracts* and are sold by University Microfilms as xerographic copy (HC) and microfilm. All requests should cite the author and the Order Number as they appear in the citation.
- Avail: US Patent and Trademark Office. Sold by Commissioner of Patents and Trademarks, U.S. Patent and Trademark Office, at the standard price of \$1.50 each, postage free. (See discussion of NASA patents and patent applications below.)
- Avail: (US Sales Only). These foreign documents are available to users within the United States from the National Technical Information Service (NTIS). They are available to users outside the United States through the International Nuclear Information Service (INIS) representative in their country, or by applying directly to the issuing organization.
- Avail: USGS. Originals of many reports from the U.S. Geological Survey, which may contain color illustrations, or otherwise may not have the quality of illustrations preserved in the microfiche or facsimile reproduction, may be examined by the public at the libraries of the USGS field offices whose addresses are listed in this Introduction. The libraries may be queried concerning the availability of specific documents and the possible utilization of local copying services, such as color reproduction.
- Avail: Issuing Activity, or Corporate Author, or no indication of availability. Inquiries as to the availability of these documents should be addressed to the organization shown in the citation as the corporate author of the document.

PUBLIC COLLECTIONS OF NASA DOCUMENTS

DOMESTIC: NASA and NASA-sponsored documents and a large number of aerospace publications are available to the public for reference purposes at the library maintained by the American Institute of Aeronautics and Astronautics, Technical Information Service, 555 West 57th Street, 12th Floor, New York, New York 10019.

EUROPEAN: An extensive collection of NASA and NASA-sponsored publications is maintained by the British Library Lending Division, Boston Spa, Wetherby, Yorkshire, England for public access. The British Library Lending Division also has available many of the non-NASA publications cited in *STAR*. European requesters may purchase facsimile copy or microfiche of NASA and NASA-sponsored documents, those identified by both the symbols # and . from ESA - Information Retrieval Service European Space Agency, 8-10 rue Mario-Nikis, 75738 CEDEX 15, France.

FEDERAL DEPOSITORY LIBRARY PROGRAM

In order to provide the general public with greater access to U.S. Government publications, Congress established the Federal Depository Library Program under the Government Printing Office (GPO), with 50 regional depositories responsible for permanent retention of material, inter-library loan, and reference services. At least one copy of nearly every NASA and NASA-sponsored publication, either in printed or microfiche format, is received and retained by the 50 regional depositories. A list of the regional GPO libraries, arranged alphabetically by state, appears on the inside back cover. These libraries are *not* sales outlets. A local library can contact a Regional Depository to help locate specific reports, or direct contact may be made by an individual.

STANDING ORDER SUBSCRIPTIONS

NASA SP-7041 and its supplements are available from the National Technical Information Service (NTIS) on standing order subscription as PB 86-903800 at the price of \$14.50 domestic and \$29.00 foreign. Standing order subscriptions do not terminate at the end of a year, as do regular subscriptions, but continue indefinitely unless specifically terminated by the subscriber.

ADDRESSES OF ORGANIZATIONS

American Institute of Aeronautics and
Astronautics
Technical Information Service
555 West 57th Street, 12th Floor
New York, New York 10019

British Library Lending Division,
Boston Spa, Wetherby, Yorkshire,
England

Commissioner of Patents and
Trademarks
U.S. Patent and Trademark Office
Washington, D.C. 20231

Department of Energy
Technical Information Center
P.O. Box 62
Oak Ridge, Tennessee 37830

ESA-Information Retrieval Service
ESRIN
Via Galileo Galilei
00044 Frascati (Rome) Italy

ESDU International, Ltd.
1495 Chain Bridge Road
McLean, Virginia 22101

ESDU International, Ltd.
251-259 Regent Street
London, W1R 7AD, England

Fachinformationszentrum Energie, Physik,
Mathematik GMBH
7514 Eggenstein Leopoldshafen
Federal Republic of Germany

Her Majesty's Stationery Office
P.O. Box 569, S.E. 1
London, England

NASA Scientific and Technical Information
Facility
P.O. Box 8757
B.W.I. Airport, Maryland 21240

National Aeronautics and Space
Administration
Scientific and Technical Information
Division (NTT-1)
Washington, D.C. 20546

National Technical Information Service
5285 Port Royal Road
Springfield, Virginia 22161

Pendragon House, Inc.
899 Broadway Avenue
Redwood City, California 94063

Superintendent of Documents
U.S. Government Printing Office
Washington, D.C. 20402

University Microfilms
A Xerox Company
300 North Zeeb Road
Ann Arbor, Michigan 48106

University Microfilms, Ltd.
Tylers Green
London, England

U.S. Geological Survey Library
National Center - MS 950
12201 Sunrise Valley Drive
Reston, Virginia 22092

U.S. Geological Survey Library
2255 North Gemini Drive
Flagstaff, Arizona 86001

U.S. Geological Survey
345 Middlefield Road
Menlo Park, California 94025

U.S. Geological Survey Library
Box 25046
Denver Federal Center, MS914
Denver, Colorado 80225

NTIS PRICE SCHEDULES

(Effective January 1, 1987)

Schedule A STANDARD PRICE DOCUMENTS AND MICROFICHE

PRICE CODE	PAGE RANGE	NORTH AMERICAN PRICE	FOREIGN PRICE
A01	Microfiche	\$ 6.50	\$13.00
A02	001-025	9.95	19.90
A03	026-050	11.95	23.90
A04-A05	051-100	13.95	27.90
A06-A09	101-200	18.95	37.90
A10-A13	201-300	24.95	49.90
A14-A17	301-400	30.95	61.90
A18-A21	401-500	36.95	73.90
A22-A25	501-600	42.95	85.90
A99	601-up	.	.
NO1		45.00	80.00
NO2		48.00	80.00

Schedule E EXCEPTION PRICE DOCUMENTS AND MICROFICHE

PRICE CODE	NORTH AMERICAN PRICE	FOREIGN PRICE
E01	\$ 7.50	15.00
E02	10.00	20.00
E03	11.00	22.00
E04	13.50	27.00
E05	15.50	31.00
E06	18.00	36.00
E07	20.50	41.00
E08	23.00	46.00
E09	25.50	51.00
E10	28.00	56.00
E11	30.50	61.00
E12	33.00	66.00
E13	35.50	71.00
E14	38.50	77.00
E15	42.00	84.00
E16	46.00	92.00
E17	50.00	100.00
E18	54.00	108.00
E19	60.00	120.00
E20	70.00	140.00
E99	.	.

*Contact NTIS for price quote.

IMPORTANT NOTICE

NTIS Shipping and Handling Charges

U.S., Canada, Mexico — ADD \$3.00 per TOTAL ORDER

All Other Countries — ADD \$4.00 per TOTAL ORDER

Exceptions — Does NOT apply to:

ORDERS REQUESTING NTIS RUSH HANDLING
ORDERS FOR SUBSCRIPTION OR STANDING ORDER PRODUCTS ONLY

NOTE: Each additional delivery address on an order
requires a separate shipping and handling charge.

1. Report No. NASA SP-7041 (55)		2. Government Accession No.		3. Recipient's Catalog No.	
4. Title and Subtitle EARTH RESOURCES A Continuing Bibliography (Issue 55)				5. Report Date November, 1987	
				6. Performing Organization Code	
7. Author(s)				8. Performing Organization Report No.	
				10. Work Unit No.	
9. Performing Organization Name and Address National Aeronautics and Space Administration Washington, DC 20546				11. Contract or Grant No.	
				13. Type of Report and Period Covered	
12. Sponsoring Agency Name and Address				14. Sponsoring Agency Code	
15. Supplementary Notes					
16. Abstract <p>This bibliography lists 368 reports, articles and other documents introduced into the NASA scientific and technical information system between July 1 and September 30, 1987. Emphasis is placed on the use of remote sensing and geophysical instrumentation in spacecraft and aircraft to survey and inventory natural resources and urban areas. Subject matter is grouped according to agriculture and forestry, environmental changes and cultural resources, geodesy and cartography, geology and mineral resources, hydrology and water management, data processing and distribution systems, instrumentation and sensors, and economic analysis.</p>					
17. Key Words (Suggested by Authors(s)) Bibliographies Earth Resources Remote Sensors			18. Distribution Statement Unclassified - Unlimited		
19. Security Classif. (of this report) Unclassified		20. Security Classif. (of this page) Unclassified		21. No. of Pages 116	
				22. Price * A06/HC	

*For sale by the National Technical Information Service, Springfield, Virginia 22161

NASA-Langley, 1987